Exploring the physiological role of an obesity-linked gene variant

Author:
Metcalfe, Louise

Publication Date:
2022

DOI:
https://doi.org/10.26190/unsworks/1629

Exploring the physiological role of an obesity-linked gene variant

Louise K. Metcalfe

A thesis in fulfilment of the requirements for the degree of Doctor of Philosophy

School of Medical Sciences,

Faculty of Medicine and Health

September 2021

1. Thesis Title and Abstract

Thesis Title

Exploring the physiological role of an obesity-linked gene variant

Thesis Abstract

An Arg457Gln missense variant in the *CREBRF* gene (encoding for Cyclic AMP Response Element Binding Protein 3 Regulatory Factor) has previously been identified to paradoxically drive both excess body weight and reduced diabetes risk in numerous Pacific/Oceanic populations. Despite its apparent critical role in whole-body metabolism, few published studies have investigated this *CREBRF* missense variant at the molecular level. This thesis describes the metabolic characterisation of a novel mouse model in which the *CREBRF* Arg458Gln variant was knocked in to replace the endogenous *CREBRF*.

To address the whole-body phenotype, male and female mice were examined on a regular chow diet or an 8-week high-fat challenge, followed by analyses of the tissue transcriptome and *in vitro* signalling to determine possible variant impacts to molecular pathways. Assessment of body composition found that lean mass and naso-anal length were significantly increased by the *CREBRF* variant in male mice, without effect on total body weight or fat mass. Glucose tolerance and indirect calorimetry assessments were likewise unchanged by genotype. Male chow-fed variant carriers displayed reduced sensitivity to insulin administration, as well as exaggerated fasting-induced trends in nutrient homeostasis, including alterations to tissue glycogen and lipid as well as plasma NEFA elevation.

Microarray analysis performed on liver and gastrocnemius muscle tissue from this cohort revealed genotype-dependent differential expression of genes contributing to protein synthesis, processing, and turnover as well as cellular respiration and nutrient metabolism. A follow-up cohort saw no significant changes to muscle function assessed by exercise endurance or grip strength performance. *In vitro* examination of insulin and glucagon signalling pathways using a primary hepatocyte model revealed significant dampening of PKB signalling in cells isolated from male mice carrying the variant.

Overall, this novel mouse model appears to show a whole-body growth phenotype effect of the *CREBRF* variant in males, with speculative roles in regulating energy homeostasis during periods of nutrient deprivation without benefit to insulin sensitivity or glucose tolerance. The mild effects of the Arg458Gln mutation in this mouse model may invite reconsideration of the link between CREBRF function and the risks of obesity and diabetes in variant allele carriers.

2. Originality, Copyright, and Authenticity Statements

ORIGINALITY STATEMENT

☑ I hereby declare that this submission is my own work and to the best of my knowledge it contains no materials previously published or written by another person, or substantial proportions of material which have been accepted for the award of any other degree or diploma at UNSW or any other educational institution, except where due acknowledgement is made in the thesis. Any contribution made to the research by others, with whom I have worked at UNSW or elsewhere, is explicitly acknowledged in the thesis. I also declare that the intellectual content of this thesis is the product of my own work, except to the extent that assistance from others in the project's design and conception or in style, presentation and linguistic expression is acknowledged.

COPYRIGHT STATEMENT

☑ I hereby grant the University of New South Wales or its agents a non-exclusive licence to archive and to make available (including to members of the public) my thesis or dissertation in whole or part in the University libraries in all forms of media, now or here after known. I acknowledge that I retain all intellectual property rights which subsist in my thesis or dissertation, such as copyright and patent rights, subject to applicable law. I also retain the right to use all or part of my thesis or dissertation in future works (such as articles or books).

For any substantial portions of copyright material used in this thesis, written permission for use has been obtained, or the copyright material is removed from the final public version of the thesis.

AUTHENTICITY STATEMENT

☑ I certify that the Library deposit digital copy is a direct equivalent of the final officially approved version of my thesis.

3. Inclusion of Publications Statement

UNSW is supportive of candidates publishing their research results during their candidature as detailed in the UNSW Thesis Examination Procedure.

Publications can be used in the candidate's thesis in lieu of a Chapter provided:

- The candidate contributed **greater than 50%** of the content in the publication and are the "primary author", i.e. they were responsible primarily for the planning, execution and preparation of the work for publication.
- The candidate has obtained approval to include the publication in their thesis in lieu of a Chapter from their Supervisor and Postgraduate Coordinator.
- The publication is not subject to any obligations or contractual agreements with a third party that would constrain its inclusion in the thesis.

☑ The candidate has declared that **their thesis contains no publications, either published or submitted for publication**.

Candidate's Declaration

I declare that I have complied with the Thesis Examination Procedure.

Table of Contents

Abstract

An Arg457Gln missense variant in the *CREBRF* gene (encoding for Cyclic AMP Response Element Binding Protein 3 Regulatory Factor) has previously been identified to paradoxically drive both excess body weight and reduced diabetes risk in numerous Pacific/Oceanic populations. Despite its apparent critical role in whole-body metabolism, few published studies have investigated this *CREBRF* missense variant at the molecular level. This thesis describes the metabolic characterisation of a novel mouse model in which the *CREBRF* Arg458Gln variant was knocked in to replace the endogenous *CREBRF*.

To address the whole-body phenotype, male and female mice were examined on a regular chow diet or an 8-week high-fat challenge, followed by analyses of the tissue transcriptome and *in vitro* signalling to determine possible variant impacts to molecular pathways. Assessment of body composition found that lean mass and naso-anal length were significantly increased by the *CREBRF* variant in male mice, without effect on total body weight or fat mass. Glucose tolerance and indirect calorimetry assessments were likewise unchanged by genotype. Male chow-fed variant carriers displayed reduced sensitivity to insulin administration, as well as exaggerated fasting-induced trends in nutrient homeostasis, including alterations to tissue glycogen and lipid as well as plasma NEFA elevation.

Microarray analysis performed on liver and gastrocnemius muscle tissue from this cohort revealed genotype-dependent differential expression of genes contributing to protein synthesis, processing, and turnover as well as cellular respiration and nutrient metabolism. A follow-up cohort saw no significant changes to muscle function assessed by exercise endurance or grip strength performance. *In vitro* examination of insulin and glucagon signalling pathways using a primary hepatocyte model revealed significant dampening of PKB signalling in cells isolated from male mice carrying the variant.

Overall, this novel mouse model appears to show a whole-body growth phenotype effect of the *CREBRF* variant in males, with speculative roles in regulating energy homeostasis during periods of nutrient deprivation without benefit to insulin sensitivity or glucose tolerance. The mild effects of the Arg458Gln mutation in this mouse model may invite reconsideration of the link between CREBRF function and the risks of obesity and diabetes in variant allele carriers.

Acknowledgments

The receipt of financial support including my Research Training Program scholarship, as well as the HDR Completion Scholarship provided by UNSW, is gratefully acknowledged. Other thanks are extended to the BRC technical staff for their care of the animals used in this thesis, and to Brendan Lee and BRIL. Thanks also go to Professor Peter Shepherd and Doctor Kate Lee of the University of Auckland, whose collaboration with especially the initial generation of the microarray data from our samples presented in this thesis is acknowledged and appreciated.

I am incredibly grateful to my supervisor Nigel Turner for always giving the necessary means and the guidance for me to succeed in first Honours and now this PhD, and for having enough faith in my research and writing skills to pull me out of my own doubts when I needed it. Huge thanks also to my co-supervisor Greg Smith, who from day one was constantly available to help out when I needed advice or unsolicited commentary on the Bledisloe, and especially for the work he put in teaching me on-the-job animal handling skills. Thanks likewise to Prof Margaret Morris for her position as my other co-supervisor.

I also must acknowledge the other members of the MBE lab, who have been a solid support throughout my time here both inside and outside of the lab itself, including but not limited to Brenna, Brendan, Hemna, Eileen, Tom, Sarah, the many Honours students--and special mention to Azrah, without whom the GTTs would have been a much paler experience! In all seriousness, the members of MBE and the broader department have very much contributed to making this journey an enjoyable one, for which I am thankful.

Special thanks also go to my family, who continued to encourage me throughout this long four years.

Publications, Oral Presentations, & Posters

Publications

Metcalfe LK, Krishnan M, Turner N, Yaghootkar H, Merry TL, Dewes O, *et al.* (2020). The Maori and Pacific specific CREBRF variant and adult height. *Int J Obesity* **44**, 748-752.

Oral Presentations

Metcalfe LK (2018). 'Exploring the physiological role of a gene variant that causes obesity.' Presented at the Neuroscience and Non-Communicable Diseases Seminar, 9 Nov, UNSW Sydney.

Metcalfe LK, Lee KL, Shepherd PR, Smith GC & Turner N (2019). 'Characterisation of the growth phenotype induced by the CREBRF "obesity variant" in knock-in mice.' Presented at the annual scientific meeting of the Australian and New Zealand Obesity Society, 16-18 Oct, Sydney, NSW.

Metcalfe LK, Shepherd PR, Smith GC & Turner N (2020). 'Metabolic characterisation of knock-in mice harbouring the CREBRF "obesity variant".' Presented at the Australasian Diabetes Congress, 11-13 Nov, virtual event.

Metcalfe LK (2020). 'Exploring the physiological role of a gene variant that causes obesity'. Presented at the Neuroscience and Non-Communicable Diseases Seminar, 20 Nov, UNSW Sydney.

Metcalfe LK, Shepherd PR, Smith GC & Turner N (2021). 'A role for the CREBRF^{R457Q} "obesity variant" in the regulation of metabolism during fasting.' Presented at the annual scientific meeting of the Australian and New Zealand Obesity Society, 20-22 Jul, virtual event.

Posters

Metcalfe LK, Shepherd PR, Smith GC & Turner N (2018). 'Metabolic characterisation of knock-in mice harbouring the "obesity variant" of CREBRF'. Poster presented at the annual scientific meeting of the Australian and New Zealand Obesity Society, 16-18 Oct, Melbourne, Vic.

List of Figures

List of Tables

Abbreviations

AA: amino acid

AN: Austronesian

BAT: brown adipose tissue

BCL6: B-cell lymphoma 6

BG: blood glucose

BMD: bone mineral density

BMI: body mass index

BSA: bovine serum albumin

BW: body weight

CBG: corticosteroid-binding globulin

ChREBP: carbohydrate response element binding protein

CLAMS: Comprehensive Laboratory Animal Monitoring System

CNS: central nervous system

CRE: cAMP response element

CREB3: cAMP-responsive element binding protein 3

CREBRF: cAMP response element binding protein 3 regulatory factor

DAVID: Database for Annotation, Visualisation and Integrated Discovery

DEGs: differentially expressed genes

DMEM: Dulbecco's Modified Eagle Medium

EDL: extensor digitorum longus

ER: endoplasmic reticulum

ERAD: ER-associated degradation

ESC: endometrial stromal cell

ETC: electron transport chain

eWAT: epididymal white adipose tissue

FA: fatty acid

FAO: fatty acid oxidation

FFA: free fatty acid

FTO: fat mass and obesity-associated

GC: Glucocorticoid

GO: gene ontology

GR: glucocorticoid receptor

GRE: glucocorticoid response element

GSEA: gene set enrichment analysis

GWAS: genome-wide association studies

HBSS: Hanks Buffered Salt Solution

HET: heterozygous

HFD: high fat diet

HGP: hepatic glucose production

HOM: homozygous

HOMA-IR: Homeostatic Model Assessment for Insulin Resistance

HPA: hypothalamic-pituitary-adrenal

HRM: high resolution meltcurve

HRP: horseradish peroxide

HSV-1: herpes simplex virus

iAUC: incremental area under the curve

InsR: insulin receptor

ipITT: intraperitoneal insulin tolerance test

IR: insulin resistance

iWAT: inguinal white adipose tissue

KEGG: Kyoto Encyclopaedia of Genes and Genomes

KI: knock-in

KO: knockout

lncRNA: long non-coding RNA

M199: Medium 199

MCL: Markov Cluster

MGI: Mouse Genome Informatics

MHO: metabolically healthy obesity

miRNA: microRNA

mTOR: mammalian target of rapamycin

mTORC1/2: mammalian target of rapamycin complex 1/2

NAFLD: non-alcoholic fatty liver disease

ncRNA: non-coding RNA

NEFA: non-esterified fatty acid

oGTT: oral glucose tolerance test

OxPhos: oxidative phosphorylation

PCA: principal component analysis

PI: Pacific Islands

PKB: protein kinase B

PPAR: Peroxisome proliferator-activated receptor

PPI: protein-protein interaction

PRAS40: proline-rich Akt substrate 40 kDa

pWAT: periovarian white adipose tissue

RER: respiratory exchange ratio

RPs: ribosomal proteins

rRNA: ribosomal RNA

RT: room temperature

S1P: site-1 protease

S2P: site-2 protease

SDS: sodium dodecyl sulphate

snoRNA: small nucleolar RNA

snRNA: small nuclear RNA

SREBP-1c: sterol regulatory element-binding protein-1c

STRING: Search Tool for the Retrieval of Interacting Genes/Proteins

T2D: type 2 diabetes

TBS: tris-buffered saline

TBST: TBS with 0.1% Tween-20

TCA: tricarboxylic acid

TF: transcription factor

TG: triglyceride

TGH: thrifty genotype hypothesis

tRNA: transfer RNA

TXNIP: thioredoxin-interacting protein

UPR: unfolded protein response

VLDL: very-low-density lipoprotein

WAT: white adipose tissue

WT: wildtype

CHAPTER 1: General Introduction

1.1 The health burden of obesity and diabetes

Obesity and diabetes are metabolic conditions of increasingly widespread significance to modern populations. The global scale and gravity of their impacts on general health, life expectancy, and quality of life encourage the search for new treatment options. In Australia, two-thirds of the adult population, and almost one in four children, is overweight or obese (AIHW, 2017); over 1.2 million Australian adults are diabetic (AIHW, 2018). The former condition has been estimated to have an annual cost to the Australian economy of $8.6 billion (AIHW, 2017); the latter condition costs at least $1.7 billion annually in directly attributable healthcare (AIHW, 2013). These figures are all rising and, with them, so too is the need for research aimed at understanding and ameliorating metabolic disease.

Mechanisms which promote, instigate, or maintain these disorders are complex, interrelated, and certainly not simple to define. Homeostatic regulation of energy intake and expenditure underpins systemic and tissue metabolic activities which are unbalanced in obesity and diabetes. Excessive lipid accumulation provokes insulin resistance, although the precise causative pathways and indeed the specific lipids involved are uncertain. The correlative link between high adiposity and metabolic ill-health is held firm, albeit differentially modulated between individuals by factors of biological heterogeneity. A predisposition towards obesity can arise from environmental factors as well as from certain genetic variations. Evolutionary imperatives have been theorised to produce an inherent predisposition to metabolic disorders in the modern environment; specific ancestral groups, such as the historically isolated Pacific Island populations, have been suggested to represent partial corroboration of this idea. No single unifying theory exists.

1.2 Metabolism

1.2.1 Energy balance and obesity

Physiological energy homeostasis is defined by the balance between energy intake and energy expenditure. Inequality between these measures over a given period of time is buffered by compensatory fluctuations between substrate storage or utilisation, resulting

in changes to body weight. In practical terms, energy intake is largely defined by diet, and expenditure by physical activity. The modern lifestyle which is typical of many developed countries increasingly incorporates (theoretically) unlimited access to calorie dense foods as well as reductions in physical activity. Such an environment is therefore conducive to chronic imbalance between energy intake and expenditure, the former exceeding the latter, leading to an excess of stored energy and consequently obesity (Romieu *et al*., 2017). In this framework, obesity can be considered to comprise a failure of energy homeostasis. Restoration (or preservation) of the correct balance warrants attention to both intake and expenditure rather than either side of the equation alone (Hill *et al*., 2012).

Obesity during prolonged overnutrition is most often typified by abnormal, excess lipid accumulation. This is deposited primarily in adipose tissue, which has significant capacity for expansion to store nutrients as fat, but subsequently also in other tissues such as skeletal muscle, heart, and liver even more so once that expansive capacity of adipose is reached. Although fat accumulation provides the most visible marker, however, obesity is a multifactorial and systemic condition. Underlying the whole-body shift to increased energy storage are diverse modifications of neuroendocrine systems on cellular as well as tissue scales, producing new metabolic patterns which represent the attempt to adapt to obesity status. Indeed, Ghanemi *et al*. (2021) have as such most recently described obesity as a "neuroendocrine reprogrammer". In like manner, energy balance and nutrient homeostasis incorporate more than lipid metabolism alone.

1.2.2 Tissue energy metabolism

The metabolic processes responsible for energy homeostasis convert nutrients to chemical energy and the substrates needed for cell function. Intracellular pools of stored nutrients can derive from dietary consumption as well as endogenous synthesis pathways. The central macronutrients of protein, carbohydrate, and lipid are postprandially digested in the mouth, stomach, and/or intestines to their component parts—namely free amino acids, monosaccharides, monoglycerides, and fatty acids. These are further metabolised upon tissue uptake for both storage and energy expenditure. Carbohydrate monomers are converted to glucose-1-phosphate for storage as glycogen; lipids are re-esterified to triglyceride (TG) for storage in lipid droplets, or to form lipoprotein particles for export. Intracellular lipid pools can additionally be populated by increased non-esterified fatty

acid flux from adipose tissue lipolysis, or via *de novo* lipogenesis. Two key pathways which facilitate the utilisation of stored nutrients in energy production are glycolysis (breakdown of glucose) and β-oxidation (breakdown of fatty acids). The former string of multi-enzymatic reactions occurs in the cytosol, the latter in the mitochondrion; the major end-products of both processes can enter the tricarboxylic acid (TCA) cycle in the mitochondrial matrix for further metabolism and subsequent ATP generation. These pathways are broadly common across tissues which otherwise possess distinct metabolic roles, capacities, and preferred fuels. In the maintenance of systemic nutrient homeostasis, however, skeletal muscle and liver are of particular importance.

Skeletal muscle comprises a significant proportion of total tissue mass and as such its metabolic activities represent an important contribution to whole-body energy metabolism even by dint of that mass alone. This tissue can therefore account for up to 30% of resting energy expenditure, despite its relatively low metabolic rate at rest, as well as up to 80% of glucose disposal in the body (DeFronzo *et al*., 1985; Zurlo *et al*., 1990; Rolfe & Brown, 1997). Muscular energy metabolism is especially vital during exercise, given the associated high energy demands, and accompanying increases in substrate utilisation. Those fuel sources can include glucose, fatty acids, and ketone bodies, as well as muscle glycogen reserves. In addition to comprising the primary site for glucose uptake and storage, skeletal muscle acts as a reservoir for amino acids, stored as protein and released as necessary to support protein synthesis or energy production (Argilés *et al*., 2016). The amino acid pool can also interact with the TCA cycle, primarily though not entirely by utilising the carbon skeletons for *de novo* synthesis of cycle intermediates to increase cycle flux and meet energy demands during exercise (Wagenmakers, 1998).

The liver represents the body's main site of gluconeogenesis, glycogenolysis, lipogenesis, and ketogenesis. Its many energetic functions are more completely reviewed elsewhere (Rui, 2014). In the postprandial state, digested carbohydrates, fatty acids, and amino acids are taken up from the circulation. Glucose is converted to glycogen for storage; free fatty acids are re-esterified for storage as TGs or are secreted as very-low-density lipoprotein (VLDL) particles. During periods of energy demand, glycolysis and β-oxidation, supplemented with carbon sources taken up from the circulation, fuel the production of new glucose (gluconeogenesis) for hepatic output into circulation. The liver is

furthermore responsible for the formation of a variety of metabolites for systemic usage including, for example, cholesterol, bile salts, lipoproteins, and ketone bodies.

There is significant crosstalk between the tissues. The greater glucose uptake seen in working muscle, for example, influences the levels of circulating hormones which in turn regulate metabolic events in the liver, provoking increased HGP to restore blood glucose levels and provide substrates for continued muscular energy metabolism (Wasserman & Cherrington, 1991). The products of muscle metabolism (for example, lactate) are transported through the circulation to the liver where they may be processed back to usable fuel sources. Hepatic ketogenesis reflects similarly systemic interplay, using NEFAs released from adipose to generate fuel for extrahepatic tissues. The concerted metabolic activities of systemic energy homeostasis are governed by stimuli including diet, exercise, and circadian rhythm; prime among the mediating factors are circulating hormones such as insulin.

1.2.3 Endocrine hormone signalling

The circulating endocrine hormone insulin, released from the β-cells of the pancreatic islets following postprandial nutrient absorption, regulates substrate movement into tissues for either oxidation or storage. Its many activities, both stimulatory and inhibitory, are implemented via a complex signalling pathway activated by the insulin receptor (Saltiel and Kahn, 2001; Taniguchi *et al.*, 2006; Humphrey *et al.*, 2015). Of particular relevance is insulin stimulation of glucose uptake and metabolism, as well as fatty acid metabolism; in the liver, insulin also suppresses gluconeogenesis. The circulating hormone glucagon is secreted from the pancreatic α-cells upon the transition from feeding to fasting states and operates as the primary hormonal counterbalance to insulin. The signalling network which is activated by its binding to the glucagon receptor accordingly impacts many of the same metabolic pathways which are regulated by insulin action. As such, glucagon can suppress the synthesis and enhance the catabolism of lipids, as well as promoting glucose release into circulation via glycogenolysis and, in the liver, gluconeogenesis (Eisenstein *et al.*, 1974; Longuet *et al.*, 2008; Oh *et al.*, 2013; Pereira *et al.*, 2020). Both hormones are linked to circadian rhythm synchronisation, further regulating the homeostatic response to nutrient intake (Sun *et al.*, 2015b; Dang *et al.*, 2016; Kalvisa *et al.*, 2018).

Tissue desensitisation to insulin, and the resultant failure of a normal insulin dose to elicit these responses, is known as insulin resistance (IR). The aetiology of this condition has recently been comprehensively reviewed (James *et al*., 2021). In brief, IR results in the increased pancreatic production and secretion of insulin, in a compensatory effort to maintain normal glucose homeostasis. Sustained overproduction can ultimately cause pancreatic β-cell failure, thereby disrupting blood glucose control and leading to type 2 diabetes (T2D) onset (as recently reviewed by Galicia-Garcia *et al*., 2020). Hyperglucagonemia has similarly been associated with diabetes, resulting from altered pancreatic α-cell proliferation and secretory regulation, and also as a compensatory consequence of glucagon resistance (Müller *et al*., 1973; Gelling *et al*., 2003; Suppli *et al*., 2016). This has traditionally been viewed in the context of driving hyperglycaemia but is equally strongly linked to disruption of amino acid signalling and lipid metabolism (Lee *et al*., 2011; Dean *et al*., 2017; Kim *et al*., 2017b; Janah *et al*., 2019). Discussion of diabetes aetiology often centres around the onset of IR in liver and/or skeletal muscle, as the (non-adipose) peripheral tissues most essential to insulin regulation of systemic energy homeostasis.

1.3 Lipotoxicity

1.3.1 Lipid-induced insulin resistance

Obesity and diabetes are both known to be underpinned by IR. Although incompletely defined, a number of different mechanisms have been proposed to promote the development of systemic IR, including the accumulation of bioactive lipids in non-adipose tissues (Kraegen *et al.*, 1991; Summers, 2006; Chavez & Summers, 2012; Turner *et al.*, 2013). Excessive tissue lipid accumulation is promoted by obesogenic environments on an organismal scale, but is also further enhanced by various factors operating at the cellular level. Alterations to adipose tissue function/metabolism that occur during obesity are thought to be intimately involved (as reviewed by Goossens, 2017). Hypertrophic and hyperplasic responses both expand adipose storage capacity in apparent direct compensation upon lipid accumulation (Jo *et al*., 2009; Arner & Spalding, 2010). Such increases in adipocyte size and number are also proven, however, to independently predict the development of IR. Controlled for body mass index (BMI), insulin resistant individuals have been found to possess a greater proportion of small

adipose cells than do insulin sensitive individuals, while their large adipose cells are fewer but larger (Weyer *et al*., 2000; McLaughlin *et al*., 2007; Johannsen *et al*., 2014; McLaughlin *et al*., 2014; Kim *et al*., 2015a). Moreover, adipogenesis is impaired with IR (Deurenberg *et al*., 1991; Yang *et al*., 2004; McLaughlin *et al*., 2007, 2014) and promotion of adipocyte differentiation improves insulin sensitivity (De Souza *et al*., 2001; McLaughlin *et al*., 2011; Eliasson *et al*., 2014). Taken together, such findings tie IR to stunted expandability of adipose tissue, and a corresponding overspill of lipids from overloaded adipose depots into insulin-sensitive peripheral tissues such as skeletal muscle and liver.

Lipids have well defined roles in signalling and gene transcription, as metabolic fuels and as structural components of cells. The combination of various backbones, headgroups and acyl chains gives rise to many thousands of lipids that are classified in distinct classes, subclasses and subgroups (Li *et al*., 2015a; Lydic & Goo, 2018). This diversity in chemical structure results in a vast spectrum of physicochemical properties across various lipids. At the level of peripheral tissues such as muscle and liver, intracellular lipid accumulation is logically caused by either heightened uptake, diminished utilisation or in some cases enhanced lipogenesis. The correlations between lipid accumulation and IR appear to be due not to changes in either lipid uptake or fatty acid oxidation (FAO) alone, but to the aberrant build-up of specific lipids with deleterious roles.

Several such lipid species have been proposed—TG, long-chain acyl-CoA, acylcarnitine, phospholipid, diacylglycerol, and ceramide content included—although for the most part their contribution to IR aetiology is incompletely defined (Meikle & Summers, 2017; Petersen & Shulman, 2017). Interplay between lipid-related mechanisms is likely, as is the existence of as-yet-unidentified, non-canonical means of inducing IR. It is now becoming more broadly accepted, however, that seemingly contradictory evidence linking certain lipid species to IR is also perhaps a reflection of lipid subcellular location, the specific subspecies present and the timing of measurements relative to lipid fluxes (Meikle & Summers, 2017; Petersen & Shulman, 2017). The same is true on a broader macronutrient scale, with dietary carbohydrate and fat sub-types shown to differentially influence liver fat accumulation and metabolic health even when comparing isocaloric diets (Hydes *et al*., 2021). The necessity of these specifics in comprehending the development of lipid-induced IR provides an indicator of the complexity of the condition.

1.3.2 Adiposity, metabolic health, and confounding factors

Lipid content and adiposity *per se* is not an unambiguous reflection of individual metabolic health. Failure of overloaded adipose tissue storage capacity leading to ectopic lipid deposition may provide the primary insult, offering a ready correlation between fat mass and metabolic syndrome. But the relationship is a complex one. A subset of the aforementioned risk alleles for obesity reportedly associates with the opposite: *lower* risks of metabolic disease (Krempler *et al*., 2002; Yaghootkar *et al*., 2016; Ji *et al.,* 2019). Lipodystrophy has been positively associated with IR (Ganda, 2000; Gavrilova *et al*., 2000; Kim *et al*., 2000). Pharmacological rescue of insulin sensitivity can be achieved despite fat mass gain (Fonseca, 2003) as is the case for thiazolidinediones. On a broader scale is the intriguing phenomenon of (so-called) "metabolically healthy obesity" (MHO) (Sims, 2001; Blüher, 2020). The phrase refers to individuals resistant to the adverse metabolic effects of weight gain including T2D, driven primarily by altered fat distribution, adipocyte morphology, and lipogenesis capacity, as well as an improved inflammatory profile compared to metabolically unhealthy obese persons (Primeau *et al*., 2011; Samocha-Bonet *et al*., 2012; Stefan *et al.*, 2013; Fabbrini *et al*., 2015; Alfadda *et al*., 2017). On an individual level, at least, it seems that the link between (total) adiposity and adverse metabolic consequences is not straightforwardly causal in all circumstances and other modulating factors exist. Overall, however, the correlation holds even for these MHO individuals. Terming the phenotype "healthy" is a simplification: meta-analyses demonstrate that the phenotype is transient and that most MHO individuals are ultimately at higher risk of developing T2D and cardiovascular disease over time (Appleton *et al*., 2013; Kramer *et al*., 2013; Eckel *et al*., 2016; Fingeret *et al*., 2018; Tsatsoulis & Paschou, 2020).

Individual adipose depots are themselves heterogeneous. Proliferative capacity, glucose and lipid metabolism, insulin sensitivity, and cytokine pattern can each differ between visceral and subcutaneous adipose tissues (Lee *et al*., 2013; Kranendonk *et al*., 2015; Guglielmi & Sbraccia, 2018). The latter depots, for instance, have a larger pool of preadipocytes, while adipogenic genes are more highly expressed and more responsive to differentiation cues than in visceral depots (Lundgren *et al.*, 2007). The different subcutaneous depots, too, have differing characteristics. Abdominal adipose provides a short-term energy store, with rapid uptake of dietary lipids and high lipolysis rates; gluteo-femoral adipose is longer-term storage, with reduced lipid turnover (Tchkonia *et*

al., 2013; Karpe & Pinnick, 2015). These distinct features have similarly distinct effects on metabolic health. Visceral fat mass is a strong predictor of IR (McLaughlin *et al*., 2011); abdominal fat has been similarly associated (Goodpaster *et al*., 1997). The gluteo-femoral depot shows the opposite: an association with a protective lipid and glucose profile, as well as decreased cardiovascular and metabolic risk (Manolopoulos *et al*., 2010). Low gluteo-femoral fat mass is rather a risk factor for unfavourable metabolic conditions, independent of other adipose tissue (Snijder *et al*., 2005). Brown adipose tissue is further still disparate in function, acting more in thermogenesis and energy balance regulation than in energy storage *per se* (Cypess *et al*., 2009; Virtanen *et al*., 2009; Vijgen *et al.*, 2011). The depot-specific functions of adipose tissue are suggested to imply an evolutionary conserved adipogenic programme (Gesta *et al*., 2006). Total fat mass provides an inadequate risk measure; preferential distribution of fat mass better reflects metabolic consequences.

Obesity furthermore exhibits sexually dimorphic characteristics, with patterns of fat content and distribution distinct between sexes. Human studies have found that females possess higher total body fat content than males (Jackson *et al*., 2002; Geer & Shen, 2009); that lipids are stored predominantly in subcutaneous adipose tissue in females, and in visceral adipose tissue in males (Schreiner *et al*., 1996; Romanski *et al*., 2000; Demerath *et al*., 2007); and that males oxidise/mobilise dietary FAs more readily than do females who are more prone to storage (Nielsen *et al.*, 2003; Uranga *et al*., 2005). Women derive proportionally more energy from fat oxidation during exercise; men primarily utilise carbohydrate oxidation (Horton *et al.*, 1998; Tarnopolsky, 2000; Mittendorfer *et al*., 2002). The consequences of these (and similar) differentiations are moreover played out in the features of metabolic syndrome. The sexes differ in comparative insulin sensitivity, glucose metabolism, circulating lipid profile, and risk of individual metabolic syndrome factors such as cardiovascular disease and hypertension, with females being less susceptible than males (Regitz-Zagrosek *et al.*, 2007; Vishram *et al*., 2014; Rochlani *et al*., 2015).

The relationship between biological sex and body composition is not merely incidental, or correlative; metabolic effects are at least partially regulated by sex hormones and by chromosomal complement. Testosterone and oestrogens differentially affect lipolysis, adipogenesis, and pathogenic lipid profile (Ramirez *et al.*, 1997; Lacasa *et al.*, 2001;

Pedersen *et al*., 2004; Singh *et al*., 2006). Oestrogens moreover regulate central and peripheral fat distribution, with inverse effects on adiposity and muscle mass (Al-Qahtani *et al*., 2017; Yasrebi *et al*., 2017; Reusch *et al*., 2018). The relationship is not strictly one-way: alterations in visceral and subcutaneous fat content can alter sex hormone profiles (Kim *et al*., 2017a). Independently of gonadal effects, the X chromosome influences food intake and is associated with fat mass gain, which is accordingly greater in XX than in XY status (Chen *et al*., 2012; Reue, 2017). Recognition of sex-based differentiation of phenotype has led the National Institute of Health to mandate that researchers consider sex as a biological variable and include both sexes in preclinical research designs (NIH, 2015; Clayton, 2018).

Ethnicity, as a proxy for genetic ancestry, is likewise a confounding factor. Total adiposity measures examined in multiethnic cohorts have consistently shown significant variation between ethnic-racial groups in both children and adults (Swinburn *et al*., 1999; Lear *et al*., 2007; Rush *et al*., 2009; Staiano *et al*., 2013a). More precise measures of intrabdominal adiposity, including comparative accumulation and distribution patterns of trunk, visceral, and liver fat, are also significantly affected by ethnicity (Nazare *et al*., 2012; Staiano & Katzmarzyk, 2012; Lim *et al*., 2019; Martos-Moreno *et al*., 2020). BMI and/or adiposity values remain strong predictors of metabolic derangements for all ethnic groups, and thus can account for significant fractions of the ethnic disparity in metabolic syndrome prevalence, but contributions to risk can nevertheless differ (Lim *et al*., 2019; Maskarinec *et al*., 2020; Martos-Moreno *et al*., 2020). For example, both Hispanic and African American cohorts exhibit high obesity and IR rates, but these risk factors accompany high non-alcoholic fatty liver disease (NAFLD) prevalence in only the former group (Agbim *et al*., 2019). Evidence suggests that ethnic-specific anthropometric targets would be of practical utility for diagnosis of metabolic health; this would require greater understanding of differential risks between populations. Nor do potential confounders operate in isolation, with sexual maturation status shown to attenuate ethnic differences in girls' adiposity (Staiano *et al*., 2013b). Many questions—regarding molecular mechanisms, interactions with factors such as diet or age, and metabolic consequences (reviewed by Reusch *et al*., 2018)—fall, however, into the many gaps in extant research and require significant further investigation before concrete conclusions may be drawn.

1.4 Obesity, Genetics, and the Environment

1.4.1 Genetic variant risk alleles

Obesity can develop from interplay between genetic and environmental (or behavioural) factors. In the broadest view, this interaction can be seen in the inter-individual variability in responses to diet which has proven to be a challenge for development of practical public health recommendations addressing obesity (Berry *et al*., 2020). Rodent studies likewise reveal complex phenotypic variation in obesity-related traits, including diet effect size, that is largely strain-dependent (Montgomery *et al*., 2013; Yam *et al*., 2020). In the ongoing attempt to identify the genes underlying an individual predisposition to obesity, large-scale genome-wide association studies (GWAS) in human populations have been used to assess associations between genetic variation and phenotypic traits. Variations at certain gene loci are associated with susceptibility (or, alternately, resistance) to weight and fat mass gain; risk alleles have been identified for monogenic or, more commonly, polygenic forms of obesity. Indeed, the *ob/ob* and *db/db* obese mice, which harbour spontaneously-arisen deficiency mutations in the genes encoding for leptin and the leptin receptor respectively, have long been utilised to study obesity aetiology (Ingalls *et al*., 1950; Hummel *et al*., 1966). In recent years, research has also identified epigenetic modifications linked to obesity and metabolic disease, as reviewed elsewhere (Chiurazzi *et al*., 2020).

Perhaps the most highly cited of these genetic contributors in humans is the fat mass and obesity-associated (FTO) gene, which harbours fifteen single nucleotide polymorphisms (SNPs) within the first intron, each one associated with increased obesity risk (Church *et al*., 2009; Speliotes *et al.*, 2010; Mao *et al*., 2017). At the time of its discovery, and until recent years, the *FTO* locus was the largest known (single) genetic influence on polygenic obesity. Crucially, however, although the *FTO* variants occur in many populations, for example European, African, or Hispanic ancestries (Dina *et al.*, 2007; Frayling *et al.*, 2007; Scuteri *et al*., 2007; Hubacek *et al.*, 2008; Liu *et al*., 2010), the association with obesity is not conclusively replicated worldwide (Ohashi *et al*., 2007; Yajnik *et al.*, 2009; Karns *et al*., 2012).

The mechanisms by which *FTO* risk alleles are theorised to operate provide a convenient illustration of the integration of genetic and other factors in obesity development. The intronic variants which induce *FTO* gain of expression act primarily via the hypothalamus

to alter neural responses to food signals and thereby influence food intake (Speakman *et al.*, 2008; Haupt *et al.*, 2009; Wiemerslage *et al.*, 2016). More broadly, the (heritable) dysregulation of food intake and behaviour is indeed suggested to be one definition of obesity (O'Rahilly & Farooqi, 2008; Wardle & Carnell, 2009; Choquet & Meyre, 2011). The behavioural susceptibility theory presents appetite as a causal factor, purporting that obesity results from genetic susceptibility to overeating in an 'obesogenic' food environment (Llewellyn & Wardle, 2015; Llewellyn & Fildes, 2017). The genetic effects of *FTO* are also modulated by factors including physical activity, aerobic fitness, and/or glycaemia (Andreasen *et al.*, 2008; Kilpeläinen *et al.*, 2011; Qi *et al.*, 2015; Celis-Morales *et al.*, 2016; Sailer *et al.*, 2016; Wagner *et al.*, 2017).

Genetic susceptibility to obesity extends further to co-morbidities encompassing a variety of metabolic disorders. The *FTO* risk alleles, for example, have been associated with not only obesity and BMI but also with cerebrocortical IR (Tschritter *et al.*, 2007), T2D (Frayling *et al.*, 2007; Freathy *et al.*, 2008; Sabarneh *et al.*, 2018), hypertension (He *et al.*, 2014), and inflammation (Fisher *et al.*, 2012). These and similar relationships to aspects of the metabolic syndrome are recapitulated in studies focussed on other gene variants shown to favour obesity which are located, for example, near *MC4R* (Loos *et al.*, 2008; Qi *et al.*, 2008), *ENPP1* (Meyre *et al.*, 2005; McAteer *et al.*, 2008), or *CDKAL1* (Steinthorsdottir *et al.*, 2007; Okada *et al.*, 2012). The correlations frequently seen between obesity and metabolic disease indicate some correspondence in the underlying molecular mechanisms, and thereby demonstrate research avenues of interest.

1.4.2 Evolution and the Thrifty Genotype Hypothesis

Theories proposed in the attempt to elucidate interactions between genetics and environment, in the context of obesity and metabolic syndrome, are many. One such explanation is provided by the Thrifty Genotype Hypothesis (TGH), initially posed by Neel (1962). According to the hypothesis, an evolutionary history incorporating repeat exposure to famine periods is a breeding ground for the positive selection of genetic features favouring efficient—that is, "thrifty"—energy balance: leveraging metabolism to maximise storage and limit expenditure of energy. In a modern environment which provides abundant sources of energy, such genes would logically predispose their carriers to obesity and metabolic syndrome (Neel, 1962, 1999). Candidate genes are occasionally proposed: the Gly482Ser variant in the *PPARGC1A* gene, for example, has a high

frequency in Polynesia and was hypothesised to contribute to the high BMI and T2D prevalence in that population (Myles *et al*., 2007, 2011). No compelling evidence, however, has been identified either for its positive selection or for an association with BMI or T2D (Myles *et al*., 2011; Cadzow *et al*., 2016).

More broadly, however, thrifty gene candidates are generally uncorroborated by population studies worldwide (Southam et al., 2009; Ayub et al., 2014; Koh et al., 2014; Steinthorsdottir et al., 2014; Wang & Speakman, 2016). The TGH is therefore somewhat controversial. It is argued (perhaps justifiably) to be inadequate as a stand-alone explanation for human susceptibility to an obesogenic environment given the multiplicity of selection pressures, of the genes and biological pathways involved, and of factors such as population dynamics (Hales & Barker, 2001; Bouchard *et al*., 2007; Speakman, 2008; Baig *et al.*, 2011; Speakman & Westerterp, 2013; Gosling *et al.*, 2015; Reales *et al*., 2017; Qasim *et al*., 2018; Garduño-Espinosa *et al*., 2019). Nevertheless, it is comparatively uncontroversial that long-term trends in body composition and metabolic capacity appear to have developed throughout hominin evolution to better ensure individual and species survival in response to local environmental pressures, including energy stress (Wells, 2006, 2017). These trends contribute to overall susceptibility to metabolic conditions including diabetes in a manner which both resembles and is exacerbated by nutritional exposure during individual lifespan. As such, the concept of an underlying determinant of *in vivo* metabolic response to the contemporary environment has persisted in the literature.

Alternative theories have been proposed, suggesting that the predisposition towards metabolic syndrome may be a function of genetic drift (rather than selection) (Speakman, 2008); or of a "thrifty phenotype" as an adaptive maternal effect associated with intrauterine growth restriction and/or as a consequence of poor nutrition in early life (Hales & Barker, 2001; Wells, 2007b, 2011; Priante *et al*., 2019); or of a "thrifty epigenotype" driven by potentially heritable epigenetic variations (Stöger, 2008). The thriftiness concept tends to be used somewhat interchangeably between these mechanisms in current discussions, operating more as umbrella terminology than referring specifically to the mechanisms of Neel's original hypothesis. As such, the proposal most recently published names PTEN as the candidate primary thrifty gene, modified *in utero* by nutrient availability rather by natural selection *per se* (Venniyoor, 2020). Bouchard

(2007) suggests five (non-mutually exclusive) genotype classes, of which "thrifty" is but one among "hyperphagic", "sedens", "low lipid oxidation", and "adipogenesis". The mitochondrial efficiency hypothesis, meanwhile, postulates that energetic thriftiness from reduced heat production is a consequence of adaptation to low-calorie diets in hot climates (Bhopal & Rafnsson, 2009).

Not all such hypotheses are mutually exclusive, or wholly incompatible with the base TGH concept. Adaptive evolutionary selection of "thrifty"-type genes, driven by feast-famine cycles, may have also been catalysed by cycles of alternating physical activity and rest (Chakravarthy & Booth, 2004). Modern disadvantage may thus be a consequence of not only dietary excess but also of comparatively sedentary lifestyle. In this scenario, where physical capacity is a key determinant of survival and thus of evolutionary adaptation, it is feasible that genes would be selected in the interests of preserving that capacity during food deprivation, as well as energy storage (Stannard & Johnson, 2004). For a more broadly integrative paradigm, Johnson *et al.* (2013) took a comparative biology approach to argue that the metabolic syndrome represents a normal physiological process—a survival mechanism to avert starvation—that has been subverted by continuous food availability. No single framework has yet been conclusively proven.

Many of these conceptual paradigms are underlain by common physiological processes. If the "thrifty" concept is indeed representative of an evolutionary adaptation designed to enhance survival during privation, then perhaps some ready parallels can be drawn from studies of starvation resistance. These have primarily been performed in *Drosophila*, revealing physiological plasticity which is both heritable and triggered by immediate circumstance. Starvation resistance is shown to be driven by a shift to greater metabolic frugality which involves alterations to carbohydrate and lipid metabolism, including redirection of glucose from oxidation in skeletal muscle to storage in white adipose tissue (WAT) (Dulloo *et al*., 2006; Rion & Kawecki, 2007). Phenotypic expression of this resistance is determined in part by nutrition. Relative proportion of dietary protein and carbohydrate influences both supply and demand of energy—where ingested carbohydrate promotes lipid storage, ingested protein is routed to the energetically demanding processes of lean mass maintenance—and the balance between these macronutrient intakes can impact body composition, lifespan, reproduction, and metabolism across multiple species including humans and mice as well as *Drosophila*

(Sørensen *et al*., 2008; Lee & Jang, 2014; Wali *et al*., 2021). Preferential utilisation of endogenous fuels by *Drosophila* during starvation, where lipids are prioritised for long-term deprivation, ensures that diets which contain more carbohydrate content and provide greater sequestration of lipid reserves also confer greater starvation resistance (Lee & Jang, 2014; Henry *et al*., 2020). The correlation with greater body lipid content is also evolutionary, seen outside diet-based studies (Chippindale *et al*., 1996; Ballard *et al*., 2008; Parkash & Aggarwal, 2012). The link to the TGH-based phenotype is clear.

Adaptations to privation may be generally maladaptive outside that environment. Trade-offs which are associated with evolutionary and physiological starvation resistance in *Drosophila* include reduced fecundity and slower development, as energy reserves are conserved (Chippindale *et al*., 1996; Lee & Jang, 2014). The net benefits of pathways activated during nutrient deprivation are context-dependent. Immune and inflammatory signals, for example, cannot be simply categorised (Fazeli *et al*., 2020). Transitions between adaptive starvation phases are orchestrated partially by hormonal loops including states of hypoleptinemia and hypercortisolemia (Steinhauser *et al*., 2018). Alterations to glucose and lipid metabolism are transduced in part by selective or tissue-specific modulation of insulin sensitivity (Soeters *et al*., 2012). Dysregulation of any of these pathways, outside survival-oriented starvation resistance, is detrimental. "Catch-up growth" in humans, seen when mechanisms active during nutrient deprivation persist during refeeding, is a risk factor for T2D (Dulloo *et al*., 2006; Dulloo, 2008). If starvation-induced physiological plasticity indeed comprises a potentially-maladaptive evolutionary holdover in human populations, then this may present the shared basis for the various TGH paradigms (even if a single gene or pathway is an insufficient driver). Further research may be required into relevant populations impacted by an apparent predisposition to metabolic dysfunction.

1.4.3 Pacific Islands: a case study

Modern Pacific Island (PI) populations have an evolutionary history of relative isolation, although ancestral migrations into and within the region were nevertheless incremental, complex, and debated. Oceania is typically considered to have experienced two major waves of migration: the Papuan people who, approx. 50,000 years ago, settled much of Near Oceania; and the Austronesian (AN)-speaking or Lapita people who, approx. 3,500 years ago, ultimately colonised Remote Oceania, reaching the most isolated islands of the

eastern and southern Pacific approx. 700-1000 years ago (Friedlaender *et al.*, 2008; Duggan *et al*., 2014; Isshiki *et al*., 2020). The location and timing of admixture between these waves, with modern PI groups exhibiting ubiquitous Papuan ancestry, provides the main point of contention. Phylogenetic analysis suggests extensive and bidirectional gene flow between the incoming AN people and the indigenous non-AN population of Melanesia, ancestors of both the modern Polynesian and AN-speaking Melanesian groups (Ohashi *et al*., 2006; Kayser *et al*., 2006, 2008; Issiki *et al*., 2018). Whether this admixture occurred when AN-speaking migrants initially passed through Melanesia, or in later exchanges, sums up the primary debate. Secondary expansion of admixed populations, considerably after the initial settlement of Polynesia, likely further contributed to the substantial genetic contacts between PI sub-populations (Wollstein *et al*., 2010; Delfin *et al*., 2012; Duggan *et al*., 2014; Skoglund *et al*., 2016; Hudjashov *et al*., 2018; Pugach *et al*., 2018). That these PI groups retain distinct genetic ancestries, largely isolated from any other global gene pools until more recent years, has rendered them attractive prospects for studying genetic predisposition to metabolic conditions.

Population studies in PI communities describe a significant prevalence of the metabolic syndrome. Modern public health statistics of urban or modernising Pacific groups are characterised by extreme obesity prevalence and high diabetes incidence. In American Samoa, for example, over 93% of the adult population were found to be overweight or obese, and 47% were diabetic (Maga *et al.*, 2007). These findings are reflected across the majority of PI countries and territories, with similar obesity rates reported for populations including Tonga, Tokelau, Nauru, and Niue (Kessaram *et al*., 2015). Compared to Europeans living in the same region, both adult and child Pacific peoples are reported to have as much as twice the obesity and three times the diabetes prevalence (Simmons *et al*., 2001; Defay *et al*., 2007; Chiavaroli *et al*., 2019). This is not purely a recent development: Polynesian men on Niihau surveyed in the early 1960s were distinctly overweight, hypertensive, and diabetic (Bassett *et al*., 1966). The trend to comparative metabolic ill-health is, however, worsening. Obesity prevalence in Western Samoa dramatically increased between 1978 and 1991 (Hodge *et al*., 1994); between 1980 and 2008, the rise in mean adult BMI was in some Pacific regions five times the mean worldwide increase (Finucane *et al*., 2011). Increase in mean fasting blood glucose was similarly unbalanced (Danaei *et al*., 2011).

Incidence of diabetes and obesity in these communities, although often grouped together, are however not the only factors. The increased obesity rates undoubtedly contribute to abnormal glucose tolerance but cannot wholly explain the significantly enhanced prevalence which persists after values are adjusted for BMI (Taylor & Zimmet, 1981a, 1981b; Zimmet *et al*., 1981). Measures of BMI are themselves not without some debate regarding their applicability to Polynesians, who are reported to have a higher ratio of lean mass to fat mass than do Europeans (Swinburn *et al*., 1999). It has therefore been suggested that different, ethnicity-based cut-offs should apply—paired with the argument that risk should anyway be based on associated comorbidities, not body composition alone (McAuley *et al*., 2002). In line with this concept, Maori women have been reported to exhibit higher fasting glucose and insulin levels, and lower insulin sensitivity, than European women of similar BMI and adiposity levels (McAuley *et al*., 2002). The diabetic phenotype may therefore be partially attributed to defects in insulin response, which other population-based surveys suggest are related to ethnic variability in insulin secretion capacity (Zimmet *et al*., 1979; Defay *et al*., 2007). The cause of this variation remains somewhat uncertain.

Population studies in the Pacific Islands have repeatedly shown the prevalence of diabetes and obesity in urban regions to be significantly greater than is found in rural or "traditional-living" groups. In 1980s Western Samoa, for instance, diabetes was nearly three times as prevalent in the urban population (10.1%) as the rural (3.6%), and obesity similarly more common (Zimmet *et al*., 1981); the following decade, the trend remained (Hodge *et al*., 1994). In roughly contemporary studies of Wallis Island Polynesians, the low diabetes prevalence found among rural residents (1.9% in men, 3.5% in women) became seven and four times greater for Wallisian men and women respectively living in urban Noumea (Taylor *et al*., 1983, 1985). Rural-urban differences have likewise been identified in Micronesian and Melanesian populations (King *et al*., 1984; Russell-Jones *et al*., 1990; Taylor *et al*., 1991; Furusawa *et al*., 2011). There seems, moreover, to be something of a gradient effect: among the non-AN Melanesian peoples of Papua New Guinea, circa 1989, both the semi-traditional and peri-urban groups had little diabetes incidence, but this was accompanied in the latter group by an unexpectedly high insulin response perhaps indicative of metabolic transition to glucose intolerance (King *et al*., 1989). The urbanisation effect appears further exacerbated by migration, with Polynesian migrant populations in New Zealand, Australia, and the USA reporting greater increased

prevalence of obesity and diabetes than observed in the native island population (Ostbye *et al*., 1989; McGarvey, 1991; Hawley & McGarvey, 2015). There has thus long been a consensus that the prevalence of metabolic syndrome in the Pacific Island region is likely driven primarily by introduction of urban, Westernising influences.

Specific environmental and lifestyle factors which underpin this population-level shift in metabolic health, and in particular glucose tolerance, are for the most part less comprehensively defined. Decline in physical activity, for example, has been associated with worsening health in this as in other populations (Weinstein *et al*., 1981; Taylor *et al*., 1983; King *et al.*, 1984; Hodge *et al*., 1994). Several studies in Samoa and American Samoa have explored the influence of dietary pattern. The "neo-traditional" or "mixed-modern" patterns, in adults, are associated with lower abdominal circumference and higher serum HDL cholesterol, and inversely associated with metabolic syndrome (DiBello *et al*., 2009; Wang *et al*., 2017). In contrast, the "modern" pattern—comprised mostly of imported, processed foods—is significantly positively associated with metabolic syndrome in adults and children alike (DiBello *et al*., 2009; Wang *et al*., 2017; Choy *et al*., 2020). This diet, which has become increasingly commonly consumed, is thus held to be a key contributor to obesity and non-communicable disease rates among Pacific Islanders; and a shift to healthier foods is recommended—here, as elsewhere—as a strategy to prevent metabolic syndrome. While these environmental factors may help drive the development of metabolic syndrome, and can potentially confound cohort study analyses, they cannot entirely resolve its outstandingly high prevalence in Pacific Island populations compared to other ethnicities affected by similar lifestyle influences.

The question is made additionally complex by evidence of a differentiated metabolic response between the Polynesian, Micronesian, and Melanesian communities of the Pacific Islands. Polynesian adult populations can exhibit diabetes prevalence exceeding 15%, often higher in women than men (Taylor & Zimmet, 1981a, 1981b; Kessaram *et al*., 2015; Lin *et al*., 2017). In Micronesia, a pair of 1970s studies reported that Nauru's diabetes rates were, at 34.4% and 44%, among the highest in contemporary literature (Zimmet *et al*., 1977, 1978). Melanesian peoples, however, (historically) possess comparatively low rates of non-communicable disease, with lower diabetes rates, abnormal glucose tolerance, and fasting blood glucose levels than Polynesians or part-Polynesians (Zimmet *et al*., 1982; Taylor *et al*., 1991; Defay *et al*., 2007). In the 1980s

Solomon Islands, fewer than 1% of Melanesians had abnormal glucose tolerance compared to 9.7% of Micronesians (Eason *et al*., 1987); two decades later, obesity rates remained likewise disparate between these populations (Furusawa *et al*., 2011). Even within Melanesian groups, distinctions are drawn: a non-AN-speaking cohort in Papua New Guinea displayed a high insulin response, whereas the AN-speaking sample had diabetes and severe hyperglycaemia (King *et al*., 1989). Genetic ancestry across PI populations, therefore, seems to provide an additional differentiator in metabolic health. Indeed, a recent study of genetic risk factors in Native Hawaiians at chromosomal and sub-chromosomal scales found risks of obesity and T2D to be significantly associated with Polynesian ancestry (Sun *et al*., 2021). This may be a further indicator in support of the concept that a predisposition to metabolic ill-health may be evolutionary and heritable, per theories of the thrifty genotype.

1.5 *CREBRF* R457Q Variant

A recent GWAS on a Samoan population identified an SNP strongly associated with BMI (Minster *et al*., 2016). Located at a highly conserved position within the *CREBRF* gene on chromosome 5, the SNP rs373863828 is a missense variant (Arg457Gln, R457Q) predicted to have a high probability of altering CREBRF function (Minster *et al.*, 2016). This R457Q variant produced significant dose-dependent increases in BMI and obesity risk while simultaneously reducing risk of type 2 and gestational diabetes. This intriguing phenotype is quite paradoxical, given the well-documented correlation between obesity and diabetes. Initially observed by Minster *et al*. (2016), these effects have since been recapitulated in subsequent studies.

The heightened obesity risk is primarily underlain by measured increases in BMI, but the variant has additionally been positively associated with increased body fat percentage, as well as waist and hip circumference (Minster *et al.*, 2016; Naka *et al*., 2017; Krishnan *et al*., 2018). More recently, associations with increased height and fat-free mass have also been described (Berry *et al.*, 2018; Krishnan *et al*., 2018; Metcalfe *et al*., 2020; Carlson *et al*., 2020; Arslanian *et al*., 2021; Oyama *et al*., 2021). The reduction in diabetes risk is retained even following adjustment for BMI but the causative factors are unknown. Studies have attributed the R457Q variant to (undefined) effects on glucose homeostasis, causing significantly lower fasting blood glucose levels (Minster *et al*., 2016; Krishnan

et al., 2018; Hanson *et al*., 2019). Associations with greater capacity for compensatory insulin secretion or with greater serum lipids are reported only inconsistently across cohorts and seem unlikely to comprise key mediators (Minster *et al*., 2016; Ohashi *et al*., 2018; Hanson *et al*., 2019; Krishnan *et al*., 2020; Lin *et al.*, 2020; Burden *et al*., 2021). Of note, carriers of the missense variant seem to develop their phenotypic differentiation early in life, with effects on weight, height, and waist circumference seen also in childhood (Minster *et al.*, 2016; Berry *et al*, 2018; Carlson *et al*., 2020; Arslanian *et al*., 2021; Oyama *et al*., 2021).

Strikingly, occurrence of this R457Q missense variant is tightly restricted by descent and geography. It is present in all surveyed Polynesian populations, with reported minor allele frequencies as high as 0.259 in the Samoan cohort, but virtually non-existent in individuals outside the Pacific Islands (Minster *et al*., 2016; Berry *et al*, 2018; Naka *et al*., 2017; Krishnan *et al*, 2018; Hanson *et al*., 2019; Lin *et al*., 2020). Indeed, presence of the missense variant in Native Hawaiians was found to be significantly correlated with proportion of Polynesian ancestry (Lin *et al*., 2020). Importantly to questions of phenotypic advantage, Minster *et al*. (2016) also identified evidence of positive selection at the Arg457Gln variant in Samoan genomes. This has not yet been matched in other reports, likely due in part to sample size limitations. The apparent evolutionary incentive for this *CREBRF* variant, despite its obesogenic effects, encourages closer examination to determine any potentially relevant selective pressures.

Analysis of *CREBRF* allele frequency among Pacific Island populations reveals that the R457Q variant common among modern Polynesians is present at only low frequencies in Micronesian and AN-speaking Melanesian groups, and wholly absent in non-AN-speaking Melanesians (Naka *et al*., 2017; Hanson *et al.*, 2019). The latter lack is relatively unremarkable: Polynesians have very limited genetic relation to non-AN-speaking Melanesians (Friedlaender *et al*., 2008). Both AN-speaking Melanesians and Micronesians, however, are reported to be (comparatively) genetically close to Polynesian populations (Issiki *et al*., 2018). That the minor allele frequency in these populations is low compared to the Polynesian values may imply that the R457Q variant appeared primarily among Polynesian ancestors, who had some admixture with native groups of near Oceania, but developed strength of frequency during their expansion across the Pacific (Naka *et al*., 2017; Hanson *et al*., 2019).

Some aspect of the colonisation process may therefore have acted as a positive selection force. The apparent phenotypic duality of the *CREBRF* variant, pairing obesity with diabetes protection, recalls the concept of the "thrifty gene" (as discussed above). This hypothesis would suggest that force to be feast/famine periods: the (logically) limited food resources during long sea voyages and early settlements of each newly discovered island (Minster *et al.*, 2016; Naka *et al*., 2017). Although Loos (2016) argues against the applicability of CREBRF to the finer details of Neel's original insulin-centric thrifty genotype hypothesis, the broader outline fits and it is in this framework that Minster *et al*. (2016) present their initial study. This evolutionary perspective, however, cannot yet provide any definitive answers regarding the stark absence of the *CREBRF* variant from almost all non-Polynesian populations, or the basis of the strong protection against T2D. Further inquiries into CREBRF action on a molecular as well as a systemic level will be needed to answer these important questions.

1.6 CREBRF and CREB3: in review

1.6.1 CREBRF

The cAMP-responsive element binding protein 3 regulatory (or recruitment) factor (CREBRF; originally identified as Luman recruitment factor, LRF) is a highly evolutionarily conserved bZIP protein. It is comprised of a basic region flanked by two leucine zippers, an acidic region, and an N-terminal transcriptional activation domain (as illustrated in Figure 1.1). At the amino acid level, there is more than 95% sequence identity between the human, mouse (GenBank GeneID 77128), and rat (GenBank GeneID 303016) homologs; the bZIP region in particular retains great similarity also to the orthologues that have been identified in *Drosophila melanogaster* (Tiebe *et al*., 2015) and in metazoans (Jindrich & Degnan, 2016). CREBRF mRNA transcripts are reportedly ubiquitous, but with levels that vary according to tissue type: especially high in heart and kidney, and low in the brain (Audas *et al.*, 2008). The CREBRF protein is tightly regulated, being highly unstable and prone to proteasomal degradation with a half-life of approximately 20 minutes (Audas *et al*., 2008). Protein expression is consequently difficult to survey, as levels typically fall below detection limits in the absence of proteasome inhibition and specific antibodies are moreover not commercially available (Audas *et al.*, 2008; Minster *et al*., 2016; Tiebe *et al*., 2019).

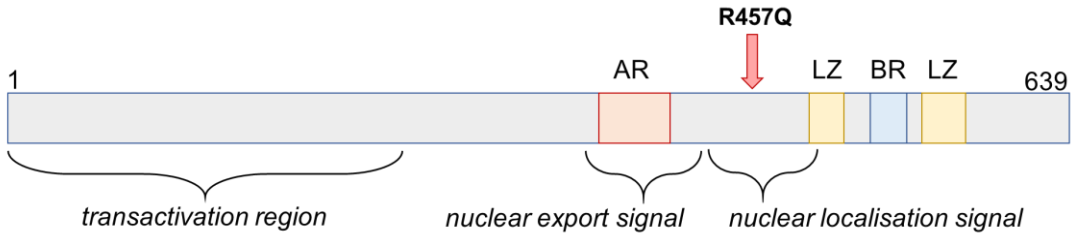

Figure 1.1: Schematic of the CREBRF protein.
Approximate location of the acidic region (AR) is indicated in red; the basic region (BR) in blue; and the leucine zippers (LZ) in yellow. Also indicated are the transcriptional activation domain as well as the locations of the hypothesised nuclear export and nuclear localisation signals. Position of the R457Q mutation is shown at the red arrow.

Initial immunofluorescence studies aiming to clarify CREBRF location and function within the cell reported that the protein was found primarily in the nucleus, where it formed discrete foci (Audas *et al*., 2008, 2016). These *in vitro* localisation efforts utilised both FLAG- and GFP-tagged CREBRF constructs, transfected into multiple cell lines, to conclude that nuclear body formation occurred under all experimental conditions, albeit with epitope tag-dependent variation in protein abundance. Indeed, these authors observed neither the wild-type CREBRF protein nor any mutant variant within the nucleus without foci formation (Audas *et al.*, 2016). Some doubt, however, has nevertheless recently been cast upon these findings: similar N-terminal epitope-tagging studies performed by another group were inconclusive, revealing mixed nuclear and cytoplasmic CREBRF localisation which varied with tag, cell line, and even from cell to cell (Tiebe *et al*., 2019; Oh-Hashi *et al*., 2021b). The cause of the discrepancy between these reports is not fully understood. The case for CREBRF function, which has been derived in great part from the earlier studies, justifies a more extended discussion of their findings despite the disagreement.

The conditions for CREBRF nuclear translocation, and consequent foci formation, are somewhat uncertain. Audas *et al*. (2016) utilised CREBRF deletion mutants to assign potential localisation sequences: distinct nuclear and sub-nuclear (foci) targeting signals within the middle region of the protein, as well as a more tentative nuclear export signal in the vicinity of the acidic region (as outlined in Figure 1.1). This theorised shuttling in and out of the nucleus implies another level of regulation for CREBRF by an as-yet unidentified factor. The equivalent mechanism in the *Drosophila* ortholog is controlled

by a 30-residue region that includes both a 14-3-3 binding site and two TORC1-sensitive phosphorylation sites, but the precise parallel is not confirmed (Tiebe *et al*., 2015). One precondition identified for the CREBRF sub-nuclear bodies, although perhaps not a trigger per se, is active transcription; pharmacological disruption of this process relocates CREBRF to the cytoplasm (Audas *et al*., 2016). Consequent speculation that mRNA templates may serve as templates for foci formation suggests CREBRF involvement with transcription activation or repression, but specificity of this regulatory activity is not fully defined.

These *in vitro* studies provided the initial evidence, on a subcellular scale, for CREBRF activity. The primary (and eponymous) function of CREBRF is to regulate activity of CREB3, a transcription factor (TF) important in cellular stress response protein folding and secretion. The direct physical interaction occurs via binding at the leucine zipper region and recruits the active, nuclear CREB3 to sub-nuclear foci. CREB3 activity is consequently reduced, firstly by sequestration away from transcriptional co-factors, and secondly by induction of its rapid turnover (Audas *et al.*, 2008, 2016). This CREBRF-mediated suppressive mechanism is not restricted only to CREB3 but has been shown to apply also to the glucocorticoid receptor (GR) as well as viral proteins (Martyn *et al*., 2012; Audas *et al*., 2016). The means by which this foci-localised degradation occurs has not been wholly elucidated but seems likely to incorporate the 26S proteasome (Baumann *et al*., 2001; Martyn *et al*., 2012). Audas *et al*. (2008, 2016) have further speculated that CREBRF foci-specific interactions might provide CREB3 (or perhaps CREBRF itself) with a separate or alternate function, likely to centre on the processes of protein (re)folding or degradation. This is not conclusively proven, however, and repression of activity remains the more definitive CREBRF foci role.

Even this key function, however, might be not uncontroversial. Oh-Hashi *et al*. (2021b) show *in vitro* that CREBRF can positively regulate CREB3 activity. The mechanism is uncertain; CREBRF did not impact CREB3 protein stability or intracellular localisation. Both the nature of the protein-protein interaction and its consequence were therefore entirely unlike previous reports. The authors suggest that the discrepancy posed by this study, which was performed in Neuro2a cells, might be due to differences in cellular context. Too few studies exist, thus far, for any more definitive conclusions. The CREBRF-CREB3 interaction, being integral to the proteins' functionality, dictates that

any review of CREBRF action should also examine CREB3. A synthetic incorporation of the latter protein's cellular and organismal activities, which have been more extensively investigated, can offer greater insights into the relatively understudied CREBRF than is otherwise feasible.

1.6.2 CREB3

The cAMP-responsive element binding protein 3 (CREB3; elsewhere identified as Luman or LZIP) is a member of the CREB/ATF family of bZIP transcription factors, sharing both structural and functional elements. More specifically it is the eponymous member of the five-member CREB3 subfamily (see Figure 1.2), which also includes CREB3-like 1 to 4 (CREB3L1-4; also identified, respectively, as OASIS, BBF2H7, CREBH, and AIbZIP). These proteins are highly conserved in their shared central bZIP domain, as indicated in Figure 1.2, but otherwise show relatively limited overall homology. Their regulation of gene transcription is primarily via binding at cAMP-responsive element (CRE) and CCAAT/enhancer-binding protein-β (C/EBPβ) sites. Although the individualised tissue expression and specific mechanics of these proteins are diverse, all CREB3 subfamily members broadly share functional roles in the context of ER and Golgi stress responses, and the regulation of cellular homeostasis (Kondo *et al*., 2011; Sampieri *et al*., 2019).

Three isoforms of CREB3 are reported: the canon protein, which comprises 371 amino acid residues in its full-length form; an atypical isoform, identical but for an additional 24-residue sequence inserted near the N-terminal; and a shortened isoform named sLZIP (for "small LZIP") which reportedly lacks a transmembrane domain. No defined three-dimensional protein structure has yet been published for the human (or rodent) CREB3 protein although certain domains and motifs have been identified. As depicted in Figure 1.2, these primary CREB3 features comprise a potent N-terminal transactivation domain, which incorporates two LxxLL motifs; a basic (DNA-binding) region; a leucine zipper; and a transmembrane domain. The full-length CREB3 is glycosylated: four potential sites for N-linked glycosylation are identifiable within the protein sequence (as noted in Figure 1.2).

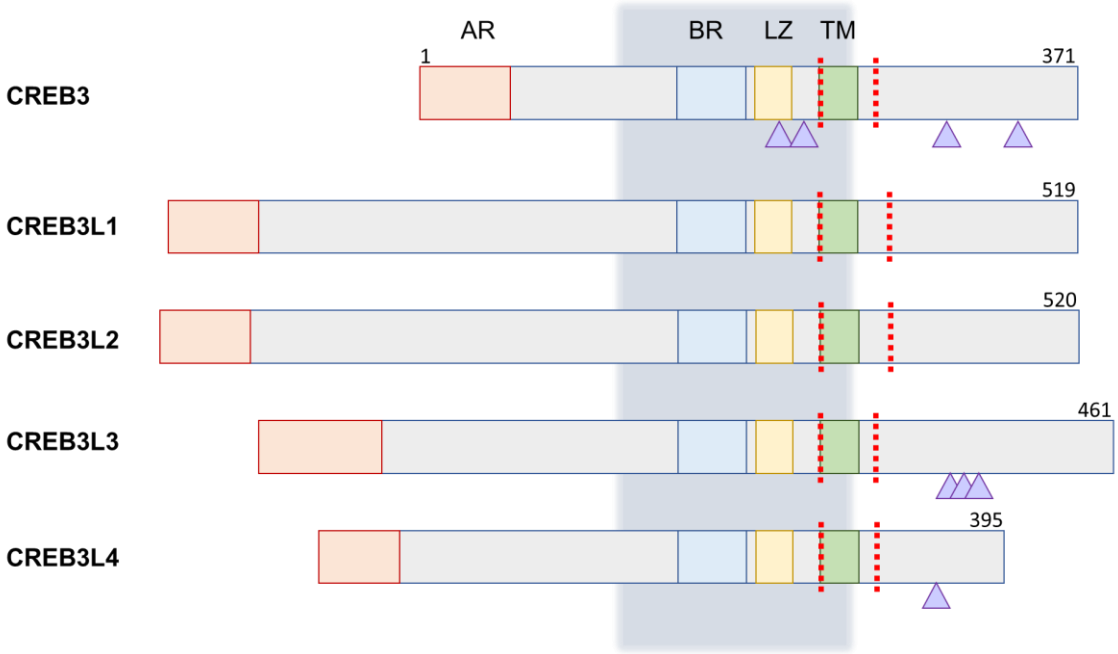

Figure 1.2: Schematics of the CREB3 subfamily of transcription factors.
The five transcription factors are here shown aligned at their homologous region, which is indicated by the grey shading and comprises a sequence of approximately 130 amino acid residues. Approximate location of the acidic region (AR) is indicated in red; the basic region (BR) in blue; the leucine zipper (LZ) in yellow; and the transmembrane region (TM) in green. Potential sites of N-linked glycosylation are indicated by purple arrowheads. Protease cleavage sites are indicated by red dashed lines.

CREB3 tissue expression, like that of CREBRF, exhibits swift protein turnover and is examined primarily at the mRNA transcript level. Mammalian *Creb3* mRNA is essentially ubiquitous, although levels are reported highest in liver and in brain tissue (Lu *et al.*, 1997; Qi *et al.*, 2009; Ying *et al.*, 2015b). CREB3 protein has more limited coverage in literature: the nuclei of central nervous system (CNS) neurons, monocytes, dendritic cells, and bone tissue-derived cell lines (Lu & Misra, 2000; Ko *et al.*, 2004; Eleveld-Trancikova *et al.*, 2010; Zeng, 2014; Kanemoto *et al.*, 2015). Expression may differ between cell maturation stages (Eleveld-Trancikova *et al.*, 2010), while post-translational modifications may also differ between cell types (Kanemoto *et al.*, 2015). Difficulties in determining protein expression may present some interpretive problems: demonstrable fluctuations in CREB3 protein levels and transcriptional activity alongside unchanging transcript levels suggest that protein degradation is, in at least some contexts, the primary regulatory mechanism (Hasmatali *et al.*, 2019).

Intracellularly, CREB3 in its full-length form is an endoplasmic reticulum (ER)-resident protein, existing as a monomer or a dimer (Nadanaka *et al*., 2007). When appropriately stimulated, the protein undergoes regulated intramembrane proteolysis prior to activity in the nucleus as a transcription factor. The proteolytic process, common among the CREB/ATF family bZIPs, entails sequential cleavage by site-1 protease (S1P) and site-2 protease (S2P) in the Golgi (as illustrated in Figure 1.2) (Raggo *et al*., 2002). The resultant active fragment, comprising 228 amino acid residues, is released for nuclear translocation. This canonical activation process seems not, however, to be strictly universal: full-length CREB3 can also act both within and without the nucleus, given alternate functions by retention of the C-terminal fragment; the truncated sLZIP isoform cannot be held within the ER membrane and so undergoes no cleavage. The divergence in processing prior to proteolysis likely represents a further fine-tuning of cellular functions.

The precise mechanistic interactions involved in CREB3 activation are currently largely undefined. Sequestration of full-length CREB3 within the ER may be mediated by the ER chaperone protein GRP78 (BiP) (Oh-hashi *et al*., 2018). Transport to the Golgi, where cleavage occurs, may be associated with the glycosylation which is identified in full-length CREB3 but lost in its proteolytic product (Hacker *et al*., 2018). Marginally more is known of S1P and S2P action. S1P cleaves CREB3 at the RxxL motif in its ER luminal domain; S2P acts within the transmembrane domain which is consequently exposed, potentially cutting as many as three sites to produce small peptide fragments derived from the segment between S1P and S2P sites (Raggo *et al*., 2002; Matsuhisa *et al*., 2020). The two cleavages require separate stimuli, as S2P action on CREB3 seems not to automatically follow cleavage by S1P (Raggo *et al*., 2002). S1P maturation is controlled by its cofactor, partner of site-1 protease (Xiao *et al*., 2020); it has been suggested that S2P may respond to cellular oxidative stress (Gu *et al*., 2014). The precise nature of these stimuli in the CREB3 context is uncertain.

1.6.3 Cell stress and protein secretion

The cellular signals which trigger CREB3 expression and activity are largely undefined. Oxidative stress may promote CREB3 activity, although the specific redox sensing mechanism outlined by Sabaratnam *et al*. (2019) is not present in the human or murine protein. CREB3 has recently been identified as a candidate component of a centralised

lipotoxicity response in *C. elegans* (Venz *et al*., 2020), although stimulation by membrane lipid disturbances has not yet been confirmed elsewhere. Lysosomal stress signals seem uninvolved (Oh-Hashi *et al*., 2019). Despite initial assumptions that the ER-resident CREB3 was heavily regulated by ER homeostasis, the stimulus is generally also thought to be distinct from canonical ER stress particularly given that the standard-use ER stressors thapsigargin and tunicamycin commonly fail to activate CREB3 *in vitro* (Chen *et al*., 2002; Nadanaka *et al*., 2007; Sanecka *et al*., 2012; Kanemoto *et al*., 2015; Kang *et al*., 2017; Oh-Hashi *et al*., 2021c). Instead, *in vitro* proteolytic activation is most consistently induced by Golgi stressors, albeit with some cell line-specific differentiation and treatment-specific effects on full-length protein which imply subtleties in the stimulating mechanism (Reiling *et al*., 2013; Kanemoto *et al*., 2015; Kang *et al*., 2017; Oh-Hashi *et al*., 2018, 2019, 2021a). Studies in human islets have independently identified *Creb3* expression in association with a common signature of Golgi stress (Bone *et al*., 2020). Overall, cellular stress signals comprise the major stimulus for CREB3 activation.

Stress-responsive CREB3 mediates the tightly regulated processes which ensure protein folding and quality control at the ER. It stimulates the transcriptional upregulation of important stress response genes, binding to unfolded protein response elements (UPRE) and/or to ER stress response elements (ERSE) within gene promoters (DenBoer *et al*., 2005). Such targets fall within both the unfolded protein response (UPR) and the ER-associated degradation (ERAD) mechanisms. These closely related ER stress-responsive signalling pathways exhibit bidirectional feedback regulation, working to enhance protein chaperone expression and promote proteasomal degradation of misfolded proteins (Dreher & Hoppe, 2018; Fun & Thibault, 2020). CREB3 is positively associated with the activity of both UPR and ERAD, shown to enhance stress-induced expression and/or activity of key proteins including, for example: the cellular homocysteine-induced ER protein (Herp); the ER degradation enhancing α-mannosidase-like protein (EDEM); and the ubiquitin segregase valosin-containing protein (VCP; p97) (DenBoer *et al*., 2005; Liang *et al*., 2006; Arora & Golemis, 2015; Singh *et al*., 2015). Endogenous CREB3 is, furthermore, itself a substrate for ERAD and proteasomal degradation which thereby provide an additional regulatory layer for CREB3 activity (Oh-Hashi *et al*., 2019, 2021c). Given the demonstrable stress-induced transcriptional regulation exercised by CREB3, and also extrapolating from the known activities of the broader CREB/ATF family in this

context, the role in ER homeostasis is commonly espoused as the protein's primary function.

The second, equally vital stress-responsive role of CREB3 is the maintenance of Golgi homeostasis. The autoregulatory Golgi stress response, which is reviewed more comprehensively by Taniguchi & Yoshida (2017), augments the apparatus' functional capacity if stress renders it insufficient. The Golgi stressor BFA, used to induce CREB3 expression and activity, acts by collapsing the Golgi and blocking secretory traffic. CREB3 subsequently upregulates the transcription of multiple genes involved in vesicle coating, delivery, tethering, and cargo selection for both anterograde and retrograde trafficking (Sanecka *et al*., 2012; Reiling *et al*., 2013; Penney, 2017; Zhang *et al*., 2017b; Howley *et al*., 2018; Penney *et al*., 2018). This increased expression of ER-Golgi transport proteins enhances secretory capacity of the cell in response to high demand. This heightened demand can be driven by cell metastasis, maturation, or differentiation, and indeed CREB3 expression is reported to be upregulated in each of these contexts and to facilitate the metastatic phenotype via trafficking effects (Eleveld-Trancikova *et al*., 2010; Kim *et al*., 2010a; Mahmoud *et al*., 2015; Howley *et al*., 2018; Hu *et al*., 2019). The UPR, which involves maximisation of protein synthesis to recover from stress, is likewise associated with greater protein secretion demand. The UPR, ERAD, and Golgi stress response arms of CREB3 function thus comprise a concerted programme to maintain ER-Golgi homeostasis.

The detrimental impacts of CREB3 deficiency emphasise its importance to the cellular stress response. *In vitro*, lack of CREB3 can stifle BFA-induced increases in ER-Golgi trafficking proteins, thereby logically increasing protein burden in the ER (Penney *et al*., 2018). Proteotoxic stress following CREB3 knockdown has been independently shown to consequently upregulate expression of ER stress indicators, protein folding chaperones, and ubiquitin-proteasome pathway genes (Hu *et al*., 2019; Zhao *et al*., 2020). That these results have been identified in glioblastoma and in murine ESCs undergoing decidualisation, both representing growth states with high demand for protein, suggests physiological relevance beyond the induced stressors of an *in vitro* system. Indeed, Penney *et al*. (2018) indicate that compromised cellular secretion capacity and resultant ER stress may account for *in vivo* dysregulation of the physiological stress response seen in CREB3-deficient mice. Suppression of CREB3 action also comprises the major

canonical target of CREBRF function, and Audas *et al*. (2008) provide *in vitro* evidence that CREBRF can consequently suppress the UPR in mouse embryonic fibroblast cells, altering the expression of key UPR proteins. Alignment between CREB3 and CREBRF activities extends beyond the cellular stress response and these intersecting functions, some derivative, are worth closer investigation.

1.6.4 CREBRF-CREB3 crosstalk and convergences

Glucocorticoid signalling represents an integral convergence between CREBRF and CREB3 activities, with functions in systemic maintenance of metabolic homeostasis. The cholesterol-derived steroid hormones signal through the glucocorticoid receptor (GR), a ligand-inducible transcription factor which acts via direct binding to glucocorticoid response elements (GREs) or via interaction with other DNA-bound factors. CREBRF and CREB3 physically interact with the GR to regulate its transcriptional activity. CREBRF acts *in vitro* as a corepressor by mediating degradation of the ligand-bound GR protein (Audas *et al*., 2008; Martyn *et al*., 2012). This interaction, like the previously described negative regulation of CREB3, occurs (*in vitro*) in discrete nuclear foci colocalised with the known GR repressor RIP140 and significantly reduces ligand-induced transactivation. CREB3 coregulation of GR activity is perhaps more complicated. Full-length CREB3 represses ligand-induced transcriptional activity by binding cytosolic GR (presumably preventing nuclear translocation) (Penney *et al*., 2018; Taylor, 2018); the sLZIP isoform provides similar negative regulation via HDAC3 recruitment (Kang *et al*., 2009; Kim *et al*., 2021b). The cleaved (N-terminal) CREB3, in contrast, binds nuclear GR (and/or target gene GREs) to activate transcription additively in the presence of GR ligands but also even in their absence (Penney *et al*., 2017; 2018). Degrees of theoretical interdependence between these combined coregulatory effects have not been speculated. Although possible that CREBRF colocalises with the GR as an incidental consequence of targeting the (bound) CREB3, the CREBRF-GR and CREB3-GR interactions *in vivo* may be independent functions if spatially or temporally separated. It is clear regardless that CREBRF and CREB3 between them manage close regulation of GR transactivation.

The interactions identified *in vitro* produce whole-body consequences *in vivo*. These have primarily been shown using CREBRF and CREB3 knockout mouse models which possess remarkably similar phenotypes ultimately underlain by (developmental)

dysregulation of hypothalamic-pituitary-adrenal (HPA) axis stress signalling. CREBRF-KO mice display a behavioural phenotype including hyperactivity, reduced anxiety-like behaviours, and impaired social recognition, which in females culminates in a maternal instinct deficit (Martyn *et al*., 2012; Frahm *et al*., 2020). This deficit is more severely present in CREB3-KO females, whose pups have a zero percent survival rate, and which show similar depressive-like behaviours (Penney *et al*., 2017). In both mouse lines these behavioural changes are accompanied by decreased circulating prolactin and/or corticosterone levels likely driven by increased GR activity associated with altered HPA axis and stress responsiveness. Larson *et al*. (in press) recently reported that genetic variation at the CREB3 locus can similarly alter behavioural stress response in purebred Yorkshire pigs. More broadly linked is the bidirectional coupling of glucocorticoid action to circadian rhythm (Caratti *et al.*, 2018; Shimba & Ikuta, 2020), which is dysregulated in CREBRF-KO mice and linked to CREB3 expression in models of adrenal disorders as well as sleep deprivation (Massart *et al*., 2014; Zhang *et al*., 2017d; Venneri *et al*., 2018; Frahm *et al*., 2020).

Penney *et al*. (2017) have theorised that the seemingly paradoxical enhancement of GR function in the CREB3-KO mice is the consequence of developmental compensation; GR activity in CREBRF-KO mice may derive directly from loss of GR degradation or indirectly from loss of CREB3 degradation (if not both). The more complex explanation may offer the better reflection: the most recent CREBRF-KO study presents the protein as a coregulator mediating GR transcriptional response, rather than purely as a corepressor (Frahm *et al*., 2020). Beyond the overt whole-body phenotypic consequences discussed here, it is feasible that the CREBRF/CREB3 association with the GR might produce additional cellular or organismal effects which are not yet explicitly linked in literature to this interaction.

CREBRF and CREB3 each play roles in early embryonic development processes. Murine reproductive systems of both sexes express CREBRF, with mRNA and protein levels in females fluctuating with oestrous cycle phase and enhanced during pregnancy (Yang *et al.*, 2013a, 2013b, 2018; Wang *et al*., 2021). CREBRF expression promotes stromal cell decidualisation, uterine receptivity and epithelial endometrial cell adhesion at implantation sites, and thereby the establishment of a maternofetal vascular connection (Yang *et al.*, 2013b; Li *et al.*, 2016; Yang *et al*., 2018). CREB3 shows similar

functionality, associated with oocyte maturation (Mahmoud *et al*., 2015), ovulation rate (Zeng, 2015), and endometrial stromal cell (ESC) decidualisation (Zhao *et al*., 2020). Both CREBRF and CREB3 seem to interact with the hormonal environment: synthesis and secretion of the sex steroid hormones oestradiol and progesterone, for example, are partially facilitated by CREB3 and induce CREBRF expression *in vitro* (Yang *et al*., 2013b; Zhao *et al*., 2016; Yang *et al*., 2018). CREB3 deficiency is associated with greater synthesis and/or secretion of testosterone in murine Leydig cells (Taylor, 2018; Wang *et al*., 2019, 2021). Female CREBRF-KO and CREB3-KO mice have lower serum prolactin, while males of the latter line have reduced testosterone (Martyn *et al*., 2012; Penney, 2017). Overarching effects on fertility seem borne out *in vivo*: litter size is reduced in mice lacking either CREBRF or CREB3, with an apparent gene dosage effect; mating pairs which are mutually homozygous for CREBRF deficiency are 100% infertile (Zeng, 2015; Penney, 2017). In this context, CREBRF and CREB3 seem to work in the same direction even if not together.

Both CREBRF and CREB3 have roles in the regulation of cell cycle progression. *In vitro,* CREBRF has been reported to promote cell proliferation; its knockdown or downregulation provokes S phase cell cycle arrest (Li *et al*., 2016; Han *et al*., 2018; Yang *et al*., 2018). In direct contrast, knockdown of CREB3 promotes cell proliferation, increasing percentage of cells in G1 phase and decreasing the percentage in S phase (Yang *et al*., 2018; Zhao *et al*., 2020; Wang *et al*., 2021). These *in vitro* effects are largely mediated by cyclins, regulated at mRNA and protein levels. Attenuation of CREBRF expression downregulates the cyclins A, B1, and D1, and CDK2 (Li *et al*., 2016; Han *et al*., 2018; Yang *et al*., 2018). CREB3 deficiency produces the opposite results, upregulating the cyclins A1, B1, B2, D2, and E, as well as CDK1 and 2 (Yang *et al*., 2018; Zhao *et al*., 2020; Wang *et al*., 2021). These studies were performed primarily in murine granulosa or endometrial stromal cells, environments predisposed to rapid proliferation under specific hormonal conditions, and may not necessarily reflect protein function in other tissue or cell types. The directly oppositional action of CREBRF and CREB3, whether mutually or incidentally coordinated, is nevertheless instructive regarding the inverse nature of their functions.

During cancer progression, CREB3 and CREBRF operate as tumour promoter and suppressor respectively, at the pivot point between autophagy and apoptosis. Their

inverse activities are reflected in reciprocal expression patterns: significantly increased CREB3 and/or significantly reduced CREBRF expression is seen in high-grade glioma, osteosarcoma, acute myeloid leukemia, gallbladder cancer, prostate cancer, and metastatic breast cancer specimens compared to controls (Jang *et al*., 2012; Kim *et al*., 2015b; Xue *et al*., 2016a, 2016b; Howley *et al*., 2018; Wu *et al*., 2019a; Wu *et al*., 2019c; Feng *et al*., 2020; Han *et al*., 2020). Tumour cell autophagy, proliferation, migration, and invasion have each been shown to be mediated by CREB3 (or sLZIP) and repressed by CREBRF expression, while the reverse is true for tumour cell apoptosis (Wu *et al*., 2019a; Feng *et al*., 2020; Kim *et al*., 2021b; Tang *et al*., 2021). Effects may be context-specific, as *in vitro* models of the reproductive environment show reversal of the CREBRF-induced autophagic effects (Yang *et al*., 2018). The involvement in metastatic progression is driven at least partially by CREB3 upregulation of ER-Golgi trafficking, which is significantly correlated with metastatic phenotype as well as reduced relapse-free and overall survival in breast cancer patients (Howley *et al*., 2018). The CREB3-CREBRF interaction in tumour cells therefore demonstrates a physiological consequence of the transport kinetics modulation, including counter-regulatory functions.

Viral infection upregulates both CREBRF and CREB3, which each exhibit antiviral activity. Indeed, the CREB3 protein was initially discovered due to its protective effects against herpes simplex virus (HSV-1) infection (Lu *et al*., 1997). The membrane-bound CREB3 precursor was found to bind and sequester human factor C-1 to prevent it from facilitating viral gene transcription and thereby HSV-1 lytic infection (Lu *et al*., 1997, 1998). By inhibiting the HIV protein Tat, CREB3 similarly attenuates the production and assembly of infectious viral particles (Blot *et al*., 2006). The role of CREBRF, although less detail is known, seems to proceed in much the same manner: sequestration of viral co-factors and repression of viral gene transcription and particle production (Audas *et al*., 2016). Despite this apparently cooperative antiviral action, however, CREB3 has also been implicated in the viral reactivation process (Lu and Misra, 2000). As such, Yadavalli *et al*. (2020) recently termed it a pro-viral host protein which mediated ER stress-induced (viral) protein synthesis. Some of its known transcriptional targets (e.g., p97/VCP, ARF4) also have pro-viral roles (Farhat *et al.*, 2016; Zhang *et al*., 2017b; Carissimo *et al*., 2019). This may suggest a dual role for CREB3, where the cytoplasmic full-length protein is anti-viral but the nuclear cleaved protein, as an active TF strongly linked to protein

synthesis and trafficking, is pro-viral. The interaction between CREB3 and CREBRF in this context, direct or indirect, is unclear.

Immune cell function is influenced by CREB3 signalling but has not been connected to CREBRF. Monocytes and dendritic cells have particularly evident CREB3 protein expression (Lu *et al*., 2000; Eleveld-Trancikova *et al*., 2010). In the latter professional antigen-presenting cells, CREB3 expression is induced by receptor activator of nuclear factor κ-B ligand (RANKL) signalling, functioning as a dendritic cell survival and maturation factor (Kanemoto *et al*., 2015). CREB3 transcriptionally upregulates the dendritic cell-specific transmembrane protein (DC-STAMP), which is stabilised and localised through interaction with CREB3, and is critical to dendritic cell immune function (Eleveld-Trancikova *et al*., 2010). CREB3 is further implicated in monocyte cell migration via chemokine signalling. The cleaved CREB3 increases transcription and protein expression of chemokine receptors (e.g. CCR1, CCR2, CXCR4) (Sung *et al*., 2008; Kim *et al*., 2010a). The full-length CREB3 directly interacts with CCR1 at the plasma membrane to enhance leukotactin-1-induced chemotaxis via the NF-κB pathway (Ko *et al*., 2004; Jang *et al*., 2007a, 2007b). This signalling pathway is at least partially subject to positive feedback: full-length CREB3 expression dose-dependently enhances NF-κB-mediated gene activation; among the genes consequently upregulated is *CREB3* (Jang *et al*., 2007a, 2007b; Kim *et al*., 2010a; Torres-Odio *et al*., 2017). The lack of any clear CREBRF link to immune cell function may be due simply to the absence of published studies in that context, rather than an absence of function.

CREB3 has neuronal functions which are primarily reported in the context of regenerative axon growth. Axonally synthesised and activated in response to nerve injury, CREB3 acts as a retrograde injury signal, able to transduce stress signals from the injury site to the cell body and consequently stimulates axonal elongation (Ying *et al*., 2014, 2015a; Hasmatali *et al*., 2019). The injury-induced UPR is mediated by CREB3 and consequently stimulates biosynthesis of cholesterol which is required for sensory axon outgrowth (Ying *et al*., 2015a). The association is corroborated *in vivo*: CREB3-deficient mice have altered hippocampal structure including truncated dendrites (Penney, 2017). This truncation is associated with reduced expression of BDNF, a neurotrophin critical to induction of the regeneration response in sensory neurons (Penney *et al*., 2018). Penney (2017) theorised that CREB3 may alter neurogenesis and neuron survival via modulation

of GR activity. Nerve injury increases circulating levels of endogenous corticosterone (rodents) and cortisol (humans), and such increases are demonstrated to regulate dendritic morphology, hippocampal volume, and increase neurite growth through GR-dependent mechanisms (Wooley *et al*., 1990; Tata and Anderson, 2010; Jafari *et al*., 2012; Lerch *et al*., 2017). There is no known association with CREBRF, although it too is expressed in the relevant tissues. These pro-growth neuronal activities seem to represent another facet of the established CREB3 roles in both ER stress and glucocorticoid signalling.

1.6.5 Cellular bioenergetics and systemic energy metabolism

CREBRF is implicated in cellular and organismal bioenergetics as a starvation response factor connected to the highly conserved mammalian target of rapamycin (mTOR) signalling pathway. The mTOR protein is the eponymous component of two separate complexes, mTORC1 and mTORC2, with central regulatory roles in growth and metabolism in response to nutrients or growth factors. *In vitro*, nutrient starvation has been shown to induce rapid significant increases in *Crebrf* mRNA levels in a mouse adipocyte model; the inhibition of mTORC1 alone by rapamycin treatment induces weaker (and tardier) increases in multiple cell types (Minster *et al*., 2016; Tiebe *et al*., 2019). The implication is that this CREBRF response to nutrient deprivation follows mTORC1-independent cell stress signalling, to which it is particularly sensitive, in addition to signals mediated by mTORC1 itself. The effect is protective: CREBRF overexpression in the same model significantly reduced cell death rate (vs. controls) within the first 6 hours of nutrient starvation, with improvements in cell survival retained through 24 hours of starvation (Minster *et al*., 2016).

Supporting these findings, Tiebe *et al.* (2015) have reported that the *Drosophila* ortholog REPTOR is similarly induced by starvation, and aids survival during nutritional stress: in *REPTOR*$^{-/-}$ flies, diluted food concentration had 50% lethality. *Drosophilae* exhibit a direct relationship between TORC1 inhibition and consequent REPTOR nuclear translocation and activity. REPTOR, complexed with its binding partner REPTOR-BP, is a key mediator of the downstream transcriptional response triggered by TORC1 inhibition. This transcriptional programme acts as a metabolic brake, decreasing protein and lipid synthesis, increasing autophagy, and consequently blunting growth and proliferative capacity. Indeed, obesity and growth defect phenotypes seen in TORC1 loss-of-function models can be rescued by REPTOR knockout. Although this TORC1-

REPTOR signalling pathway may not be wholly replicated in the mammalian context, the physical association between CREBRF and Crebl2 (the REPTOR-BP ortholog) has been reported in mice (Tiebe *et al*., 2019). The recapitulated protection against nutrient deprivation further suggests that any other potential parallels are also due consideration.

CREBRF protection against starvation is suggested to be linked to (perhaps longer-term) effects on energy storage. *CREBRF*-KO mice have significantly lower body weight than WT for both sexes (Martyn *et al*., 2012); *REPTOR*-KO flies are similarly leaner, with less TG/weight and less glycogen/protein content than WT (Tiebe *et al*., 2015). This whole-body phenotypic effect seems at least partially underpinned by an altered transcriptional programme. *In vitro*, CREBRF expression is induced by adipogenesis and can in turn induce adipogenic marker expression in an adipocyte cell line, suggesting that the protein can enhance storage of lipid content (Minster *et al*., 2016). It promotes ATP production, basal glycolysis, and both basal and maximal respiration levels (Minster *et al*., 2016). *REPTOR*-KO flies show downregulation of gluconeogenesis and TG biosynthesis genes, paired with upregulation of genes involved in lipid and glycogen breakdown, in addition to the aforementioned effects on genes downstream of TORC1 (Tiebe *et al*., 2015). This role in mediating glucose and lipid storage, utilisation, and metabolism seems to align with the mammalian *in vitro* model. The CREBRF involvement in nutrient homeostasis nevertheless requires further study to elucidate these effects beyond the two extant reports as described here.

Unlike CREBRF, CREB3 is not explicitly involved with the starvation response per se but has nevertheless been peripherally implicated in hepatic nutrient metabolism. Regulatory roles in hepatic gluconeogenesis have been suggested for both the canonical (cleaved) and the sLZIP isoforms (Zeng, 2015; Kang *et al.*, 2020). The latter isoform has the more convincing connection: Kang *et al*. (2020) show that starvation-induced sLZIP expression promotes gluconeogenic enzyme expression and glucose levels in human liver cells and murine primary hepatocytes; and, *in vivo*, show abnormal blood glucose homeostasis in sLZIP transgenic mice. Observations regarding the canonical CREB3 were made primarily in CREB3-deficient mice, which (in contrast) exhibit increased fasting blood glucose concentration, without any significant change to insulin or glucose tolerance, and perhaps therefore indicate an opposite effect to sLZIP (Zeng, 2015; Penney, 2017). Molecularly, CREB3 may also be involved in mediating (nutrient-

sensitive) upregulation of *Foxo1*, *Sirt1*, and *Glut1* transcripts in response to high fat or high glucose (Penney, 2017). The role of CREB3 in lipid metabolism is not clearly delineated. Penney (2017) reports that it can mediate HFD-induced increases in lipid-related genes including acetyl-CoA synthetase 2, which catalyses formation of malonyl-CoA for local regulation of the mitochondrial enzyme carnitine palmitoyltransferase I in the prelude to β-oxidation. CREB3 also stimulates transcription of apolipoprotein A-IV (ApoA4), which is likewise highly expressed in steatotic liver and can increase secretion rates to reduce hepatic lipid burden (VerHague *et al*., 2013; Cheng *et al*., 2016; Kang *et al*., 2017). Further associations between CREB3 and hepatic glucose or lipid metabolism are unknown.

Systemic effects of CREB3 functions may ultimately impact body composition. Both canonical CREB3 and sLZIP are implicated in adipose, muscle, and bone differentiation. Endogenous CREB3 stimulates osteoclastogenesis (Kanemoto *et al*., 2015); CREB3-interacting proteins DC-STAMP and RANKL are closely involved in bone resorption and remodelling (Miyamoto, 2006; Chiu *et al*., 2017; Park *et al*., 2017a). sLZIP can suppress myogenic gene expression (An *et al*., 2014); it represses PPARγ2 and enhances Runx2 transcriptional activity, thereby suppressing adipogenesis and promoting osteogenesis (Kim & Ko, 2014). Mice overexpressing sLZIP show greater bone mass and mineral density, faster bone formation, and reduced fat mass (Kim & Ko, 2014; Kim *et al*., 2020). CREB3-KO mice seem to possess the opposite associations: they are likewise reported to lack (perhaps any) visceral fat content (Penney, 2017), accompanied by severe reductions in body weight compared to WT animals (Zeng, 2015). It has been suggested that this leanness phenotype may derive from dysregulation of energy balance in the CNS, and particularly appetite/satiety signalling. CREB3 targets include ApoA4 and FoxO1, both of which are able to regulate hypothalamic POMC neurons to suppress or promote food intake (Kim *et al*., 2006; Shen *et al*., 2008). Bienvenu *et al*. (2020) suggested CREB3 as a candidate gene involved in anorexia nervosa aetiology, part of a neuron differentiation and dopamine signalling pathway.

There is little to no explicit overlap between CREBRF and CREB3 activities in systemic energy metabolism. Although both proteins seem to be involved in homeostatic responses to nutrient availability, current knowledge would suggest that they address different facets. Where CREBRF is primarily associated with mTORC1 signalling, CREB3 has

roles in hepatic glucose and lipid metabolism. With the tentative exception of the *in vitro* adipocyte model, where it is linked to adipogenesis, CREBRF has not yet been shown to act in tissue differentiation. The distinct phenotypic similarities between CREB3-KO and CREBRF-KO mouse models, particularly in the reduced weight and fat mass which are seen in both lines, do nevertheless leave open the possibility that CREBRF may also act (even if only indirectly) in the fat-muscle-bone axis as shown for CREB3. A cohesive model which draws together these disparate associations, seen at molecular and tissue as well as whole-body levels, remains to be defined for the conjunction of CREBRF, CREB3, and systemic energy metabolism.

1.7 CREBRF variant: phenotype, interactions, theories

1.7.1 Summary of literature

Knowledge of the molecular interactions and/or functions of the CREBRF R457Q variant protein is limited. The 3T3-L1 mouse adipocyte model used by Minster *et al*. (2016), transfected to overexpress either wildtype or variant CREBRF, remains the sole (published) study into the cellular bioenergetic context. The variant protein was observed to alter cellular energy storage, with slightly weaker expression of adipogenic markers but significantly greater lipid/TG accumulation than the WT protein (Minster *et al*., 2016). Cellular energy usage was also differentially impacted: measures of mitochondrial respiration, ATP production, and basal glycolysis were increased by the WT but decreased by the variant overexpression (compared to empty vector controls) (Minster *et al*., 2016). This apparent cellular shift towards a "thriftier" phenotype, increasing storage and decreasing usage of energy, reflects the broader phenotype and the TGH. Indeed, the overexpressed CREBRF conferred protection against cellular nutritional stress (Minster *et al*., 2016), although the WT and variant proteins produced similar effects when it might have otherwise been expected that the variant would further promote survival. This could, potentially, be due to the model: protein overexpression may force effects to artificially hit their ceiling, masking any differentiation that is due to, for example, an altered half-life.

But the precise molecular mechanisms underlying the bioenergetic shift which is seen with variant CREBRF activity are uncertain. Nor is it known whether the effects seen in Minster *et al.* (2016)'s adipocyte model are also visible in other cell or tissue types, or

indeed *in vivo*. Further research is required to determine what other CREBRF actions, whether effected independently or via CREB3, are impacted by this mutation (and what else is impacted in turn) on organismal and/or molecular scales. Extant theories are nearly wholly speculative in nature: the mutated residue may impact intracellular localisation, altering longevity of CREBRF nuclear activity; it may impact protein turnover and half-life, whether positively or negatively. Considering what we know of CREBRF functions more broadly, some aspects warrant closer attention as possible candidates for variant action. These include cell stress, glucocorticoid signalling, and the starvation response.

1.7.2 Cell stress signalling

The CREBRF missense variant could potentially interact with the cellular ER, Golgi, or oxidative stress responses. The connection is primarily theoretical. Facilitation of these signalling pathways, which seek to restore homeostasis following insult, comprises the main known function of CREB3 (Reiling *et al*., 2013; Kanemoto *et al.*, 2015; Kang *et al*., 2017; Oh-Hashi *et al*., 2018, 2019; Bone *et al*., 2020). This function is further shown to be at least partially regulated, presumably indirectly via action on CREB3, by the WT CREBRF protein (Audas *et al*., 2008). Dysregulation of CREB3 will compromise protein folding and cellular secretory capacity, increasing protein burden and ER stress, and CREBRF (over)activity can likewise suppress the stress response (Audas *et al*., 2008; Penney *et al*., 2018; Hu *et al*., 2019; Zhao *et al*., 2020). It is therefore logically feasible that any variant-induced alterations to CREBRF action might impact these outcomes.

Cellular stress signalling is furthermore associated with obesity and diabetes pathogenesis. This is particularly true of ER stress, which is heightened by chronic hyperglycaemia and hyperlipidemia conditions to produce an adverse cellular environment in multiple tissues, as reviewed more comprehensively elsewhere (Fernandes-da-Silva *et al*., 2021). Briefly, ER stress in liver and adipose contributes to inflammation and IR, while in the pancreas it can impair insulin synthesis and induce β-cell apoptosis (Back & Kaufman, 2012; Cnop *et al*., 2012; Rocha *et al*., 2016). Alleviation of ER stress in diet-induced obese or diabetic mice can improve systemic insulin sensitivity and glucose tolerance as well as enhancing insulin action specifically in liver and adipose tissues (Ozcan *et al*., 2006; Zanotto *et al*., 2016; Wang *et al*., 2018). These links between CREBRF, cellular stress, and diabetes pathogenesis may provide grounds

for a speculative further link between these three factors and the CREBRF missense variant association with protection against diabetes.

1.7.3 Glucocorticoid signalling

The mechanistic basis underlying the effects of the CREBRF variant on whole-body metabolism could involve glucocorticoid regulation. Although the variant protein has not itself been explicitly connected, both CREBRF and CREB3 impact glucocorticoid signalling via interactions with the GR (as outlined above). There is furthermore a logical thematic link: glucocorticoids are critical to systemic energy metabolism, regulating glucose supply to ensure survival under stress and starvation conditions. Glucocorticoids also play roles in, for example, immune cell function, reproductive or gonadal function, hepatic glucose homeostasis, musculoskeletal physiology, and neural signalling, processes also broadly linked to the WT CREBRF and/or CREB3.

Chronic glucocorticoid imbalance produces pathophysiological conditions (e.g., Cushing syndrome, Addison's disease, steroid diabetes mellitus). Peripheral glucocorticoid metabolism is seen to be altered under conditions such as genetic obesity and acute HFD exposure (Drake *et al*., 2005). Chronic glucocorticoid exposure has been seen to result in central obesity, muscle atrophy, hyperglycaemia, IR, suppressed BAT function, and reduced bone mineralisation and mass, among other features of a perturbed energy metabolism (Tanaka *et al*., 2017; Thuzar *et al*., 2018). The reverse associations have also been proven: GR genetic ablation and/or pharmacological inhibition, even when tissue-selective, can demonstrably improve systemic insulin sensitivity and glucose tolerance, as well as attenuate the weight gain and altered body composition induced by HFD (Zinker *et al*., 2007; Shimizu *et al*., 2015; Cooper *et al*., 2016; Mueller *et al*., 2017; Kroon *et al*., 2018). A closer examination of these facets in individuals possessing the CREBRF variant may aid any theorising as to the relationship between that variant and GR signalling.

1.7.4 Starvation response

The starvation response, in which both WT and variant CREBRF appears to play a role, is especially integral to speculation of missense variant function. Periods of fasting initiate a homeostatic response to maintain glucose supply which is essential to meet whole-body energetic requirements. In the liver, the initial stages of this response are defined by glycogenolysis and gluconeogenesis which serve to release new glucose into

circulation. These glucose levels are maintained in part by diminished uptake in muscle and adipose tissues, and by the transition in muscle and liver from glucose to FAs (released by adipose lipolysis) and, ultimately, to ketone bodies as the major fuel source. As precursor stores become progressively depleted, further glucose synthesis uses carbons sourced from lipolysis-derived glycerol and from proteolysis-derived amino acids. Given that uninhibited breakdown of protein will inevitably produce loss in function, including reduced muscle mass, the body's secondary priority during fasting is the preservation of protein mass.

The signalling cascades which regulate tissue responses to feeding, fasting, and refeeding are in large part governed by pancreatic hormones insulin and glucagon. The dysregulated secretion and action of these circulating hormones, as is seen in diabetes, contributes to the metabolic derangements in the condition which is perhaps typified by abnormal fuel usage. The CREBRF missense variant is strongly associated with protection against diabetes as well as with nutrient response (Minster *et al*., 2016; Krishnan *et al.*, 2018; Hanson *et al*., 2019; Krishnan *et al*., 2020). Perhaps these aspects of CREBRF function share a more direct connection than is yet understood in the current literature, which might therefore allow some elucidation of the mechanisms underlying whole-body variant effects.

Intracellularly, the starvation response proceeds via specific transcription factors to induce and maintain the requisite gene expression programmes. The precise positioning of the starvation-induced CREBRF, whether the wild-type or the variant, in this molecular context is uncertain. The WT protein reportedly acts (with Crebl2) downstream of mTORC1 inhibition following nutrient deprivation (Tiebe *et al*., 2015; Minster *et al*., 2016; Tiebe *et al*., 2019), but the nature of the missense variant interaction is unknown. The potential for tissue specificity in such as CREBRF variant response has likewise not been ascertained. If CREBRF indeed affects other, more central starvation factors in mediating the post-mTORC1 fasting response, then perhaps potential molecular interactions and signalling pathways may be more conclusively discerned. These might then allow more informed theorising as to the missense variant impact.

1.8 Conclusion

Human studies have identified the *CREBRF* R457Q variant as a major driver of excessive weight gain and/or lean mass growth in Pacific Island populations (Minster *et al*., 2016; Naka *et al*., 2017; Krishnan *et al*., 2018; Arslanian *et al*., 2021). Although the wildtype CREBRF protein has been linked to nutrient homeostasis and the starvation response, as well as glucocorticoid and cell stress signalling, current literature cannot answer whether these functions might be altered for carriers of the variant protein. With the notable exception of the initial Minster *et al.* (2016) 3T3-L1 adipocyte overexpression model, very few published studies have investigated the action of the CREBRF R457Q variant at the molecular level in either *in vitro* or *in vivo* contexts.

The current project therefore aims to address this gap in the literature using a novel mouse model where the CREBRF R458Q missense variant has been knocked in to replace the endogenous CREBRF on an FVB/N background. We wish to characterise, firstly, the whole-body metabolic phenotype of the variant knock-in (KI) mouse model; and, secondly, any molecular pathways impacted by variant function. The latter focus will be approached via the tissue transcriptome, biomolecule and protein expression, and *in vitro* signalling in a primary hepatocyte model. Characterisation of this novel animal model is expected to permit a better understanding of how obesity develops in many Polynesian individuals and the metabolic link to risk of diabetes.

CHAPTER 2: General Methods

Detailed methods specific to each study can be found in the methods section for the relevant chapter. General techniques common to multiple chapters are detailed below.

2.1 Animal Studies

CREBRF Arg458Gln gene variant mice were generated by MEGA Gene Engineering Facility (Moss Vale, NSW) via CRISPR/Cas9 technology. Sequences are provided in Table 2.1, indicating the substitutions made. Mouse genotyping was performed externally by Garvan Molecular Genetics (Garvan Institute of Medical Research) via real-time PCR in a 384-well plate format using a LightCycler 480 (Roche Diagnostics, IN, USA) combined with Sito9-based High Resolution Meltcurve (HRM) analysis. PCR conditions and primer sequences are given in Tables 2.2 and 2.3.

All animal experiments were conducted in accordance with National Health and Medical Research Council (NHMRC) and Animal Care and Ethics Committee (ACEC) guidelines and performed under UNSW ethics numbers 15/48B or 18/78A.

Table 2.1: *CREBRF* R458Q sequences used in generation of the variant mouse line.

	Nucleobase sequence*
Crebrf-R458Q WT	GTTATGAAAATGACTCTGTAGAGGACTTGAAG GAGATGACGTCCATATCTTCTCGGAAGAGAGG GAAAAGAAGGTACTTCTGGGAGTATAGTGAGC AGCTTACACCATCACAGCAAGAGAGGATTCTG AGGCCTTC**T**GAGTGGAATC**G**AGATACCTTGCC AAGTAATATGTACCAGAAAAATGGCTTACATC ATG
Crebrf-R458Q Δ MUT	GTTATGAAAATGACTCTGTAGAGGACTTGAAG GAGATGACGTCCATATCTTCTCGGAAGAGAGG GAAAAGAAGGTACTTCTGGGAGTATAGTGAGC AGCTTACACCATCACAGCAAGAGAGGATTCTG AGGCCTTC**C**GAGTGGAATC**A**AGATACCTTGCC AAGTAATATGTACCAGAAAAATGGCTTACATC ATG

*Sequences shown are selected portions surrounding the two single base substitutions (T>C & G>A), as indicated in red.

Table 2.2: PCR conditions used for mouse genotyping.

STEP	TEMPERATURE	TIME
Initial Denaturation	94°C	10 s
Amplification (30 cycles)	94°C 65 – 55°C 60°C	10 s 30 s 1 min/kb
Final Extension	72°C	3 min
Hold	4 – 10°C	

Table 2.3: *CREBRF* primer sequences used in mouse genotyping (WT vs HOM).

Forward primer	GGATTCTGAGGCCTTCTGA
Reverse primer	CCTCTTACCATGATGTAAGCCA
PCR product size	~85 Bp

2.1.1 Animal housing and diets

Animals were maintained on either a standard control "chow" rodent diet (71% of calories from carbohydrate, 8% calories from fat, 21% calories from protein, ~3 kcal/g; Gordon's Specialty Stock Feeds, Yanderra, NSW, Australia), or high fat diet (HFD) made in-house as previously described (45% kcal from fat; 4.7 kcal/g; based on rodent diet D12451, Research Diets, USA; Turner *et al*., (2007)). HFD macronutrient content is described in Table 2.4. Mice were housed in a temperature-controlled room (22 ± 1°C) on a 12/12 hr light/dark cycle, monitored weekly, with *ad libitum* access to food and water. Cages were mixed-genotype, and genotype-specific food intake was therefore not directly measured.

Mice were culled by cervical dislocation either in a fed state or following a 15-16 hr overnight fast. The latter period was of a duration chosen to ensure significant shifts in nutrient handling and metabolism, including a state of glycogen depletion (Jensen *et al*., 2013). Tissues were collected in a timely manner, weighed, and immediately freeze-clamped and snap-frozen in liquid nitrogen. Blood was collected from cardiac puncture or as trunk blood at the time of cull into tubes containing trace amounts of tripotassium ethylenediaminetetraacetic acid (K3-EDTA) (Sarstedt) and stored on ice before being centrifuged at 2,000 g for 5 min at 4°C. The top layer of plasma was carefully collected into a fresh tube and stored at -80°C along with other tissues.

Table 2.4: Macronutrient composition of the in-house HFD.

	(g/kg)
Lard	220
Safflower Oil	30
Cornstarch	170
Sucrose	202
Casein	230
Methionine	3
Choline Bitartrate	4
Gelatin	20
Wheat Bran	50
Vitamin Mix§	13
Mineral Mix§	45
Trace Mineral Mix#	13

§ Vitamin and mineral composition as per AIN-76 rodent diet standard (AIN, 1977) with the exception of subsequently recommended modifications (Reeves, 1989), used as commercially available mixtures (MP Biomedicals). # Trace Mineral Mix (MP Biomedicals, Cat # 0296026401).

2.1.2 Body composition analysis

Total body fat mass and lean mass in mice was measured using nuclear magnetic resonance with the EchoMRI-900 Body Composition Analyzer (EchoMRI Corporation Pty Ltd, Singapore). Calibration was performed using a canola oil standard. Percentage fat or lean mass was calculated according to total body weight measured on the day. Naso-anal length was measured using a ruler in mice under isoflurane anaesthesia.

2.2 Biochemical Analyses

2.2.1 Sample homogenisation

Freeze-clamped muscle tissue was powdered prior to analysis using a Cellcrusher tissue pulveriser (Cellcrusher, Cork, Ireland), which was maintained at below freezing temperatures using liquid nitrogen to prevent thawing of samples.

All liver and muscle tissues were homogenised in ice-cold lysis buffer (20 mM Tris-HCl [pH 7.4], 150 mM NaCl, 1% nonidet NP-40, 10 mM EDTA, 1 mM ethylene glycol-bis(β-aminoethyl ether)-N,N,N’,N’-tetraacetic acid [EGTA], 10 mM sodium pyrophosphate [$Na_4P_2O_7$], 10% glycerol) supplemented with protease and phosphatase inhibitors (100

mM sodium fluoride [NaF], 2 mM sodium orthovanadate [Na_3VO_4], 4 µg/mL leupeptin, 100 µg/mL phenylmethylsulfonyl fluoride [PMSF], 4 µg/mL aprotinin, 1 µg/mL pepstatin, 30 µM ALLN). Liver tissue was powdered using a rotor-stator homogeniser. Powdered muscle tissue was homogenised using a Precellys 24 homogeniser (Bertin Technologies, France) at 6,500 g for 30 s and subsequently nutated for 1 hr at 4°C. Following nutation, lysates were centrifuged at 13,000 g for 10 min at 4°C and the supernatant retained.

2.2.2 Determination of protein content

Total protein content was quantified using the Pierce BCA protein assay kit (Thermo-Fisher Scientific, USA) as per manufacturer's instructions. All samples were incubated with BCA reagent for 20 min at 37°C before relative absorbance was measured at 570 nm on a microplate reader (iMark™, Bio-Rad Laboratories, CA, USA). Total protein concentration was calculated from a bovine serum albumin (BSA; 0-1 mg/ml) standard curve.

2.2.3 Immunoblotting

Sample lysates were diluted to appropriate concentrations (20-40 µg of protein) and denatured in Laemmli sample buffer (10% glycerol, 8 mM Tris-HCl, 1% sodium dodecyl sulphate [SDS], 0.02% bromophenol blue, 5% 2-mercaptoethanol) at 37°C for 30 min. Samples were resolved on tris-based SDS-PAGE electrophoresis prepared using a Bio-Rad Criteron system alongside a molecular weight marker (Kaleidoscope Plus prestained standards, Bio-Rad) to confirm molecular weight of proteins of interest. Gel recipes are described in Table 2.5. Gels were run at 130 V for 90-110 min and proteins were transferred onto a polyvinylidene difluoride (PVDF) membrane (Immobilon-P, EMD Millipore, MA, USA) at 4°C at 65 V for 2 hr or 16 V for 16 hr.

Transferred membranes were blocked in Tris buffered saline with 0.1% Tween-20 (TBST) and 5% skim milk solution for 1 hr at room temperature (RT). Membrane sections were incubated with primary antibody (as specified in Table 2.6) diluted 1:1000 in primary antibody solution (1% BSA w/v, 0.5% Phenol Red v/v, 0.1% Tween 20 v/v, 3.1 mM sodium azide in tris-buffered saline [TBS]) at 4°C on a rotator overnight. Following incubation, excess primary antibody was removed from the membranes by repeated washes in TBST before incubation in the appropriate secondary antibody (specified in Table 2.6) diluted 1:10,000 in TBST and 5% skim milk solution for 1 hr at RT. After

several washes in TBST, immunolabelled proteins were detected using a chemiluminescence reagent (Clarity Western ECL Substrate, Bio-Rad) and imaged using a ChemiDoc MP (Bio-Rad). Intensity of bands was quantified using ImageJ 1.52a densitometry software (NIH, MD, USA). When necessary, membranes were stripped with 0.5 M NaOH, then blocked and probed with a new primary antibody.

Table 2.5: Gel recipes used for immunoblotting.

	10- and 15-well		**18- and 26-well**	
Separating buffer (per gel)				
	8%	**10%**	**7.5%**	**10%**
H_2O	3.95 ml	3.6 ml	4.5 ml	4.73 ml
40% Acrylamide	1.5 ml	1.88 ml	1.82 ml	3.29 ml
1.5 M Tris pH8.8	1.9 ml	1.88 ml	-	-
10% SDS	75 µl	75 µl	-	-
10% APS	75 µl	75 µl	182 µl	246 µl
TEMED	4.5 µl	3 µl	18 µl	24.3 µl
2% Bis	-	-	1.0 ml	1.81 ml
4x separating buffer (stock)	-	-	2.5 ml	3.38 ml
Stacking buffer (per gel)				
H_2O	2.175 ml		2.5 ml	
40% Acrylamide	375 µl		600 µl	
1.5 M Tris pH6.8	375 µl		-	
10% SDS	30 µl		-	
10% APS	30 µl		100 µl	
TEMED	3 µl		10 µl	
2% Bis	-		320 µl	
4x stacking buffer (stock)	-		1.5 ml	

APS (ammonium persulphate); TEMED (Tetramethylethylenediamine). 4x separating and stacking buffers made in-house.

Table 2.6: Antibodies used for immunoblotting

Antibody	MW (kDa)	Secondary Antibody	Supplier	Catalogue Number
Phospho-Acetyl-CoA Carboxylase (Ser79)	280	Rabbit	CST	3661
Phospho-Akt (Ser473)	60	Rabbit	CST	9271
Phospho-Akt (Thr308)	60	Rabbit	CST	2965
Akt	60	Rabbit	CST	9272
β-actin	43	Mouse	SCBT	sc-47778
Phospho-β-Catenin (Ser552)	92	Rabbit	CST	5651
CD36	88	Rabbit	SCBT	sc-9154
Phospho-CREB (Ser133)	43	Mouse	CST	9196
FATP1	63	Rabbit	SCBT	sc-25541
Phospho-FoxO1 (Ser256)	82	Rabbit	CST	9461
FoxO1	78-82	Rabbit	CST	2880
GAPDH	37	Rabbit	CST	2118
Phospho-Glycogen Synthase (Ser641)	85-90	Rabbit	CST	3891
Glycogen Synthase	84	Rabbit	CST	3886
Phospho-GSK3α/β (Ser21/9)	46, 51	Rabbit	CST	9331
GSK3α/β	46, 51	Rabbit	CST	5676
HSP70	72,73	Rabbit	CST	4872
Phospho-IGF-1 Receptor β (Tyr1135/1136)/Insulin Receptor β (Tyr1150/1151)	95	Rabbit	CST	3024
Insulin Receptor β	95	Rabbit	CST	3025
Phospho-IRE1 (Ser724)	110	Rabbit	Abcam	ab48187
Phospho-mTOR (Ser2448)	289	Rabbit	CST	5536
Total OXPHOS Rodent WB cocktail	***a***	Mouse	Abcam	ab110413
Phospho-p44/42 MAPK (Erk1/2) (Thr202/Tyr204)	42, 44	Rabbit	CST	4377
Phospho-PKA C (Thr197)	42	Rabbit	CST	5661
PKA C-α	42	Rabbit	CST	4782
Phospho-PRAS40 (Thr246)	40	Rabbit	CST	2997
Smad2/3	52, 60	Rabbit	CST	8685
TXNIP	55	Rabbit	CST	14715
VDAC	32	Rabbit	CST	4866
pan 14-3-3 (K19)	27	Rabbit	SCBT	sc-629
Secondary Antibodies				
Anti-rabbit IgG produced in goat, HRP-linked			CST	7074
Anti-mouse IgG produced in horse, HRP-linked			CST	7076

a OXPHOS cocktail contains 5 mAbs, against CI subunit NDUFB8 (20 kDa), CII subunit SDHB (30 kDa), CIII subunit UQCRC2 (48 kDa), CIV subunit MTCO1 (40 kDa), and CV subunit ATP5A (55 kDa). CST (Cell Signalling Technology, MA, USA); SCBT (Santa Cruz Biotechnology, TX, USA); Abcam (Cambridge, UK). GAPDH (glyceraldehyde 3-phosphate dehydrogenase); GSK3 (glycogen synthase kinase 3); HSP70 (heat shock protein 70 kDa); IRE1 (inositol-requiring enzyme 1); MAPK (mitogen-activated protein kinase); TXNIP (thioredoxin-interacting protein); VDAC (voltage dependent anion channel 1).

2.2.4 Triglyceride measurements

Triglycerides in tissues and plasma were measured using an enzymatic colorimetric assay. Briefly, the assay uses lipoprotein lipase to break down TGs into glycerol and free fatty acids (FFA). In the presence of ATP and glycerol kinase, the glycerol is converted to glycerol-3-phosphate, which is then oxidised by glycerol phosphate oxidase to yield hydrogen peroxide. In the presence of horseradish peroxidase, hydrogen peroxide reacts with 4-chlorophenol and 4-aminophenazone to generate a rose-coloured quinoneimine dye. The colour intensity is directly proportional to the TG concentration in the sample.

Tissue samples were homogenised in 4 mL of chloroform:methanol (2:1 vol/vol) and extracted on an orbital mixer at RT for 3 hr (liver) or 22 hr (muscle). 2 mL of sulphuric acid (1 M) was added to the extract, vortexed, and the phases separated by centrifugation at 2,000 g for 10 min. The lipid-containing lower phase was collected using glass pipettes into 7 mL glass scintillation vials and extracts dried down at 37°C. Lipids were resuspended in 300 µL of absolute ethanol. Lipid extract and plasma samples were plated at 5 µL in a 96-well microplate. Samples from plasma and liver were incubated with 300 µL of GPO-PAP reagent (Triglycerides GPO-PAP, Roche) for 25-30 min at 37°C and absorbance read at 490 nm using a microplate reader (VERSAmax™, Molecular Devices, CA, USA). Following discontinuation of the Roche GPO-PAP product, muscle lipid samples were incubated with 200 µL of Triglycerides liquid reagent (Pointe Scientific, MI, USA) for 25-30 min at 37°C and absorbance read at 505 nm. TG concentration was calculated against a glycerol standard curve (Precimat Glycerol 21 mg/dL, Roche; 0-0.26mg/mL).

2.2.5 Glycogen measurements

Glycogen content in liver, quadriceps, and gastrocnemius tissue was measured using a colorimetric assay (Infinity Glucose (Ox), Thermo). Briefly, isolated glycogen is hydrolysed using amyloglucosidase to form β-D-glucose, which is then oxidised by glucose oxidase to yield D-gluconic acid and hydrogen peroxide. In the presence of horseradish peroxidase, hydrogen peroxide reacts with 4-hydroxybenzoic acid and 4-aminoantipyrine to generate a red quinoneimine dye. The 1:1 stoichiometry of this reaction ensures colour intensity is proportional to the glucose concentration in the sample.

Frozen tissue (15-30 mg) was digested in 200 µL of 1 M potassium hydroxide at 70°C for 1 hr with regular mixing. Precipitation of glycogen was facilitated by the addition of 1.75 mL 95% ethanol and 75 µL saturated sodium sulphate (Na_2SO_4) followed by incubation at -80°C for 1 hr and centrifugation at 13,000 g for 10 min at 4°C. The glycogen pellet was dissolved in 200 µL water and an additional ethanol precipitation was performed. The final pellet was air-dried at RT and dissolved in 0.3 mg/ml amyloglucosidase (Sigma Aldrich, MO, USA) solution prepared in sodium acetate buffer (0.25 M, pH 4.75) and incubated at 37°C overnight. Samples were plated at 10 µL in a 96-well microplate and incubated with 250 µL of Glucose Oxidase reagent for 15 min at 37°C. Absorbance was read at 500 nm on a microplate reader (VERSAmax™, Molecular Devices). Glucose content was determined against a glucose (0-2 mM) standard curve.

2.3 Statistics

Statistical analysis relevant to individual chapters are detailed therein. In general, data were assessed for normality by the D'Agostino and Pearson normality test and for outliers by the two-sided Grubbs' test, with subsequent analysis by unpaired or paired t-tests and standard or repeated measures two- or three-way ANOVA where appropriate. Where a significant effect was identified by the ANOVA, post hoc testing was conducted to determine differences between groups. Data are presented as means ± SEM, with statistical significance accepted at $p < 0.05$. Statistical analysis was performed in GraphPad Prism software (Prism 8, Version 8.0.2).

CHAPTER 3: Metabolic Characterisation of CREBRF R458Q Knock-In Mice

3.1 INTRODUCTION

Obesity is one of the most significant contemporary health issues, due both to its sharply rising global prevalence and the substantial number of adverse health problems that are associated with the obese state. While reduced physical activity and overconsumption of calorie dense foods are no doubt major precipitates for the increased obesity rates worldwide, there is also intense interest in discovering genetic variants that may predispose individuals to weight gain and the associated co-morbidities of obesity. A recent genome-wide association study on a Samoan population identified a novel missense variant in the *CREBRF* gene (rs373863828, Arg457Gln), which was found only in Pacific Island populations (Minster *et al*., 2016). This R457Q missense variant produced a paradoxical phenotype of significantly increased obesity risk simultaneous with reduced diabetes risk, lacking any definitive mechanistic basis which might explain these effects.

The body composition effects induced by this *CREBRF* missense variant in Polynesian populations are primarily demonstrated by increased BMI, with the effect sizes in adults ranging from 1.28 kg/m^2 to 3.09 kg/m^2 per copy of the R457Q variant allele (Minster *et al*., 2016; Naka *et al*., 2017; Krishnan *et al*., 2018; Lin *et al*., 2020). To appropriately contextualise these figures, the R457Q effect is dramatic even compared to that of the *FTO* gene polymorphisms which, at ~0.39 kg/m^2 increase to BMI per allele, produce the largest previously-published effect size (Speliotes *et al*., 2010). The physiological source of this increased BMI in R457Q variant carriers has been an evolving debate. Minster *et al*. (2016) initially indicated a positive association with total and regional adiposity, later backed up by observations of greater waist and hip circumference in variant carriers (Naka *et al*., 2017; Krishnan *et al*., 2018; Lin *et al*., 2020). More recent studies associate the R457Q variant with greater height and/or lean mass (Krishnan *et al*., 2018; Hanson *et al*., 2019; Carlson *et al*., 2020; Lin *et al*., 2020; Metcalfe *et al*., 2020). These variant-associated phenotypes are reported in both men and women, typically without any statistical interaction between sex and genotype even when effect sizes differ (Krishnan *et al*., 2018; Carlson *et al*., 2020; Metcalfe *et al*., 2020). Hawley *et al*. (preprint) provide the primary exception, describing a male-specific effect on height and female-specific

changes to fat mass. Nor are body composition effects confined to adulthood. Separate cohorts have found associations between the variant allele and increased total body weight, fat-free mass, height, waist circumference, and/or BMI in infancy and childhood (Minster *et al*., 2016; Berry *et al*., 2018; Arslanian *et al*., 2021). The body composition phenotype exhibited by R457Q variant carriers, therefore, seems to be present across PI cohorts even if not all studies report (on) the same specific measures.

The metabolic phenotype seen in carriers of the *CREBRF* variant primarily impacts diabetes risk, as visible through odds ratio analyses. Presence of the R457Q variant is consistently associated with statistically significant decreases in the likelihood of developing T2D (OR 0.49-0.59) as well as GDM (OR 0.13-0.19) in both univariable analysis and after adjustment for confounding factors such as BMI (Minster *et al*., 2016; Krishnan *et al.*, 2018; Hanson *et al*., 2019; Krishnan *et al*., 2020). This protective effect was initially linked foremost to significant reduction in fasting glucose levels (0.09 mM per variant allele) evident even in non-diabetic subjects, with the effect becoming more pronounced after adjustment for BMI (0.12 mM) (Minster *et al*., 2016). Subsequent meta-analysis, incorporating three Samoan cohorts, confirms -0.05 mM fasting glucose per copy of missense allele in participants both with and without obesity (Russell *et al.*, preprint). Other variant-carrying populations, however, have not reproduced this effect (Lin *et al.*, 2020). No consistent correlations with either fasting insulin levels or homeostatic model assessment for IR (HOMA-IR) have yet been reported. Hanson *et al*. (2019) report a higher HOMA-B in variant carriers which may represent greater capacity for compensatory insulin secretion, as indicated by Burden *et al.* (2021)'s more recent study utilising hyperinsulinemic-euglycaemic clamps, a more precise surrogate measure, which links the missense variant to greater glucose-stimulated insulin secretion without impact on insulin sensitivity index or glucose disposal. Association with serum lipids in variant carriers is observed only inconsistently across cohorts and seems to be neither independent of BMI nor a mediator of the reduced GDM risk (Minster *et al*., 2016; Ohashi *et al*., 2018; Krishnan *et al*., 2020; Lin *et al.*, 2020). Protective effects against diabetes have thus been linked to glucose homeostasis and to insulin secretion, but without overt or consistent links to (whole-body) insulin sensitivity or obesity-associated comorbidities the causative mechanisms remain uncertain.

Extant literature cannot yet provide definitive answers regarding either the strong predisposition towards obesity or the protection against T2D which are associated with the missense variant. Nor is it wholly clear whether these two facets interact or operate independently. A recent study does, however, suggest that BMI and T2D odds are not decoupled in variant carriers, and that the variant allele might produce both direct and indirect effects (Russell *et al*., preprint). The CREBRF protein is primarily recognised to negatively regulate activity of the transcription factor CREB3 and has further been implicated in cellular and organismal bioenergetics as a starvation response factor, conferring protection against nutrient deprivation (Audas *et al.*, 2008, 2016; Minster *et al*., 2016). Although this seems relevant, mechanistic links to the variant phenotype at systemic and tissue levels remain uncertain. To address this in more detail, the present study sought to examine the metabolic phenotype of a novel knock-in mouse model for the *CREBRF* missense variant. Heterozygous and homozygous carriers of both sexes, and their wildtype counterparts, underwent comprehensive metabolic characterisation on a standard laboratory diet and in response to a high fat diet.

3.2 METHODS

3.2.1 Animal maintenance and study

Male and female wildtype (WT), heterozygous (HET), and homozygous (HOM) *CREBRF* R458Q knock-in mice were generated, with an average of 22 litters required to generate animals of each genotype for the desired sample size (minimum n = 32 per genotype per sex). Subsets used in lower-powered endpoint analyses comprised at least 3 independent litters per group. Mice were housed and maintained as described in section 2.1 from 8 weeks of age to 20 weeks. After four weeks on the standard control "chow" diet, mice were randomly allocated to remain on the chow diet or to receive the in-house-made HFD *ad libitum* for eight weeks. Body composition analysis was performed as described in section 2.1.2, and biochemical analyses as described in section 2.2.

3.2.2 Glucose and insulin tolerance

Mice were fasted for 5 hr and then given either an oral gavage of glucose (3 g/kg lean mass) or intraperitoneal injection of insulin (1.0 U/kg lean mass; Actrapid, Novo-Nordisk, Copenhagen, Denmark). Blood glucose levels were monitored using an Accu-Chek glucometer (Roche Diagnostics, Castle Hill, NSW, Australia). For the oral glucose tolerance test (oGTT), glucose was analysed at baseline and at 15, 30, 60, and 90 min post gavage, while for the insulin tolerance test (ITT) glucose levels were determined at baseline and at 10, 20, 30, 45, and 60 min post injection. During the oGTT, additional blood was collected from the tail tip at baseline and at 15, 30, and 60 min following glucose gavage to measure plasma insulin.

3.2.3 Insulin ELISA

Plasma insulin levels were measured using an Ultrasensitive Mouse Insulin ELISA Kit (Crystal Chem, Illinois, USA). Briefly, the assay uses two monoclonal antibodies, one immobilised on coated microplate wells and the other conjugated with horseradish peroxide (HRP), to bind insulin present in the sample. Hydrogen peroxide, in the presence of HRP, provokes oxidation of 3,3',5,5'-tetramethylbenzidine substrate to form a water-soluble blue reaction product. The kinetic reaction is halted by acidification, and intensity of the resultant yellow pigment is proportional to the insulin concentration in the sample. Plasma samples were plated as singletons at 5 µL with 95 µL sample diluent in an insulin antibody-coated 96-well microplate. Following incubation for 2 hr at 4°C, well contents were aspirated and washed five times to remove unbound material before addition of anti-

insulin enzyme conjugate and incubation at RT for 30 min. Wells were washed seven times, enzyme substrate added, and the plate incubated for 40 min at RT in the absence of direct light. The reaction was stopped using sulphuric acid and absorbance read at 630 nm and 450 nm on a microplate reader (VERSAmax™) within 30 min, with the former reading taken as background. Insulin concentration was calculated against an insulin standard curve (0-12.8 ng/ml).

3.2.4 Indirect calorimetry

Whole body energy expenditure (determined as whole-body oxygen consumption [mL O_2/min] and/or as heat [kcal/min]) and respiratory exchange ratio (RER) were assessed using an Oxymax Indirect Calorimeter (Comprehensive Laboratory Animal Monitoring System [CLAMS], Columbus Instruments, USA). Mice aged 18 weeks were housed individually over a 24 hr period (12 hr light/dark cycle, 0600-1800 hrs), following a 16 hr acclimatisation period at 21-23°C. The system was calibrated using a standard gas mixture of 0.489% CO_2 and 20.4% O_2. Samples of exhaust air were collected over a period of 1 min and measured every 20 mins. The RER was calculated from direct VCO_2 and VO_2 readings over the 24 hr period according to the following equation:

$$RER = \frac{VCO_2}{VO_2}$$

Energy expenditure (or 'heat') was likewise calculated from VCO_2 and VO_2 readings according to the following equation:

$$EE = VO_2 \times (3.815 \times (1.232 + RER))$$

3.2.5 NEFA measurements

Non-esterified fatty acid (NEFA) content in plasma was measured using an enzymatic colorimetric assay (NEFA C kit, Wako Pure Chemical Industries, Osaka, Japan). Briefly, the assay uses acyl-CoA synthase to catalyse the acylation of CoA by the FA in the sample. The acyl-CoA product is oxidised by acyl-CoA oxidase to produce hydrogen peroxide which, in the presence of peroxidase, allows the oxidative condensation of 3-methyl-N-ethyl-N (β-hydroxyethyl)-aniline with 4-aminoantipyrine. The resultant pigment is proportional to the NEFA concentration in the sample. Plasma samples were plated at 5 μL in a 96-well microplate and incubated at 37°C with reagents according to manufacturers' instructions. Absorbance was read at 550 nm on a microplate reader (VERSAmax™) following each incubation period, with the initial reading taken as

background. NEFA concentration was calculated against an FFA standard curve (0-10 mM).

3.2.6 Statistical analysis

Measures of body composition, indirect calorimetry, and endpoint tissue weight were analysed by ordinary two-way ANOVA. Glucose and insulin tolerance tests were analysed by repeated measures two-way ANOVA. Endpoint measures of circulating factors and tissue nutrient homeostasis were analysed by three-way ANOVA, with post-hoc testing conducted by Sidak's multiple comparisons tests. Male and female data were analysed separately. Data are presented as means ± SEM, with statistical significance accepted at $p < 0.05$. Statistical analysis was performed in GraphPad Prism software (Prism 8, Version 8.0.2).

3.3 RESULTS

3.3.1 Generation of *CREBRF* R458Q KI mice

To better understand how the *CREBRF* missense variant impacts the whole-body metabolic phenotype, we generated a novel mouse line with the R458Q variant knocked in to replace the WT protein. Confirmation of the functional R458Q knock-in was accomplished by real-time PCR and HRM analysis as represented in Figure 3.1. Tissue expression of the CREBRF protein could not be assessed due to lack of an appropriate commercially available primary antibody, in line with previous reports (Tiebe *et al*., 2019).

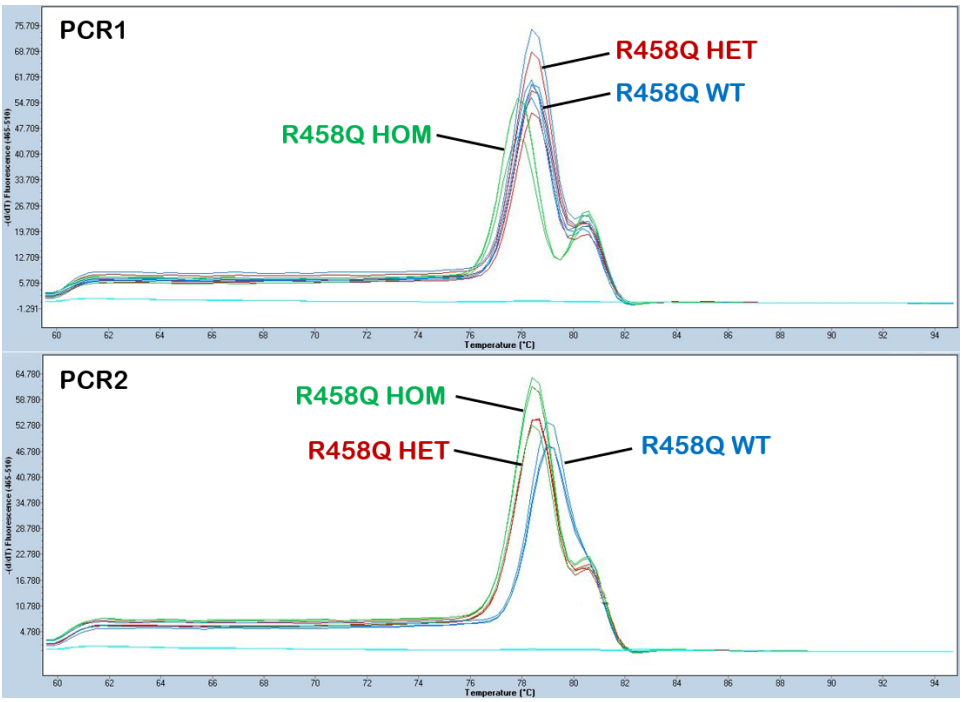

Figure 3.1: Genotype confirmation of *CREBRF* R458Q variant mice.
Representative HRM results of two PCR conditions for KI mice, presented as derivative melting peaks. PCR1 distinguishes WT/HET from HOM samples; PCR2 distinguishes WT from HET/HOM samples. WT samples are shown in blue, HET samples in red, HOM samples in green, and the negative control (H_2O) in cyan.

3.3.2 Body composition

The human variant allele has been repeatedly associated with increased BMI and/or adiposity measures (Minster *et al.*, 2016; Naka *et al*., 2017; Krishnan *et al*., 2018; Lin *et al.*, 2020). Total body weight of the HOM and HET mice on the chow diet was however not significantly different from WT mice across the course of the study for either sex (Figure 3.2A-B). Total body fat mass and the weight of individual adipose depots, measured at the conclusion of the feeding regime, was similarly unaffected by genotype for both male and female mice (Figure 3.2C-D, Tables 3.1, 3.2). Nor did the R458Q variant appear to promote preferential distribution of fat mass across depots (Tables 3.1, 3.2) as had been speculated for human carriers (Minster *et al*., 2016; Hawley *et al.*, preprint). There was no genotype difference in the weight of several key organs (Table 3.1), but EchoMRI lean mass measurements showed that male HOM chow-fed mice did have significantly greater lean mass than their WT counterparts at 20 weeks of age (Figure 3.2E), an effect present from 12 weeks of age (Figure 3.2G). The genotype difference was dose-dependent, with the HET animals demonstrating an intermediate increase in lean mass (Figure 3.2E,G). Female mice did not display any genotype-dependent differences in lean mass (Figure 3.2F).

To examine the effects of diet on body composition, an HFD was introduced to half the cohort at 12 weeks of age and maintained for 8 weeks. Both male and female sexes experienced the expected significant increases in body weight, total fat content, and white adipose depot size following HFD feeding, but there was no diet-induced development of a genotype effect (Figure 3.2A-D, Tables 3.1, 3.2). The effect on lean mass which was identified in chow-fed male mice was not present in HFD-fed mice of either sex (Figure 3.2E-F).

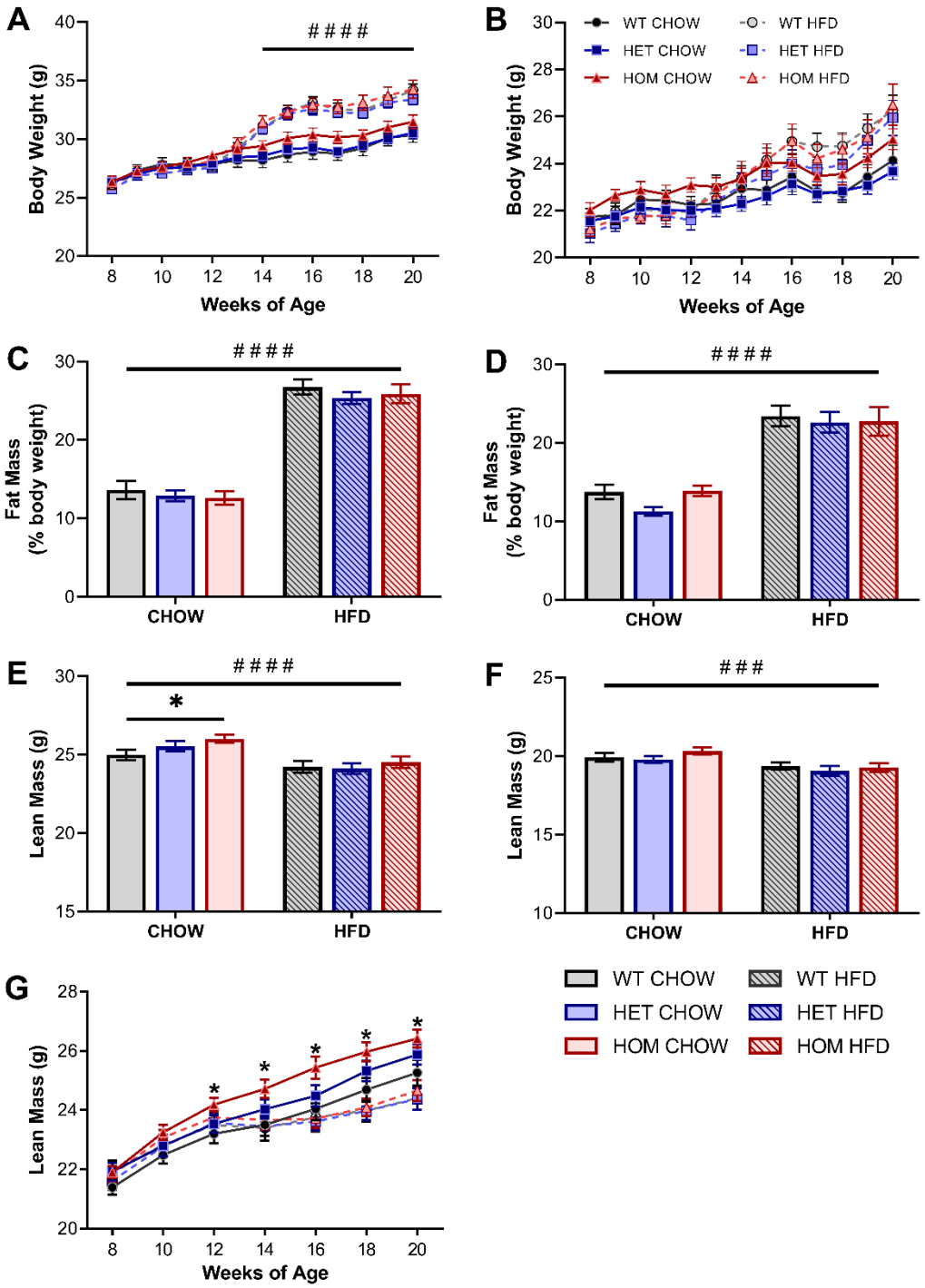

Figure 3.2: Body composition phenotype of *CREBRF* R458Q variant mice.

A-B. Body weight of (A) male and (B) female mice throughout the study (HFD began at 12 weeks of age). **C-D.** Fat mass at 20 weeks post-birth of (C) male and (D) female mice, presented as a proportion of total body weight. **E-G.** Total lean mass at 20 weeks post-birth of (E) male and (F) female mice, and of (G) male mice throughout the study. Data are presented as mean ± SEM, *n* = 17-24. * $p < 0.05$ effect of genotype; ### $p < 0.001$, #### $p < 0.0001$ main effect of diet by two-way ANOVA.

Table 3.1: Tissue weights of male *CREBRF* R458Q variant mice at 20 weeks.

	CHOW			HFD			P-values		
	WT	**HET**	**HOM**	**WT**	**HET**	**HOM**	**G**	**D**	**G x D**
Fed BW (g)	30.1 ± 0.83	31.0 ± 0.70	31.3 ± 1.04	34.3 ± 0.91	33.8 ± 0.60	34.7 ± 1.13	ns	< **0.0001**	ns
Fasted BW (g)	27.6 ± 0.61	27.9 ± 0.67	28.6 ± 0.40	32.2 ± 0.57	31.7 ± 0.71	32.2 ± 0.97	ns	< **0.0001**	ns
Fed eWAT (% BW)	1.64 ± 0.23	1.66 ± 0.13	1.86 ± 0.26	3.78 ± 0.11	3.67 ± 0.14	3.54 ± 0.17	ns	< **0.0001**	ns
Fasted eWAT (% BW)	2.04 ± 0.20	1.92 ± 0.15	1.68 ± 0.10	3.75 ± 0.12	3.92 ± 0.15	3.82 ± 0.19	ns	< **0.0001**	ns
Fed iWAT (% BW)	0.61 ± 0.06	0.66 ± 0.04	0.77 ± 0.08	1.33 ± 0.08	1.11 ± 0.05	1.39 ± 0.16	ns	< **0.0001**	ns
Fasted iWAT (% BW)	0.75 ± 0.07	0.68 ± 0.05	0.64 ± 0.04	1.25 ± 0.09	1.12 ± 0.06	1.19 ± 0.10	ns	< **0.0001**	ns
Fed BAT (% BW)	0.47 ± 0.03	0.42 ± 0.04	0.43 ± 0.04	0.56 ± 0.03	0.54 ± 0.03	0.63 ± 0.04	ns	< **0.0001**	ns
Fasted BAT (% BW)	0.46 ± 0.05	0.41 ± 0.03	0.36 ± 0.02	0.50 ± 0.03	0.40 ± 0.03	0.43 ± 0.01	< **0.05**	ns	ns
Fed Liver (% BW)	4.65 ± 0.13	4.75 ± 0.14	4.70 ± 0.15	4.21 ± 0.09	4.16 ± 0.16	4.08 ± 0.11	ns	< **0.0001**	ns
Fasted Liver (% BW)	3.86 ± 0.06	3.76 ± 0.06	3.66 ± 0.11	3.45 ± 0.10	3.30 ± 0.07	3.27 ± 0.07	ns	< **0.0001**	ns
Fed Heart (% BW)	0.46 ± 0.01	0.46 ± 0.01	0.45 ± 0.02	0.41 ± 0.02	0.41 ± 0.01	0.41 ± 0.02	ns	< **0.001**	ns
Fasted Heart (% BW)	0.48 ± 0.02	0.49 ± 0.01	0.49 ± 0.02	0.44 ± 0.02	0.44 ± 0.01	0.41 ± 0.01	ns	< **0.001**	ns
Fed Kidneys (% BW)	1.54 ± 0.05	1.53 ± 0.02	1.45 ± 0.03	1.25 ± 0.04	1.28 ± 0.03	1.26 ± 0.04	ns	< **0.0001**	ns
Fasted Kidneys (% BW)	1.45 ± 0.03	1.45 ± 0.03	1.53 ± 0.04	1.24 ± 0.06	1.23 ± 0.02	1.21 ± 0.03	ns	< **0.0001**	ns

Data are presented as mean ± SEM, *n* = 8-13. Statistics by ordinary two-way ANOVA. BW = body weight; eWAT = epididymal white adipose tissue; HFD = high fat diet; iWAT = inguinal white adipose tissue; BAT = brown adipose tissue; G = genotype, D = diet.

Table 3.2: Tissue weights of female *CREBRF* R458Q variant mice at 20 weeks.

	CHOW			HFD			P-values		
	WT	**HET**	**HOM**	**WT**	**HET**	**HOM**	**G**	**D**	**G x D**
Fed BW (g)	24.6 ± 0.94	23.8 ± 0.60	24.8 ± 0.83	27.3 ± 0.88	26.3 ± 1.10	25.9 ± 0.83	ns	< **0.01**	ns
Fasted BW (g)	21.8 ± 0.69	21.5 ± 0.43	22.5 ± 0.29	24.0 ± 0.99	24.2 ± 0.91	25.6 ± 1.14	ns	< **0.001**	ns
Fed pWAT (% BW)	1.27 ± 0.25	0.98 ± 0.18	1.57 ± 0.21	3.31 ± 0.30	3.02 ± 0.36	2.71 ± 0.48	ns	< **0.0001**	ns
Fasted pWAT (% BW)	1.12 ± 0.25	0.85 ± 0.09	1.20 ± 0.13	2.60 ± 0.43	2.85 ± 0.55	3.11 ± 0.54	ns	< **0.0001**	ns
Fed iWAT (% BW)	0.83 ± 0.08	0.67 ± 0.06	0.78 ± 0.06	1.31 ± 0.05	1.22 ± 0.07	1.25 ± 0.09	ns	< **0.0001**	ns
Fasted iWAT (% BW)	0.63 ± 0.08	0.69 ± 0.09	0.65 ± 0.05	0.97 ± 0.12	1.06 ± 0.12	1.17 ± 0.10	ns	< **0.0001**	ns
Fed BAT (% BW)	0.47 ± 0.03	0.42 ± 0.04	0.47 ± 0.03	0.47 ± 0.02	0.43 ± 0.02	0.43 ± 0.03	ns	ns	ns
Fasted BAT (% BW)	0.40 ± 0.05	0.41 ± 0.03	0.42 ± 0.04	0.54 ± 0.04	0.42 ± 0.02	0.45 ± 0.02	ns	< **0.05**	ns
Fed Liver (% BW)	4.99 ± 0.11	5.03 ± 0.11	4.95 ± 0.13	4.33 ± 0.04	3.99 ± 0.08	4.13 ± 0.17	ns	< **0.0001**	ns
Fasted Liver (% BW)	4.33 ± 0.09	4.26 ± 0.15	4.16 ± 0.18	3.81 ± 0.19	3.58 ± 0.07	3.56 ± 0.10	ns	< **0.0001**	ns
Fed Heart (% BW)	0.50 ± 0.02	0.48 ± 0.01	0.46 ± 0.01	0.41 ± 0.01	0.47 ± 0.03	0.44 ± 0.03	ns	< **0.01**	ns
Fasted Heart (% BW)	0.55 ± 0.02	0.52 ± 0.02	0.52 ± 0.02	0.48 ± 0.02	0.47 ± 0.01	0.43 ± 0.01	ns	< **0.0001**	ns
Fed Kidneys (% BW)	1.25 ± 0.03	1.25 ± 0.04	1.23 ± 0.02	1.05 ± 0.02	1.06 ± 0.01	1.09 ± 0.05	ns	< **0.0001**	ns
Fasted Kidneys (% BW)	1.34 ± 0.04	1.35 ± 0.03	1.29 ± 0.03	1.26 ± 0.04	1.15 ± 0.03	1.15 ± 0.04	ns	< **0.0001**	ns

Data are presented as mean ± SEM, *n* = 8-11. Statistics by ordinary two-way ANOVA. BW = body weight; pWAT = periovarian white adipose tissue; HFD = high fat diet; iWAT = inguinal white adipose tissue; BAT = brown adipose tissue; G = genotype, D = diet.

To further pursue effects on whole-body growth, we measured naso-anal length. The R458Q variant had a dose-dependent effect on 8-week-old males, significantly increasing length in HOM compared to WT mice (Figure 3.3A-B). This effect was not seen in female mice of the same age. Follow-up measurements at 18 weeks of age were not statistically significant but reflected a similar trend to greater length in chow-fed HOM mice of both sexes (Figure 3.3C-D). HFD feeding seemed associated with greater length in WT but not HOM mice, with no genotype effects.

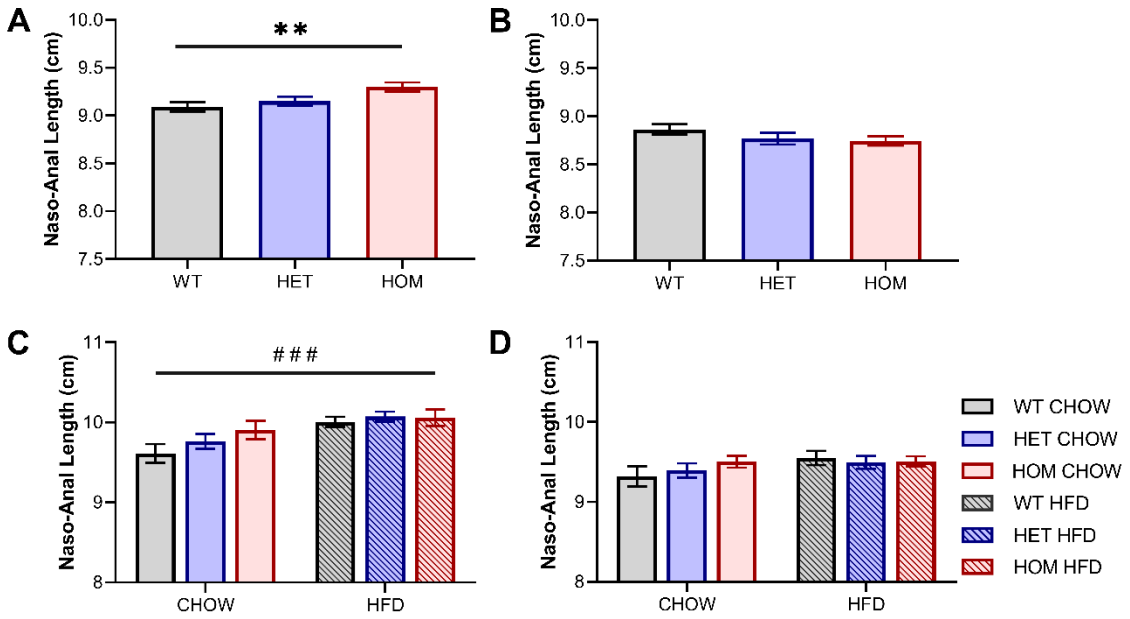

Figure 3.3: Lengths of *CREBRF* R458Q variant mice.

Naso-anal length at 8 weeks post-birth for (A) male and (B) female mice fed on a chow diet (n = 25-34), and at 18 weeks post-birth for (C) male and (D) female mice fed on chow or HF diets (n = 7-19). Data are expressed as mean ± SEM. ** $p < 0.01$, HOM vs WT by two-tailed unpaired Student's t test, $p = 0.0047$ ordinary one-way ANOVA test for linear trend; ### $p < 0.001$ main effect of diet by ordinary two-way ANOVA.

3.3.3 Glucose and insulin tolerance

The CREBRF variant has been linked to reduced diabetes risk and lowered blood glucose levels in human carriers (Minster *et al*., 2016; Krishnan *et al.*, 2018; Hanson *et al*., 2019; Krishnan *et al*., 2020). To determine whether the R458Q variant impacted glycaemic control in our mice, oral glucose tolerance tests (oGTT) were performed to assess whole-body glucose tolerance at 10 and 16 weeks of age. The blood glucose and plasma insulin responses of male and female mice at the earlier time-point (2 weeks preceding HFD introduction) were indistinguishable between WT, HET, and HOM animals (Figure 3.4).

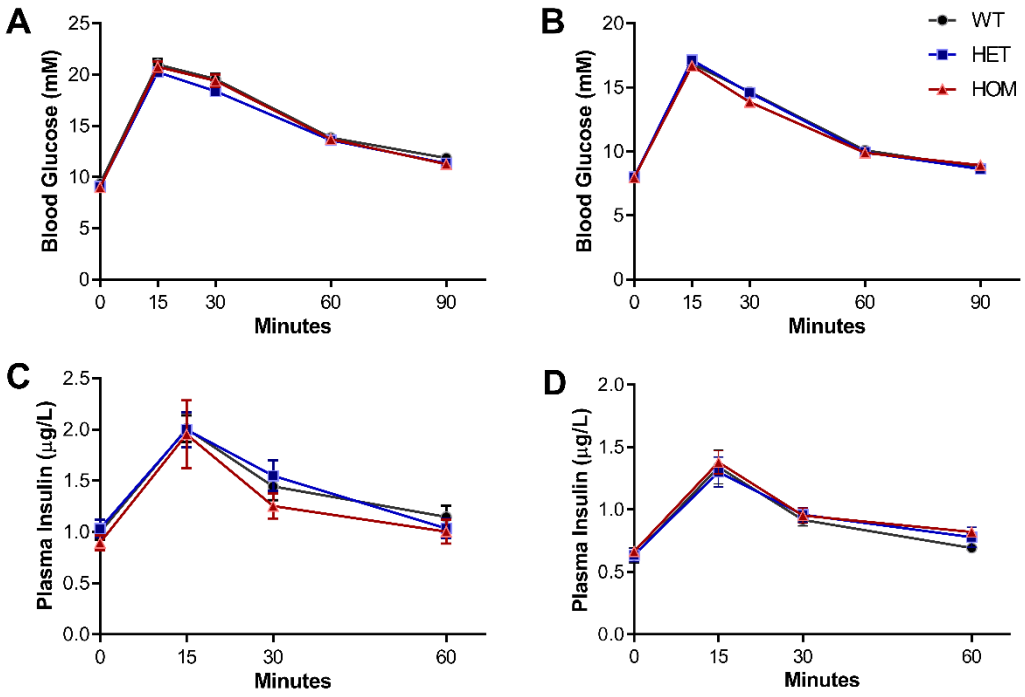

Figure 3.4: Glucose tolerance in 10-week-old *CREBRF* R458Q variant mice.
A-B. Blood glucose response to glucose administration for (A) male and (B) female mice (*n* = 13-19). **C-D.** Plasma insulin levels during oGTT for (C) males and (D) females (*n* = 8-16). Data are presented as mean ± SEM.

At the 16-week timepoint (4 weeks into the feeding regime), glucose clearance of both sexes was significantly impaired by HFD-feeding but remained absent of any genotype effect (Figure 3.5A-D). Plasma insulin levels during the oGTT were likewise unchanged by genotype in male mice, but in females were mildly increased in HOM mice compared

to WT (Figure 3.5E-F). HFD feeding significantly heightened plasma insulin levels for both sexes, although the diet effect was of greater magnitude for females in HOM mice, and for males in WT mice. Curiously, this latter observation mirrored the blood glucose response which likewise displayed a less prominent effect of diet in the male HOM mice than in WT or HET counterparts.

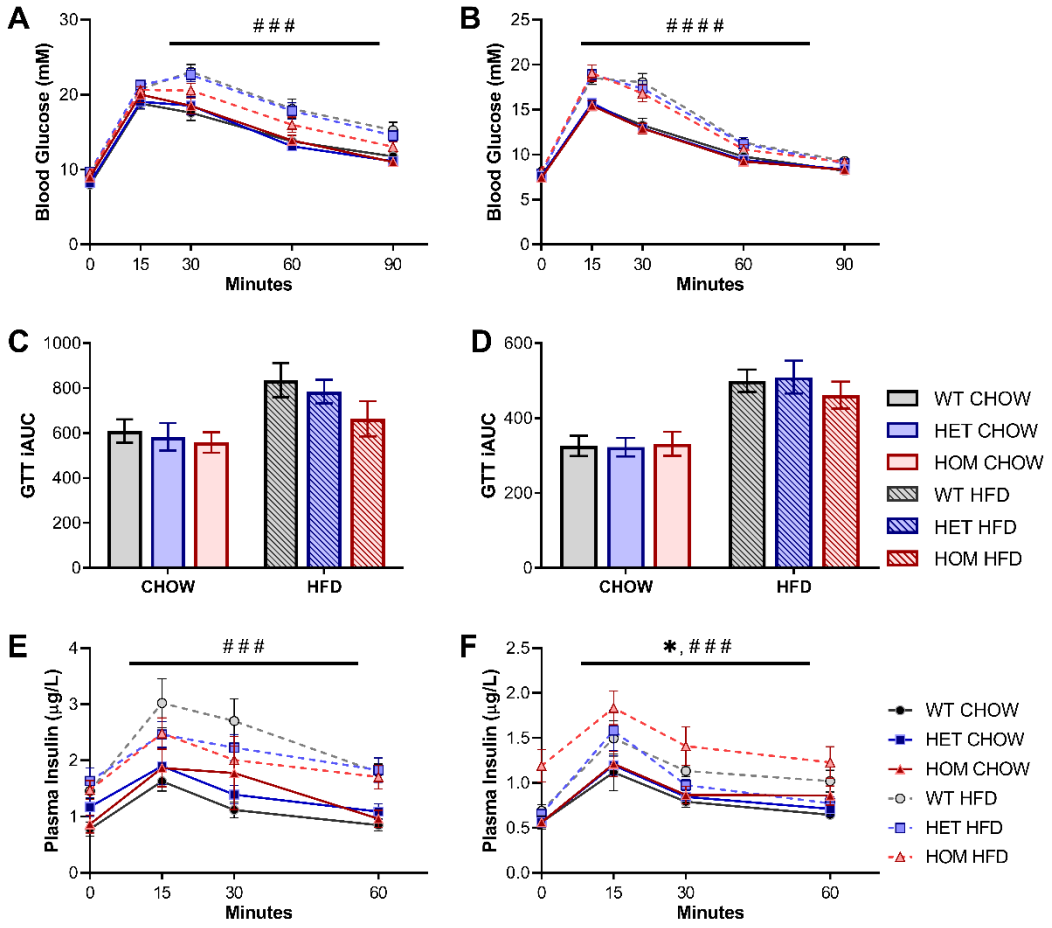

Figure 3.5: Glucose tolerance in 16-week-old *CREBRF* R458Q variant mice.
A-D. Blood glucose response to glucose administration for (A) male and (B) female mice, showing incremental area under the curve (iAUC) for (C) males and (D) females (n = 13-19). **E-F.** Plasma insulin levels during oGTT for (E) males and (F) females (n = 8-16). Data are presented as mean ± SEM. * $p < 0.05$ main effect of genotype; ### $p < 0.001$, #### $p < 0.0001$ main effect of diet by RM two-way ANOVA.

We further assessed whole-body insulin sensitivity via intraperitoneal insulin tolerance test (ipITT). Male and female mice aged 11 weeks displayed no genotype difference in blood glucose response to insulin administration (Figure 3.6A-B). At 17 weeks, male HOM mice on a chow diet exhibited a significantly less pronounced fall in glucose levels post-injection than was seen in WT counterparts (Figure 3.6C). This seeming comparative reduction in sensitivity to insulin administration was not overtly dose-dependent, but chow-fed HET males did display an intermediate response, positioned between WT and HOM groups. The genotype effect was absent in HFD-fed male mice. Unexpectedly, the insulin sensitivity of male HOM mice also appeared largely unaffected by HFD-feeding, with the glucose response of mice carrying the double variant not different between diet groups. In contrast, insulin tolerance of female mice was changed by diet but not genotype (Figure 3.6D).

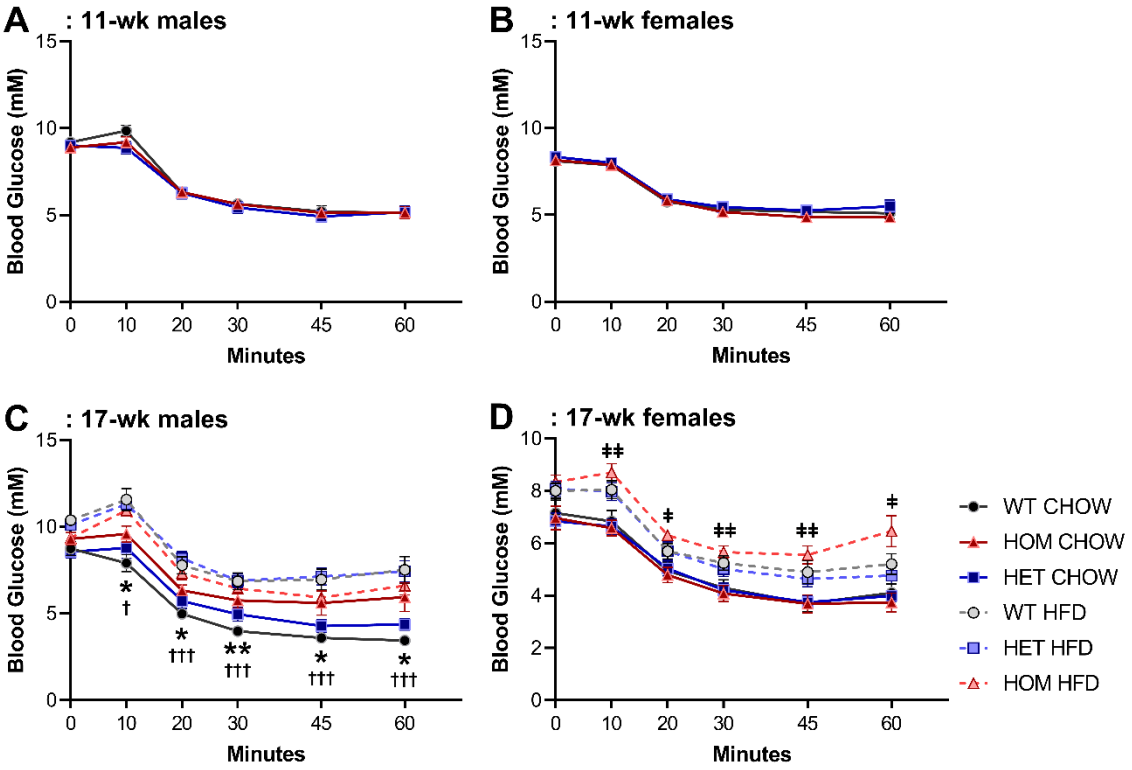

Figure 3.6: Insulin tolerance in *CREBRF* R458Q variant mice.

Blood glucose response to insulin administration in 11-week-old (A) males and (B) females (n = 18-31); and in 17-week-old (C) males and (D) females (n = 10-18). Data are presented as mean ± SEM. * $p < 0.05$, ** $p < 0.01$ WT chow vs HOM chow; † $p < 0.05$, ††† $p < 0.001$ WT chow vs WT HFD and vs HET HFD; ǂ $p < 0.05$, ǂǂ $p < 0.01$ all chow groups vs HOM HFD by RM two-way ANOVA and Dunnett's multiple comparisons.

3.3.4 Indirect calorimetry

Given that CREBRF has been previously associated with altered tissue bioenergetics (Minster *et al.*, 2016), we additionally performed indirect calorimetry to determine whether the R458Q variant impacted measures of whole-body energy metabolism and expenditure in our knock-in mouse model. Whole-body energy expenditure (as measured by heat production) was significantly increased for HFD-fed male and female mice compared to their chow-fed counterparts (Figure 3.7A-B). Whole-body energy metabolism was assessed through the respiratory exchange ratio (RER) as a surrogate for substrate utilisation. As expected, HFD-fed mice exhibited an RER significantly lower than their chow-fed counterparts (Figure 3.7C-D). The lower RER seen for HFD-fed mice indicates greater utilisation of lipids as the primary fuel source, while the higher RER values observed for chow-fed mice indicate the relatively greater contribution of carbohydrates being metabolised. No differences were observed between genotypes for either parameter.

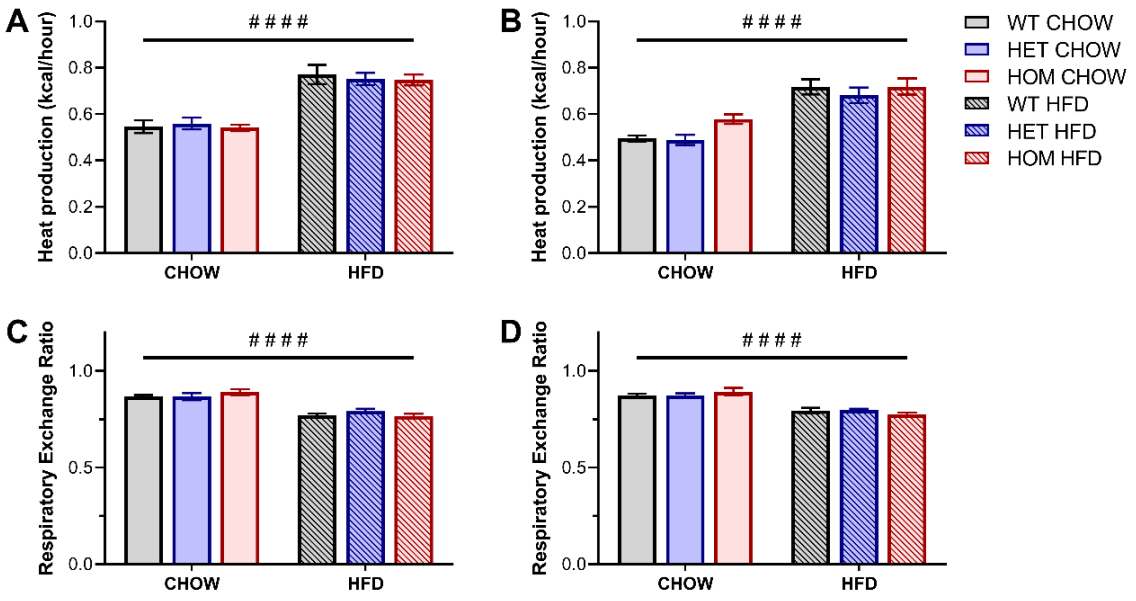

Figure 3.7: Whole-body energy expenditure in *CREBRF* R458Q variant mice.
A-B. Heat production, normalised to lean mass, in (A) male and (B) female mice. **C-D.** Respiratory exchange ratio (RER) in (C) male and (D) female animals. Values represent an average over a 24-hr data collection period (12 hr light and 12 hr dark phase). Data are presented as mean ± SEM, n = 6-8. #### $p < 0.0001$ main effect of diet by ordinary two-way ANOVA.

3.3.5 Circulating factors

Plasma and tissue biochemical analyses were performed on samples taken from WT and HOM mice in either the fed state or following overnight fasting, which aimed to induce conditions more likely to stimulate activity of the starvation factor CREBRF (Minster *et al*., 2016; Tiebe *et al*., 2019). Blood glucose levels were significantly depressed in response to fasting in both sexes, but there was no significant genotype effect on glucose levels in either the fed or the fasted state (Table 3.3). The presence of the R458Q variant likewise had no effect on plasma insulin levels in either male or female mice, but the expected decrease in insulin due to fasting and, in females, increase in response to high fat feeding were apparent (Table 3.3).

Plasma TG was unaltered by genotype in male mice (Table 3.3). In females, however, the R458Q variant was associated with a decrease in plasma TG levels (Table 3.3). In contrast, circulating NEFAs in male mice were increased in HOM animals, with this change largely driven by a more pronounced increase in fasting NEFA levels in mice carrying the R458Q variant (Table 3.3). Female mice did not present the same pattern, with a clear fasting effect, but the absence of any differences produced by genotype (Table 3.3).

Table 3.3: Circulating factors in *CREBRF* R458Q variant mice at 20 weeks.

		Chow		HF		P-values			
		WT	**HOM**	**WT**	**HOM**	**G**	**F**	**D**	**G x F**
Male	Fed BG (mM)	8.52 ± 0.22	8.63 ± 0.13	8.47 ± 0.23	8.70 ± 0.28	ns	**< 0.0001**	ns	ns
	Fasted BG (mM)	5.53 ± 0.27§§§§	5.99 ± 0.63§§§§	6.11 ± 0.23§§§§	6.44 ± 0.31§§§§				
	Fed Insulin (µg/L)	1.40 ± 0.17	1.68 ± 0.41	2.67 ± 0.50	2.44 ± 0.55	ns	**< 0.0001**	**< 0.05**	ns
	Fasted Insulin (µg/L)	0.51 ± 0.06	0.46 ± 0.04	0.58 ± 0.07§§§	0.59 ± 0.05§§				
	Fed TGs (mM)	2.03 ± 0.20	2.08 ± 0.19	1.39 ± 0.14	1.44 ± 0.15	ns	ns	**< 0.01**	ns
	Fasted TGs (mM)	2.21 ± 0.29	1.66 ± 0.13	1.83 ± 0.18	1.80 ± 0.12				
	Fed NEFAs (mM)	0.40 ± 0.07	0.40 ± 0.08	0.38 ± 0.07	0.49 ± 0.05	**< 0.05**	**< 0.0001**	ns	ns
	Fasted NEFAs (mM)	0.77 ± 0.07	1.19 ± 0.14*,§§§§	0.80 ± 0.09§	0.92 ± 0.13§				
Female	Fed BG (mM)	7.95 ± 0.18	8.54 ± 0.18	7.88 ± 0.23	8.18 ± 0.14	ns	**< 0.0001**	ns	ns
	Fasted BG (mM)	5.30 ± 0.20§§§§	5.61 ± 0.38§§§§	5.55 ± 0.34§§§§	5.16 ± 0.27§§§§				
	Fed Insulin (µg/L)	0.63 ± 0.11$^{##}$	0.76 ± 0.10	2.07 ± 0.53	1.04 ± 0.24	ns	**< 0.001**	**< 0.01**	ns
	Fasted Insulin (µg/L)	0.48 ± 0.13	0.51 ± 0.05	0.53 ± 0.06§§§	0.48 ± 0.04				
	Fed TGs (mM)	2.55 ± 0.13	2.89 ± 0.25$^{#}$	2.44 ± 0.26	1.90 ± 0.11	**< 0.05**	ns	**< 0.0001**	ns
	Fasted TGs (mM)	3.52 ± 0.36$^{##}$	2.70 ± 0.23$^{#}$	2.19 ± 0.16	1.73 ± 0.15				
	Fed NEFAs (mM)	0.45 ± 0.09	0.42 ± 0.04	0.32 ± 0.10	0.48 ± 0.03	ns	**< 0.0001**	ns	**< 0.05**
	Fasted NEFAs (mM)	1.21 ± 0.12§§§§	1.00 ± 0.08§§§	1.13 ± 0.06§§§§	0.99 ± 0.09§§				

Data are presented as mean ± SEM, n = 5-11. ***** $p < 0.05$ vs WT counterpart; **§** $p < 0.05$, **§§** $p < 0.01$, **§§§** $p < 0.001$, **§§§§** $p < 0.0001$ vs fed state counterpart; **#** $p < 0.05$, **##** $p < 0.01$ vs HFD counterpart by three-way ANOVA, Sidak's post-hoc. BG = blood glucose; NEFA = non-esterified fatty acid; TG = triglyceride; G = genotype; F = fed state; D = diet; G x F = interaction between genotype and fed state.

3.3.6 Tissue nutrient homeostasis

As a broad measure of tissue nutrient homeostasis, glycogen and TG contents were measured in both liver and muscle. Glycogen stores in both tissues were as expected significantly depleted by the overnight fasting for all mice, with a greater decline observed in the liver (Figure 3.8A-D). The presence of the *CREBRF* R458Q variant in male mice did not significantly impact glycogen content in either tissue, but in the fasted state there was a trend for variant-induced reductions (Figure 3.8A,C). There was an overall trend ($p = 0.0565$) for female liver glycogen to be significantly reduced in HOM mice, and unlike the males this effect was more prominent in the fed state animals (Figure 3.8B); the pattern was reflected also in quadriceps glycogen content (Figure 3.8D).

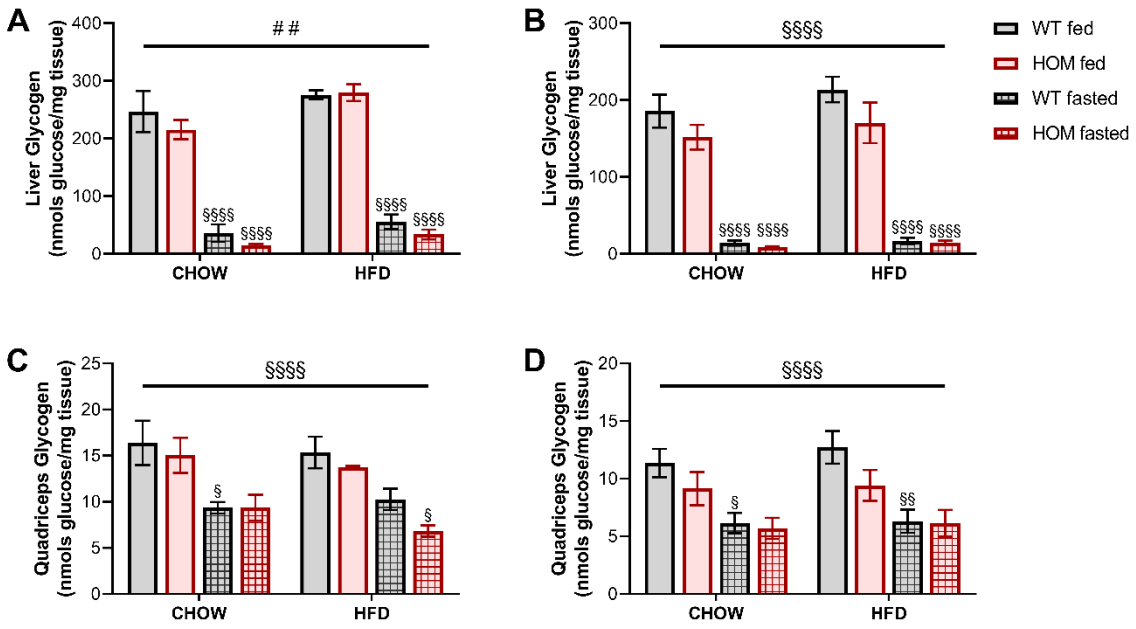

Figure 3.8: Tissue glycogen content in *CREBRF* R458Q variant mice.

A-B. Liver glycogen content in (A) male and (B) female mice. **C-D.** Quadriceps glycogen in (C) male and (D) female mice. Data are presented as mean ± SEM, $n = 6$. ## $p < 0.01$ main effect of diet; § $p < 0.05$, §§ $p < 0.01$, §§§§ $p < 0.0001$ effect of fasting by three-way ANOVA and Sidak's multiple comparisons test.

Hepatic TG accumulation in chow-fed male mice was significantly increased both by fasting and by the presence of the R458Q variant (Figure 3.9A). HFD feeding blunted the fasting- and genotype-induced TG changes. Female mice exhibited a similar overall pattern in hepatic TG levels among both chow- and HFD-fed animals, but without significant genotype effects (Figure 3.9B). Quadriceps muscle TGs were predominantly influenced by the HFD in both male and female mice (Figure 3.9C-D). Female muscle displayed a significant interaction between fed state and genotype, with the overnight fast associated with a relative decrease in TG in WT animals, and a relative increase in their HOM counterparts. A significant variant-induced decrease in quadriceps TG levels was observed in HFD-fed male mice in the fed state.

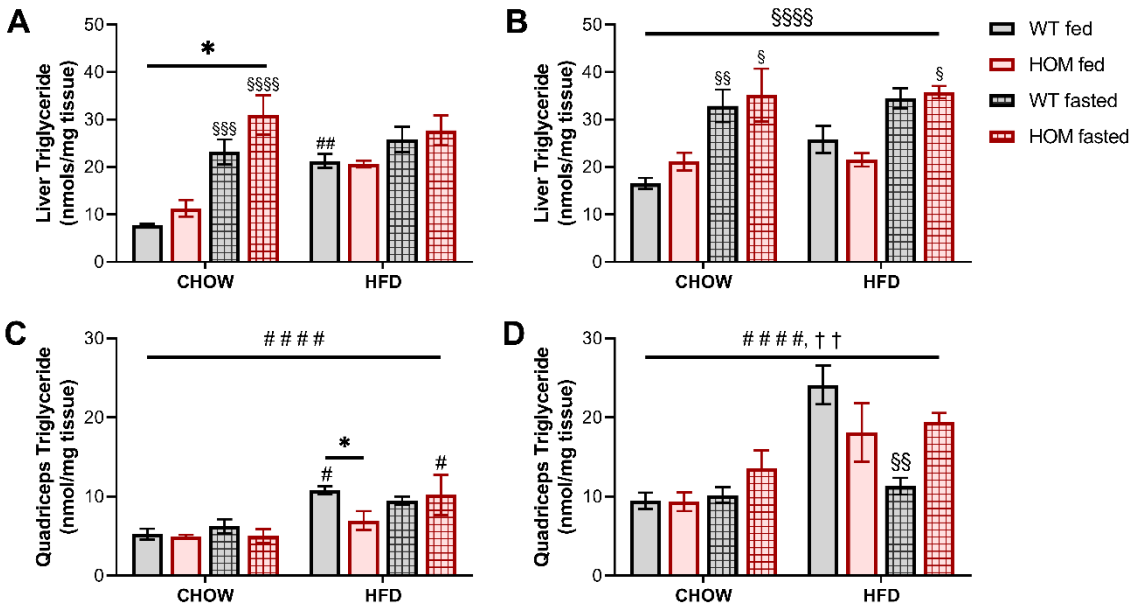

Figure 3.9: Tissue lipid content in *CREBRF* R458Q variant mice.

A-B. Liver TG accumulation in (A) male and (B) female mice. **C-D.** Quadriceps TG accumulation in (C) male and (D) female mice. Data are presented as mean ± SEM, n = 6. * $p < 0.05$ main effect of genotype by ordinary two-way ANOVA; †† $p < 0.01$ interaction between genotype and fed state; # $p < 0.05$, ## $p < 0.01$, ### $p < 0.001$, #### $p < 0.0001$ effect of diet; § $p < 0.05$, §§ $p < 0.01$, §§§§ p < 0.0001 effect of fasting by three-way ANOVA and Sidak's multiple comparisons test.

3.3.7 Protein expression

Tissue expression of selected proteins involved in metabolic signalling was examined in liver and quadriceps muscle from KI mice. The livers of chow-fed HOM male mice in the fasted state showed reduced protein kinase B (PKB)^{473} phosphorylation compared to WT animals (Figure 3.10A). There was no clear effect of genotype on PKB^{473} expression in the fed state, while HFD-fed animals had reduced expression regardless of genotype (Figure 3.10B). Expression of phosphorylated FoxO1^{256}, a PKB substrate, seemed reduced in liver tissue from fasted HOM mice when examined at high protein concentrations (Figure 3.10C), but at the standard concentration reflected PKB^{473} expression without overt genotype differentiation (Figure 3.10A). In contrast, hepatic expression of phosphorylated PKB^{473} in female mice trended higher with presence of the R458Q variant, but without statistical significance (Figure 3.10D). The HFD feeding regime seemed to increase PKB phosphorylation levels in female but not male fed-state mice.

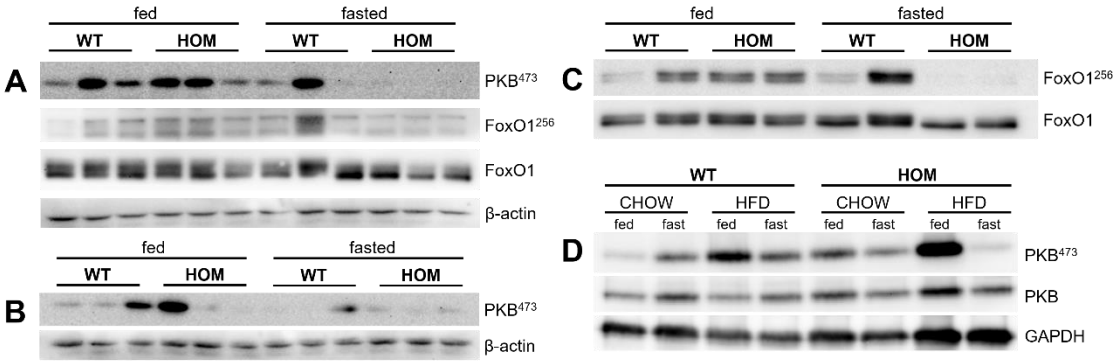

Figure 3.10: Hepatic insulin signalling pathway in *CREBRF* R458Q variant mice. Protein expression in liver tissue was assessed via immunoblot for phosphorylated PKB^{473} in (A) chow-fed and (B) HFD-fed male KI mice. **C.** Phosphorylated and total FoxO1^{256} in male chow-fed animals, loaded at 100 µg/well. **D.** Phosphorylated and total PKB^{473} expression in liver tissue of chow- and HFD-fed female mice. Tissues from both fed and overnight (16 hr) fasted animals were examined. Whole protein lysates were loaded at 30 µg/well with the exception of panel C. GAPDH and β-actin were used as housekeepers. Images are representative.

Further analyses of protein expression were primarily restricted to liver and quadriceps muscle of chow-fed male mice, which had shown the greatest whole-body effects of the variant protein. Markers of oxidative and lipid metabolism, pathways known to be associated with the CREBRF protein (Tiebe *et al*., 2015; Minster *et al*., 2016), were evaluated for potential involvement in missense variant activity. Oxidative phosphorylation complex subunit expression in liver and muscle was unchanged between WT and HOM animals (Figure 3.11A, 3.12A). In muscle, the mitochondrial voltage-dependent anion channel (VDAC) was more highly expressed in fasted than fed animals but unaffected by genotype (Figure 3.12B,D). Markers of lipid metabolism in the KI mice suggested trends in liver and quadriceps were similarly independent of the R458Q variant (Figure 3.11C, 3.12C). Protein expression of phosphorylated (inactive) acetyl-CoA carboxylase was slightly elevated in HOM compared to WT liver tissues (Figure 3.11C).

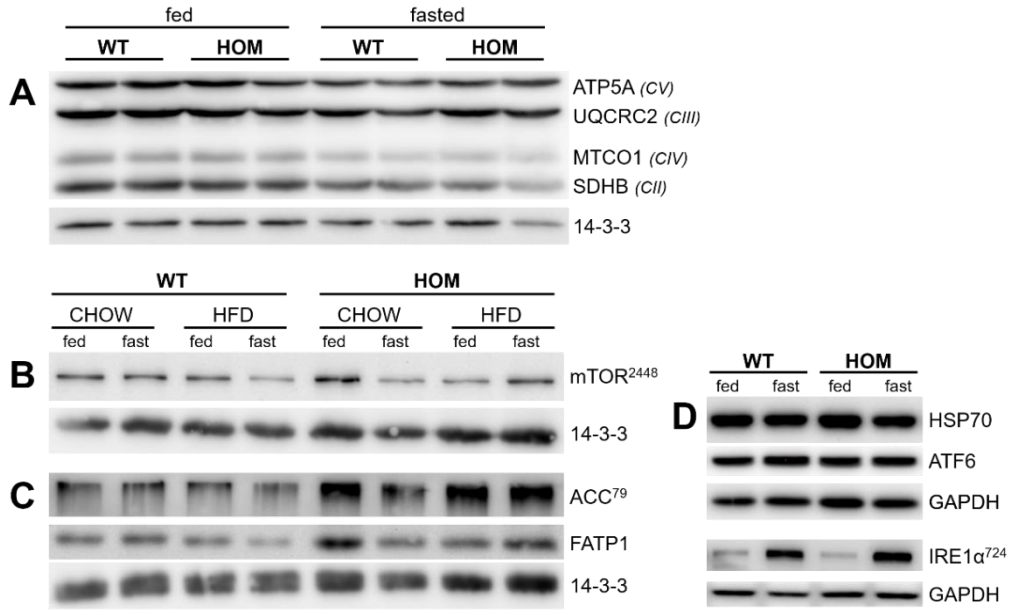

Figure 3.11: Hepatic protein expression of oxidative and lipid metabolism markers in male *CREBRF* R458Q variant mice.

Protein expression in liver tissue from male KI mice was assessed via immunoblot for (A) components of the electron transport chain complexes, (B) phosphorylated mTOR^{2448}, (C) lipogenesis and lipid transport proteins, and (D) markers of cell stress. Liver tissues were taken from both fed and overnight (16 hr) fasted male animals, chow-fed unless otherwise indicated. Whole protein lysates were loaded at 30 µg/well. Pan 14-3-3 was used as a housekeeper. Images are representative. FATP (fatty acid transport protein 1).

CREBRF and its regulatory target CREB3 are also strongly associated with ER stress (Audas *et al*., 2008; Penney *et al*., 2018). Markers of the ER stress or unfolded protein responses including HSP70 and ATF6, however, showed no variation in expression between WT and HOM liver (Figure 3.11D). Phosphorylation of IRE1α responded to fasting but lacked a genotype effect (Figure 3.11D). Muscle expression of proteins known to be involved in regulating metabolism and growth, including SMAD2/3 and ERK, was not different between genotypes (Figure 3.12B,E).

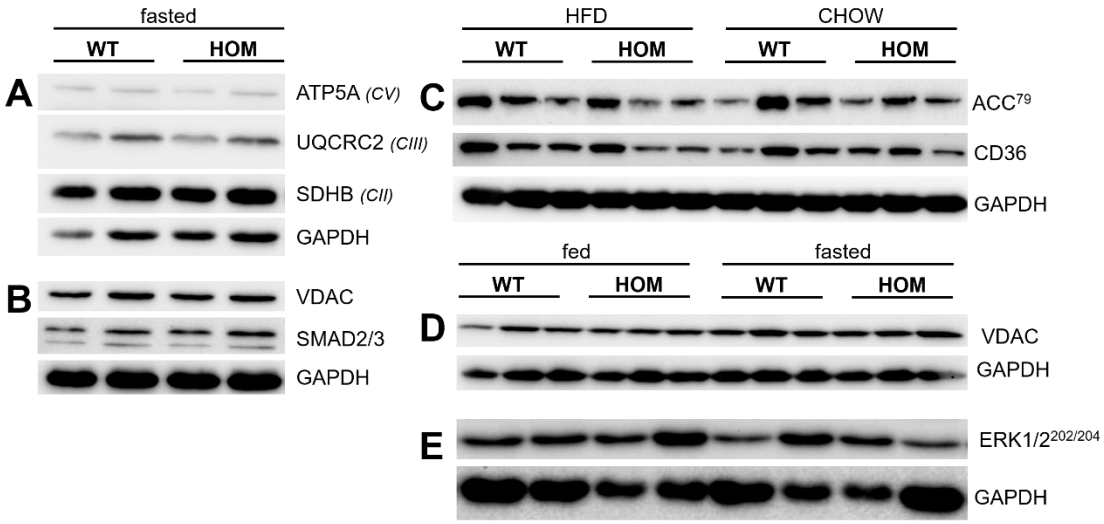

Figure 3.12: Quadriceps muscle protein expression of metabolic markers in male *CREBRF* R458Q variant mice.

Protein expression in skeletal muscle tissue from male KI mice was assessed via immunoblot for (A) components of the electron transport chain complexes and (B) VDAC and SMAD2/3 in fasted animals. **C.** Markers of lipid metabolism in chow-fed and HFD-fed mice. **D-E**. Comparison of fed and fasted tissue expression of (D) VDAC and (E) ERK1/2. Tissues were taken from both fed and overnight (16 hr) fasted male animals, chow-fed unless otherwise indicated. Whole protein lysates were loaded at 30 µg/well. GAPDH was used as a housekeeper. Images are representative.

3.4 DISCUSSION

While there is an obvious link between the growing obesity epidemic and environmental factors, there has also been great interest in searching for genetic factors that may contribute to this condition. To date the most prominent genetic variant linked with excess body weight is the recently identified R457Q variant in the *CREBRF* gene, a missense variant with a presence restricted to Pacific Islands (PI) populations (Minster *et al*., 2016; Naka *et al*., 2017; Krishnan *et al*., 2018). Despite these reports, in the current study mice with this variant knocked in displayed minimal differences to their wildtype counterparts when assessed for a variety of metabolic traits. Over the course of the study, HOM mice were indistinguishable from WT animals when assessed for changes in body weight and fat mass, despite excess body weight being the most overt and well-reported effect of the variant in human studies. This lack of difference between genotypes persisted when mice were placed on a HFD to provide a more obesogenic environment.

Precise measures of body fat content, such as those which we have been able to determine for our KI mouse model, are rarely reported in human studies of the R457Q variant. Human studies most commonly utilise BMI as the chosen measure of obesity, reporting (with few exceptions) significant increases due to the minor allele. Use of BMI is not without its detractors. Most relevant here is the dubious nature of its ability to consistently represent comparative adiposity between ethnicities via uniform cut-off values developed for a specific population (Goossens, 2017). At a given BMI, Pacific Islanders have been reported to possess a higher ratio of lean mass to fat mass (i.e., less body fat mass) than, for example, Asian Indians or Europeans (Swinburn *et al*., 1999; Rush *et al*., 2009). It has also been suggested (again with reference to Pacific Island populations) that BMI cut-offs should be based on associated comorbidities, not body composition alone (McAuley *et al*., 2002). Given the discrepancies between chosen methods of assessment, exact comparison between mouse and human phenotypes are perhaps not wholly straightforward**.**

For adiposity measures beyond BMI, Minster *et al*. (2016) attributed increased body fat percentage to the missense variant, while some subsequent studies also reported increased waist and hip circumference in carriers of the variant (Naka *et al*., 2017; Krishnan *et al*., 2018). A recent clinical study, however, indicated that a cohort of Maori and Pacific pregnant women with obesity did not differ in BMI, waist circumference, or gestational

weight gain between variant carriers and non-carriers (Krishnan *et al*., 2020). An adult Samoan cohort comprised of participants from the original GWAS sample, recruited to follow up on the adiposity effects in variant carriers, curiously found no significant association between genotype and percent body fat (Hawley *et al*., preprint). The disparity among these findings may lend credence to the theory that preferential distribution of fat content from visceral to subcutaneous adipose depots could offer a better reflection of metabolic consequences than total adiposity, and perhaps contribute to the otherwise paradoxical CREBRF variant phenotype. This is not the case in the KI mouse model, which lacks variant-dependent alterations across individual adipose depots, but it may remain a viable theory in the human context. Hawley *et al*. (preprint) provide the only known human study to measure body fat distribution and show that the *CREBRF* variant was associated with greater android and trunk fat mass in Samoan women. Gynoid and peripheral fat mass was not significantly increased in variant carriers, but analysis of fat deposition patterns did not present a genotype effect. The missense variant in Native Hawaiian carriers showed no clearly characterised impact on fat distribution (Lin *et al*., 2020). There is likely a more complex phenotypic effect of the missense variant than is otherwise yet defined in published literature, or indeed seen within our mouse model.

We have identified that the missense variant significantly increases lean mass and naso-anal length in our male KI mice, with a dose- (and sex-) dependent effect. Samoan male and female carriers of the variant were recently reported to exhibit increased total lean mass during both infancy and adulthood (Arslanian *et al*., 2021; Hawley *et al*., preprint). These findings appear to reflect the phenotype of our KI male mice and may indicate that some underlying correlations in mechanism could exist. Increased fat-free mass in human variant carriers could potentially skew simple BMI measurements. Indeed, the infant lean mass effects associated with the *CREBRF* variant appear without any accompanying impact on BMI (Arslanian *et al*., 2021), while in Hawley *et al*. (preprint)'s recent report they appear in male adults without the trend to greater BMI reaching statistical significance. Likewise, association of the missense variant with body composition or obesity measures may also be influenced by its effects to increase human height as well as length in our KI male mice (Hanson *et al*., 2019; Metcalfe *et al*., 2020; Carlson *et al*., 2020; Lin *et al*., 2020; Oyama *et al*., 2021; Hawley *et al*., preprint; Lee *et al*., preprint). Dual effects on fat-free mass and height imply that the missense variant could produce a growth phenotype, resulting in greater overall body size, which is present in human

carriers—albeit partially masked by PI-typical obesity. In keeping with these observations, animal models studying the WT CREBRF protein are also shown to experience growth-related effects, with mice and flies lacking the protein being lighter and smaller (Martyn *et al*., 2012; Tiebe *et al*., 2015).

The increased fat-free mass exhibited by variant carriers could not be attributed to any specific organ in the KI mice, perhaps therefore implying a common mechanism with cumulative organismal effect. Greater understanding of the phenotype might develop from a closer investigation of the key components of fat-free mass, namely muscle and bone, which tend to develop in parallel. Arslanian *et al*. (2021) attribute the infant fat-free mass phenotype to greater bone accretion as well as muscle mass, although the lack of any association between missense variant and bone mass in Samoan adults may suggest that variant-induced skeletal effects may lose their significance by the time adult proportions are attained (Hawley *et al*., preprint). Like skeletal muscle, which has greater mass in PI than European populations, bone is also known to exhibit greater mineral content and density as well as length in Polynesian groups (Reid *et al*., 1986; Cundy *et al*., 1995; Grant *et al*., 2005). A possible musculoskeletal growth phenotype induced by the *CREBRF* missense variant, as seems to be indicated by recent reports, could comprise further exaggeration of an extant PI phenotype but perhaps awaits additional corroborating reports. Whether these effects might be played out in mass, functional capacity, or composition of muscle or bone remains to be tested in our KI mouse model as well as the relevant human populations.

The second major facet of the known *CREBRF* missense variant phenotype, namely a decreased diabetes risk (Minster *et al*., 2016; Hanson *et al*., 2019; Krishnan *et al*., 2020), similarly seems to be poorly recapitulated in the murine model. The missense variant in our KI mice had limited overall effect on glucose clearance during a glucose tolerance test in both male and female mice. Insulin tolerance testing in the male and female KI mice revealed that the blood glucose response to insulin administration is largely unaffected by the missense variant, and if anything hints at an induction of insulin resistance by the variant in chow-fed male animals, where there was an attenuation in insulin-induced effects. Taken together, this combination of minimally altered glucose homeostasis, unchanged basal levels of glucose or insulin, and the subdued response to

insulin which is seen in our male KI mice entirely fails to provide any overt reproduction of the human phenotype.

Comparatively few studies report on specific metabolic factors which may contribute to the human R457Q missense variant effects on diabetes. Minster *et al*. (2016) reported significantly lower fasting glucose levels (0.09 mM per variant allele) even in non-diabetic subjects, with the effect more pronounced after adjustment for BMI. No consistent correlations with either fasting insulin levels or HOMA-IR have been reported. Recent associations with higher HOMA-B and increased glucose-stimulated insulin release, without effect on insulin sensitivity or resistance, imply that the R457Q variant may enhance β-cell capacity for compensatory insulin secretion (Hanson *et al*., 2019; Burden *et al*., 2021). Hanson *et al*. (2019), however, indicate that this association was attenuated when adjusted for BMI; in normoglycemic overweight/obese men of Maori and Pacific ancestry, the association was significant for early phase insulin secretion consistent with T2D prevention (Burden *et al*., 2021). Others have recently speculated that, in humans, the protective effects against T2D and GDM may derive from the greater (height-related) muscle and bone mass that has been reported in variant carriers and predicted to enhance glucose disposal (Krishnan *et al*., 2020; Arslanian *et al*., 2021; Hawley *et al*., preprint). The similarly increased lean mass and length of our male KI mice seen without positive effects on glucose homeostasis does not align with this tenet, and deeper study would be needed to untangle the potential origins of the contrast between phenotypes displayed by mouse and human missense variant carriers. Indeed, it is possible that more challenging or different diet regimen, or an experimental model of induced T2D, might be required to reveal an underlying genotype effect in the KI mice (if one exists).

The initial theory proposed by Minster *et al.* (2016) to explain the phenotype seen in human variant carriers would expect the *CREBRF* variant to produce a "thriftier" balance between energy storage and expenditure. Our KI mice, however, did not present any whole-body impact of genotype on either heat production or respiratory exchange ratio measures when examined via indirect calorimetry. Nor did the protein expression of mitochondrial respiratory complex subunits in liver or quadriceps suggest any molecular change to oxidative phosphorylation in mice carrying the missense variant. The concept of the thrifty genotype is integrated with the fasting state, as a theorised evolutionarily

adapted mechanism to survive prolonged nutrient deprivation (Neel, 1962). Both wildtype and variant CREBRF have been shown *in vitro* to promote cell survival during nutritional stress (Minster *et al*., 2016). We therefore examined our KI mice following overnight fasting using biochemical measures as proxies for energy storage. Taken together, the combined fasting-induced trends in tissue glycogen and lipid contents, as well as plasma NEFA levels, imply that the missense variant may indeed have a role in regulating energy homeostasis during periods of nutrient deprivation.

The hint towards an exaggerated fasting response, observed in male mice carrying the double variant, is perhaps not sufficiently definitive to draw firm conclusions based on the current sample alone. Given that both the wild-type and variant *CREBRF* are induced by starvation, it does however seem logical that these conditions would promote greater activity and thus more overt genotype differentiation (Tiebe *et al*., 2015; Minster *et al*., 2016). The (wild-type) CREBRF response to nutrient deprivation follows mTORC1-independent cell stress signalling, to which it is particularly sensitive, in addition to signals mediated by mTORC1 inhibition (Minster *et al*., 2016; Tiebe *et al*., 2019). Indeed, the *Drosophila* ortholog mediates the downstream transcriptional response triggered by TORC1 inhibition, and its absence renders flies more sensitive to starvation (Tiebe *et al*., 2015). A missense variant-induced differentiation in the fasting response, on tissue or organismal scales, may also contribute to effects on glucose disposal or insulin response, if not potentially longer-term effects on bioenergetics. Given the relatively minor effect size in our KI mice, however, speculation may be strengthened by investigation of a greater sample size to improve experimental power, or perhaps of a more severe deprivation protocol than the overnight fast used in the current study. Modelling extreme nutritional stress, for example through a starvation period greater than 24 hr, or until significant weight loss is achieved, may be required to potentiate any physiological manifestation of the theorised evolutionary adaptation to starvation (Jensen *et al*., 2013; Kanshana *et al*., 2021). Alternately, the wildtype CREBRF association with circadian rhythm may warrant closer attention to oscillation of parameters during the fasting period (Frahm *et al*., 2020).

The male R458Q KI mice exhibited genotype effects only when fed the regular chow diet. Phenotypic differentiation between WT and HOM animals was neither exacerbated nor even retained following HFD challenge. In contrast, the human variant phenotype was

theorised to have emerged as a consequence of the modern obesogenic environment but now seems to appear irrelevant of diet or nutritional environment exposures (which tends not to be specifically reported but is implied in the highly heterogeneous recruitments of study participants). Loos (2016) speculates that the predisposition to greater BMI in variant carriers, given that it is established early in life, is perhaps not further increased by dietary or other environmental stimuli throughout later years; but there is no indication that the phenotype is not retained in such an environment. It is possible that this discrepancy between human and murine variant carriers may be partially contributed to by diet composition. An HFD with fat content from coconut oil, more appropriate to the traditional PI diet, can produce metabolic effects in rodents different from those which are induced by a lard-based HFD such as that which was used in our study (Turner *et al.*, 2009; Montgomery *et al*., 2013; Zicker *et al*., 2019; Ströher *et al*., 2020). Such differences could potentially influence any interaction between genotype and environment in the KI mice.

The male KI mice, if not humans, appear to experience an approximation of such interaction in the key phenotypic measures. This was most apparent in the ITT, where the blood glucose response was significantly dampened by HFD-feeding in WT animals and yet unchanged between HOM diet groups. It is perhaps worth acknowledging in this context that the heightened insulin levels during an ITT far exceed those which would typically be experienced during normal physiological fluctuations, for example increased postprandial secretion, and the results in this framework are accordingly distanced from being a true mirror of physiological effect. The combined effect is perhaps insufficient to assert any true protective effect against HFD-induced defects in metabolic outcomes in carriers of the double variant. Given that diet is rarely noted in human variant studies, its interaction with the variant cannot be directly compared as for the KI mouse model. Meta-analysis has however shown that the protection against T2D in humans is greater for variant carriers without obesity than those with obesity (Russell *et al.*, preprint). In genotype-stratified groups, only the double variant carriers did not exhibit a significant association between BMI and higher T2D odds (although this result was statistically under-powered due to the low T2D case load in that group). It is perhaps feasible, therefore, that the variant phenotype is in some way influenced by nutritional environment (or its impacts on body composition) even if this interaction does not play out the same way in mice and humans.

The phenotypic effects seen with the missense variant in our male KI mice developed with age. The proposed male growth phenotype was reflected at the earliest timepoint in greater naso-anal length of male mice aged 8 weeks; increased lean mass emerged in variant carriers initially at 12 weeks and developed further in subsequent weeks as animals aged. These effects on body composition preceded the variant-induced altered metabolic outcome seen in the ITT at 17 weeks of age (an effect which was wholly absent in younger mice). This development of phenotype throughout the study time-course invites the question of further genotype differentiation appearing in older mice, beyond our 20-week endpoint. The comparatively early effect on body composition perhaps indicates that this may be the primary operation of the missense variant in these mice. In humans, phenotypic differentiation during childhood is similarly based in alterations to body composition (Minster *et al.*, 2016; Berry *et al*., 2018; Arslanian *et al*., 2021; Oyama *et al*., 2021). The greater lean mass seen in variant carriers during infancy developed with time and Arslanian *et al*. (2021)'s prediction that BMI effects might emerge as the children grow older seems to be borne out in the later report of a lean mass-driven increase to BMI in adult variant carriers (Hawley *et al*., preprint). Perhaps the murine and human missense variant phenotypes impact body composition independent of interaction between genetic and environmental factors and prior to influence over metabolic outcomes. Even partial dependence on age or age-related metabolic condition might, however, confuse manifestation of the missense variant phenotype and thus contribute to conflicting reports.

The missense variant phenotype in our KI mice had striking sexual dimorphism. Genotype effects were observed only in males, presenting a wholly disparate response in addition to the more standard sex differences which were seen even between the wild-type animals for all measures taken. In contrast, human studies have reported variant-associated phenotypes in both men and women, although association analyses are commonly adjusted for sex, perhaps due to limited sample sizes. Stratification by sex has shown that effect sizes may differ between males and females but statistical interaction between sex and genotype, when tested, is typically not seen (Krishnan *et al*., 2018; Carlson *et al*., 2020; Metcalfe *et al*., 2020). Berry *et al*. (2018) did however show a significant interaction between variant and sex in New Zealand resident children for both weight and zBMI at four years of age. Hawley *et al*. (preprint) have most recently reported an effect on fat mass which is significant only in women, as well as a male-specific effect

on height. Biological sex may, therefore, selectively influence aspects of missense variant function in human carriers without the magnitude of the murine dimorphism. The underlying basis for the lack of phenotype replication in the female KI mice could perhaps, if identified, aid our understanding of *CREBRF* variant action.

Body composition and biological sex are well-known to interact. Metabolic effects are at least partially regulated by sex hormones and by chromosomal complement (Nielsen *et al.*, 2003; Al-Qahtani *et al*., 2017; Reue, 2017; Reusch *et al.*, 2018). Indeed, sexual dimorphism of body composition produces greater total lean mass, lower total fat mass, and larger, stronger bones in adult human males compared to females (Wells, 2007a). The pattern is perhaps not wholly unlike that associated with the CREBRF missense variant, which likewise increases lean mass and height (or length) most prominently in males while greater impacts on fat mass are seen in human women (Metcalfe *et al.*, 2020; Hawley *et al*., preprint). Indeed, CREBRF itself has likewise been associated with sex steroid hormones oestradiol and progesterone (Yang *et al.*, 2013b; Yang *et al*., 2018). Its primary target CREB3 interacts with the androgen receptor and appears to have a role in modulating steroidogenesis and testosterone levels, and perhaps therefore maintenance of secondary sex characteristics (Zhao *et al*., 2016; Penney, 2017; Wang *et al*., 2019). Both the CREBRF and CREB3 knockout mouse lines are reported to possess significant fertility defects (Penney, 2017). On these grounds, therefore, the CREBRF missense variant might legitimately have direct or indirect interactions underlying the sex-dependence seen in our KI mice. Further research might be warranted to develop this dimorphic link to understand its consequences and/or origins in human as well as murine carriers of the missense variant.

In conclusion, comprehensive metabolic phenotyping of mice harbouring the *CREBRF* R458Q variant revealed only limited effects of the mutation, which did not reproduce either the increased obesity or decreased diabetes risk initially reported in human variant carriers. The presence of clear but non-significant trends may encourage possible phenotypic manifestation in nutritional challenge contexts with greater experimental power. Translational discrepancies, which perhaps limit the model's utility for elucidation of mechanisms, may reflect the more complex and multifactorial nature of the metabolic interactions which are present in humans. The influence of these interactions on the

CREBRF missense variant likely necessitates a more challenging protocol to reproduce or understand the phenotypic consequences in this mouse model.

CHAPTER 4: Tissue Transcriptome Profiling of CREBRF R458Q Knock-In Mice

4.1 INTRODUCTION

Gene expression programmes underpin molecular response to short- and long-term environmental and/or physiological stimuli. Coordinated modulation of transcriptional activity thereby drives biological processes and ultimately links genotype to phenotype. This activity drives expression of not only messenger RNA (mRNA), synthesised from protein-coding genes and destined for ribosomal translation and proteome function, but also non-coding RNA (ncRNA). The latter classification includes ribosomal (rRNA), transfer (tRNA), small nuclear (snRNA), small nucleolar (snoRNA), micro (miRNA), and long non-coding (lncRNA) RNAs. Although traditionally considered to be non-functional "junk" RNA, ncRNAs have important roles in development, physiology, and pathology (Amaral *et al*., 2013; Bhatti *et al*., 2021). Alternative splicing of gene exons facilitates further heterogeneity (Kalsotra & Cooper, 2011). RNA synthesis and maturation are tightly regulated in order to maintain genetically encoded response networks, which are both robust and plastic, resilient and adaptive. Dynamic remodelling of the transcriptome is key to adaptation and transgenerational inheritance, fuelling phenotypic variation and evolutionary change, as well as more immediate biological signalling (López-Maury *et al*., 2008; Amaral *et al*., 2013). Measurement of the transcriptome therefore promises the chance to analyse these gene expression networks.

Progressive technological advances have produced numerous experimental approaches to study variation in gene expression. Two of the most commonly utilised are RNA sequencing (RNA-Seq) and microarray techniques. These have individual strengths and weaknesses—microarrays can, for example, more stably detect alternatively spliced genes—but both offer generally consistent and complementary results (Chen *et al.*, 2017; Nazarov *et al.*, 2017). The contributions of these developing transcriptomic techniques to scientific understanding of RNA biology and genetically encoded signals are more fully reviewed elsewhere (Stark *et al*., 2019; Longo *et al*., 2021). Transcriptomic profiling is typically used to identify differentially expressed gene transcripts as well as differentially spliced mRNAs, and thereby characterise overrepresented clusters or pathways in specific tissues or indeed single cells (de Klerk & 't Hoen, 2015; Aldridge & Teichmann, 2020). Consequent analyses offer biological insight into phenotypic differentiation, aiding

identification of genes and regulatory mechanisms associated with particular traits. Such techniques would be accordingly valuable in elucidating the CREBRF missense variant phenotype on a molecular level, with no transcriptomic data yet published in current literature despite grounds for a potentially direct influence on gene expression.

CREBRF activity can be reasonably expected to impact the transcriptome. Any variation to the protein's action would logically likewise alter gene expression. The mechanism behind such transcriptomic effects is, however, somewhat uncertain. The CREBRF protein is reported to contain an apparently potent transactivation domain at its N-terminus, suggestive of a capacity to stimulate gene expression in its own right as a putative TF (Audas *et al*., 2016). Subcellular localisation studies provide further indication of a role in transcription activation or repression. *In vitro*, CREBRF is present within the nucleus under conditions of active transcription; it is relocated to the cytoplasm when transcription is pharmacologically inhibited (Audas *et al*., 2016). This implied transcriptional influence appears able to produce whole-body *in vivo* impacts: the phenotypic effect seen in *Drosophila* lacking the CREBRF ortholog, REPTOR, is at least partially underpinned by an altered gene expression pattern (Tiebe *et al*., 2015). Even without such evidence that CREBRF may act as a genuine TF, it possesses an indirect regulatory role on transcription via its suppressive action on CREB3 and the GR (Martyn *et al*., 2012). These TFs, which possess their own regulatory relationship seemingly independent of CREBRF, contribute to the regulation of multiple cellular and systemic processes. Some of these processes also implicate CREBRF in their action and may therefore be indicative of likely transcriptomic consequences.

Cell and animal models demonstrate some thematic overlap in CREBRF and CREB3 transcriptomic effects. Among these commonalities is a role in the anti-viral and immune response. CREBRF sub-nuclear foci are thought to mediate repression of genes necessary for viral proliferation, an action dependent on CREBRF transactivation potential (Audas *et al*., 2016). CREB3 physically interacts with viral proteins to likewise prevent viral gene transcription and attenuate lytic infection (Lu *et al*., 1997; Lu *et al*., 1998; Blot *et al*., 2006). The individual anti-viral transcriptomic effects seem to be of sufficient impact to attract targeting by viral proteins for disruption (Jin *et al*., 2000; Blot *et al*., 2006; Audas *et al*., 2016). As a TF, CREB3 additionally promotes immune response through increasing chemokine receptor gene transcription as well as maturation of the professional antigen-

presenting dendritic cells (Sung *et al*., 2008; Eleveld-Trancikova *et al*., 2010; Kim *et al*., 2010a). It also dose-dependently enhances NF-κB-mediated gene activation (Jang *et al*., 2007a, 2007b). Some CREB3 gene targets are, however, known to promote viral replication, and the heightened CREB3 nuclear expression and transcriptional activity which is induced following HSV-1 and HCV infection may therefore have ambiguities (Zhang *et al*., 2017b; Yadavalli *et al*., 2020). Both CREBRF and CREB3 impact gene expression during viral infection, suggesting that even this limited example of their independent activities can produce observable influence on the transcriptome.

The interconnected branches of a theorised CREBRF-related transcriptional network can also converge at specific focal points. One critical example is forkhead box protein O1 (FoxO1), a TF thought to be a downstream gene target of both CREB3 and the GR (Qin *et al.*, 2014; Zeng, 2015). Its closely regulated action is induced in states of energy deprivation, and associated with energy metabolism, particularly in insulin-responsive tissues. In skeletal muscle, FoxO1 regulates muscle differentiation and fibre typing specification, resulting in atrophy (Kamei *et al.*, 2004; Xu *et al*., 2017). In liver, FoxO1 drives upregulation of gluconeogenesis, such that blocking FoxO1 nuclear expression can lower blood glucose and combat hyperglycaemic diabetes (Zhang *et al*., 2006; Mihaylova *et al*., 2011; Ozcan *et al*., 2012). Although the GR has elsewhere been decisively linked to FoxO1 (Waddell *et al*., 2008), direct functional evidence connecting FoxO1 and CREB3 is limited. Penney (2017) suggests that dysregulated FoxO1 signalling in CREB3-KO mice, alongside differentially expressed candidate nutrient sensors, mediates the increased blood glucose concentration seen in that model.

The relationship between CREBRF and FoxO1, outlined primarily in *Drosophila*, is perhaps the most crucial of the interactions yet described here. REPTOR, the CREBRF ortholog, is a validated FOXO gene target (Teleman *et al*., 2008), but the relationship is otherwise more of mimicry than regulation. Flies which lack REPTOR show a whole-body phenotype which parallels that seen in FOXO knockout animals, including a strongly reduced lifespan (Tiebe *et al*., 2015). Double-KO mutants die as larvae, suggesting that the function of these proteins is not merely overlapping but perhaps redundant. Tiebe *et al*. (2015) further provide the most conclusive published evidence that this CREBRF ortholog can itself act as a TF, together with its binding partner (REPTOR-BP), the Crebl2 ortholog. REPTOR-dependent gene expression reveals that

the REPTOR/REPTOR-BP complex likely binds the same enhancer regions as FOXO, with the FOXO-binding motif being the most enriched in the dataset (Tiebe *et al*., 2015). Indeed, 40% of the REPTOR gene targets are also targeted by FOXO. No studies have yet explored this exact relationship outside *Drosophila*, but CREBRF and CREBL2 have been shown to interact in mice (Tiebe *et al*., 2019). The transcriptional effects may feasibly be likewise preserved across species.

The transcriptional activity of CREBRF (and REPTOR) appears closely bound to the metabolic response to stress conditions. For REPTOR, complexed with its binding partner, this activity is primarily visible in a state of nutrient deprivation. Active TORC1 blocks nuclear accumulation of REPTOR; when this repression is released, the active REPTOR/REPTOR-BP transcriptional complex helps mediate the downstream signalling pathway which is triggered by TORC1 inhibition (Tiebe *et al*., 2015). In S2 cells, targeting this pathway revealed nearly 200 genes which are induced by rapamycin and dependent upon both components of the REPTOR/REPTOR-BP complex. Similar quantities are dependent on either component individually. The rapamycin-induced transcriptional response in *Drosophila* is significantly stifled in REPTOR-KO larvae, only sharing approximately 10% of the genes differentially regulated in control animals. Tiebe *et al.* (2015) thus propose that REPTOR might target stress response genes to act as a metabolic brake; the known convergence in FOXO and TOR signalling links these closer (Teleman *et al.,* 2008). This transcriptional activity may underlie the starvation- and rapamycin-induced increases in CREBRF expression which are reported in multiple cell models, as well as explain the associated effects on cellular energy conservation and utilisation (Minster *et al*., 2016; Tiebe *et al*., 2019). Both REPTOR and CREBRF, using knock-out and overexpression models respectively, are shown to aid survival during nutritional stress (Tiebe *et al*., 2015; Minster *et al*., 2016). If the CREBRF transcriptional impact can be connected with phenotypic response, further investigation of that conjunction is therefore warranted.

The stress- and nutrient-responsive transcriptional functions which are associated with CREBRF suggest its likely involvement in key peripheral tissues which contribute to metabolic homeostasis. Indeed, the CREBRF cofactor, Crebl2, was recently shown to regulate lipid and glucose metabolism in both muscle and liver cells, with cell type-specific impacts (Tiebe *et al*., 2019). It is probable that the CREBRF missense variant,

which is likewise thought to influence substrate metabolism and storage (Minster *et al*., 2016), also acts within muscle and liver on an organismal scale in response to similar nutritional or energetic stress conditions. The potential impacts of this variant on WT transcriptional function, either direct or indirect, have not previously been examined in published literature. In this chapter, therefore, the primary aim was to characterise the tissue transcriptomes of fasted WT and HOM KI mice in gastrocnemius muscle and in liver. We sought to thereby gain insights into molecular signalling pathways or functions which might be impacted by presence of the R458Q variant during nutritional stress including possible tissue-specific influences and/or correlation with known CREBRF regulatory functions.

4.2 METHODS

4.2.1 Transcriptome microarray expression profiling

Transcriptome expression profiling was performed on muscle and liver tissues taken from randomly selected 20-week-old male and female *CREBRF* R458Q gene variant mice (WT and HOM) characterised in Chapter 3, after overnight fast intended to provoke nutrient stress conditions conducive to the metabolic suppression in which CREBRF is implicated. In the absence of any initial muscle-specific phenotype data for the KI mice, the gastrocnemius, as a large hindlimb muscle important for locomotion with mixed fibre type distribution, was taken for this analysis. Dissected tissue samples were immediately snap-frozen in liquid nitrogen and stored at -80°C prior to transport to the University of Auckland, New Zealand for RNA extraction and microarray analysis.

Extracted RNA samples were analysed using Clariom™ D mouse assays (Applied Biosystems™, Thermo-Fisher), covering >214,000 transcripts in >66,100 genes to facilitate both exon- and gene-level expression profiles. Microarrays were processed and analysed according to manufacturer's instructions. Briefly, raw microarray data were extracted from fluorescence intensities before pre-processing and normalisation using the signal space transformation-robust multiarray analysis (SST-RMA) algorithm method. Detection above background p-values were computed. Splicing index was defined as the log2 ratio of exon to gene intensity.

Probe sets for uncharacterised LOC transcripts or with gene name absent were excluded from further analyses. Probe sets were ascribed chromosome location according to Mouse Genome Informatics (MGI), using reference genome Build 39. Predicted genes or pseudogenes which were not present in this resource, utilised as a proxy for irrelevance, were excluded. Where microarray typing of transcripts conflicted with MGI annotation, the more up-to-date MGI resource was used.

4.2.2 Gene set enrichment analysis (GSEA)

For biological interpretation of these transcriptomic data, gene set enrichment analysis was performed to identify enriched processes, functions, and/or pathways within the set of differentially expressed genes which met our established criteria ($p < 0.05$, fold change > 1.2 or SV > 5). Functional annotation analyses used the Database for Annotation, Visualisation and Integrated Discovery (DAVID, [https://david.ncifcrf.gov/home.jsp] v.6.8) and the Search Tool for the Retrieval of Interacting Genes/Proteins (STRING)

database [www.string-db.org] (Szklarczyk *et al*., 2019). Enriched KEGG (Kyoto Encyclopaedia of Genes and Genomes) pathways and gene ontology (GO) biological process (BP) terms were extracted from both databases (Ashburner *et al*., 2000; Kanehisa *et al*., 2017). The DAVID pathway viewer was used to display genes from selected enriched pathways on KEGG pathway maps to facilitate biological interpretation of response networks. STRING was used to identify and display interaction relationships between encoded proteins.

The DAVID analysis used a modified Fisher's Exact test to measure gene enrichment in annotation terms, with *p*-values further adjusted for approximate control of the false discovery rate (FDR) using the adaptive linear step-up lowest slope method. Functional annotation clustering parameters set classification stringency at 0.70 and EASE score at 0.05. The STRING analysis used FDR-corrected *p*-values calculated via the Benjamini-Hochberg method. The minimum required interaction score was set at "high confidence" (0.700). Clustering via the Markov Cluster (MCL) algorithm used an inflation value of 1.7, according to the calculated optimal trade-off between sensitivity and positive predictive value (Brohée & van Helden, 2006).

4.3 RESULTS

4.3.1 Genomic profile overview

CREBRF has been associated with nutrient-sensitive transcriptional regulation of metabolism but this has not been investigated in the context of the missense variant (Tiebe *et al*., 2015; Minster *et al*., 2016; Tiebe *et al.*, 2019). The current study therefore examined the transcriptome of gastrocnemius and liver tissues from fasted mice carrying the CREBRF R458Q variant. Visualisation of global transcriptomic trends by principal component analysis (PCA) showed distinct separation of sex-based clusters in both gastrocnemius and (more prominently) liver tissue samples (Figure 4.1). This overall difference between the transcriptomes of male compared to female mice was reinforced by differing degrees of genotype dependence. The gastrocnemius tissue transcriptome demonstrated clear genotype separation in the male samples which was not similarly defined in females (Figure 4.1A,C). Genotype groups did not strongly cluster in liver but were marginally tighter in male samples (Figure 4.1B,D). Overall, the PCA suggested that any trend for remodelling of the transcriptome in response to the CREBRF missense variant was most visible in the male mice and further analyses therefore concentrated on these data.

Microarray analysis identified 2380 probes in gastrocnemius tissue, and 1890 in liver tissue, with significant differential expression in the R458Q HOM compared to WT mice. Following the exclusion of probes which lacked gene names, referred to uncharacterised loci, or could not be attributed to the reference genome, transcript mapping to chromosomes did not reveal any particular genomic origins of the variant-induced changes, although chromosome 19 was perhaps overrepresented among protein-coding genes in both tissues (Figures 4.2A, 4.3A). Refined datasets included 1798 differentially expressed genes (DEGs) in gastrocnemius and 1154 in liver. This quantitative disparity between tissues mirrored the PCA genotype clustering effects, and furthermore had no considerable overlap between specific transcripts. 134 transcripts (4.4%) were differentially expressed in both gastrocnemius and liver tissues, of which 77 were regulated in opposing directions.

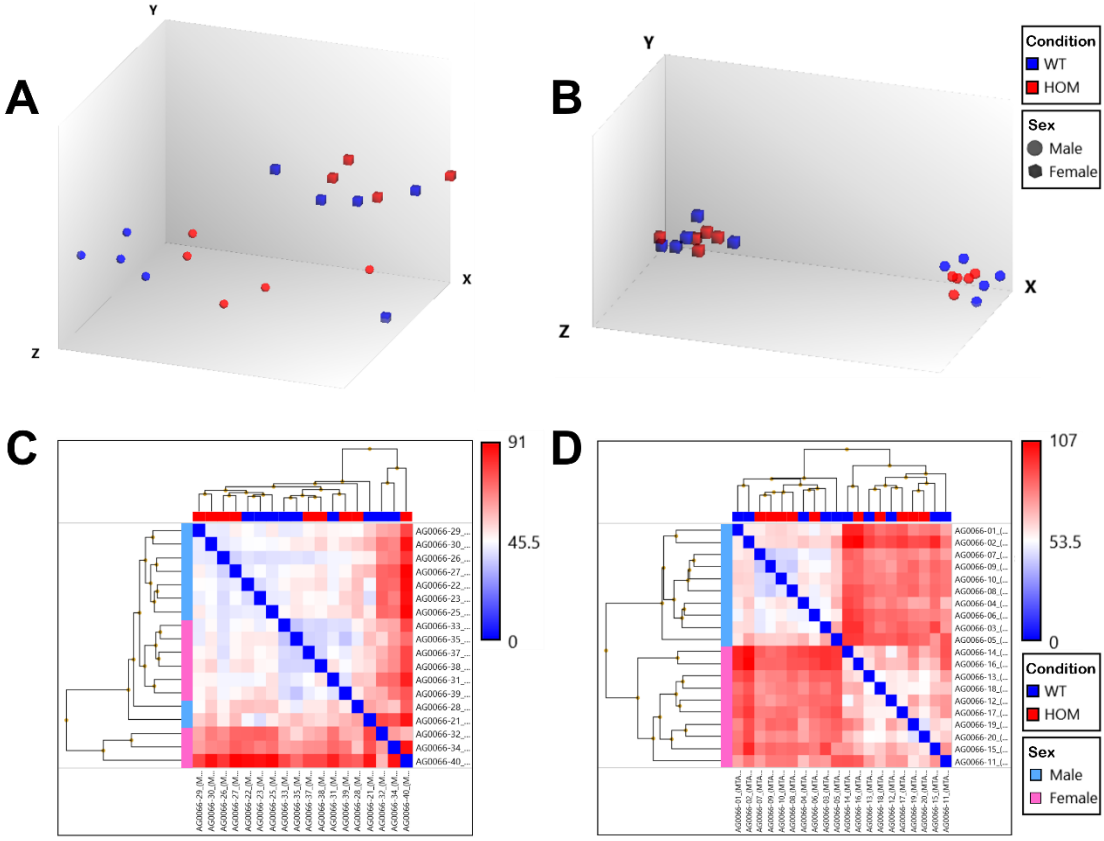

Figure 4.1: Principal component analysis of differentially expressed transcripts in CREBRF R458Q variant mice.

A-B. Cluster plots of (A) gastrocnemius and (B) liver tissue PCA, separating male (spheres), female (cubes), WT (blue) and HOM (red) samples (n = 4-5). **C-D.** Hierarchical clustering heatmaps for (C) gastrocnemius and (D) liver samples, indicating degrees of difference between samples. Images provided by Dr Kate Lee, University of Auckland.

The missense variant-induced changes in gastrocnemius tissue were classifiable as 28% protein-coding genes and more than 50% ncRNA genes (Figure 4.2). The latter group was comprised primarily of snRNA, snoRNA, and rRNA transcripts but also included miRNA and lncRNA. These had distinct expression patterns: protein-coding and pseudogene transcripts were each 80% downregulated in HOM gastrocnemius, while the snRNA, snoRNA, and rRNA transcripts were each more than 95% upregulated and together represented 70% of the total upregulation in this tissue. Protein-coding genes of the R458Q liver transcriptome comprised more than 60% of the total changes, with less than 8% represented by the three major ncRNA groups together (Figure 4.3). These distinct transcriptomic profiles showed tissue-specific results which were therefore assessed separately between tissues and transcript types.

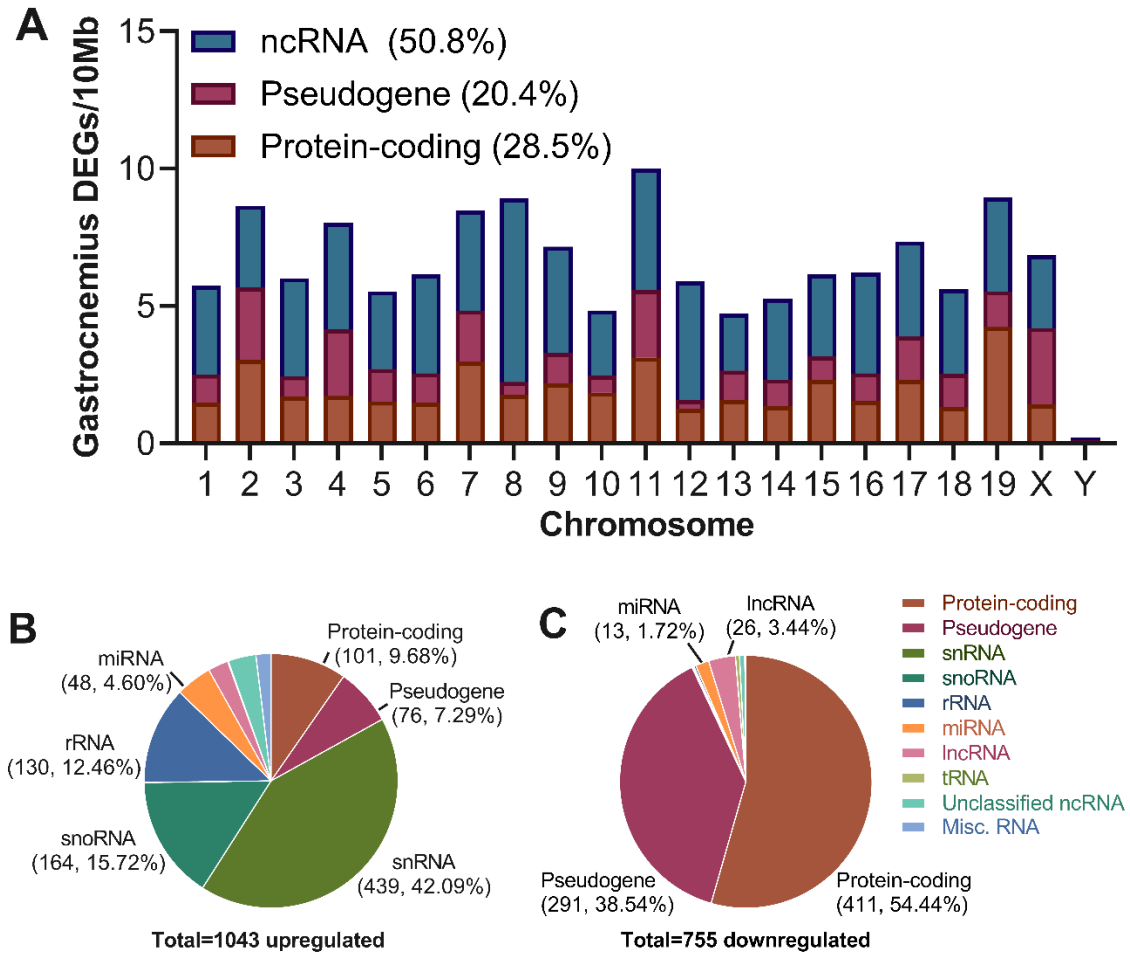

Figure 4.2: Genomic profile of male R458Q gastrocnemius muscle tissue.

A. Chromosome distribution of significant DEGs, presented as number of protein-coding, pseudogene, and ncRNA transcripts per 10Mb, in gastrocnemius (*n* = 4-5 per genotype). **B-C.** Proportional breakdown of (B) upregulated and (C) downregulated transcripts by RNA classification. lncRNA also includes antisense and intronic lncRNA transcripts. Misc. RNA includes ribozyme, RNase RNA, scRNA, SRP RNA genes and gene segment transcripts. Does not depict the 5 differentially expressed tRNA genes from the mitochondrial genome, which are not included in the percentage values.

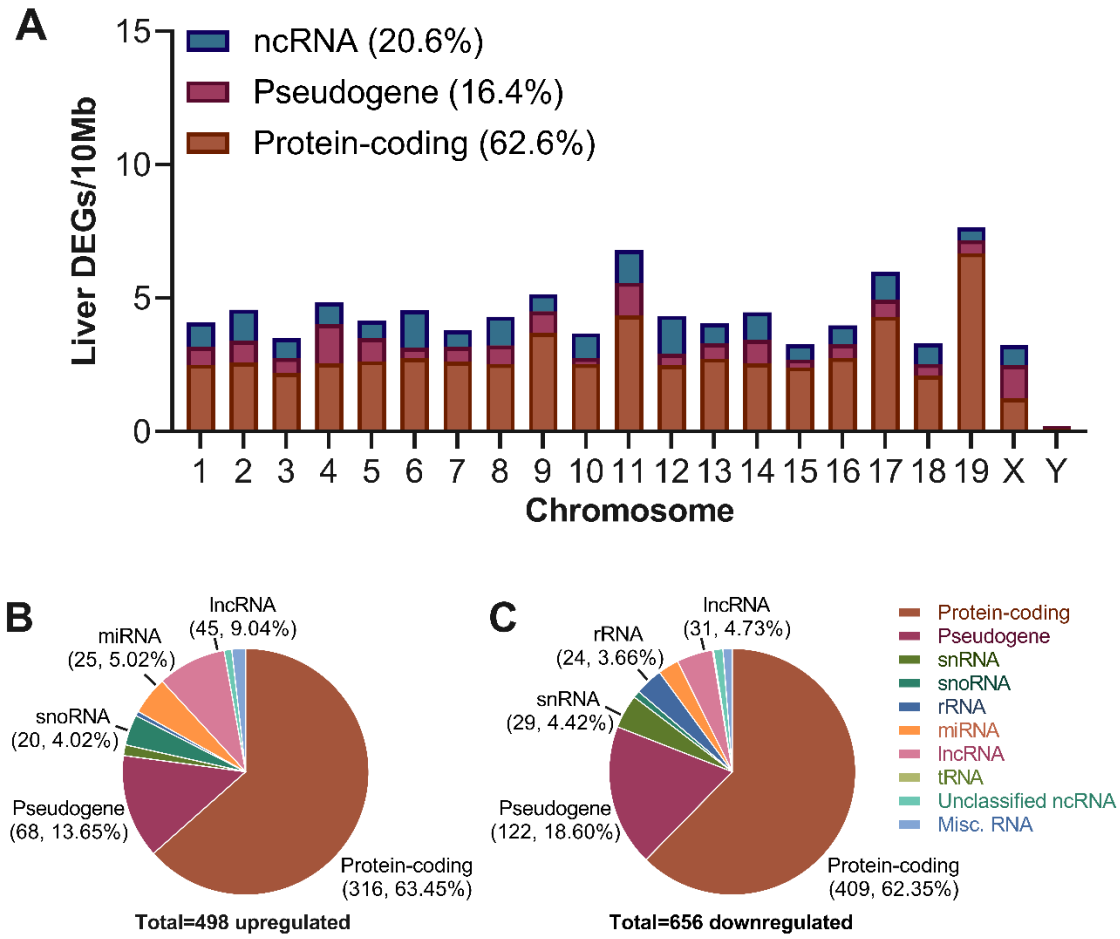

Figure 4.3: Genomic profile of male R458Q liver tissue.

A. Chromosome distribution of significant DEGs, presented as number of protein-coding, pseudogene, and ncRNA transcripts per 10Mb, in liver (*n* = 5 per genotype). **B-C.** Proportional breakdown of (B) upregulated and (C) downregulated transcripts by RNA classification. lncRNA also includes antisense and intronic lncRNA transcripts. Misc. RNA includes ribozyme, RNase RNA, scRNA, SRP RNA genes and gene segment transcripts.

4.3.2 ncRNA transcript expression

The abundance and highly tissue-selective distribution of ncRNA transcripts which were differentially expressed in R458Q mice encouraged closer examination of these genotype-dependent targets. Analysis was necessarily somewhat limited by the predicted gene model (Gm) transcripts, identified by sequence comparison and typically poorly characterised without clear functional evidence, which comprised 57% of the gastrocnemius and 29% of the liver gene sets in the current study. These Gm transcripts were heavily concentrated in the snRNA, snoRNA, and pseudogenes categories in the gastrocnemius.

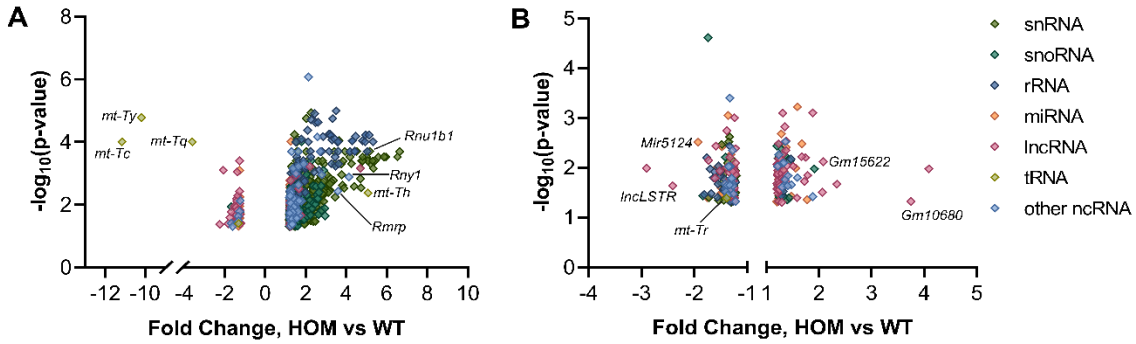

Figure 4.4: Differentially expressed ncRNA gene transcripts in male R458Q tissues. Significantly up- and down-regulated ncRNA transcript expression in **(A)** gastrocnemius and **(B)** liver tissues is plotted as fold change against -$\log_{10}$(p-value). Transcripts are classified as snRNA (dark green), snoRNA (teal), rRNA (dark blue), miRNA (orange), lncRNA (pink), tRNA (light green), and other ncRNA (light blue) according to MGI annotation of reference genome build 39.

Transcripts classified as small nuclear RNA (snRNA) were the most abundant ncRNA type, comprising nearly 25% of all differential expression in the gastrocnemius tissue where only one snRNA transcript was downregulated (Figure 4.4A). Only six of these 440 snRNA genes were named rather than predicted: *Rnu1a1*, *Rnu1b1*, *Rnu1b2*, *Rnu1b6*, *Rnu11*, *Rnu12*. Small nucleolar RNA (snoRNA) transcripts represented 9% of total differential expression, again with only a single downregulated transcript. The 38 named snoRNAs included H/ACA and C/D boxes as well as small Cajal body-specific RNA. Known snRNAs and snoRNAs act on other RNA molecules, demonstrating a strong and largely unidirectional influence of the R458Q variant on these spliceosome and RNA pre-processing activities in the gastrocnemius. The hepatic transcriptome, in contrast,

included only 36 Gm-predicted snRNA transcripts (3%) which were primarily downregulated in HOM animals (Figure 4.4B). Hepatic snoRNAs were likewise less impacted, comprising 26 transcripts (2%) which showed >75% upregulation in the presence of the missense variant.

The 132 differentially expressed rRNA gene transcripts in gastrocnemius tissue, representing 7% of the total, demonstrated distinct transcriptional targeting of 5S rRNA in CREBRF variant carriers (>98% upregulated). Many of these genes, found as neighbouring clusters on chromosome 8, appear coregulated and cannot be distinguished in Figure 4.4A where they share both fold-change and significance values (48 transcripts concentrated within 7 shared values). Given that 5S rRNA is transcribed exclusively by RNA polymerase III (Pol III), the R458Q transcriptome was examined for additional targets of this polymerase. These included the scRNA genes *Rny1* and *Rny3*, encoding ribonucleases, the RNase MRP and RNase P RNA genes *Rmrp* and *Rpph1*, and the SRP RNA genes *Rn7s1* and *Rn7s2*, all of which were likewise upregulated in R458Q gastrocnemius. Similar examination of the R458Q liver transcriptome demonstrated fewer affected genes, of which 89% showed negative rather than positive fold-changes, compared to gastrocnemius (Figure 4.4B). There was, however, similar emphasis on Pol III transcriptomic targets in particular 5S rRNA, *Rpph1*, and *Rny1*/*3*. The six tRNA transcripts differentially expressed in HOM mice were encoded in the mitochondrial genome, with the (downregulated) neighbouring *mt-Tc* and *mt-Ty* genes the most significantly impacted.

Differentially expressed miRNA transcripts comprised less than 4% of the total alteration to gene expression in either gastrocnemius or liver tissues and largely could not be associated with well-characterised biological functions or molecular interactions. Taken collectively, genotype-dependent expression of miRNA transcripts lacked any concerted directional or (characterised) functional trends. The *Drosha* and *Ago1*/*2* genes, although not themselves ncRNA, encode proteins required for maturation of precursor miRNA and were differentially expressed in variant mice. Differentially expressed lncRNAs similarly did not demonstrate concerted up- or down-regulation (Figure 4.4). Very few of the 53 gastrocnemius and 75 liver lncRNA transcripts have been associated with known biological function (Table 4.1). Survey of neighbouring genes suggested potential coregulation of hepatic lncRNAs with *Herpud1*, *Vamp1*, *Ngef*, *Fnip2*, and *Dph6* mRNA

transcripts on the same DNA strand, and *Stip1*, *Hist2h3b*, *Hist2h3c2*, *Slc25a33*, *Gck*, and *Apoa4* mRNA transcripts on the opposite strand.

Pseudogenes comprised 15-20% of the genotype-dependent changes to transcript expression in each tissue. Although these genomic regions have typically been defined as containing defective copies of genes, lacking functional protein-coding potential and consequently often excluded from transcriptomic analyses, more recent evidence indicates multiple protein-, RNA-, and DNA-based mechanisms by which pseudogenes can play biological roles (Cheetham *et al*., 2020). We therefore included these transcripts in analysis of the current study. Indeed, of the 60-70% of predicted pseudogenes in each gastrocnemius and liver which were matched to their parent genes, more than 25% mimicked the differential expression of that parent gene within the same tissue.

Table 4.1: Differential expression of lncRNA genes with known functions in male R458Q tissues.

Gene ID	Fold change	Function	Reference
Gastrocnemius			
Dubr	-1.27	Positive regulation of myogenesis	(Wang *et al*., 2015b)
Liver			
C730036E19Rik	-2.41	Liver lipid and fasting metabolism	(Batista *et al*., 2019)
Gm11967	-1.26	Fasting metabolism; PPARα	
Gm15622	2.08	Liver lipid metabolism; SREBP1C	(Ma *et al*., 2020)

4.3.3 Gastrocnemius GSEA

The CREBRF missense variant was associated with significant differential expression of 512 protein-coding and 367 pseudogene transcripts in the gastrocnemius, represented in Figure 4.5. Largest positive fold changes among protein-coding transcripts in HOM animals were seen for *Trim63*, *Tmem140*, *Cyr61*, *Pnpla2*, and *Phaf1*. Greatest downregulation was shown by *Nr4a1*, *Mpz*, *Irs2*, *Slc25a25*, and *Bcl6*. Transcripts showing differential expression with greatest statistical significance included *Atp5g2*, *Ndufa3*, *Babam1*, *Rpl28*, and *Eif3k*.

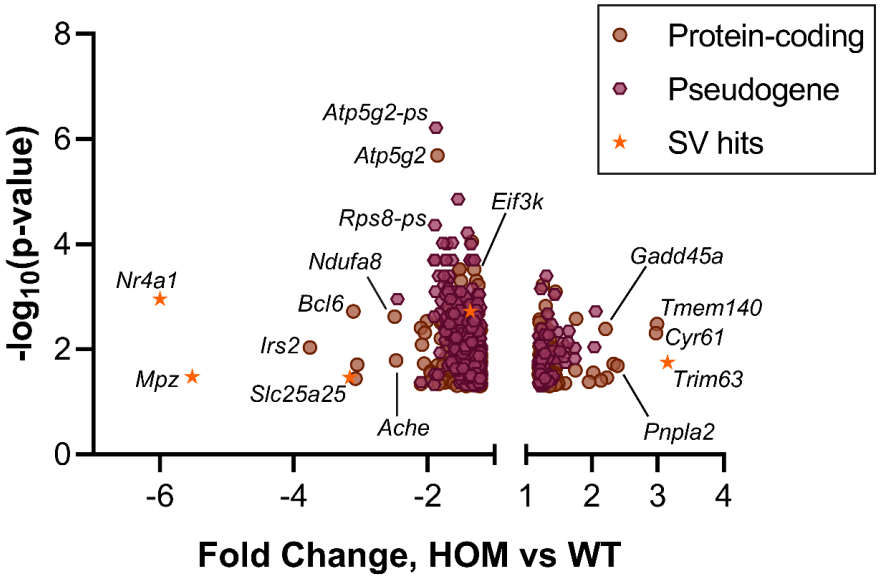

Figure 4.5: Differential expression of protein-coding and pseudogene transcripts in male R458Q gastrocnemius.

Significantly up- and down-regulated expression of protein-coding (brown) and pseudogene (maroon) transcripts are plotted as fold change against -$\log_{10}$(p-value). DEGs also showing significant alternate splicing are represented using stars. Key genes showing greater fold-change or significance are labelled.

Annotation of transcriptomic data via GSEA on the basis of shared biological or functional properties was performed using both DAVID and STRING aggregative resources, which utilise differing parameters for gene/protein networks components, to promote stringency and maximise coverage of gene and pathway reference databases. Significant overrepresentation in KEGG pathways or GO terms was used to indicate a possible functional profile of the transcriptional alterations seen in R458Q variant tissues.

Table 4.2: Enriched KEGG pathways for gastrocnemius DEGs in male CREBRF R458Q missense variant mice.

Pathway ID	Pathway Description	DAVID				STRING_DB		
		Count	Fold enrichment	*p*-value	FDR	Count	Strength	FDR
Downregulated DEGs								
mmu03010	Ribosome	17/145	5.37	**8.13e-8**	**1.43e-5**	21/128	0.92	**2.51e-10**
mmu05010	Alzheimer's disease	17/177	4.40	**1.27e-6**	**1.12e-4**	14/167	0.63	**6.5e-4**
mmu05016	Huntington's disease	17/198	3.93	**5.55e-6**	**3.26e-4**	15/187	0.61	**6.5e-4**
mmu00190	Oxidative phosphorylation	14/139	4.61	**9.07e-6**	**3.99e-4**	13/129	0.71	**3.9e-4**
mmu05012	Parkinson's disease	14/149	4.30	**1.93e-5**	**6.80e-4**	12/138	0.64	**1.2e-3**
mmu04932	Non-alcoholic fatty liver disease (NAFLD)	13/157	3.79	**1.47e-4**	**4.32e-3**	11/146	0.58	**7.0e-3**
mmu04714	Thermogenesis	-	-	-	-	16/223	0.56	**7.2e-4**
mmu04550	Signalling pathways regulating pluripotency of stem cells	8/138	2.65	**3.04e-2**	0.729	-	-	-
mmu01100	Metabolic pathways	38/1269	1.37	**3.31e-2**	0.729	-	-	-
Upregulated DEGs								
mmu04740	Olfactory transduction	13/1080	2.37	**4.43e-3**	0.266	-	-	-

"-" indicates pathways which were not identified by the relevant annotation database. Statistically significant ($p < 0.05$) values are bolded. Count refers to the number of R458Q input genes/number of total genes in pathway.

Analysis (via DAVID) identified 24% of the genes downregulated in R458Q gastrocnemius in KEGG pathways, of which six were significantly enriched (Table 4.2). The KEGG pathway most significantly associated with the down-regulated genes was "ribosome" (mmu03010). The greater than 5-fold enrichment was driven by genes coding for cytosolic and mitochondrial ribosomal proteins (RPs), which included both large (60S) and small (40S) ribosome subunit components. The "oxidative phosphorylation" (mmu00190) pathway exhibited second-strongest fold enrichment, produced by downregulation of nuclear-encoded electron transport chain (ETC) subunit or assembly factor transcripts. This group was also the primary driver underlying enrichment of the remaining four doubly-identified KEGG pathways, all referring to pathological conditions: "Alzheimer's disease" (mmu05010), "Huntington's disease" (mmu05016), "Parkinson's disease" (mmu05012), and the seemingly off-target "non-alcoholic fatty liver disease (NAFLD)" (mmu04932). Due to the comparatively small number of upregulated transcripts in the HOM gastrocnemius, only the "olfactory transduction" (mmu04740) KEGG pathway was enriched (Table 4.2). The association was driven by 13 olfactory receptor genes and was not significant after FDR correction.

Greater proportions of both the downregulated (53%) and the upregulated (41%) gene sets were annotated with GO terms based on biological process (Figure 4.6A-B). Transcript downregulation was most significantly enriched in "translation" and "response to oestradiol" terms (Figure 4.6A). Additional terms identified by both analyses included reference to microtubule organisation and anchoring, intracellular transport, and response to corticotropin-releasing hormone. The five terms enriched by R458Q-induced upregulation referred to the spliceosome and ribosome, GPCR signalling, lipoprotein lipase activity, and sensory perception, although these associations were not significant after FDR correction (Figure 4.6B). Functional annotation clustering via DAVID was used to group annotation terms with similar, redundant, and heterogeneous contents (Figure 4.6C). The most highly enriched of these clusters in the gastrocnemius dataset reproduced the KEGG pathway analyses. The remaining functional clusters were primarily structured around molecular function or protein interaction, and highlighted nuclear hormone activity, histone-related processes, and cAMP binding as significant to the R458Q-associated downregulation of gastrocnemius transcripts. Annotation for upregulated transcripts did not produce clusters.

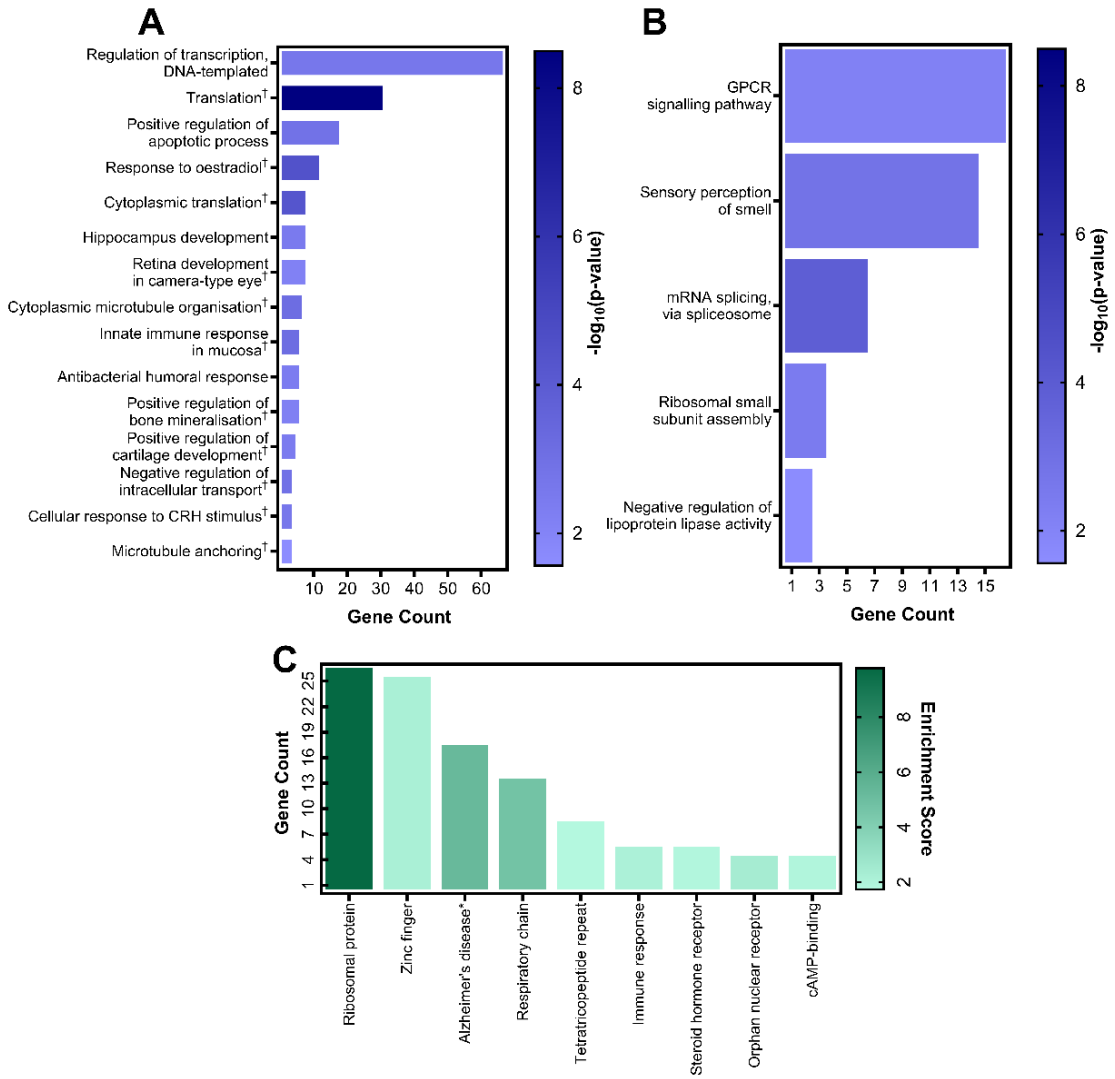

Figure 4.6: Functional annotation of male R458Q gastrocnemius transcripts.

A-B. Representation of the fifteen most significant GO-BP terms associated with (A) downregulated and (B) upregulated DEGs, organised by gene count. Bar colour represents enrichment significance (-$\log_{10}$(p-value)) provided by DAVID annotation, scale shared between panels. **C.** Representation of the functional annotation clusters associated with downregulated DEGs, organised by gene count. Bar colour represents cluster enrichment score provided by DAVID annotation; cut-off set at 1.5. † GO-BP terms identified by both DAVID and STRING analyses. * cluster includes three neurodegenerative and oxidative phosphorylation KEGG pathways. All terms included have $p < 0.05$ enrichment, driven by more than two genes unless supported by both databases.

4.3.3 Liver GSEA

The CREBRF missense variant was associated with significant differential expression of 725 protein-coding and 190 pseudogene transcripts in the liver, represented in Figure 4.7. Largest positive fold changes among these hepatic transcripts in HOM animals were seen for *Cyp8b1*, *Cyp7a1*, *Onecut1*, *Apoa4*, and *Hist1h1c*. Greatest downregulation was shown by *Bcl6*, which had the largest fold-change in any direction for either tissue, followed by *Serpina6*, *Hspa1a*, *Insig1*, and *Hsd17b6*. Transcripts showing differential expression with greatest statistical significance included *Chordc1*, *Ptch1*, *Slc5a3*, *Flcn*, and *Herpud1*.

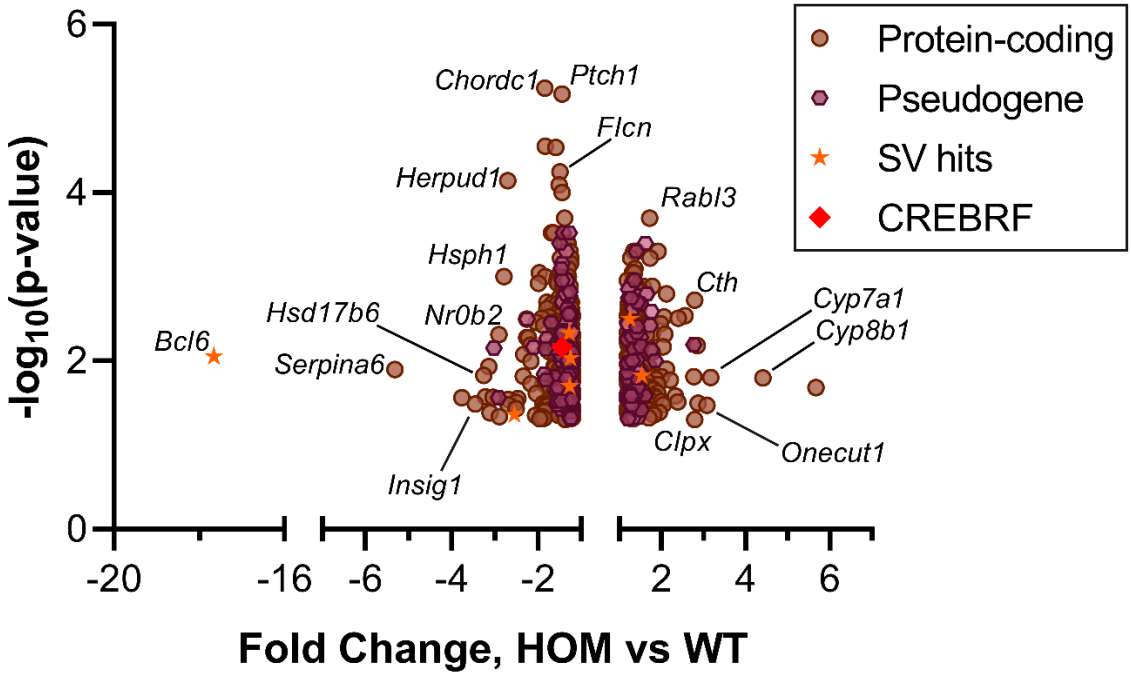

Figure 4.7: Differential expression of protein-coding and pseudogene transcripts in male R458Q liver.

Significantly up- and down-regulated expression of protein-coding (brown) and pseudogene (maroon) transcripts are plotted as fold change against -$\log_{10}$(p-value). DEGs also showing significant alternate splicing in liver are represented using stars. *CREBRF* is indicated in red. Key genes showing greater fold-change or significance are labelled.

Table 4.3: Enriched KEGG pathways for downregulated liver DEGs in male CREBRF R458Q missense variant mice.

Pathway ID	Pathway Description	DAVID				STRING_DB		
		Count	**Fold enrichment**	***p*-value**	**FDR**	**Count**	**Strength**	**FDR**
mmu04141	Protein processing in endoplasmic reticulum	16/168	4.28	**4.04e-6**	**8.77e-4**	17/161	0.74	**1.35e-5**
mmu05322	Systemic lupus erythematosus	12/147	3.67	**3.91e-4**	**4.25e-2**	-	-	-
mmu05034	Alcoholism	13/202	2.89	**1.68e-3**	0.121	-	-	-
mmu04540	Gap junction	8/86	4.18	**2.82e-3**	0.153	8/85	0.69	**3.24e-2**
mmu05164	Influenza A	11/171	2.89	**4.52e-3**	0.171	11/165	0.54	**3.28e-2**
mmu05203	Viral carcinogenesis	13/231	2.53	**5.04e-3**	0.171	-	-	-
mmu04915	Oestrogen signalling pathway	8/98	3.67	**5.84e-3**	0.171	-	-	-
mmu01100	Metabolic pathways	42/1269	1.49	**6.29e-3**	0.174	43/1296	0.23	**3.28e-2**
mmu00140	Steroid hormone biosynthesis	7/87	3.62	**1.23e-2**	0.282	-	-	-
mmu05215	Prostate cancer	7/88	3.58	**1.30e-2**	0.282	-	-	-
mmu02010	ABC transporters	5/46	4.89	**1.83e-2**	0.343	-	-	-
mmu04140	Regulation of autophagy	4/26	6.92	**1.90e-2**	0.351	-	-	-
mmu00053	Ascorbate and aldarate metabolism	4/27	6.66	**2.10e-2**	0.351	-	-	-
mmu00040	Pentose and glucuronate interconversions	4/33	5.45	**3.56e-2**	0.483	-	-	-
mmu00500	Starch and sucrose metabolism	4/32	5.62	**3.29e-2**	0.476	-	-	-
mmu00052	Galactose metabolism	4/32	5.62	**3.29e-2**	0.476	-	-	-
mmu00830	Retinol metabolism	6/89	3.03	**4.67e-2**	0.597	-	-	-
mmu04210	Apoptosis	-	-	-	-	13/135	0.70	**6.40e-4**

"-" indicates pathways which were not identified by the relevant annotation database. Statistically significant ($p < 0.05$) values are bolded. Count refers to the number of R458Q input genes/number of total genes in pathway.

Table 4.4: Enriched KEGG pathways for upregulated liver DEGs in male CREBRF R458Q missense variant mice.

Pathway ID	Pathway Description	DAVID				STRING_DB		
		Count	**Fold enrichment**	***p*-value**	**FDR**	**Count**	**Strength**	**FDR**
mmu01100	Metabolic pathways	36/1269	2.08	**1.29e-5**	**1.94e-3**	40/1296	0.32	**1.90e-3**
mmu00120	Primary bile acid biosynthesis	5/16	22.89	**5.07e-5**	**3.82e-3**	5/16	1.33	**1.90e-3**
mmu01130	Biosynthesis of antibiotics	11/214	3.77	**6.00e-4**	**3.02e-2**	-	-	-
mmu00270	Cysteine and methionine metabolism	5/40	9.16	**1.98e-3**	0.060	6/46	0.95	**6.40e-3**
mmu00220	Arginine biosynthesis	4/19	15.42	**1.99e-3**	0.060	4/19	1.16	**1.44e-2**
mmu01230	Biosynthesis of amino acids	6/76	5.78	**3.54e-3**	0.089	6/75	0.74	**4.30e-2**
mmu04146	Peroxisome	6/83	5.30	**5.17e-3**	0.111	-	-	-
mmu03320	PPAR signalling pathway	5/80	4.58	**2.28e-2**	0.426	-	-	-
mmu03008	Ribosome biogenesis in eukaryotes	5/83	4.41	**2.57e-2**	0.426	-	-	-
mmu00330	Arginine and proline metabolism	4/49	5.98	**2.82e-2**	0.426	-	-	-

"-" indicates pathways which were not identified by the relevant annotation database. Statistically significant ($p < 0.05$) values are bolded. Count refers to the number of R458Q input genes/number of total genes in pathway.

Enrichment analysis of the downregulated hepatic gene set via DAVID identified 32% of the input in KEGG pathways, with seventeen pathways associated with a combined 114 genes (Table 4.3). The pathway most significantly associated with the down-regulated genes was “protein processing in the endoplasmic reticulum” (mmu04141). The greater than 4-fold enrichment was driven by genes encoding ubiquitin ligase complex and ERAD components as well as the three primary UPR sensor proteins PERK, ATF6, and IRE1. The remaining three pathways which were identified by both databases as enriched were “gap junction” (mmu04540), “Influenza A” (mmu05164), and “metabolic pathways” (mmu01100) (Table 4.3).

Enrichment analysis of the upregulated hepatic gene set identified 24% of the input in KEGG pathways, with the five pathways to reach sufficient statistical strength driven by only 45 genes (Table 4.4). The most significantly enriched KEGG pathway was the broad-spectrum “metabolic pathways”, enriched two-fold in R458Q compared to WT liver. The “primary bile acid biosynthesis” (mmu00120) pathway was the second-most significant hit, with greater than 22-fold enrichment due partially to the relatively small number of genes in the full population. Both analyses also identified significant enrichment of the “cysteine and methionine metabolism” (mmu00270), “arginine biosynthesis” (mmu00220), and “biosynthesis of amino acids” (mmu01230) KEGG pathways, suggesting that the R458Q variant had broad impacts on amino acid metabolism in the liver (Table 4.4).

Enrichment of GO terms referring to biological process among downregulated hepatic transcripts primarily supported the pathway analysis, including three separate terms relating to unfolded protein and ER stress responses as well as two “negative regulation of transcription” terms (Figure 4.8A). Both databases also identified circadian clock entrainment and regulation of gene expression, retrograde protein transport, glucose metabolic process, and cellular response to starvation. Transcripts upregulated in HOM liver were enriched for two amino acid-related terms, aligning with KEGG pathway analysis, as well as rRNA modification, methylation, response to virus, and nucleocytoplasmic transport (Figure 4.8B).

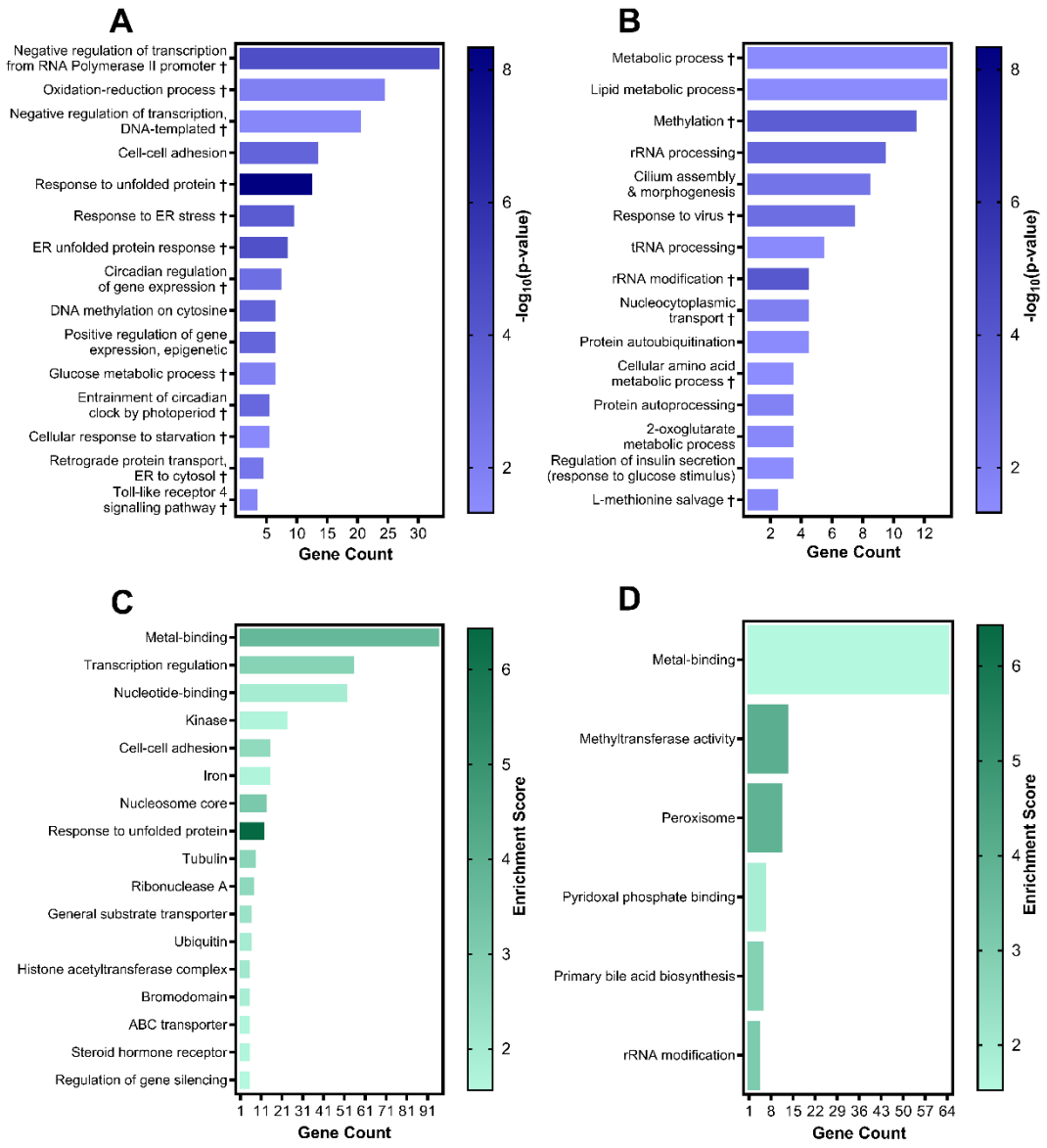

Figure 4.8: Functional annotation of male R458Q liver transcripts.

A-B. Representation of the fifteen most significant GO-BP terms associated with (A) downregulated and (B) upregulated DEGs, organised by gene count. Bar colour represents enrichment significance ($-\log_{10}$(p-value)) provided by DAVID annotation, scale shared between panels. **C-D.** Functional annotation clusters associated with (C) downregulated and (D) upregulated DEGs, organised by gene count. Bar colour represents cluster enrichment score provided by DAVID annotation, scale shared between panels; score cut-off is set at 1.5. † GO-BP terms identified by both DAVID and STRING analyses. All terms included have $p < 0.05$ enrichment, driven by more than two genes unless supported by both databases.

DAVID clustering of annotated liver DEGs primarily re-identified KEGG pathway analyses as the most significantly enriched functional groups but also highlighted additional molecular functions (Figure 4.8C-D). Downregulation of histone family transcripts, histone acetyltransferase activity, and bromodomain-containing proteins (which recognise acetylated lysine residues) was represented across four clusters to suggest altered chromatin regulation in R458Q liver. Annotations also included multiple clusters indicative of altered trafficking and transport mechanisms as well as comparatively more generic and less strongly enriched molecular function terms which suggested decreases to ubiquitin and nucleotide-binding proteins. Metal-binding activity clusters were significantly enriched for both up- and down-regulated gene sets.

4.3.4 Alternative splicing

Splice variants promote heterogeneity in gene expression networks, enhancing adaptive response plasticity. The extreme abundance of snRNA and snoRNA transcripts which were differentially expressed in especially the R458Q gastrocnemius could logically reflect alterations in spliceosomal activities of our KI mice. We therefore identified differential splice variation in R458Q gastrocnemius and liver tissues in order to further explore genotype-dependent transcriptional changes (Figure 4.9).

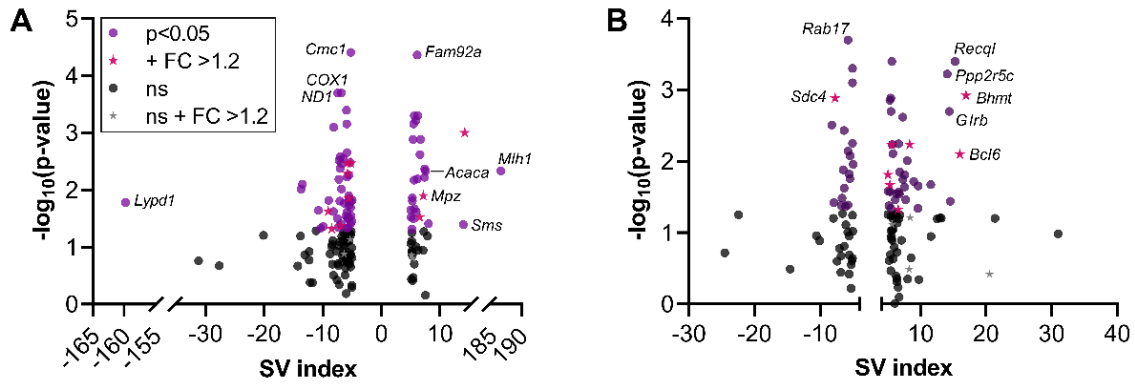

Figure 4.9: Splice variant expression in male R458Q variant mice.

Alternate splicing of mRNA transcripts in (A) gastrocnemius and (B) liver tissue was identified by microarray analysis as significantly differing ratios of exon to gene intensity. Transcripts also showing differential gene expression in gastrocnemius or liver are represented using stars; splicing index values which were not significant ($p < 0.05$) are coloured black.

The R458Q tissue transcriptome exhibited alternate splicing for 83 gastrocnemius and 56 liver transcripts for which the ratio of exon to gene intensity was significantly different to WT tissue (Figure 4.9). Genotype-dependent splicing was accompanied by differential gene expression for eighteen transcripts, indicative of potentially greater alterations to function in these areas (Figure 4.9). These R458Q-associated changes were most broad-ranging in *Bcl6* and *Lmbrd2* transcripts, which were downregulated in both tissues as well as alternately spliced in the liver. Hepatic *Bcl6* presented the greatest fold change and second-highest SV score. Gastrocnemius splice variation included *Slc25a25*, *Mpz*, *Tatdn1*, *Nr4a1*, and *Trim63*, which were downregulated in the same tissue, in addition to *Aass*, *D3Ertd751e*, *F10*, *Lrrcc1*, and *Ppp2r5e*, which were differentially expressed in the liver (Figure 4.10A). Additional hepatic transcripts which were differentially spliced and expressed were *Bhmt*, *Sdc4*, *Cntrl*, *Cyp2a4/5*, *Ralgapa2*, and *1810008I18Rik* (Figure 4.9B). There was no obvious correlation with gene function or chromosomal positioning.

These SV index counts were insufficient to produce highly significant enrichment of KEGG pathways or GO terms when analysed by DAVID (Tables 4.5, 4.6). The gastrocnemius sample indicated genotype involvement in Parkinson's disease which, although not significant after FDR correction, reinforced the similar association seen for downregulated transcripts in this tissue. Curiously, gastrocnemius and liver SV indices each included genes relating to nervous system development (GO:0007399) and the dopaminergic synapse (mmu04728). Individual splice variants did however reflect specific missense variant-associated biological functions, as exemplified by *Cmc2*, *ND1*, and *COX1* in R458Q gastrocnemius, which comprised three of the four most significant splice variants and again highlighted decreases to muscle mitochondrial respiration.

Table 4.5: Enriched KEGG pathways for gastrocnemius and liver splice variant transcripts in male *CREBRF* R458Q missense variant mice.

Pathway ID	Pathway Description	Count	Fold enrichment	*p*-value	FDR
Gastrocnemius					
mmu05012	Parkinson's disease	5/149	7.59	**3.58e-3**	0.390
mmu05150	Staphylococcus aureus infection	3/50	13.57	**1.92e-2**	1.000
mmu04924	Renin secretion	3/71	9.56	**3.69e-2**	1.000
mmu04971	Gastric acid secretion	3/72	9.43	**3.79e-2**	1.000
Liver					
mmu04728	Dopaminergic synapse	3/134	9.06	**3.84e-2**	1.000

Table 4.6: Enriched GO-BP terms for gastrocnemius and liver splice variant transcripts in male CREBRF R458Q missense variant mice.

GO-term	Biological Process	Count	*p*-value	FDR
Gastrocnemius				
GO:0008344	Adult locomotory behaviour	4/69	**1.79e-3**	0.884
GO:0007156	Homophilic cell adhesion via plasma membrane adhesion molecules	4/163	**1.92e-2**	1.000
GO:0070050	Neuron cellular homeostasis	2/10	**3.43e-2**	1.000
GO:0042053	Regulation of dopamine metabolic process	2/10	**3.43e-2**	1.000
GO:0010467	Gene expression	2/12	**4.10e-2**	1.000
GO:0021952	Central nervous system projection neuron axonogenesis	2/12	**4.10e-2**	1.000
GO:0051932	Synaptic transmission, GABAergic	2/12	**4.10e-2**	1.000
GO:0042417	Dopamine metabolic process	2/14	**4.77e-2**	1.000
Liver				
GO:0007399	Nervous system development	5/377	**2.15e-2**	1.000
GO:0032508	DNA duplex unwinding	2/18	**4.96e-2**	1.000

4.3.5 Protein-protein interaction networks

To better visualise the effects of the CREBRF missense variant on gastrocnemius and liver tissues at a system level, we constructed protein-protein interaction (PPI) networks using STRING-DB for all differentially expressed or spliced protein-coding gene loci in each tissue. This approach calculated significant associations between proteins which contribute jointly to a shared function, drawing from experimental, literature, and other evidence (Szklarczyk *et al.*, 2019). PPI networks identified significant interaction enrichment (p < 1.0e-16) within R458Q-associated datasets for both gastrocnemius and liver tissues (Figure 4.10, 4.11). High degree of interconnection represented a coordinated rather than incidental transcriptional programme in missense variant carriers.

Visualisation of the relationships connecting PPI network nodes illustrated different clustering patterns in gastrocnemius and liver tissue protein-coding gene expression (Figure 4.10, 4.11). Representation of protein groupings via MCL analysis generated >60 clusters in each tissue, some of which comprised only two nodes with a single connection. The gastrocnemius dataset showed concentration on ribosome and mitochondrial respiration functions, with transcription-related nodes forming a comparatively looser grouping (Figure 4.10). The liver dataset was dominated by a cluster of 73 nodes, centrally incorporating histone- and ubiquitin-related proteins, to which distinct function could not be readily attributed (Figure 4.11).

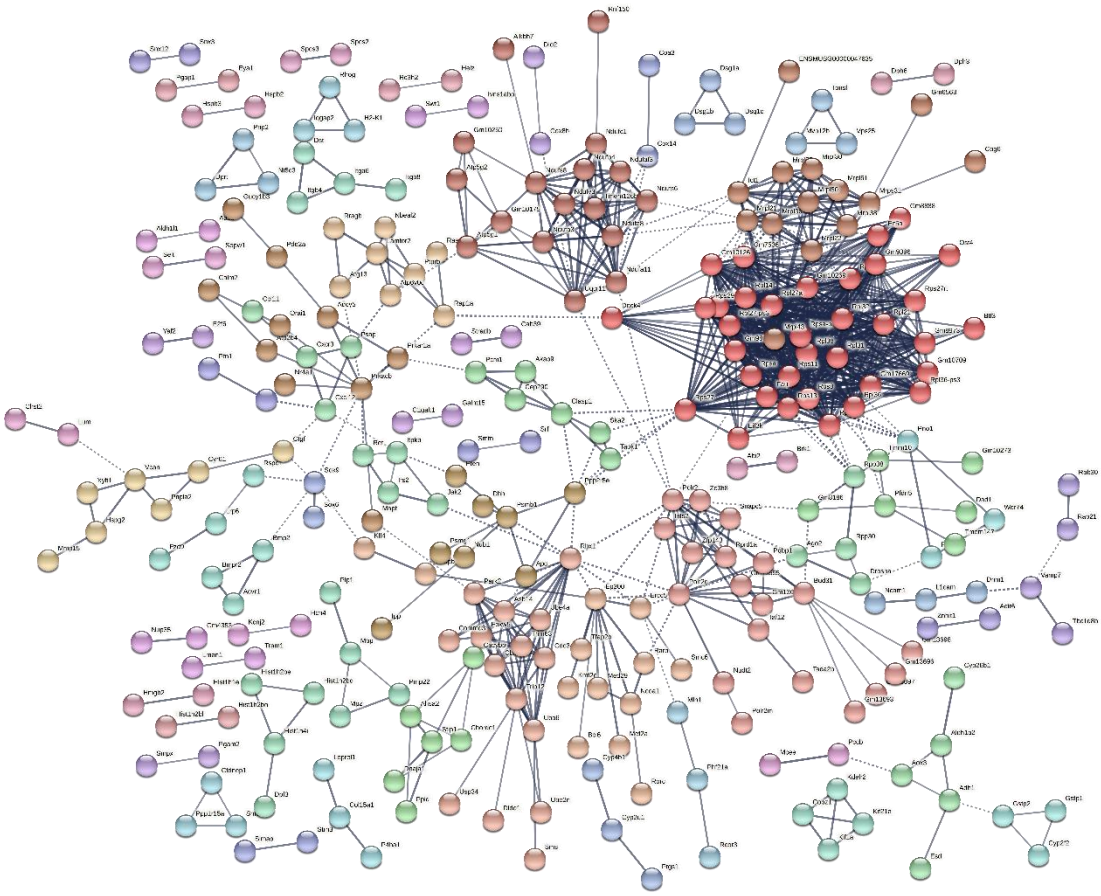

Figure 4.10: PPI network generated from protein-coding DEGs in male R458Q gastrocnemius.

STRING analysis identified 607 nodes (proteins) connected by a total 983 edges, with 3.24 average node degree. Colours correspond to 64 identified MCL functional clusters. Disconnected proteins are hidden to better highlight enriched interactions.

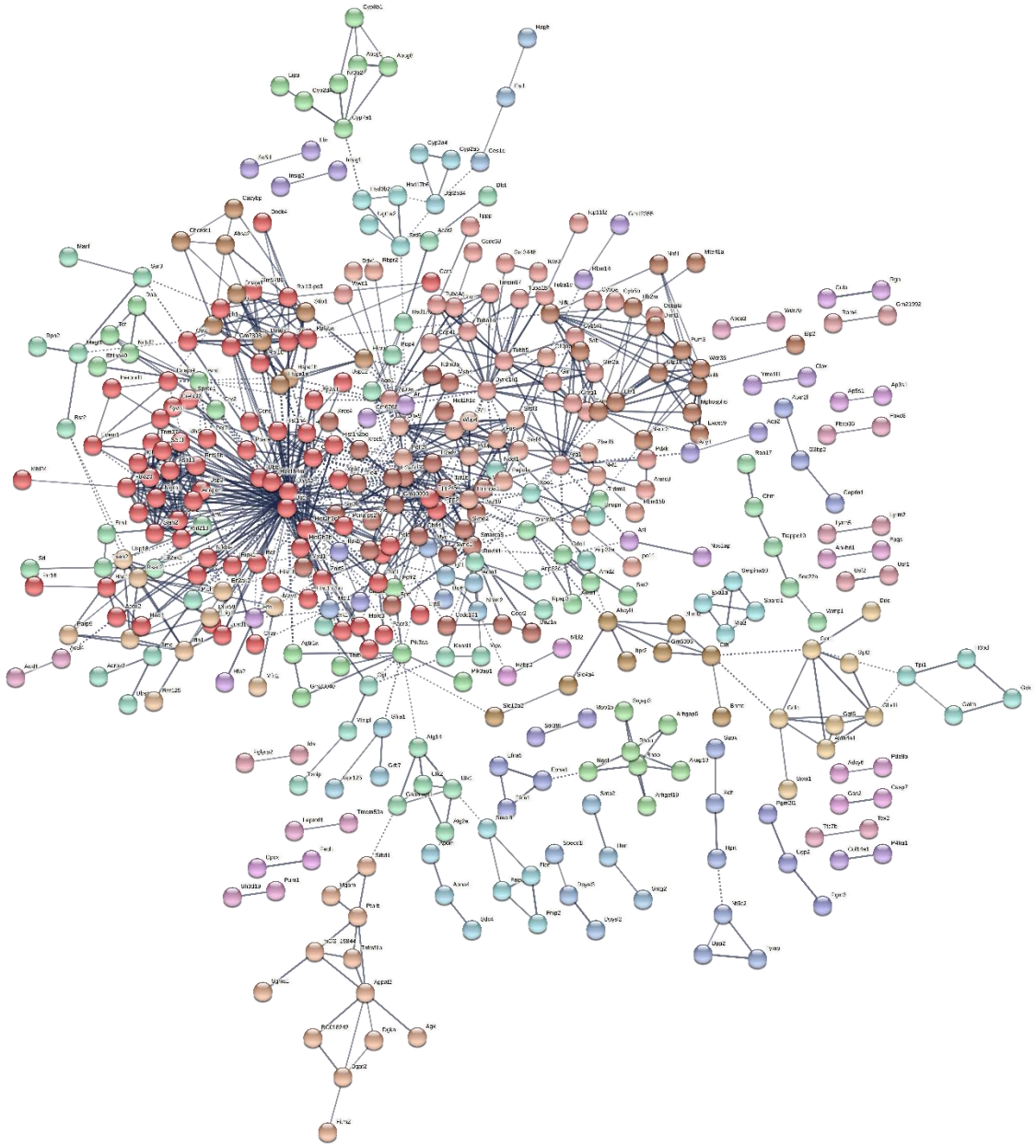

Figure 4.11: PPI network generated from protein-coding DEGs in male R458Q liver. STRING analysis identified 790 nodes (proteins) connected by a total 958 edges, with 2.43 average node degree. Colours correspond to 69 identified MCL functional clusters. Disconnected proteins are hidden to better highlight enriched interactions.

4.3.5 Canonical TF target overlap

CREBRF has potential transactivation activity, as identified in *Drosophila*, and furthermore has regulatory links to transcription factors including CREB3, the GR, and FOXO (Audas *et al*., 2008; Martyn *et al*., 2012; Tiebe *et al*., 2015; Martyn *et al*., 2016). To determine their potential relevance to the missense variant function we therefore investigated correlations between known targets of these TFs and the differentially expressed transcripts in R458Q mice. Direct comparison with gene targets modulated by the rapamycin-induced REPTOR/REPTOR-BP (CREBRF/CREBL2 ortholog) complex in *Drosophila* (Tiebe *et al*., 2015) was complicated by species difference with minimal correlation. Enrichment analysis indicated overlap in affected KEGG pathways for "galactose metabolism", "pentose and glucuronate interconversions", "metabolic pathways", "retinol metabolism", and "protein processing in the ER" (Table 4.7).

CREB3 activity was not visibly impacted by presence of the R458Q variant, with target gene transcripts both up- and down-regulated in the HOM liver (Table 4.8). Given the limited number of known CREB3-specific targets, as well as the differential expression of genes related to cAMP/PKA signalling pathways in liver and muscle, analysis was extended to cAMP-response element (CRE) binding sites more broadly. Comparison against published CREB target genes (Zhang *et al*., 2005) demonstrated mild overlaps with the R458Q tissue transcriptomes, representing 11% of total R458Q protein-coding DEGs. CREB targets with altered expression in gastrocnemius were primarily downregulated (53 of 59) in variant carriers (Figure 4.12A), but the 76 transcripts altered in liver had no distinct directional effect (Figure 4.12B).

.

Table 4.7: Enriched KEGG pathways for REPTOR-regulated genes in *Drosophila melanogaster* larvae.

Pathway ID	Pathway Description	DAVID			
		Count	**Fold enrichment**	***p*-value**	**FDR**
dme00980	Metabolism of xenobiotics by cytochrome P450	15/61	3.7	**2.7e-5**	**1.4e-3**
dme00480	Glutathione metabolism	15/62	3.6	**3.2e-5**	**1.4e-3**
dme00982	Drug metabolism – cytochrome P450	14/61	3.5	**1.2e-4**	**3.5e-3**
dme04142	Lysosome	15/93	2.4	**2.7e-3**	5.9e-2
dme00052	Galactose metabolism†	8/34	3.5	**5.7e-3**	0.10
dme04141	Protein processing in endoplasmic reticulum†	17/126	2.0	**7.7e-3**	0.11
dme00565	Ether lipid metabolism	6/23	3.9	**1.5e-2**	0.19
dme00040	Pentose and glucuronate interconversions†	8/43	2.8	**2.1e-2**	0.23
dme01100	Metabolic pathways†	73/901	1.2	**2.7e-2**	0.24
dme00561	Glycerolipid metabolism	8/46	2.6	**2.9e-2**	0.24
dme00051	Fructose and mannose metabolism	6/27	3.3	**2.9e-2**	0.24
dme00564	Glycerophospholipid metabolism	9/59	2.3	**3.8e-2**	0.27
dme04130	SNARE interactions in vesicular transport	5/20	3.8	**3.9e-2**	0.27
dme00071	Fatty acid degradation	6/30	3.0	**4.4e-2**	0.28
dme00830	Retinol metabolism†	6/31	2.9	**5.0e-2**	0.30

The gene set here analysed by DAVID identified REPTOR-dependent differential transcript expression seen following 6 hr rapamycin treatment using WT and REPTOR-KO *Drosophila melanogaster* larvae (Table S4, Tiebe *et al*., 2015). † indicates pathways which were also significantly enriched in the differentially expressed R458Q tissue transcriptome as analysed by DAVID.

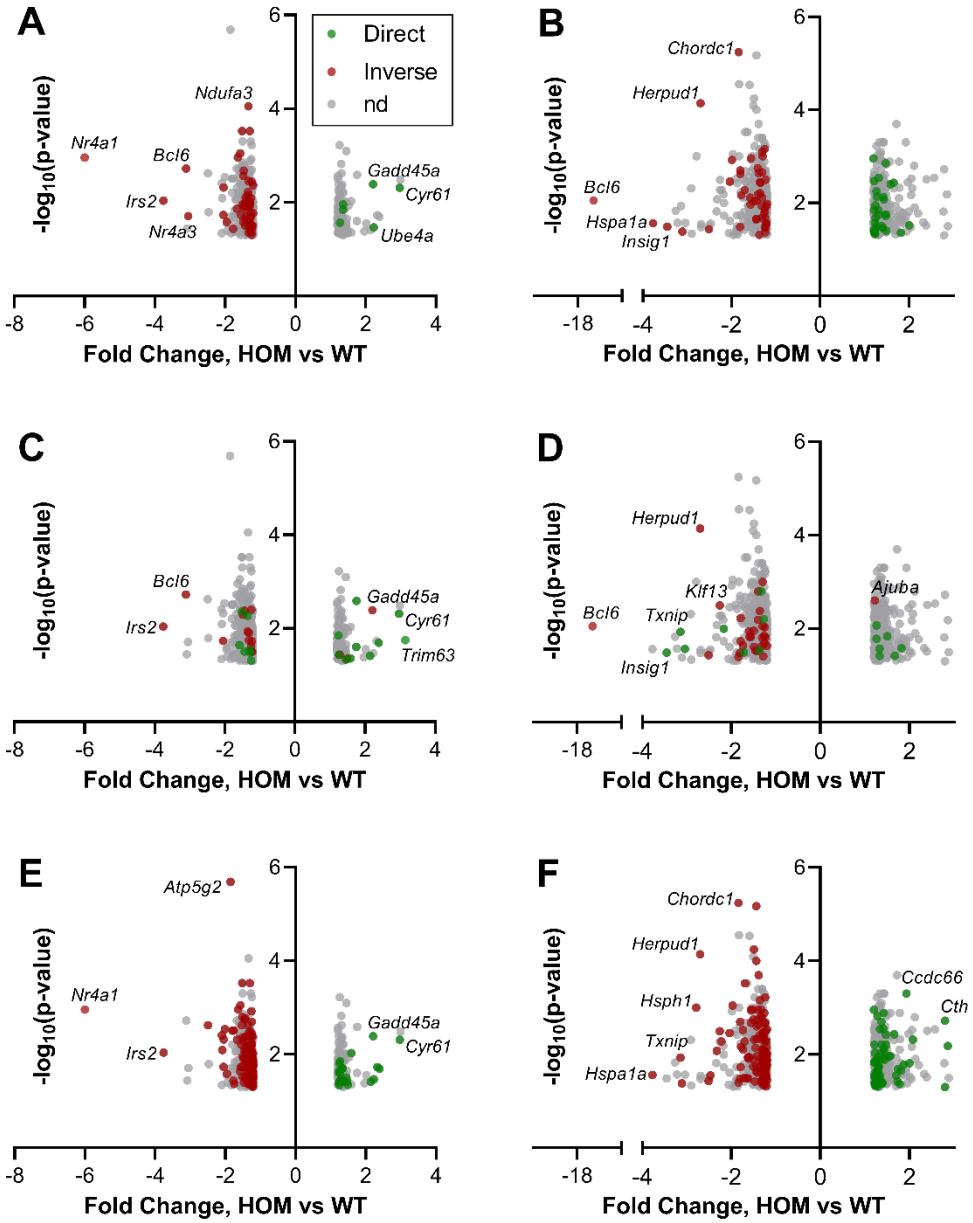

Figure 4.12: Comparison of male R458Q DEGs and canonical TF target gene sets. **A-B**. CRE-binding target genes identified in (A) gastrocnemius (58 transcripts, 11.5% of total protein-coding DEGs) and (B) liver (76, 10.5%). **C-D.** GRE-binding target genes identified in (C) gastrocnemius (33, 6.4%) and (D) liver (45, 6.2%). **E-F.** FOXO gene targets identified in (E) gastrocnemius (158, 30.9%) and (F) liver (185, 25.6%). DEGS are plotted as fold change against -$\log_{10}$(p-value) using the R458Q transcriptome values. DEGs for which the R458Q-induced fold-change is directly (positively) associated with canonical TF action are shown in green; DEGs with an inverse association with canonical TF action shown in red; DEGs not detected (nd) in TF gene sets shown in grey.

Table 4.8: CREB3 gene targets differentially expressed in male R458Q variant liver.

Gene ID	R458Q effect	CREB3 effect	Associated Pathway	Reference
Apoa4	↑↑	↑	Lipid, appetite	(Sanecka *et al*., 2012)
Dcstamp	↑	↑	Immune function	(Kanemoto *et al*., 2015)
Ddc	↑↑	↑	Appetite	(Penney *et al*., 2018)
Edem1	↓	↑	ERAD	(DenBoer *et al*., 2005)
Herpud1	↓↓	↑	ER stress/ERAD	(Liang *et al*., 2006)
Insig1	↓↓↓	↑	UPR, cholesterol	(Ying *et al*., 2015a)
Insig2	↑	↑	UPR, cholesterol	(Ying *et al*., 2015a)

Arrows indicating direction of R458Q effect also indicate magnitude of fold change.

Glucocorticoid signalling produces both stimulatory and suppressive effects on target gene transcription. Using published datasets (Kuo *et al*., 2012; Johnson *et al*., 2021) as reference, differential expression of dexamethasone-responsive genes was identified in both gastrocnemius and liver transcriptomes of R458Q mice (Figure 4.12C-D). These glucocorticoid response element (GRE)-containing genes included the transcripts subject to most dramatic and/or significant differential expression in gastrocnemius (*Irs2*, *Trim63*, *Cyr61*) and liver (*Herpud1*, *Insig1*, *Bcl6*). The mild overlap comprised 6.3% of the total genotype-affected transcripts in each tissue, with no overt directionality or correlation to the GR-mediated induction or repression of gene transcription.

Genotype-dependent effects on transcript abundance more greatly impacted FOXO gene targets (Figure 4.12E-F). Comparison against a published murine dataset (Webb *et al*., 2016) identified 31% of gastrocnemius and 26% of liver protein-coding DEGs in the R458Q transcriptome. The majority of the relevant affected transcripts were downregulated in gastrocnemius (134 of 158) and in liver (125 of 185). Enrichment analysis performed on the R458Q-FOXO overlap most strongly identified the KEGG "ribosome" and "protein processing in the ER" pathways which were also prominently enriched in the complete R458Q gene set (Table 4.9).

Table 4.9: Significantly enriched KEGG pathways for FOXO-regulated genes in male R458Q variant mice.

Pathway ID	Pathway Description	DAVID				STRING_DB		
		Count	**Fold enrichment**	***p*-value**	**FDR**	**Count**	**Strength**	**FDR**
Gastrocnemius								
mmu03010	Ribosome†	12/145	8.37	**1.27e-7**	**1.61e-5**	10/127	1.04	**2.40e-5**
mmu05016	Huntington's disease†	6/198	3.07	**4.35e-2**	1.000	-	-	-
Liver								
mmu04141	Protein processing in endoplasmic reticulum†	9/168	4.90	**4.30e-4**	0.071	9/168	0.81	**7.9e-3**
mmu05164	Influenza A†	8/171	4.28	**2.38e-3**	0.198			
mmu04146	Peroxisome†	5/83	5.52	**1.22e-2**	0.673			
mmu00220	Arginine biosynthesis†	3/19	14.46	**1.75e-2**	0.703			
mmu04915	Oestrogen signalling pathway†	5/98	4.67	**2.12e-2**	0.703			
mmu04140	Regulation of autophagy†	3/26	10.56	**3.16e-2**	0.875	7/137	0.79	**4.56e-2**
mmu05017	Spinocerebellar ataxia	-	-	-	-	7/140	0.78	**4.56e-2**
mmu04150	mTOR signalling pathway	-	-	-	-	7/156	0.73	**4.56e-2**
mmu05010	Alzheimer's disease††	-	-	-	-	11/359	0.56	**4.56e-2**
mmu05014	Amyotrophic lateral sclerosis	-	-	-	-	11/364	0.56	**4.56e-2**

Enriched pathways are ordered by significance. "-" indicates pathways which were not identified by the relevant annotation database. Statistically significant ($p < 0.05$) values are bolded. Count refers to the number of R458Q input genes/number of total genes in pathway. † indicates pathways which were also significantly enriched in the complete R458Q gene set from the same tissue; †† indicates that the pathway was enriched in the different tissue.

The differentially expressed transcripts identified as possible targets of these three TFs had mild overlap between gene sets (Figure 4.13). This was strongest in both tissues between CREB and FOXO shared targets, perhaps partially a function of the greater abundance of genotype-affected FOXO targets. All three TFs target 5 gastrocnemius DEGs and 3 liver DEGs. There was no consistent regulatory pattern in TF and genotype interactions.

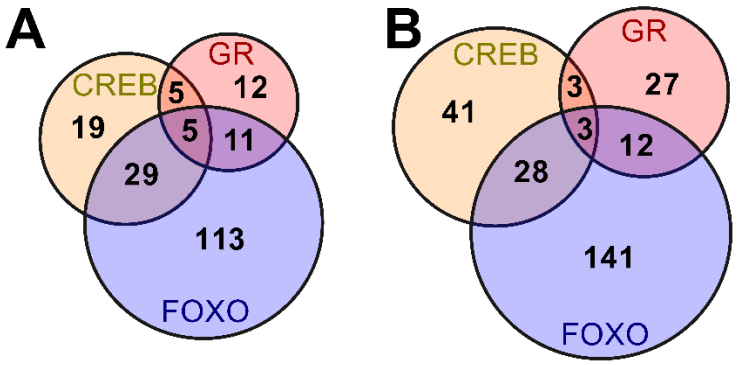

Figure 4.13: Numerical breakdown of TF-associated gene set overlaps.
The number of DEGs in male R458Q (A) gastrocnemius and (B) liver transcriptomes which were identified in published gene sets as potential targets of CREB, GR, and/or FOXO transcriptional activity.

4.4 DISCUSSION

Remodelling of the tissue transcriptome can reveal coordinated gene expression programmes which govern immediate biological signalling as well as evolutionary genotypic and phenotypic variation. A putative transcription factor, CREBRF is reported to facilitate the starvation-induced transcriptional programme downstream of mTORC1, as well as interact with other TFs key to metabolic signalling, although literature is limited. The current study examined potential transcriptional influence of the CREBRF missense variant in gastrocnemius and liver tissues of R458Q KI mice, which has not yet been explored. The tissue- and sex-specific genotype effects were mild but GSEA revealed pathway enrichment relating to protein synthesis, turnover, processing, and trafficking as well as cellular respiration and fuel metabolism, broadly correlating to a speculative role in bioenergetic homeostasis.

Dramatic tissue- and genotype-dependent changes to non-coding RNA imply altered cellular transcription and translation machinery in CREBRF missense variant mice. Although representing less than 14% of differentially expressed liver transcripts, ncRNA in the HOM gastrocnemius comprised over 50% of total transcripts, upregulated almost without exception. These muscle-specific effects of the R458Q variant imply greater transcriptional activity of RNA polymerases II and III, which synthesise the most-impacted ncRNA transcripts (Listerman *et al*., 2007; Nikitina *et al*., 2011; Barba-Aliaga *et al.*, 2021). The R458Q liver transcriptome, although lacking the same pronounced ncRNA effects, had enrichment of gene ontology terms relating to Pol II transcription and nucleosome assembly, suggesting a more moderate but still relevant genotype effect. Altered expression of genes encoding DNA-, chromatin-, histone-, and polymerase-interacting proteins in both gastrocnemius and liver produced enriched functional clustering likewise further implicating the CREBRF variant in processes regulating gene expression and potentially the regulatory epigenome (Alabert & Groth, 2012; Park *et al*., 2017b; Klemm *et al*., 2019). Upregulated expression of snoRNA and snRNA content in R458Q gastrocnemius similarly implies enhanced spliceosome and RNA processing activities (Bohnsack & Sloan, 2018; Baldini *et al*., 2021; Morais *et al.*, 2021), complementing the heightened polymerase activity, and indeed was again accompanied by enrichment of similar ncRNA modification and processing GO terms in the liver. The implied genotype-dependent impacts suggest concentrated tissue-specific involvement in cellular transcriptional and RNA processing machinery.

Translational machinery likewise showed significant genotype-dependent impacts in the R458Q gastrocnemius. Specific transcriptional targeting of the upregulated nuclear-encoded 5S rRNA molecule may be partially related to its similarly selective import into mitochondria where it is associated with mitochondrial ribosomes and critical for mitochondrial translation (Smirnov *et al*., 2011). Taken together with differential expression of protein-coding genes important in mitoribosome biogenesis (e.g., *Rbfa*), the 5S rRNA expression suggests genotype influence on mitochondrial, as well as cytoplasmic ribosome components. The logical presumption that this enhanced rRNA expression might increase muscle protein translation is however complicated by decreased expression of nuclear and mitochondrial ribosomal protein (RP) mRNA, and of mitochondrial transfer RNA, in HOM tissues. Indeed, the "ribosome" KEGG pathway was most strongly enriched among downregulated gastrocnemius transcripts, implying potential reductions in translational machinery and action. Opposition may simply represent dysregulation, perhaps exacerbated by compensatory responses to initial CREBRF variant-induced alterations.

Inverse transcription and translation rate juxtaposition is precedented. Constitutive Pol III activity in transgenic models produces a futile RNA cycle, with high transcription rates but reductions in total and RP mRNA levels and in global translation efficiency (Willis *et al*., 2018; Bonhoure *et al*., 2020). Parallels to the R458Q gastrocnemius transcriptome, which similarly demonstrates greater Pol III-transcribed rRNA levels but relative decreases in over 75% of mRNA transcripts including ribosomal proteins, may imply a similar phenotype of metabolic inefficiency in CREBRF variant carrier muscle. Dysregulation of ribosome subunit composition may reflect intrinsic regulation of translation through generation of "specialised ribosomes" which can disrupt translation efficiency either globally or preferentially, targeting specific mRNA subsets (Xue & Barna, 2012; Shi *et al.*, 2017; Genuth & Barna, 2018). The unknown potential of such skewed translation rates in the current KI mouse model could somewhat undercut proposed physiological relevance of differential RNA transcript expression but presents its own functional consequences. Ribosome subunit heterogeneity, driven even by loss of individual RPs, can diminish cellular growth rates and delay global growth as a result of decreased protein synthesis and greater protein catabolism (Kirn-Safran *et al*., 2007; Cheng *et al*., 2019). The transcriptional and translational machineries are themselves regulated by growth signals including nutrient availability, cellular stress, and ATP/GTP

intracellular pool size, via mTOR signalling (Mayer & Grummt, 2006; Wei *et al*., 2009; Chaillou *et al.*, 2014). Altered transcription of ribosome components and biogenesis, dysregulating protein synthesis, may therefore both reflect and facilitate reduced growth signalling in CREBRF R458Q gastrocnemius.

Dysregulation of protein turnover balance is further represented by differential expression of atrophic factors in the R458Q gastrocnemius transcriptome. Although no relevant pathway enrichment was observed, the top ten upregulated transcripts in HOM muscle included *Trim63* (MuRF1) and *Gadd45a*. These encode vital mediators of stress-induced skeletal muscle atrophy, potentially thereby linking the R458Q variant to myofibrillar and sarcoplasmic protein ubiquitination, myonuclear remodelling, and repression of anabolic signalling and energy production (Ebert *et al*., 2012; Baehr *et al*., 2021). Interestingly, these genotype-dependent DEGs implicate atrophic response to both fasting and muscle denervation (Rudolf *et al*., 2013a; Khan *et al*., 2014; Ehmsen *et al*., 2021). Downregulation and splice variation of myelination protein transcripts (e.g., *Mpz, Mbp*, *Pmp22*) reflects CNS diseases known to produce muscle atrophy, weakness, fibre remodelling, and altered oxidative metabolism (Lang *et al*., 2017; Dalise *et al*., 2020; Tepavčević, 2021). Mpz/Mbp-related peripheral nerve development is associated with cAMP-dependent signalling, which is altered in dystrophic skeletal muscle, while neuromuscular junction remodelling is a focal point of fasting-induced and mTORC1-driven sarcopenia (Guo *et al*., 2013; Rudolf *et al*., 2013b; Ham *et al*., 2020b). Both cAMP and mTORC1 signalling are independently linked to CREBRF (Audas *et al*., 2008; Tiebe *et al*., 2015, 2019). Downregulation of genes known to promote skeletal muscle growth (e.g., *Smpx, Pgam2, Slc38a2, Orai1*) or differentiation (e.g., *Dubr*, *Srf*) further supports an atrophic shift in the HOM dataset. Severe downregulation of the three NR4A orphan nuclear receptors, which promote skeletal muscle oxidative capacity, mass, strength, and/or fatigue resistance (Chao *et al*., 2007; Pearen *et al*., 2008; Tontonoz *et al*., 2015; Cortez-Toledo *et al*., 2017), may hint at functional consequences. An atrophic transcriptional shift in R458Q mice could perhaps represent concerted induction of catabolic signalling more broadly in the KI gastrocnemius and contribute to the similarly muscle-specific effects on protein translation.

The R458Q liver, unlike muscle, demonstrated coordinated transcriptional suppression of not ribosome biogenesis, but protein processing pathways. Downregulation of ERAD-

and UPR-related transcripts drove significant enrichment of the "protein processing in the ER" KEGG pathway in R458Q liver. These mechanisms respond to misfolded protein accumulation, controlling proteasomal degradation and cell survival pathways respectively (Hwang & Qi, 2018). Deficiency of individual ER stress response components can disturb glucose or lipid homeostasis, mitochondrial function, protein translation and secretion, or cell survival (Francisco *et al.*, 2011; Eura *et al*., 2012; Sha *et al*., 2014; Sun *et al.*, 2014). Loss of ERAD components can cause inappropriate protein accumulation of the UPR sensor IRE1α (Sun *et al.*, 2015a). CREBRF suppresses CREB3-mediated enhancement of the stress-induced expression of UPR and ERAD pathways (DenBoer *et al*., 2005; Liang *et al*., 2006; Arora & Golemis, 2015; Singh *et al*., 2015). Reduced transcription of these pathways in HOM compared to WT liver may indicate that the CREBRF missense variant can strengthen this suppressive effect. Whether this might reflect decreased stressors, sensitivity, or capacity of response is less clear. Indeed, CREB3 knockdown can itself induce proteotoxic stress (Penney *et al*., 2018; Hu *et al*., 2019; Zhao *et al*., 2020), while loss of ERAD has similar consequences (Francisco *et al*., 2010; Sun *et al*., 2014). Alternately, diminished proteotoxic stress response activity is linked to reductions in protein synthesis and processing (Francisco *et al.*, 2011; Kristensen *et al*., 2018; Sun *et al*., 2020). This latter circumstance, perhaps indicative of hepatic energy sparing measures and/or diminished energy production (Kristensen *et al*., 2018; Liu *et al*., 2020), would appear to parallel other changes to protein synthesis likewise present in the HOM tissue transcriptome.

Transcriptional regulation and suppression of protein processing in CREBRF missense variant mice further extends to intracellular transport. Genes involved in cytoskeletal organisation and microtubule dynamics (e.g., *Sntb2*, *Sntg2*, *Utrn*) as well as subcellular vesicle formation and/or motility (e.g., *Dync1h1*, *Dynll1*, *Kif1a*, *Trappc10*) were targeted in both R458Q tissues, downregulating nucleocytoplasmic transport. These decreases run counter to the known effects of CREB3 activity, which heightens expression of ER-Golgi transport proteins in response to Golgi stress and/or greater protein secretion demand (Sanecka *et al.*, 2012; Reiling *et al*., 2013; Penney, 2017; Zhang *et al*., 2017b; Howley *et al*., 2018; Penney *et al*., 2018). Although the current study has no exact overlap in the impacted genes, the broader pathway effects may again frame the CREBRF missense variant as enhancing WT inhibition of CREB3 action. Consequences of diminished intracellular trafficking machinery can include reduced protein secretion, degradation, or

recycling, suggesting that R458Q regulation has potential to impact not only protein synthesis and quality control mechanisms but also downstream processing. Accompanied by differential expression of solute carrier genes, repression of trafficking machinery in liver and muscle perhaps further reflects intracellular signalling capability and generalised decrease in cell activity (Bhat *et al*., 2019; Schulze *et al*., 2019).

The mitochondrion was strongly represented in the differentially regulated transcriptome of male KI gastrocnemius. Functional annotation of downregulated mRNA transcripts indicated R458Q-associated enrichment of mitochondrial oxidative phosphorylation (OxPhos) as well as mitochondrial transcription and ribosome biogenesis. Deficiency of ETC complex subunits and assembly factors in this mouse model can (even individually) disrupt assembly and function of ETC complexes I, IV, and V to increase reactive oxygen species generation and inflammation, impair mitochondrial OxPhos, and reduce ATP production (Natera-Naranjo *et al*., 2012; Andrews *et al*., 2013; Kmita *et al*., 2015). Depletion of the mitochondrial ATP-Mg^{2+} and P_i shuttle, ScAMC-2 (*Slc25a25*), or of proteins involved in biosynthesis and cellular uptake of creatine (*Gatm*, *Slc6a8*), which serve as energy buffers for ATP replenishment, can also diminish metabolic efficiency and ATP production in skeletal muscle (Anunciado-Koza *et al*., 2011; Nabuurs *et al*., 2013; Russell *et al*., 2014). Transcriptional disturbance of mitochondrial energetics in R458Q gastrocnemius is logically coupled to dysregulation of protein turnover, which is a significant contributor to resting metabolic rate, with mitochondrial disruption partially causative in multiple atrophy models (Muller *et al*., 2007; Romanello *et al*., 2010; Schutz, 2011; Powers *et al*., 2012; Ibebunjo *et al*., 2013; Hyatt *et al*., 2019; Yokokawa *et al*., 2020). It also aligns with Minster *et al*. (2016)'s *in vitro* model showing reduced cellular ATP production and respiration following CREBRF variant overexpression. Given that *in vivo* decreases in skeletal muscle mitochondrial respiratory capacity are also provoked by extended fasting in responses geared to energetically sustain cellular processes and thereby survival (Monternier *et al*., 2015; Bourguignon *et al*., 2017; Roussel *et al*., 2018), these R458Q results may support Minster *et al*. (2016)'s theory of "thrifty" variant metabolism.

Loss of muscle oxidative capacity is observed in metabolic pathologies. The altered OxPhos mRNA expression in HOM gastrocnemius powered statistical enrichment of KEGG pathways related to Alzheimer's, Huntington's, and Parkinson's diseases, which were strongly grouped in functional clustering analysis. Correlation between

mitochondrial deficiencies and neurodegenerative disorders is reported in muscle biopsy samples (Shoffner *et al.*, 1991; Cardellach *et al.*, 1993), but logically better established in the affected brain regions (Manczak *et al.*, 2004; Chakravorty *et al.*, 2019; Intihar *et al.*, 2019; Müller-Nedebock *et al.*, 2019; Galber *et al.*, 2021). Reduced muscle OxPhos cannot alone prove genotype-dependent development of the three named diseases, particularly given the highly tissue-specific transcriptomic changes. Muscle mitochondrial dysfunction is strongly associated in literature with systemic dyslipidaemia and insulin resistance (Formentini *et al.*, 2017; Genders *et al.*, 2020). That these metabolic consequences are not readily apparent in the current analysis advises against presumption of whole-body dysregulation. Indeed, unlike the clear repression of OxPhos mRNA in HOM muscle, hepatic transcripts were both up- (e.g., *Atp10d*, *Atp5s*) and down-regulated (e.g., *Ndufb11*, *Coq10a*) in insufficient number for meaningful impact. The *Park2* splice variant in HOM gastrocnemius, when found in skeletal muscle, is associated with contractility and mitochondrial function rather than Parkinson's disease (Gouspillou *et al.*, 2018). Possible neurodegenerative connections cannot be excluded, given that CREBRF/CREB3 are expressed in the brain (Ying *et al.*, 2015b), but would require examination of neuronal tissues not undertaken in the present study.

Fuel metabolism processes potentially also contributed to modified cellular energetics in the hepatic R458Q transcriptome. Genotype-dependent differential expression implicated reduced glycophagy (*Gabarapl1*, *Stbd1*) and carbohydrate interconversion (e.g., *H6pd*, *Ugp1*, *Mgam*) pathway flux, and presented associations with lipid deposition, hepatic steatosis, and fatty liver disease (e.g., *Apom*, *C730036E19Rik*, *Gm15622*) as well as FA α- and β-oxidation (e.g., *Acsl1, Acsl4, Them7)* (Donnelly *et al.*, 2004; Joseph *et al.*, 2015; Li *et al.*, 2015b; Batista *et al.*, 2019; Ma *et al.*, 2020; Shi *et al.*, 2020). Significant enrichment of "glucose metabolic process", "cellular response to glucose stimulus" and "cellular response to starvation" GO terms suggests that the R458Q variant primarily affected carbohydrate fuel metabolism following nutrient deprivation. Absence of lipid-related pathway enrichment was unexpected, with links to WT and variant CREBRF seen in literature (Tiebe *et al.*, 2015; Minster *et al.*, 2016; Tiebe *et al.*, 2019). Given that regulation of glucose and lipid metabolism is often integrated to coordinate fuel switching (Rui, 2014; Singh *et al.*, 2020), however, missense variant-induced bioenergetic adaptations seen in the overnight-fasted KI mice may likewise shift from glucose to lipid as fasting conditions progress.

Hepatic DEGs across both glucose and lipid pathways reflected fasting-induced expression changes which were perhaps exemplified by significant downregulation of major nutrient sensors and TFs. Glucokinase (*Gck*), carbohydrate response element binding protein (ChREBP; *Mlxipl*), and B-cell lymphoma 6 (*Bcl6*) are highly responsive to nutritional status, with mRNA and protein expression depleted *in vivo* by fasting (Ruan *et al*., 2016; Rennert *et al*., 2018; Sommars *et al*., 2019). These changes in HOM liver may functionally suppress TF activity: direct ChREBP gene target *Txnip*, encoding a negative regulator of glucose uptake, showed more than three-fold decrease in expression compared to WT (Yoshihara, 2020; Noblet *et al*., 2021). These hepatic mediators of glucose signalling cooperatively govern the homeostatic production and disposal of glucose (Sols *et al.*, 1964; Dentin *et al.*, 2004; Chutkow *et al.*, 2008; DeBalsi *et al*., 2014; Yang *et al.*, 2017). Genetic loss of murine hepatic *Bcl6* mimics the fasting-induced transcriptional programme controlling lipid metabolism (Sommars *et al*., 2019). Neither gluconeogenesis nor lipid catabolism genes were significantly provoked above WT levels in R458Q liver, somewhat belying this starvation factor theory, but perhaps due merely to comparative strength of effect between these major hepatic pathways and the mild missense variant phenotype.

The hepatic KI transcriptome was significantly associated with amino acid (AA) biosynthesis, salvage, and metabolic pathways. Upregulation of methionine and cysteine downstream metabolism reflects altered oxidative stress conditions underlain by homocysteine (Hcy) and glutathione homeostasis in HOM liver. Increased flux through hepatic Hcy removal pathways, driven by key transmethylation and transsulphuration enzymes (e.g., *Bhmt*, *Bhmt2*, *Cth*), not only forestalls detrimental impacts of elevated Hcy levels but also enhances the generation of antioxidant glutathione and hydrogen sulphide generation (Tyagi *et al*., 2005; Ai *et al*., 2017; Paul *et al*., 2021). Consequent mitigation of cellular and oxidative stress in HOM liver may be reflected in, for example, decreased mRNA expression of *Herpud1*, which responds to homocysteine-induced ER stress, and of cystine cellular uptake (*Slc3a1*) and lysosomal export (*Ctns*) transporters sensitive to oxidative stress (Wu *et al*., 2020a). Protective transcriptional changes in the HOM liver may also, however, reflect adaptation to greater stress rather than actual metabolic health. Indeed, *Bhmt* and *Cth* mRNA and activity are likewise significantly increased in streptozotocin-diabetic rats (Jacobs *et al*., 1998; Ratnam *et al*., 2006), and the latter

enzyme also in HFD-fed mice (Hwang *et al*., 2013). This aspect of AA metabolism may further the CREBRF association with stress response activity.

AA-related transcripts upregulated by the CREBRF variant also implicate fuel metabolism processes. Many of the enzymes affected in the current study (e.g., *Aldh4a1*, *Got1*, *Gpt2*, *Hal*) catalyse reversible anaplerotic reactions, degrading AAs including proline, histidine, aspartate, alanine, and arginine to produce glutamate and TCA cycle metabolites important for cellular energy generation. Polyamine synthesis enzymes are likewise upregulated in HOM liver, perhaps responding to cellular stress (Gilad *et al.*, 2001). Upregulation of (cataplerotic) deamination and urea cycle enzymes (e.g., *Glud1*, *Arg1*, *Asl*) as well as of the mitochondrial glutamate transporters (*Slc25a12*, *Slc25a22*) needed to provide substrate for those reactions highlights differential hepatic handling of glutamate in CREBRF variant carriers. Crucially, glutamate deamination not only stimulates excess nitrogen clearance through ureagenesis, but also releases its carbon skeleton for gluconeogenesis, thusly interfacing between AA and carbohydrate metabolism (Brosnan, 2000). Genotype-dependent changes in AA pathway flux may not overload extant metabolic capacity, being unaccompanied by similarly concerted differential expression of major TCA cycle and/or gluconeogenic enzymes.

Flux through these AA-related pathways, including induction of enzymatic expression, is largely governed by protein intake and catabolism (Clifford *et al*., 1972; Kersten *et al*., 2001; Sokolovič *et al*., 2008; Majaw & Sharma, 2015; Zhang *et al*., 2019). Enhanced AA signalling via mTORC1, which also responds to nucleotide and polyamine content, coordinates nutrient-sensitive growth (Emmanuel *et al*., 2017*;* Hoxhaj *et* al., 2017; Tabbaa *et al.*, 2021). The combination of increased TCA and urea cycle activity and altered AA, polyamine, and nucleotide levels, as indicated in the R458Q liver transcriptome, is elsewhere associated with higher energy demands and reduced protein synthesis (Willis *et al*., 2018; Bonhoure *et al*., 2020). Potential systemic consequences on energy homeostasis include AA-induced tissue crosstalk. The liver-pancreas feedback loop couples AA signalling to secretion of glucagon, a fasting-induced hormone known to stimulate hepatic AA turnover and ureagenesis as well as gluconeogenesis and lipid oxidation (Solloway *et al*., 2015; Wewer Albrechtson *et al.*, 2019; Winther-Sørensen *et al*., 2020). Skeletal muscle wasting, as implied by atrophic transcripts in R458Q gastrocnemius, is promoted by liver alanine catabolism and can in turn provide AAs for

hepatic gluconeogenesis during energetic stress (Lecker *et al*., 2004; de Lange *et al*., 2007; Nakao *et al*., 2019; Okun *et al*., 2021). AA signalling in KI mice may further support a role for the missense variant in nutrient-responsive growth mechanisms.

Primary bile acid biosynthesis was the most strongly enriched KEGG pathway among upregulated R458Q liver transcripts. Key upregulated rate-limiting enzymes in this pathway (e.g., *Cyp7a1*, *Cyp8b1*) control bile pool size and composition (Pandak *et al*., 2001), implying greater flux in HOM than WT animals. Their activity is likely derepressed by *Nr0b2* downregulation, which diminishes negative feedback regulation to cause abnormal bile acid accumulation (Kerr *et al*., 2002; Wang *et al*., 2002). Enhanced biosynthesis is predicated on hepatic cholesterol content, which provides the major bile acid building block. Altered transcription of sterol-responsive genes (e.g., *Insig1*, *Rnf145*, *Stard4*) may imply comparatively higher intracellular concentrations in HOM livers. Cholesterolgenic activity is reflected in suppressed mRNA expression of negative regulators (e.g., *Insig1*, *Rnf145*), while downregulation of sterol transporters (e.g., *Abcg5*, *Abcg8*, *Stard4*) implies slowed cholesterol efflux into bile or endocytic recycling compartments (Engelking *et al*., 2005; Wang *et al*., 2015a; Zhang *et al*., 2017a; Iaea *et al*., 2020). Given that bile acids are critical signalling molecules, their enhanced biosynthesis has potentially systemic consequences. Greater esterification of FAs to cholesterol can offer a physiological buffer against excess lipid deposition, as may be implicated in R458Q mice. Cholesterol and/or bile salt export defects produce intrahepatic cholestasis and liver damage (Kruglov *et al*., 2011; Bhattacharya, 2019). Increased bile acid pool size and cholic acid: chenodeoxycholic acid ratios provoked by Cyp7a1/Cyp8b1 activity are linked to dyslipidemia, obesity, and diabetes (Bloks *et al*., 2004; Pathak & Chiang, 2019). Discernment of metabolite flux through these pathways may better clarify murine missense variant action in this context as well as the potential for deleterious consequences in variant carriers.

The CREBRF R458Q variant was associated with innate immunity and antiviral responses. Both liver and gastrocnemius transcriptomes of HOM mice show differential expression of immunoglobulin heavy and light chain variable domain transcripts, and of T cell receptor alpha joining or variable transcripts, indicating heightened immune response. CREB3 and NF-κB cooperatively modulate inflammation responses (Jang *et al*., 2007a, 2007b; Torres-Odio *et al*., 2017); downregulated NF-κB mRNA in R458Q

liver may suggest functional juxtaposition with the CREBRF variant. Significant variant-induced hepatic expression of transcripts encoding antiviral factors suggests more defined functions, including cytoplasmic sensing of viral nucleic acids (*Ifih1*), virus-induced autophagy (*Trim23*), and restriction of viral capsids (*Trim34*), replication (*Rsad2*), or translation (*Ifit1*), as well as regulation of type I IFN or RIG-I signalling (*Rnf125*, *Trim14*) (Arimoto *et al*., 2007; Jia *et al*., 2017; Sparrer *et al*., 2017; Mears & Sweeney, 2018; Dias *et al*., 2019; Ebrahimi *et al*., 2020; Ohainle *et al*., 2020). Both CREBRF and CREB3 similarly promote immune response during viral infection, preventing viral gene transcription primarily via physical interactions (Lu *et al*., 1997; Lu *et al*., 1998; Blot *et al*., 2006; Audas *et al*., 2016). The CREBRF missense variant may provide additional contributions to a coordinated host defence and innate immunity response, presenting metabolic health signals not necessarily driven by more prominent nutrient sensing mechanisms.

Dysfunctional metabolic signalling in peripheral tissues has well-established links to insulin resistance and/or diabetes aetiology. Such pathways which show altered gene expression in CREBRF variant carrier mice include dysregulation of steroid hormone (Sharma & Singh, 2020), bile acid (Wu *et al*., 2020b), and retinol (Manolescu *et al.*, 2010; Obrochta *et al*., 2015) metabolism in addition to well-known links with glucose and lipid metabolism. Such evidence is, however, largely circumstantial. Transcripts which more directly influence insulin signalling do not reveal clear associations. Although R458Q-induced downregulation of skeletal muscle *Irs2* can impair insulin signalling (Guo *et al*., 2006; Agarwal *et al*., 2013; Eckstein *et al*., 2017), downregulated *Pten* implies the opposite effect, with even partial reduction able to improve muscle insulin sensitivity (Wijesekara *et al*., 2005; Wong *et al*., 2007). Patterns of differential gene expression in the liver transcriptome are similarly contradictory, correlated with both impairment (e.g., *Pik3ca*, *Pik3ap1*, *ApoM*, *Apoa4*) and enhancement (e.g., *Appl1*, *Bcl6*, *miR-378*) of insulin sensitivity (Cheng *et al*., 2009; Liu *et al*., 2014; Senagolage *et al*., 2018; Kurano *et al*., 2020; Yao *et al*., 2020). The human CREBRF missense variant has not been specifically associated with peripheral insulin signalling, rendering comparison with the murine transcriptomic effects in this context largely ineffectual. Despite pathway-level correlations, the otherwise ambiguous R458Q transcriptomic influence cannot illuminate diabetes- or IR-related phenotypes in variant carriers.

Interconnection between the metabolic pathways enriched in the KI transcriptome may imply underlying transcriptional programmes even if translational relevance of mRNA expression is unclear. Correlations between muscle mitochondrial respiration and protein turnover, alongside differential expression of individual nutrient-sensitive genes, are jointly indicative of fasting state metabolism. UPR sensory proteins are associated with viral infection, immunoglobulin synthesis, and innate immunity (Janssens *et al*., 2014; Choi & Song, 2020). ER stress produces greater hepatic cholesterol accumulation (Kovacs *et al.*, 2009; Henkel *et al*., 2017; Röhrl & Stangl, 2018), while ERAD deficiency disrupts cholesterol export and elevates bile acid levels (Bhattacharya, 2019). These apparent parallels to the R458Q liver transcriptome may imply relevant causative links, and indeed UPR-induced cholesterol biosynthesis in axonal regeneration is mediated via CREB3 (Ying *et al*., 2015a). The weight of individual factors in the current dataset is perhaps debatable, but notable TFs (e.g., *Bcl6*, *Mlxipl*, *Ppara*, *Nr0b2*) can even individually produce broad-ranging consequences across lipid, glucose, bile acid, and/or circadian metabolism (Wei *et al*., 2011; Wu *et al*., 2016; Sommars *et al*., 2019; Agius *et al*., 2020). These factors might offer a basis from which to seek potential mediating factors or pathways able to facilitate a concerted R458Q transcriptional programme.

Circadian rhythm desynchrony may represent genotype influence on one such transcriptional programme. Enriched gene ontology terms in R458Q liver included circadian clock entrainment and regulation of gene expression, with multiple circadian clock components significantly down-regulated (*Bhlhe40*, *Cry2*, *Nr1d2*, *Per2*) or alternately spliced (*Arntl*, *Dbp*) in HOM compared to WT mice. Disruption of this homeostatic regulatory control, which is integrated with feeding-fasting and hormonal secretion cycles, impacts multiple CREBRF variant-affected pathways. Of the current dataset, for example, Dec1 (encoded by *Bhlhe40*), Rev-erbβ (*Nr1d2*), and Per2 each independently influence lipid metabolism, glucose tolerance, bile acid synthesis, and/or nucleotide metabolism in addition to clock regulation (Noshiro *et al.*, 2007; Grimaldi *et al*., 2010; Bugge *et al*., 2012; Fujita *et al*., 2016; Chen *et al*., 2021). Knockdown of clock components alters AA and nucleotide metabolic cycling as well as antiviral host response (Krishnaiah *et al*., 2017; Borrmann *et al*., 2021). Although relative expression of these genes naturally fluctuates across the 24-hour cycle, as determined by complex autoregulatory feedback loops, the R458Q-induced decreases represent multiple circadian phases rather than depletion of any time- or fed state-dependent cluster (Woller

et al., 2016; Kinouchi *et al*., 2018; Brown and Doyle, 2020), and seem not to (transcriptionally) activate compensatory redundancies shown elsewhere to mitigate targeted dysregulation (Bugge *et al*., 2012; Ikeda *et al*., 2019). Suppressive effects may rather imply less efficient transactivation by the cascade initiator Bmal1 (*Arntl*) splice variant. Hepatic loss of SHP (*Nr0b2*) and of OGT can delay Bmal1-dependent gene expression and liver circadian adaptation upon restricted feeding (Li *et al*., 2013b; Wu *et al*., 2016). Closer elucidation of circadian desynchrony drivers in the R458Q liver, potentially nutrient-sensitive, might reveal broader associations and/or implications of this vital homeostatic mechanism.

The greater genotype separation shown by PCA in male compared to female KI transcriptomes, consistent with the sex-specific manifestation of whole-body genotype effects described in Chapter 3, suggests that the CREBRF variant phenotype is partially underlain by sexually dimorphic signalling in the current R458Q mouse model. This can have specific molecular drivers. Pharmacological or genetic loss of BCL6 activity in mice, for example, alters sex-biased DNA methylation and chromatin accessibility to derepress female-biased genes, feminising male liver (Lau-Corona *et al*., 2017; AlOgayil *et al*., 2021). *Bcl6* downregulation in male HOM liver may introduce similar bias, although the distinct PCA separation between male and female transcriptomes suggests otherwise. Murine fasting responses show greater AA metabolism gene expression in females than males, as we observed for HOM compared to WT livers, perhaps also predisposing variant carriers to this female-biased AA flux to FA synthesis and TCA cycle metabolites (Della Torre *et al*., 2018; Bazhan *et al*., 2019). Dimorphism may also be linked to altered sex steroid signalling, as implied in R458Q liver by upregulated androgen receptor and downregulated steroid biosynthesis and metabolism enzyme (e.g., *Hsd17b6*, *Hsd3b2*, *Srd5a2*) transcript expression, while GO term enrichment suggested genotype-dependent response to oestradiol in gastrocnemius. Such gene expression shifts may derive from CREBRF variant alteration of WT interactions with CREB3. CREBRF and CREB3 are associated with synthesis and secretion of oestradiol, progesterone, and/or prolactin in female models (Martyn *et al*., 2012; Yang *et al*., 2013b; Zhao *et al*., 2016; Yang *et al*., 2018). CREB3 further regulates steroidogenesis via GR- and PKA-responsive nuclear receptors NR4A1 and SHP, which respectively promote and repress testosterone synthesis (Song *et al*., 2002; Martin *et al*., 2008; Vega *et al*., 2015; Wang *et al*., 2019). Their downregulation in R458Q muscle and liver cannot prove similar effects

but indicates the potential for genotype-dependent steroidogenic changes. Study of steroidogenic tissues could further clarify CREBRF missense variant interactions with sex steroid hormone action and associated gender bias.

The best-established CREBRF regulatory target, CREB3, was not differentially transcribed in R458Q tissues. This was perhaps unsurprising given that its negative regulation by CREBRF is post-translational (Audas *et al.*, 2008; Martyn *et al.*, 2012; Audas *et al*., 2016). Possible downstream missense variant influence is not thereby precluded, but variable modulation of CREB3 gene targets (e.g., *Apoa4*, *Dcstamp*, *Herpud1*) in R458Q liver cannot define genotype-dependent suppression or promotion of CREB3 transactivation potential. Mild overlaps with CRE-binding site gene sets imply possible missense variant interaction with CREB family transactivation more broadly, complemented by downregulation of CREB cofactors *Ep300* in gastrocnemius and *Crebbp* in liver. Although gastrocnemius R458Q effects were suppressive, this was unclear in liver and the relatively low proportions of CREB-related genes cannot underlie all variant-induced differential expression. Genotype-dependent changes to upstream cAMP-PKA signalling, including calcium channel (*Orai*), adrenoceptor (*Lmbrd2*, *Akap11*), adenylate cyclase (*Adcy5*, *Adcy6*), and PKA subunit (*Prkar1a*) regulation, further implicate CREB as well as PPARα and Rap1 signalling pathways (Briassoulis *et al.*, 2016; Paek *et al.*, 2017). That the PKA signalling network involves phosphorylation signalling cascades not visible in transcript expression highlights the limitations of the current dataset in discerning molecular interactions in R458Q tissues. Pathway-level correlations showing the oppositional variant- and CREB-induced actions on ER stress and protein processing, as discussed above, may therefore represent one consequence of such combined transcript- and protein-related interactions. If the CREBRF missense variant indeed enhances WT suppression of CREB transactivation, the broad spectrum of cAMP-PKA pathways also indicates potentially wide-ranging signalling consequences which may not be facilitated specifically by CREB3.

One possible mediating factor is CREBH, a TF which is closely related to CREB3 and found primarily in the liver. With broad regulatory influence on multiple metabolic pathways, CREBH was recently identified as a potential target for prevention or mitigation of diet-induced obesity, insulin resistance, and/or hepatic steatosis (Krumm *et al*., 2021; Yang *et al*., 2021). The hepatic R458Q transcriptome upregulated specific

CREBH-induced genes (e.g., *Apoa4*, *Insig2*, *Cyp7a1*, *Kiss1*) as well as broader functional overlaps including glucose and lipid metabolism, inflammatory response, and circadian rhythm (Vecchi *et al*., 2009; Lee *et al*., 2010; Chanda *et al*., 2011; Chanda *et al*., 2013; Misra *et al*., 2014; Xu *et al*., 2014; Wang *et al*., 2016; Kim *et al*., 2017b; Satoh *et al*., 2020; Kim *et al*., 2021a). Although *Crebh* mRNA was not altered in R458Q mice, variant-induced downregulation of ERAD components can feasibly reduce turnover of CREBH protein, which is targeted for degradation by the Sel1/Hrd ERAD complex (Bhattacharya *et al*., 2018; Wei *et al.*, 2018; Kim *et al*., 2021a). Circadian clock components which are differentially expressed and/or spliced in the KI liver also regulate CREBH proteolytic activation (Zheng *et al*., 2016; Kim *et al*., 2021a). Hepatic CREBH is induced during fasting, influencing systemic energy homeostasis (Lee *et al*., 2010; Chanda *et al*., 2013; Bhattacharya *et al*., 2018; Wei *et al.*, 2018), and could thusly participate in proposed variant-associated exaggeration of fasting response. This may not provide mechanistic basis for R458Q action, per se, but highlights that potential facilitators may not be explicitly represented in the current transcriptomic dataset.

Alterations to the R458Q transcriptome may also implicate steroid hormone signalling. Glucocorticoids (GCs) are the main biological mediator of response to chronic stress (Mattos *et al*., 2013; Crawford *et al.*, 2021), and influence pathways enriched in the R458Q tissues. Acute or chronic stress-induced GCs can respectively stimulate or decrease skeletal muscle mitochondrial biogenesis and function (Duclos *et al*., 2001; Weber *et al*., 2002; Duclos *et al.*, 2004; Kobayashi *et al*., 2020), with the latter depletion of intracellular ATP preceding a GC-stimulated atrophic transcriptional programme (Troncoso *et al.*, 2014; Liu *et al*., 2016; Britto *et al*., 2018). Hepatic GC signalling promotes AA metabolism and ureagenesis during high protein turnover (Cousin *et al*., 1982; Gotoh *et al*., 1997; Gilad *et al*., 2001; Okun *et al*., 2015), and influences bile acid homeostasis which can in turn alter GC synthesis and clearance (Rose *et al*., 2011; McMillin *et al*., 2015; Xiao *et al*., 2016). Correlations to GC-stimulated activities might imply a systemic physiological basis underlying effects on skeletal muscle and hepatic metabolic processes represented in the R458Q transcriptome.

Mechanistically, the link is less clear. Although the broader mitochondrial, atrophic, and AA metabolism transcriptomic effects imply enhanced GC signalling in murine missense variant carriers, specific GC-sensitive gene targets were not consistently similarly

regulated in R458Q tissues. The interaction could logically derive from CREBRF-mediated degradation of the GR, elsewhere shown to produce *in vivo* transcriptional consequences (Martyn *et al.*, 2012; Audas *et al.*, 2016). Repression of GR activity, as for CREB3, might therefore indicate that the missense variant can enhance this WT protein interaction. Discrepancies at the pathway level may represent GR crosstalk with sex steroid receptor transactivation (Ruiz *et al*., 2020), or its synchronisation of liver circadian clock components (Oishi *et al*., 2005; Reddy *et al*., 2007; Quagliarini *et al*., 2019). Indeed, two-thirds of the GC-associated DEGs were also CREB or FOXO targets. CREBRF also modulates circulating GC levels in circadian and stress response conditions (Martyn *et al*., 2012; Frahm *et al*., 2020). These HPA axis effects are not delineated in gastrocnemius or liver, but reduced corticosteroid-binding globulin (CBG; *Serpina6*) mRNA in HOM liver could influence GC bioavailability and transport to target organs. Thusly altered clearance and signalling in peripheral tissues could potentiate systemic R458Q effects on growth, glucose homeostasis, lipid metabolism, and/or basal metabolic rate (Sinha *et al*., 2018). Changes are not readily predictable, however, given that rodent CBG deficiency has been associated with both hyper- and hypo-corticosteronism, attributable to the finely-controlled balance between total and free (unbound, bioactive) corticosterone levels (Mattos *et al*., 2013; Moisan & Castanon, 2016; Gulfo *et al*., 2019; Crawford *et al.*, 2021). The somewhat ambiguous interaction between GC signalling and the CREBRF missense variant may be better elucidated through a more targeted analysis of the *in vivo* GC effects, perhaps modelling GC provision or inhibition.

CREBRF is suggested to share functions with FOXO signalling in *Drosophila* (Tiebe *et al*., 2015). Activated during oxidative and energetic stress, FOXO has broad regulatory roles in cellular metabolism which include transducing nutrient sensing to control the carbohydrate-lipid metabolic switch in muscle and liver (Cheng & White, 2011; Kodani & Nakae, 2020; Yang *et al*., 2021). That we identified more than a quarter of R458Q-associated changes in muscle and liver transcriptomes as FOXO targets might support that this overlap also exists in mice. The differential expression cannot, however, prove whether the CREBRF missense variant limited its own WT transactivation capacity or blocked that of FOXO. Mutual redundancy, seen in double-KO lethality compared to viable loss of either protein alone (Tiebe *et al*., 2015), may suggest partial operation of both mechanisms on the affected gene subset. Indeed, it remains possible that R458Q transcriptional effects and/or the CREBRF/FOXO overlap could extend beyond

transcriptome changes observable in the current study. Redundancy also offers a potential explanation for the overall mild changes to murine variant phenotype. FOXO function is tightly controlled by post-translational modification and cofactor interactions (Zhang *et al*., 2021). Downregulation of transcripts encoding mediators of FOXO negative feedback (*Nr0b2, Nlk*), glucose-stimulated transcription (*Ogt*), and DNA-binding and subsequent degradation (*Cbp, Ep300*) might underlie CREBRF variant-induced dysfunction (van der Heide & Smidt, 2005; Housley *et al*., 2009; Kim *et al*., 2010b; Wei *et al*., 2011). This interference with FOXO regulation, visible on a mechanistic basis, can also reinforce the gene set overlap as a specific if not necessarily targeted impact of the CREBRF missense variant.

Acting as a purported TF, CREBRF primarily mediates the transcriptional response downstream of (inactivated) mTORC1 during nutrient deprivation or rapamycin treatment to relieve its suppression of catabolic activity (Tiebe *et al*., 2015, 2019). Only ER stress and heat shock response gene expression, however, responded to both the CREBRF missense variant and rapamycin-induced WT function. Functional annotation did not highlight mTORC1 signalling in the R458Q tissue transcriptome, perhaps indicating retention of the WT role as a starvation factor downstream of mTORC1. The link is not without thematic correlation. Nutrient-sensitive metabolic processes implicated in both the current study and mTORC1/2 function include ribosomal biogenesis (Mayer & Grummt, 2006; Ham *et al*., 2020a), skeletal muscle atrophy (Bentzinger *et al*., 2013; Quy *et al*., 2013; Ham *et al*., 2020b), mitochondrial activity (Morita *et al*., 2013; Rosario *et al*., 2019), amino acid and nucleotide metabolism (Emmanuel *et al*., 2017*;* Hoxhaj *et* al., 2017; Tabbaa *et al*., 2021), the actin cytoskeleton and secretory pathways (Jacinto *et al*., 2004), and hepatic glucose and lipid homeostasis (Hagiwara *et al*., 2012; Ricoult & Manning, 2013; Mao & Zhang, 2018). These processes also incorporate shared functions of other TFs. AA catabolism, for example, is related not only to mTORC1 signalling but is synergistically induced by CREB and the GR during fasting (Korenfeld *et al*., 2021). FOXO pathways likewise converge with mTORC1 (Teleman *et al*., 2008). Such regulatory overlaps among R458Q-affected pathways are not wholly unexpected, given their metabolic importance, but can complicate distinction between missense variant effects.

Several DEGs regulate mTORC1 or mTORC2 in R458Q muscle or liver. In the latter tissue, downregulation of *Flcn* and its binding partners (*Fnip1*, *Fnip2*) may imply lessening of their mTORC1 suppression during AA starvation (Tsun *et al*., 2013; Meng & Ferguson, 2018). Circadian clock components, downregulated in R458Q liver, can both suppress mTORC1 and promote mTORC2 stability (Zhang *et al*., 2014; Tian *et al*., 2018; Wu *et al*., 2019b). In gastrocnemius, downregulation of *Rragb* and *Lamtor2*, components of the Rag-Ragulator complex mediating AA-sensitive mTORC1 translocation (Bar-Peled *et al*., 2012), suggests the missense variant reduces mTORC1 activity; downregulation of *Stradb* and *Cab39l*, involved in AMPK activation and thereby mTORC1 inhibition, suggests the opposite. Overall ambiguity of mTORC1/2 regulatory associations may indicate more nuanced modulation of the WT role in mediating starvation-induced transcription. Given prior reports of rapamycin-induced CREBRF expression (Minster *et al*., 2016; Tiebe *et al*., 2019), the decreases to *Crebrf* mRNA in fasted HOM liver imply either muted transcriptional response or, if CREB3- and GR-related speculation of enhanced functionality holds, overactivity of the missense variant protein. Either answer would, however, complexify the overexpression model used previously to establish CREBRF variant *in vitro* effects on energy storage and utilisation (Minster *et al*., 2016). An underlying genotype-dependent link to mTORC1/2 bioenergetic regulation might be more conclusively identified using rapamycin-treated CREBRF missense variant KI models.

In conclusion, the tissue transcriptome of *CREBRF* R458Q mice demonstrated sex- and tissue-dependent changes in the presence of the missense variant compared to WT counterparts. Enrichment analysis of the differentially expressed transcripts in male gastrocnemius and liver suggested a potential role in bioenergetic homeostasis, mediated by nutrient-sensitive catabolism, and perhaps associated with FOXO-linked transcription. Genotype separation was, however, relatively mild. These findings may encourage further study in this area, with attention to interventions focused on nutrient or stress which might develop the theorised variant-induced changes in transcriptional programming.

CHAPTER 5: Musculoskeletal Characterisation of CREBRF R458Q Knock-In Mice

5.1 INTRODUCTION

The CREBRF missense variant has been strongly linked to increased growth in humans. Initial characterisation of the R458Q mouse model in Chapter 3 of this thesis was suggestive of some similar influence on fat-free mass in male variant carriers. Fat-free mass is primarily understood to be comprised of muscle and bone. These components are often grouped together, at times referred to jointly as the "functional muscle-bone unit" based on the developmental and mechanical interactions between the two (Schoenau, 2005). Bone and muscle cells share mesenchymal cell precursors; development of each is affected by shared influences including genetic and signalling factors such as IGF1, the GR, or Wnt (Karasik & Kiel, 2008). Mice lacking myostatin, for example, present with both increased muscle mass and greater bone mineral density (BMD) (Montgomery *et al*., 2005; Hamrick *et al*., 2006). The duality is present throughout the human lifespan: bone mineral content and muscle mass accumulate in parallel during (healthy) childhood, and remain proportional during adulthood (Proctor *et al*., 2000; Ashby *et al*., 2011). The forces exerted by skeletal muscle on bone provoke adaptation, such that strength of muscle and of bone are correlated in children and adolescents (Schönau *et al*., 1996; Goodman *et al*., 2015). Any phenotypic influence on fat-free mass, whether induced by genetic or environmental stimuli, would accordingly predicate investigation of both muscle and bone components.

The physiological contributions of skeletal muscle and bone composition include not only strength and mobility but also systemic energy metabolism. Skeletal muscle comprises the primary site for glucose uptake and storage in the body, and further functions as a reservoir for amino acid content. Energy expenditure and substrate utilisation in muscle are vital to whole-body homeostasis; sustainable levels of work, as determined by intensity and duration of exercise, are governed by steady-state ATP synthesis flux, set by relative contributions of glycolysis and oxidative phosphorylation (Conley *et al*., 2001; Hargreaves & Spriet, 2020). Bone remodelling is an energy-demanding process, such that the balance between bone formation and resorption depends on energetic homeostasis (Suzuki *et al*., 2020); as a proposed endocrine organ, bone likewise contributes in turn to systemic energy metabolism via bone-derived circulating factors (Lee *et al*., 2007; Lee &

Karsenty, 2008; Suchacki *et al*., 2017; Zhou *et al*., 2021). Many of these factors, including osteocalcin, lipocalin 2 (Lcn2), and parathyroid hormone-related protein (PTHrP), modulate systemic glucose tolerance and uptake in adipose, liver, and/or skeletal muscle peripheral tissues (Motyl *et al.*, 2010; Mizokami *et al*., 2014; Zhang *et al*., 2017c; Capulli *et al.*, 2018). Alternate mechanisms of energy regulation involve increased mitochondrial biogenesis via osteocalcin (Ferron *et al.*, 2012), inhibition of food intake via a hypothalamic MC4R-dependent pathway triggered by Lcn2 (Mosialou *et al*., 2017), or enhanced WAT browning and FAO via PTHrP-stimulated pathways (Zhang *et al*., 2017c).

Given their involvement in systemic metabolism, muscle and bone can logically also contribute to metabolic conditions when homeostasis is upset. Fat-free mass has, for example, been inversely associated in men and women with risks of insulin resistance, prediabetes, and abnormalities in glucose homeostasis (Diaz *et al*., 2019; Ghachem *et al*., 2019; Zaniqueli *et al*., 2020; LeCroy *et al*., 2021). Similarly, metabolic syndrome is linked to dysregulated muscle metabolism and morphology, and deterioration of muscle mass (Eriksson *et al*., 1994; Mårin *et al*., 1994; Oberbach *et al*., 2006; Holloszy, 2009; Park *et al*., 2009; Kim *et al.*, 2010c; Guerrero *et al*., 2016; Han *et al*., 2019; Lewis *et al.*, 2019; Bergman & Goodpaster, 2020). Exercise interventions to forestall reductions in muscle functional capacity, which can incorporate decreased muscle strength and quality as well as greater fatigability (Park *et al*., 2006; Ijzerman *et al*., 2012; Kawamoto *et al*., 2016; Orlando *et al*., 2017; Merchant *et al*., 2020; Senefeld *et al*., 2020a, 2020b, 2020c; Shen *et al*., 2020), have been demonstrated to also prevent further deterioration of overall metabolic health (Meex *et al*., 2010; Bacchi *et al*., 2012; Van Tienen *et al*., 2012; Sparks *et al*., 2013; Pino *et al*., 2019). The skeletal system is also subject to diabetic complications including increased bone brittleness and fracture risk underlain by compromised bone microarchitecture (Bonds *et al*., 2006; Holloway *et al*., 2018; Starup-Linde *et al*., 2018; Ho-Pham & Nguyen, 2019; Yamamoto *et al*., 2019; Lee & Hwang, 2020). Impairment of musculoskeletal composition and function in metabolic disease conditions further positions fat-free mass as important to metabolic homeostasis contexts.

Polynesian populations present a musculoskeletal phenotype which, like their predisposition to obesity and metabolic syndrome in the modern environment, is distinct from European average body composition measures. The greater mean BMI of Pacific

Islanders compared to Europeans is accompanied by possession of greater lean or muscle mass, and perhaps also greater height (Swinburn *et al*., 1999; Rush *et al*., 2009). Skeletal composition seems likewise enhanced. Bone mineral content and density are significantly greater in Polynesian than European cohorts (Reid *et al*., 1986; Cundy *et al*., 1995; Grant *et al*., 2005). This may help to explain why the increased femoral neck length of Polynesians compared to European or Asian groups, typically taken as a risk factor for fracture, is accompanied by low incidence of bone fracture (Chin *et al*., 1997). The underlying reasons for these ethnic disparities are less simply discerned. Beverly and Evans (1986) made the early suggestion that bone density was driven by local stressors, and thus a reflection of the peak physical effort required in different socioeconomic circumstances. The key developmental driver, however, is perhaps common to both the muscular and the skeletal phenotypes. The greater bone mineral acquisition in Polynesian adults is partially accounted for by greater body weight, and in children is entirely explained by height and weight (Cundy *et al*., 1995; Grant *et al*., 2005). The strongest predictor of BMD in a healthy cohort of Pacific Island women was lean mass (Casale *et al*., 2016). Stride (2016) argues that this dual musculoskeletal phenotype is at least partially caused by genetic effects on bone-muscle precursor mesenchymal cells. The potentially heritable predisposition to increased muscle and bone mass in Pacific Island populations is perhaps particularly suggestive in the context of region-specific genetic variant alleles which influence body composition and growth.

Musculoskeletal involvement in the CREBRF missense variant phenotype has received comparatively limited attention thus far. Increased fat-free mass is reported in Samoan variant carriers of both sexes during infancy and adulthood (Arslanian *et al*., 2021; Hawley *et al*., preprint); we have demonstrated increases to lean mass in male murine variant carriers. Lee *et al*. (preprint) report that this increased lean mass is linked to decreased circulating myostatin levels in male variant carriers. Tangentially associated (and more reproducibly evidenced) are R457Q variant-induced increases to height in children and adults (Berry *et al*., 2018; Krishnan *et al*., 2018; Hanson *et al*., 2019; Carlson *et al*., 2020; Metcalfe *et al*., 2020; Oyama *et al*., 2021; Hawley *et al*., preprint). Indirect associations in the literature are likewise scarce. CREBRF lacks links to the musculoskeletal system beyond a recently reported miRNA-regulated role in yak skeletal muscle development (Ji *et al*., 2020). Its key regulatory target, CREB3, may suppress myogenic gene expression via disruption of α-actinin-4 (ACTN4) activity (An *et al*.,

2014). CREB3 furthermore has a role in bone remodelling, shown to interact with multiple osteogenic mediators to promote osteoclast differentiation and activation, and consequently enhance bone mass and mineral density as well as stimulating bone formation during healing (Miyamoto, 2006; Kim & Ko, 2014; Kanemoto *et al*. 2015; Chiu *et al*., 2017; Kim *et al*., 2020). At one remove further is the GR, differentially regulated by both CREBRF and CREB3, which facilitates muscle atrophy as well as reduction of bone mass and mineralisation (Abu *et al*., 2000; Waddell *et al.*, 2008; Rauch *et al*., 2010; Tanaka *et al*., 2017). There seems, therefore, to be some tentative theoretical grounds to speculate that the CREBRF missense variant produces phenotypic effects on muscle and/or bone composition, which may in turn influence the more established effects on diabetes risk.

The production of phenotypic effects on muscle and/or bone composition by the CREBRF missense variant could in turn influence the more established effects of genotype on diabetes risk. In the interests of further developing our understanding of the fat-free mass phenotype, we used a pilot cohort of mice harbouring the CREBRF R458Q variant, choosing to examine male animals in order to establish whether the dose-dependent genotype effect on body composition which we had previously identified only in this sex might be underlain by muscle- and/or bone-specific effects. In this chapter the aim was to characterise the musculoskeletal characteristics of chow-fed WT and HOM male KI mice, and to determine whether muscle function or nutrient homeostasis were impacted by presence of the R458Q variant in this model.

5.2 METHODS

5.2.1 Animal maintenance and study

Male *CREBRF* R458Q gene variant mice (WT and HOM) fed a regular chow diet were bred and housed as detailed in Chapter 2. Assessment of body composition at 14, 17, and 20 weeks of age, and of length at 18 weeks, was likewise performed as previously described (Section 2.1.2). Mice were sacrificed in a fed state and tissues collected at 20 weeks of age, with biochemical analyses performed as per sections 2.2.4-5.

5.2.2 Exercise endurance testing

Exercise endurance was measured on an Exer-6M Treadmill (Columbus Instruments, USA) fitted with an electrical stimulus shock grid. Male KI mice aged 16 weeks were acclimatised to the treadmill for 3 days prior to testing, followed by a rest day. Acclimatisation protocol each day comprised two bouts of low intensity treadmill activity for 10 min, separated by a 5 min rest period. Treadmill speed during these bouts was set at 5 m/min on the first day; at 5 m/min and at 5 m/min increasing by 1 m/min/min to 10 m/min on the second day; and at 5 m/min increasing by 1 m/min/min to 10 m/min and at 10 m/min on the third day. On the day of testing, mice were subjected to a low intensity exercise endurance protocol as follows: 5 m/min for 5 mins, followed by an increase of 1 m/min/min until a speed of 10 m/min was reached, and maintained for 10 mins. The speed was subsequently further increased by 1 m/min/min to 15 m/min, which was maintained for 10 mins, before being likewise increased to 20 m/min and maintained at that speed for the remainder of the test. Mice were monitored until 10 lapses onto the shock plate, whereupon the stimulus was removed, and the final running time and distance of each animal was recorded.

5.2.3 Grip strength

Forelimb grip strength was determined using the Chatillon [DFE II] Digital Force Gauge (Ametek STC). Male KI mice aged 17 weeks were held by the tail and lowered towards the metal triangular pull bar on the horizontal grip strength meter. Once mice had gripped the bar with both forelimbs, the mice were pulled backward in the horizontal plane until the grasp was released. The force of grip was measured as the peak tension in newtons (*N*). The test was repeated ten times, as two sets of five consecutive tests with a rest break between, and the average of each mouse recorded. Mice unable to complete all ten tests were excluded from analysis.

5.2.4 Hindlimb bone measurements

Hindlimbs dissected from 20-week mice were stored in ethanol at 4°C prior to manual removal of remaining muscle and connective tissues and joint dislocation. Dimensions of femurs and tibiae were quantified using digital callipers. Anatomical locations measured on the femur included widths of the femoral head and bicondylar joint, and shaft depth at the third trochanter and immediately above the bicondylar joint. Missing data for femoral length and head width measures due to bones broken during collection. Tibial measurements assessed widths of the articular surfaces across the proximal epiphysis, from most medial point of the medial condyle to most lateral point of the lateral condyle, and across the distal epiphysis, between medial and lateral malleoli. Shaft depth was measured at the cranial point of inflection on the tibial tuberosity, and immediately above distal epiphysis. Total length and mass were measured for both bone types.

5.2.5 Statistical analysis

Change in body composition measures over time were analysed by ordinary two-way ANOVA with post-hoc testing of WT vs HOM by Sidak's multiple comparisons. All other measures were analysed by unpaired t-tests with Welch's correction. Data are presented as means ± SEM, with statistical significance accepted at $p < 0.05$. Statistical analysis was performed in GraphPad Prism software (Prism 8, Version 8.0.2).

5.3 RESULTS

5.3.1 Body composition

The human CREBRF missense variant allele has been associated with increased BMI and/or adiposity measures (Minster *et al.*, 2016; Naka *et al.*, 2017; Krishnan *et al.*, 2018; Lin *et al.*, 2020) as well as increased height and/or fat-free mass (Carlson *et al.*, 2020; Metcalfe *et al.*, 2020; Arslanian *et al.*, 2021; Oyama *et al.*, 2021). Total body weight was however not different between WT and HOM male chow-fed mice across the course of the current study (Figure 5.1A), as was anticipated from our earlier study (Figure 3.2). Percent fat mass was likewise undifferentiated by genotype at 20 weeks (Figure 5.1B), but displayed some disparity in change over time over the course of the study. HOM mice experienced relative loss of fat mass following the exercise endurance trials (across the 14-17 week measures), significantly different to the gains exhibited by WT animals during the same time period (Figure 5.1C). HOM mice subsequently regained fat mass during the final (sedentary) weeks of the study (Figure 5.1C). Neither lean mass nor naso-anal length of this mouse cohort were significantly changed in HOM animals (Figure 5.1D-F), failing to reproduce the phenotype previously seen in the KI mice detailed in Chapter 3. Total fat and lean mass at 20 weeks, as well as length, were significantly greater than recorded by the initial cohort (Figures 3.2, 3.3).

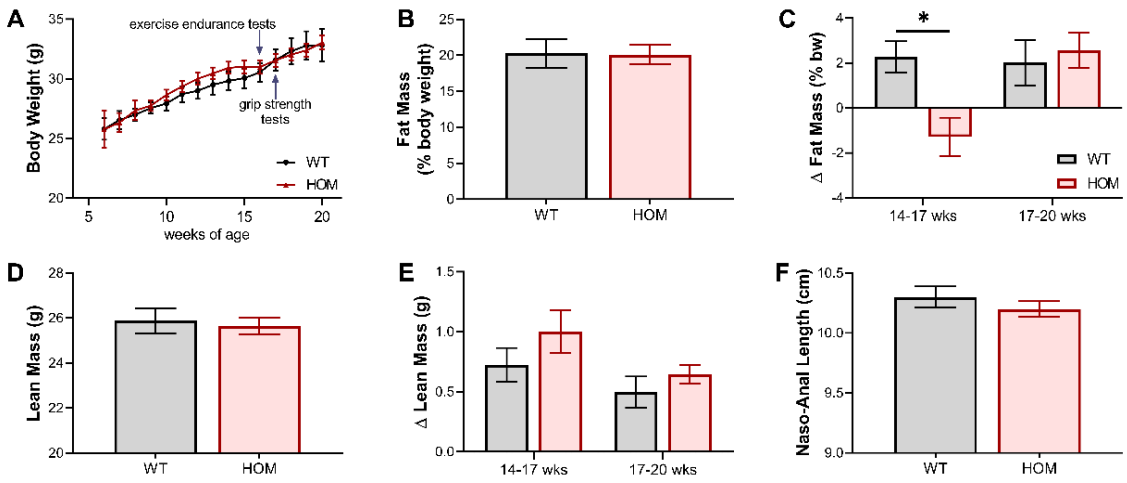

Figure 5.1: Body composition of chow-fed male *CREBRF* R458Q variant mice.

A. Body weight of male mice throughout the study. Total (B) fat mass as a proportion of body weight and (D) lean mass of male mice at 20 weeks of age. Change in (C) percent fat mass and (E) lean mass across indicated time points. **F.** Naso-anal length of male mice at 18 weeks. Data are shown as mean ± SEM, n = 9-15. Data were analysed by ordinary two-way ANOVA, * $p = 0.0134$ by Sidak's multiple comparisons test.

Given previously published associations between the CREBRF missense variant and greater fat-free mass (Arslanian *et al*., 2021; Hawley *et al*., preprint), we further examined the mass of individual hindlimb skeletal muscles despite the lack of genotype effect on total lean mass in the current cohort. The quadriceps and gastrocnemius muscles, which as the larger muscles might accordingly be expected to provide the greater or otherwise more relevant contribution to a phenotype, showed no alterations to their mass between the WT and HOM mice (Figure 5.2A-B). The tibialis, extensor digitorum longus (EDL), and soleus reflected a trend to reduced mass in mice carrying the variant *CREBRF*, which reached significance in the former two fast-twitch muscles (Figure 5.2C-E).

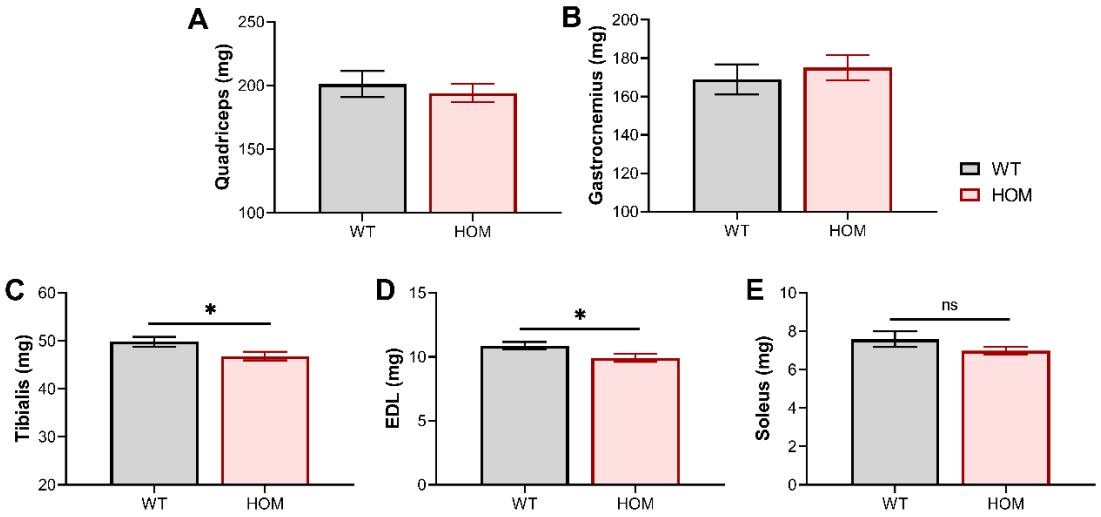

Figure 5.2: Hindlimb skeletal muscle mass of male *CREBRF* R458Q variant mice. Average weight of 20-week male (A) quadriceps, (B) gastrocnemius, (C) tibialis, (D) EDL, and (E) soleus muscles. Data are shown as mean ± SEM, n = 8-15. * $p < 0.05$ HOM vs WT by unpaired t-test with Welch's correction.

5.3.4 Hindlimb bone dimensions

The potential influence of the R458Q variant on fat-free mass in male mice was further explored via the femur and tibia bones. Presence of the *CREBRF* variant had no significant effect on length or mass of either hindlimb bone (Figure 5.3A-B), nor on femoral head and bicondylar widths when assessed individually (Figure 5.3C). Femur depth was significantly greater in the HOM mice than the WT at both the upper and lower placements (Figure 5.3D). The overall trend, incorporating width and depth measures,

suggested that the femurs of HOM mice were (marginally) thicker although not longer than those of their WT counterparts. In contrast, the tibiae were not visibly affected by genotype in any of the width measures taken (Figure 5.3E).

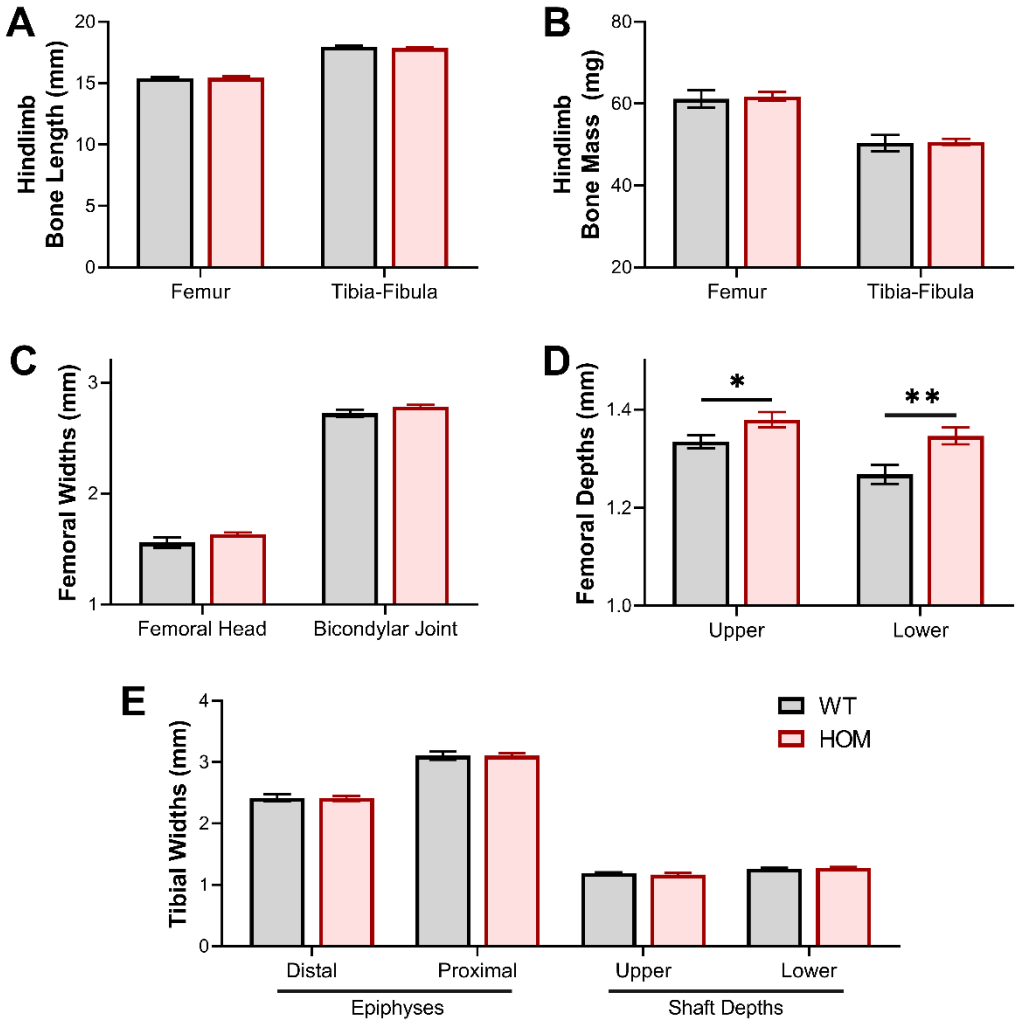

Figure 5.3: Hindlimb bone dimensions of 20-week male *CREBRF* R458Q variant mice.

A-B. Femoral and tibia-fibula bone (A) length and (B) mass. **C.** Femur bone width at femoral head and bicondylar joint. **D.** Cross-sectional depth of the femoral shaft at the third trochanter (upper) and above the bicondylar joint (lower). **E.** Tibial bone width measurements taken across the distal and proximal epiphyses, and shaft depths at the tibial tuberosity (upper) and above the distal epiphysis (lower). Data are shown as mean ± SEM, n = 7-15. * p = 0.0443, ** p = 0.0066 HOM vs WT by unpaired t-test with Welch's correction.

5.3.2 Functional muscle assessments

To determine whether a muscle performance phenotype might be reflected in these mice, functional assessments of exercise capacity and muscle strength were conducted. The KI mice showed no significant difference in the distance run on treadmill exercises, although there was an apparent trend for this endurance capacity to be reduced in HOM compared to WT mice (Figure 5.4A). Forelimb grip strength, quantified as peak tension exerted on the forelimb grip bar, was unaffected by genotype (Figure 5.4B).

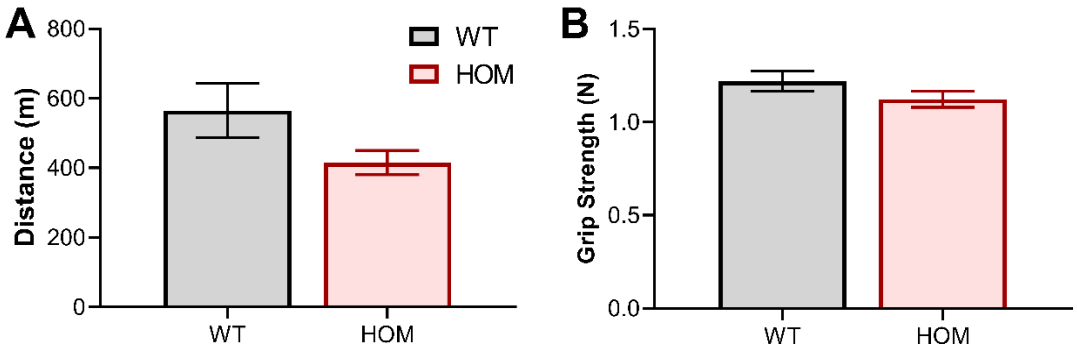

Figure 5.4: Functional assessment of chow-fed male *CREBRF* R458Q variant mouse muscle.

A. Distance covered by 16-week-old chow-fed male mice during an exercise endurance test (n = 9-15). **B.** Forelimb grip strength of 17-week-old male mice, as average of ten attempts, measured as the peak tension in newtons (N) (n = 8-11). Data are shown as mean ± SEM.

5.3.3 Skeletal muscle nutrient homeostasis

Glycogen and triglyceride content was evaluated as a reflection of energy storage in quadriceps and gastrocnemius muscle tissues. No significant genotype differences were observed in the stored glycogen of either muscle (Figure 5.5A). The R458Q variant was however associated with greater lipid content in the same two hindlimb muscles, with a statistically significant effect in the gastrocnemius (Figure 5.5B). Curiously, triglyceride deposition in these animals was significantly greater than the values seen in the equivalent group from the earlier cohort. Glycogen values were similar across both cohorts.

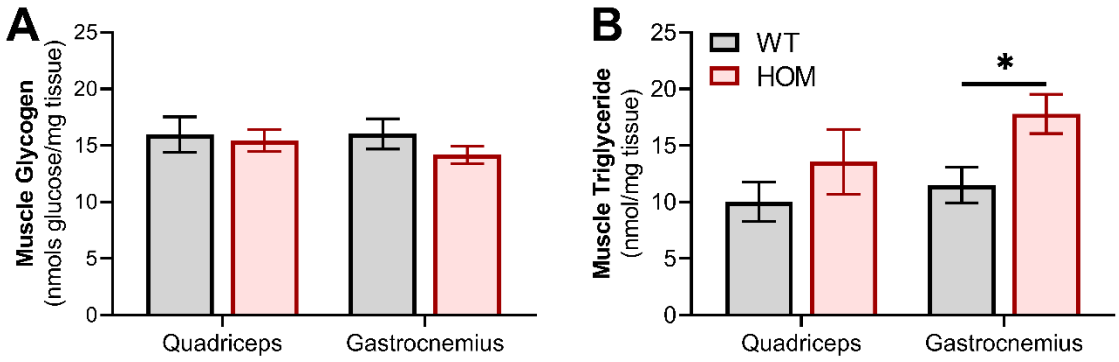

Figure 5.5: Biochemical analysis of hindlimb skeletal muscle from chow-fed male *CREBRF* R458Q variant mice.

(A) Glycogen content and **(B)** triglyceride content of quadriceps and gastrocnemius muscles from 20-week-old male mice in the fed state. Data are shown as mean ± SEM, *n* = 9-15. * $p = 0.0139$ HOM vs WT by unpaired t-test with Welch's correction.

5.4 DISCUSSION

Fat-free mass composition is integral to strength and mobility as well as energy metabolism. Skeletal muscle and bone show proportional accumulation and mutually adaptive development. The CREBRF missense variant found in Pacific Island populations was initially linked primarily to increased adiposity but has also been (inconsistently) associated with greater lean mass and height in humans (Carlson *et al.*, 2020; Metcalfe *et al.*, 2020; Arslanian *et al.*, 2021; Oyama *et al.*, 2021). Despite this growth phenotype, reported to derive from increases to both muscle and bone mass, the current (pilot) study showed only a very mild musculoskeletal phenotype in male mice carrying the CREBRF R458Q variant. Selected hindlimb skeletal muscles had reduced mass in homozygous R458Q mice compared to wild-type counterparts, accompanied by greater femoral width but not mass. Total body composition and functional muscle capacity trends were not significant.

Total lean and fat mass were not significantly different between WT and HOM mice at any individual time-point across the current study. This does not reflect human studies, which near-unanimously associate the CREBRF missense variant with body composition phenotypes affecting either fat or lean mass if not both (Minster *et al.*, 2016; Krishnan *et al.*, 2018; Carlson *et al.*, 2020; Lin *et al.*, 2020; Metcalfe *et al.*, 2020; Arslanian *et al.*, 2021; Oyama *et al.*, 2021). Genotype-dependent change in total percent fat mass over time may, however, indicate some potentially instructive variant-induced changes. The loss in whole-body fat content, which was seen only in mice carrying the CREBRF variant, coincides with exercise endurance testing and could potentially represent a reaction to that physiological stressor. Indeed, CREBRF activity is known to interact with glucocorticoid signalling, which governs the major biological stress response and facilitates lipolytic decreases in adipose tissue following exercise training (Campbell *et al.*, 2009; Martyn *et al.*, 2012; Rosa *et al.*, 2014; Frahm *et al.*, 2020). Any missense variant alteration of that relationship might accordingly influence the murine body composition response to exercise stress, although further studies would be needed for definitive proof of this supposition.

Genotype-dependent influence on lean mass was represented at the level of selected individual muscles, rather than total whole-body measures. Given the absence of any concerted impacts on total lean mass or body composition, however, the implications of

these hindlimb muscle-specific reductions for broader physiological function are somewhat limited. Mechanistic origins of the altered muscle mass hold potential to elucidate a basis for CREBRF variant interaction but generally lack evidential support in the current study. Muscle phenotype responds to multiple hypertrophic and atrophic stimuli, including the mTOR and fasting-induced signalling pathways with which CREBRF has previously been associated and which may therefore be differentially influenced by the R458Q variant (Tiebe *et al.*, 2015; Minster *et al.*, 2016; Tiebe *et al.*, 2019). Remodelling can further demonstrate complex expression patterns including, for example, dependence on muscle fibre type (Talmadge *et al.*, 2004; Jia *et al.*, 2019). Given that the R458Q-affected tibialis and EDL are both fast-twitch muscles, such an explanation is feasible, but perhaps somewhat mitigated by the near-significant reduction seen in slow-twitch soleus muscle. Absence of any change to quadriceps or gastrocnemius may otherwise imply that the genotype effect has an absolute limit rather than proportional amplification, and thus disappears in the larger muscles.

Few human studies examine fat-free mass in CREBRF variant carriers. Lin *et al*. (2020) have provided the only (published) measures to distinguish between arm and leg lean mass, and moreover report no genotype effect on any fat-free measures in the Hawaiian cohort. This cannot guide interpretation of the murine muscle-specific changes but may help explain absence of any differences in lean mass or length in the current study. The muscle-based phenotype currently minimally reported in literature develops somewhat inconsistently across surveyed human geographic or ethnic populations (Metcalfe *et al*., 2020; Lin *et al*., 2020; Arslanian *et al.*, 2021; Lee *et al*., preprint). The additional complicating factor of species translation, and the comparatively milder murine phenotype, render it perhaps unsurprising that the small sample size of the current study cannot outcompete biological variability to produce a significant genotype difference in total body composition measures.

The CREBRF R458Q variant was associated with greater femoral width in the HOM mice. This effect on bone is perhaps somewhat explicable in view of the phenotypes elsewhere reported which link both human and murine missense variants with increased growth, incorporating both lean mass and height (Carlson *et al*., 2020; Arslanian *et al*., 2021; Lin *et al*., 2020; Metcalfe *et al.*, 2020; Hawley *et al*., preprint). Muscle and bone are developmentally correlated, showing proportional growth and strength (Proctor *et al*.,

2000; Ashby *et al*., 2011; Goodman *et al*., 2015). The human R457Q variant has also been associated with greater bone mass accretion in infant carriers (Arslanian *et al*., 2021). That Hawley *et al*. (preprint) reported this effect to be absent in an adult population (which retained a muscle mass phenotype) may suggest a comparatively mild bone phenotype, perhaps with an absolute limit on variant-induced bone mass increases, losing significance as adult proportions are reached. Indeed, a weak phenotypic effect in this regard might explain the absence of variant-induced tibial changes in the KI mice.

Alternately, the disparity between human infant and adult cohorts could indicate some additional environmental influence, perhaps unrelated adaptive responses to age or activity, masking variant-induced changes. Human R457Q variant effects on total bone mass cannot be wholly equated to the murine hindlimb bone dimension measurements of the current study. Indeed, murine femoral mass was not significantly different in variant carriers despite greater width, although variations in trabecular bone structure, which was not analysed in the current study, remain a possibility. This may have implications for CREBRF variant impacts on bone density and therefore strength or related functional outcomes. As for muscle, bone has a bidirectional adaptive relationship with physical activity and performance. Mouse lines bred for high voluntary wheel running, for example, have been shown to possess thicker femora, with larger femoral heads, without change to bone length (Kelly *et al*., 2006; Castro & Garland, 2018). Extrapolation to the similar CREBRF variant femoral effects could perhaps imply analogous activity-based effects in exercise-trained variant carriers. Variability in musculoskeletal characteristics displayed by exercised mice renders bone morphology, taken by itself, an unclear indicator of functional consequences (Plochocki *et al*., 2008; Castro & Garland, 2018). More extensive study would be needed to ascertain reproducibility and implications of such missense variant effects.

The current study presented preliminary testing of treadmill endurance and of forelimb grip strength which did not find the R458Q variant to be associated with any significant alterations to inherent skeletal muscle functional capacity. Examination of skeletal muscle performance in the presence of the CREBRF missense variant cannot yet allow for comparison between human and murine carriers. The recent Soifua Manuia (Good Health) study, which enrolled adult Samoan participants in a follow-up to an earlier 2010 study, incorporated measurements of handgrip strength and objective physical activity in

its study protocols (Hawley *et al*., 2020). These results are however yet to be published. No other human studies have (reported having) undertaken similar measurements and as such can offer no specific interpretative guidance for how the R458Q KI mouse model might either reproduce or mistranslate the human phenotype. Similarly little relevant data pertains to the WT CREBRF, limited primarily to the hyperactivity observed in CREBRF-KO mice (Martyn *et al*., 2012; Frahm *et al*., 2020). In this absence of literature, and also considering the small sample size and non-significant results of the current study, extensive speculation is largely unsupported. Given that total lean mass was not impacted by genotype in the assessed cohort, the similar absence of significant functional effect is perhaps not unexpected but certainly seems to indicate no obvious amplification of metabolic efficiency. Assessment of physical performance in murine or human cohorts which do display variant-induced increases to lean mass as previously reported might offer more conclusive results.

Any phenotypic effect of the CREBRF variant on fat-free mass morphology or function might also receive potential influence from strain or species. Indeed, the genetic variance between mouse strains has been shown to substantially contribute to baseline muscle mass as well as to functional overload-induced mass gains (Kilikevicius *et al*., 2016). Murine exercise capacity, including intrinsic and forced running endurance, is likewise significantly influenced by genetic background (Haramizu *et al*., 2009; Kvedaras *et al*. 2017; Massett *et al*., 2019). Evidence has likewise been found that genetic background impacts exercise capacity and response in humans (Vellers *et al*., 2018; Harvey *et al*., 2020). That genetics can influence if not drive inter-individual variation in skeletal muscle performance supports that the CREBRF missense variant could hold the potential to exert similar influence. It also, however, underlines the species translation barrier separating human and murine variant phenotypes. The overall absence of any pronounced variant muscle phenotype in the KI mouse model cannot exclude possible effects in human variant carriers, which may be subject to additional or polygenic influences. PI populations are known to have greater muscle and bone mass than European or other groups (Reid *et al*., 1986; Cundy *et al*., 1995; Swinburn *et al*., 1999; Grant *et al*., 2005; Rush *et al*., 2009). If any related influence of the CREBRF R457Q variant was to comprise augmentation of this baseline predisposition, the effects may not be independently visible in a model lacking this PI genetic background.

Although intrinsic muscle function in the KI mouse model was not significantly altered by presence of the CREBRF missense variant, an interaction might more feasibly be precipitated by more direct intervention to induce muscle hypertrophy or atrophy. Incorporation of mechanical loading or unloading strategies into the R458Q KI model, provoking adaptive muscle responses, might thusly facilitate understanding of any variant-associated factors affecting muscle mass and growth (Mirzoev, 2020; Murach *et al*., 2020). Whereas the current study sought to ascertain endurance capacity on a single occasion, following only a short acclimatisation period, muscle exercise performance in animal as well as human research develops over time. Consecutive bouts of exercise, each accompanied by acute metabolic adaptations at the molecular and cellular level during recovery, produce cumulative effects to ultimately induce remodelling of substrate metabolism pathways in addition to functional improvements in exercise performance (Pilegaard *et al*., 2000). This can include greater skeletal muscle capacity for substrate storage as well as metabolic efficiency (Hearris *et al*., 2018; Fuller *et al*., 2019), but alterations are not limited to that tissue. Given that CREBRF has functions in these realms of oxidative metabolism and nutrient handling as aforementioned (Minster *et al*., 2016; Tiebe *et al*., 2019), it is perhaps liable also to interact with these pathways in response to chronic exercise-based (and not only starvation-based) stressors. Indeed, CREBRF may exhibit greater activity, and perhaps more pronounced variant-induced genotype differentiation, when stimulated by such an environment of physiological stress.

The nature and magnitude of the adaptive changes which are elicited by exercise training are significantly influenced by both the intensity and the duration of exercise (Hildebrandt *et al*., 2003; Ahmadi *et al*., 2021; Shirai *et al*., 2021). In rats, for example, eight weeks of moderate-intensity continuous training versus isocaloric high-intensity interval training produced significantly greater positive responses in metabolic gene expression (compared to sedentary animals) under the latter protocol (Ahmadi *et al*., 2021). Endurance training of differing durations in mice was recently shown not to alter body or muscle mass, but differentially impacted protein ubiquitination and oxidative stress (Shirai *et al*., 2021). Low-intensity treadmill activity, such as that used to test the KI mice, can acutely produce transient metabolic changes in mice which after six weeks of training are more robust but do not indicate pathway remodelling (Fuller *et al*., 2019). Given that the minimal variant phenotype which is seen in the mouse model likely requires some potentiation, it is perhaps not unexpected that the KI mice, being essentially untrained sedentary animals,

do not show significant differentiation between WT and HOM endurance exercise performance. A more in-depth assessment of skeletal muscle potential performance in KI mice might be better facilitated by looking at whether the variant produces differential response to prolonged exercise training of perhaps greater intensity. Functional outcomes can include not only time to exhaustion but also speed as well as voluntary exercise patterns (De Bono *et al*., 2006; Kelly *et al*., 2006; Kvedaras *et al*. 2017). The latter is perhaps of especial relevance given that the hyperactivity phenotype of CREBRF-KO mice, being the sole report of CREBRF-associated impacts on physical performance, was more behavioural than physiological in cause. Such more complex testing protocols may be equally useful in revealing (or excluding) a variant phenotype.

Given the proposed connections between CREBRF and nutrient-sensing and/or homeostasis (Tiebe *et al.*, 2015; Minster *et al*., 2016; Tiebe *et al*., 2019), we examined storage of glycogen and lipid in our KI mouse skeletal muscle. The similarity in glycogen content between WT and HOM mice was perhaps not unexpected: neither WT nor missense variant CREBRF has been specifically associated with glycogen content. While this is partially a natural consequence of the limited literature available on the protein, even the broader associations with altered systemic glucose metabolism in human variant carriers are not consistently observed (Minster *et al.*, 2016; Lin *et al*., 2020). In fed state animals, with the starvation-induced CREBRF presumably less actively involved in nutrient homeostasis, variant-induced impacts on stored carbohydrate would likely be accordingly minimised. Although glycogen stores are depleted by exercise, the effect is primarily acute and followed by resynthesis. Low-intensity treadmill exercise as performed in the current study would be neither strenuous nor repetitive enough to produce longer-term changes visible at endpoint in these mice (Fuller *et al*., 2019). Any interaction between variant and exercise-induced glycogen utilisation would likewise not be visible in this measure under the current protocol. The apparent lack of missense variant impacts to glycogen content in the current KI mouse model might have implications for glucose metabolism in variant carriers more generally. Such interpretations would likely, however, necessitate more stringent protocols or energy-demanding conditions to conclusively exclude any genotype-dependent effect on skeletal muscle carbohydrate storage.

The missense variant was associated with greater skeletal muscle triglyceride accumulation in male R458Q KI mice. Variant-induced enhancement of lipid storage was likewise reported in Minster *et al*. (2016)'s 3T3-L1 adipocyte overexpression model, perhaps indicating that the missense variant may induce these effects somewhat independent of tissue type. Given the absence of any whole-body adiposity phenotype in the KI mice, however, this extrapolation is perhaps of limited relevance and overly speculative. The endpoint measurement cannot ascertain whether the greater accumulation is a product of altered synthesis or breakdown. Parallels can perhaps be derived from a recent *in vitro* study in which knockdown of the CREBRF cofactor Crebl2 increased muscle cell triglyceride content, mediated by enhanced glucose uptake (Tiebe *et al*., 2019). Direct translation of this mechanism is unrealistic, and similarly cannot be taken to straightforwardly evidence that the missense variant might induce a reduction in CREBRF-Crebl2 complex activity, given that Tiebe *et al*. (2019) and the current study utilise wholly distinct models, focusing on different components of that complex. The similarity in lipid effect may nevertheless imply that the CREBRF R458Q variant could likewise alter glucose uptake and, given its lack of effect on glycogen, perhaps subsequently acts to direct these carbons towards lipid rather than glycogen synthesis. This might imply utility to investigating glucose (as well as lipid) metabolism more closely in this KI model.

Skeletal muscle mass and nutrient homeostasis are both impacted by fasting. Limited availability of energy substrates triggers adaptive catabolic responses and consequently atrophic mechanisms (Ibrahim *et al*., 2020). Energetic pathways are likewise impacted by exercise and these impacts on, for example, breakdown or oxidation of intramuscular triglyceride content have furthermore been shown to be enhanced when exercise occurs in the fasted state (De Bock *et al*., 2005; Van Proeyen *et al*., 2011). The corollary is also proven, with altered muscle FA uptake (and thus utilisation) shown to impact exercise capacity during fasting (Iso *et al*., 2018, 2019). Given that both fasting and low-intensity exercise prefer energy derived from FA substrates (Egan & Zierath, 2013; Iso *et al*., 2019), it would be interesting to know whether their combination might produce any interplay with the altered TG accumulation which comprised the most overt effect in muscle of mice carrying the R458Q missense variant in the current study. Although both exercise and fasting represent demands on energy, these two conditions have been suggested to stimulate different (and perhaps opposing) molecular responses such that

their combination in animals as well as humans is not a straightforward augmentation of energy demand, but rather produces changes which are unlike those elicited by either stimulus alone (Hildebrandt & Neufer, 2000; Jaspers *et al*., 2017). Interaction of these combined with missense variant would consequently also not be straightforward.

It may be that the introduction of a fasting state would present additional impacts on skeletal muscle metabolism in the R458Q KI mouse model, which may render missense variant-associated effects more prominent. Indeed, overnight fasting has elsewhere provoked genotype-dependent effects on exercise capacity which are not visible when the same transgenic rodents are tested in the fed state (Pedersen *et al*., 2005; Iso *et al*., 2018). The possibility is particularly promising given that both WT and variant CREBRF are linked not only to nutrient handling but specifically to the starvation response (Tiebe *et al*., 2015; Minster *et al*., 2016; Tiebe *et al*., 2019). This is true even beyond the exercise context. Fasting-induced muscle atrophy would likewise offer another lens through which to explore CREBRF variant effects on muscle mass and growth; especially given that this proteolytic mechanism operates via the GR (Wing & Goldberg, 1993; Waddell *et al*., 2008), which is strongly linked to the operation of CREBRF (Audas *et al*., 2008; Martyn *et al*., 2012; Frahm *et al*., 2020). The current study showed exceedingly minor effects of the variant on skeletal muscle mass in fed state animals; whether fasting conditions might exacerbate or remove the difference between genotypes could help elucidate protein physiological function.

Skeletal muscle mass and functional capacity of R458Q KI mice was primarily examined for the potential source or consequences of previously established lean mass increases in variant carriers, but secondarily also for variant-associated metabolic changes. The speculative scope of these potential changes is perhaps most commonly derived from the well-reported finding that the human CREBRF variant is associated with protection against risk of diabetes (Minster *et al*., 2016; Hanson *et al*., 2019; Krishnan *et al*., 2020). Skeletal muscle is essential to whole-body glucose disposal and homeostasis and this role is often compromised in diabetes, a metabolic condition which furthermore is itself associated with deteriorations in muscle strength and mass (Cetinus *et al*., 2005; Park *et al*., 2006; Park *et al*., 2009; Guerrero *et al*., 2016). The junction between these three aspects of missense variant, muscle, and diabetes is therefore of logical interest. The R458Q KI mice, which found only limited or non-significant differences between WT

and HOM hindlimb skeletal muscle, were broadly unable in the current study to provide insight into a diabetes-related paradigm. This is perhaps unsurprising given that the KI mouse model has not been studied in a diabetic setting which might properly allow elucidation of possible variant interaction with diabetes-associated muscle decline (Ostler *et al*., 2014). Human studies have not reported any similar such investigation. It may be that any such phenotypic effects are not translated verbatim across species, given that these KI mice have in other regards been shown not to reproduce the human variant phenotype, but would be due further consideration for human and/or murine variant carriers in an appropriate model.

In conclusion, examination of musculoskeletal characteristics in male mice carrying the CREBRF missense variant demonstrated only mild genotype effects on reduced tibialis and EDL mass, increased femur thickness, and greater muscle triglyceride accumulation. Body composition could not reproduce the phenotypes reported either in human populations or in the earlier mouse cohort described in Chapter 3 of this thesis and did not significantly impact muscle function in the presence of the variant allele. The theoretical development of any musculoskeletal phenotype in this mouse model may be more conclusively studied using exercise- or nutrient-based interventions, but inconsistent associations in the primarily-sedentary, chow-fed animals of this pilot cohort cannot establish a fat free mass-driven phenotype.

CHAPTER 6: Molecular Signalling in Hepatocytes from CREBRF R458Q Knock-In Mice

6.1 INTRODUCTION

Systemic energy metabolism is vitally connected to whole-body homeostatic maintenance. Its physiologic regulation entails complex signalling contributions from multiple metabolic tissues including muscle, bone, adipose, and liver. Of the endocrine organs, the liver is particularly essential as a nutrient state sensor for maintaining both carbohydrate and lipid homeostasis (van den Berghe, 1991; Rui, 2014). Much of the relevant hepatic regulation is enacted via the coordinated action of hormonal signals. Insulin and glucagon, secreted from pancreatic β-cells and α-cells respectively, induce generally oppositional counter-regulation. In the transition from the fed to the fasted state, circulating insulin levels, and therefore signalling, become reduced; concurrent elevations in glucagon secretion and signalling enforce that suppression. In the postprandial state, the inverse is true. The balance between insulin and glucagon levels can accordingly govern the hepatic response to nutrient state, including maintenance of euglycemia as well as lipid metabolism and energy balance more broadly. That this governance is not purely counter-regulatory in all respects, but can involve gradation or modulation as well as synergy, indicates fine-tuned control mechanisms. Alterations in hepatic homeostatic processes following stimulation by these two major pancreatic hormones can inform broader physiological regulatory response mechanisms.

Insulin signalling provides systemic regulation of postprandial nutrient metabolism. In the liver, these signals can be broadly classified as promoting anabolic metabolism, modulating glucose and lipid homeostasis as well as cell growth and survival (Saltiel & Kahn, 2001; Taniguchi *et al*., 2006; Santoleri & Titchenell, 2019). Coordination of glucose flux to control postprandial concentrations is facilitated by multiple insulin-stimulated mechanisms. Most directly related is the suppression of hepatic glucose production (HGP), inhibiting glycogenolysis and repressing gluconeogenic gene expression, supplemented by signals to downstream processes which ultimately lead to increased hepatic uptake of circulating glucose (Petersen *et al*., 1998; Iozzo *et al*., 2003; Noguchi *et al.*, 2013). Insulin seems to regulate HGP partially by extra-hepatic mechanisms, primarily the suppression of circulating adipocyte-derived FFA levels, but the direct action on liver tends to predominate unless it becomes otherwise defective

(Rebrin *et al*., 1995; Edgerton *et al*., 2006; Titchenell *et al*., 2015; Bergman & Iyer, 2017; Titchenell *et al*., 2017). Insulin also acts directly on the liver to modulate lipid metabolism, producing increased *de novo* lipogenesis, enhanced triglyceride esterification and secretion, postprandial lipoprotein clearance, and suppression of FAO (Biddinger *et al*., 2008; Laatsch *et al*., 2009; Leavens & Birnbaum, 2011; Haas *et al*., 2012). Postprandial insulin signalling has further been linked to hepatic regulation of circadian rhythms, repressing transcription of circadian genes regulated by feeding (Dang *et al*., 2016; Kalvisa *et al*., 2018). These hepatic regulatory activities position insulin signalling as vital for systemic homeostatic metabolism.

The hepatic glucagon signalling network is primarily active during states of nutrient deprivation. Many of its major signalling targets respond to fasting-induced signals and can be broadly classified as attempts to source or produce energy. The canonical pathway has long been characterised: glucagon regulates the conversion of stored hepatic glycogen into glucose and subsequently its release into the portal circulation, allowing a rapid response to reductions in blood glucose levels (Jakob & Diem, 1974; Magnusson *et al*., 1995). The hormone can also, however, facilitate regulation of multiple other cellular processes including the hepatic production of new glucose, with glucagon known to exert significant transcriptional control to upregulate gluconeogenic genes (Koo *et al.*, 2005; Mihaylova *et al*., 2011; Wu *et al*., 2018). Glucagon signalling suppresses lipid synthesis and enhances lipid catabolism, decreasing liver lipid content (Foretz *et al.*, 1999; Longuet *et al*., 2008; Nason *et al*., 2020). These aspects closely mirror the traditional starvation response in its first two phases. Indeed, the transcriptional response to glucagon exposure in primary hepatocytes is time-dependent: expression of gluconeogenic genes peaks at two hours post-glucagon administration, followed by FAO gene upregulation peaking at 24 hours (Lv *et al*., 2017). Glucagon signalling further impacts broader bioenergetic signalling, not necessarily glucose- or lipid-dependent, including synchronisation of the peripheral circadian clock (Sun *et al*., 2015b), activation of the cellular energy sensor AMPK, and the cessation of mTORC1 activity (Kimball *et al*., 2004; Berglund *et al*., 2009). Where insulin facilitates the disposal and utilisation of excess energetic stores, hepatic glucagon signalling seeks to conserve or produce energy during scarcity.

Hormonal counter-regulation can be observed at key junctions in insulin- and glucagon-stimulated signalling cascades, and indeed is evidenced even for individual proteins

involved in glucose and/or lipid metabolism. The glucagon-activated gluconeogenic transcriptional programme operates primarily via CREB, in cooperation with coactivators which are likewise activated by glucagon during fasting conditions and are inhibited by insulin signalling in the fed state (Chrivia *et al.*, 1993; Arias *et al.*, 1994; Koo *et al.*, 2005; Patel *et al*., 2014). Key rate-limiting gluconeogenic enzymes are also upregulated by FoxO1. Glucagon stimulates both FoxO1 gene expression and, by promoting nuclear translocation and stability, its transcriptional activity (Daitoku *et al*., 2004; Matsuzaki *et al*., 2005; van der Heide & Smidt, 2005; Wondisford *et al*., 2014; Wu *et al*., 2018; Kodani & Nakae, 2020). During the fed state, insulin acts via PKB to trigger FoxO1 ubiquitination, nuclear exclusion, and consequent proteasomal degradation (Matsuzaki *et al*., 2003). Hepatic lipid metabolism is similarly receptive to hormone- and nutrient-responsive homeostatic mechanisms: overnutrition prompts lipid synthesis to store excess energy; deprivation prompts lipid breakdown, to utilise those stores. Expression and activity of the lipogenic sterol regulatory element-binding protein-1c (SREBP-1c), for example, are promoted by insulin and repressed by glucagon, targeting not only transcription but proteolytic processing, protein stability, and occupancy at gene promoters via multiple redundant mechanisms (Foretz, 1999; Azzout-Marniche *et al*., 2000; Cagen *et al*., 2005; Yellaturu *et al*., 2009a, 2009b; Li *et al*., 2010; Yecies *et al*., 2011; Lee *et al*., 2014; Tong *et al*., 2016; Tian *et al*., 2016; Wang *et al*., 2016; Li *et al*., 2019). The contrast is likewise visible in the context of hepatic lipid catabolism: where insulin inhibits peroxisomal FAO (Hamel *et al*., 2001), glucagon enhances FAO by multiple complementary pathways which are primarily but not exclusively transcriptional (Longuet *et al*., 2008; von Meyenn *et al*., 2013; Lv *et al*., 2017; Nason *et al*., 2020; Perry *et al*., 2020). The directly oppositional hormonal signalling suggests coordination reflective of the broader nutrient state response.

Nutrient state-based hormonal counter-regulatory measures can also be illustrated acting on the mTOR signalling pathway. When activated during nutrient replete conditions, mTORC1 promotes protein synthesis and growth. Insulin is well-known to promote this signalling pathway via multiple PKB-mediated mechanisms (Proud, 2006; Vander Haar *et al.*, 2007; Huang & Manning, 2009). Nutrient deficient conditions produce the opposite effect, promoting instead autophagy and amino acid catabolism. Following glucagon stimulation, mTOR complex signalling is inhibited by promotion of complex dissociation and reduction of mTOR catalytic activity (Kimball *et al*., 2004; Xie *et al*., 2011; Wu *et*

al., 2019b). The hormonal signalling effects, although broadly oppositional, do not however simply present as an on/off switch. Although glucagon represses phosphorylation and activity of mTOR substrates 4E-BP1 and S6K1, which insulin induces, it does not similarly repress factors further downstream of S6K1 (Kimball *et al*., 2004). These counterintuitive effects, which are achieved by concurrent glucagon-stimulated activation of the extracellular signal-regulated protein kinase 1-p90(rsk) signalling pathway, suggest that signals transduced downstream of mTOR can be precisely modulated in response to hormone administration (Kimball *et al*., 2004). Nor are the hormonal imperatives on mTOR signalling evenly balanced: coadministration of insulin and glucagon in a perfused rat liver model shows that the repressive effects of the latter are dominant (Baum *et al*., 2009). The counter-regulation, with its emphasis on glucagon-induced tuning of mTOR signalling, reflects broader hepatic interests in ensuring energy preservation during nutrient deprivation.

Insulin and glucagon do not entirely forgo a degree of mutual activity. Of special interest is the mutual effect of glucagon and insulin on the serine/threonine kinase PKB. That insulin administration will phosphorylate PKB, which is extremely integral to the insulin signalling network, at Ser473 and at Thr308 is common knowledge (Alessi *et al*., 1996; Titchenell *et al*., 2017). Kim *et al*. (2018) recently discovered that hepatic glucagon signalling, both *in vivo* and *in vitro*, can also phosphorylate PKB at the same site. The study further found that joint administration of glucagon and insulin will enhance this phosphorylation above levels achieved by either hormone alone, implying distinct signalling pathways (Kim *et al*., 2018). Such interactions between pancreatic hormones, whether synergistic, cooperative, or simply replicative, highlight the complexities of their regulatory actions which, in extending beyond simple direct oppositional counter-regulation, may necessitate closer investigation to explicate.

Pancreatic hormones are far from the sole regulatory factors governing hepatic response to nutrient-based stimuli, but rather operate in coordination with parallel and/or overlapping pathways involving sensors of sugars or carbohydrates, of lipids, or of amino acids. Postprandial glucose availability activates sensors such as LXR and liver glucokinase, which have regulatory roles in cholesterol, lipid, and glucose metabolism (Anthonisen *et al*., 2010; Massa *et al*., 2011; Bindesbøll *et al*., 2015). The three major peroxisome proliferator-activated receptor isoforms (PPARα, PPARβ/δ, PPARγ) have

distinct roles in the liver, as recently reviewed by Wang *et al*. (2020), but together comprise major transcriptional sensors of fatty acids and fatty acid derivatives with broad-ranging effects on hepatic and systemic metabolism (Poulsen *et al*., 2012; Contreras *et al*., 2013). Amino acids signal primarily via the mTOR complexes, shown to modulate hepatic and systemic lipid metabolism via mTORC1, and PKB signalling via mTORC2 (Tato *et al*., 2011; Dai *et al*., 2015; Uno *et al*., 2015). Selective activation is differentiated by nutrient/starvation conditions accompanying amino acid provision (Tato *et al*., 2011). The extensive regulatory impacts of these and other nutrient sensors reflect their importance to hepatic metabolism.

Maintenance of homeostasis in the hepatic environment involves numerous tightly interwoven signalling networks. Presenting the hormonal signals as divorced from alternate nutrient sensing pathways is a largely artificial construct, for ease of digestion, rather than an accurate reflection of the adaptive, multifaceted mechanisms involved. Glucose directly stimulates insulin secretion and suppresses glucagon secretion; the hormones, as discussed, can operate as nutrient sensors and cooperatively maintain euglycemia by facilitating glucose uptake or production as necessitated. Amino acids promote α-cell proliferation and secretion of glucagon, which feeds back to reduce amino acid signalling apparently independent of its glucose-related regulatory functions (Unger *et al*., 1970; Dean *et al*., 2017; Hayashi & Seino, 2018; Suppli *et al*., 2020; Winther-Sørensen *et al*., 2020). These hormonal regulatory functions merge in many respects with carbohydrate-, lipid-, and amino acid-responsive signals. Nutrient sensing mechanisms are however complicated by more than simple downstream overlap in shared signalling pathways or targets. Rather, the sensors cooperate by design, providing additional layers of regulation, such that pathway activation may be determined by the combination of inputs. Liver glucokinase, for example, responds to the dual postprandial increases in glucose and insulin (Massa *et al*., 2011). The regulatory functions of SREBP-1c and ChREBP, TFs which respond to increased insulin and carbohydrate concentrations respectively, are overlapping but distinct, and consequently ensure that the liver's full capacity for lipid synthesis is reached only when both stimuli are present (Linden *et al*., 2018). The balance between these regulatory signals is therefore strongly integrated with maintenance of normal metabolism.

Pancreatic hormone secretion and signalling is dysregulated in diabetes. The field is dominated by investigation into the roles played by hyperinsulinemia and insulin resistance. Although these are unequivocally central to the condition, more recent studies have also begun to focus on the well-reported elevation of circulating glucagon in people with diabetes (Unger & Cherrington, 2012; Lee *et al.*, 2016; Bisgaard Bengtsen & Møller, 2021). In the diabetic context, hyperinsulinemia and/or hyperglucagonemia contribute to hyperglycaemia through failure to ensure proper glucose homeostasis. The inappropriate responses elicited, however, are neither limited to glucose control nor wholly straightforward: metabolic disease can for example demonstrate pathway-selective insulin resistance, such that effects on glucose metabolism are impaired while lipogenic effects are increased (Otero *et al*., 2014). Chronic hyperinsulinaemia in insulin-resistant syndromes can promote hepatic lipid accumulation (Wolfrum *et al*., 2004; Steneberg *et al*., 2015; Meroni *et al*., 2020), alter amino acid metabolism (Rozance *et al*., 2020), or suppress hepatic autophagy (Liu *et al*., 2009). Chronic hyperglucagonemia, traditionally causally linked to hyperglycaemia, has recently been theorised to potentially induce glucagon resistance in the liver and therefore improve glucose homeostasis (Bozadjieva Kramer *et al*., 2021); such resistance, however, may also dysregulate lipid and amino acid/protein metabolism and generally lacks uniform consequences (Janah *et al*., 2019; Galsgaard, 2020; Suppli *et al*., 2020; Winther-Sørensen *et al*., 2020). Perturbation of these hormones, and by extension their complex hepatic signalling networks, seems to be integrated with the diabetic phenotype; examination of their interactions might therefore be informative.

The CREBRF R457Q missense variant has an established protective effect against T2D in human carriers (Minster *et al*., 2016; Krishnan *et al.*, 2018; Hanson *et al*., 2019; Krishnan *et al*., 2020). Published studies have not as yet been able to provide a definitive basis for this effect, which is accompanied in some cohorts by reduced blood glucose levels or increased insulin secretion but is overall without consistent links to potential mediating factors across studies (Minster *et al*., 2016; Ohashi *et al*., 2018; Hanson *et al*., 2019; Krishnan *et al*., 2020; Lin *et al.*, 2020; Burden *et al*., 2021). Molecular or tissue-specific studies have not been undertaken and as such there has been little focus on the pancreatic hormone signals which are dysregulated in the diabetic condition. There is, however, a clear association between WT CREBRF and nutrient-responsive energy metabolism: CREBRF expression is induced by starvation and linked with both glucose

and lipid metabolism *in vitro*, via associations with Crebl2 and FoxO1 (Tiebe *et al*., 2015; Minster *et al*., 2016; Tiebe *et al*., 2019). An indirect connection to (hepatic and systemic) glucose homeostasis is provided by starvation-induced expression of the shortened CREB3 isoform, sLZIP, which can promote gluconeogenic enzyme activity in human and murine liver cells with consequences on *in vivo* glucose tolerance (Kang *et al.*, 2020). CREBRF variant activity on diabetes risk (or growth phenotypes) might feasibly involve altered nutrient-responsive signalling in peripheral tissues such as liver. With the exception of this last example, however, these associations have largely not been specifically studied in the liver. Current literature, therefore, cannot indicate whether CREBRF, either WT or variant, acts on the relevant hepatic signalling networks, or how such an interaction might influence cellular or systemic processes.

Given these limitations, the current study investigated potential impacts of the CREBRF missense variant on hepatic signalling in the R458Q KI mice. Although the study described in Chapter 3 could not strongly indicate a role for the missense variant in the regulation of hepatic metabolism, the fasting-induced genotype differentiation in nutrient storage as well as the hepatic transcriptome (Chapter 4) also do not dissuade more targeted examination of hormone-stimulated signalling networks. The isolated primary hepatocyte model provides an opportunity to investigate molecular signalling in a controlled environment. Precise regulation of extracellular influences, including nutrient supply and hormonal stimuli, restricts confounding factors to allow clearer evaluation of interactions or mechanisms. In this chapter the aim was to characterise metabolic molecular pathways in primary hepatocytes isolated from WT and HOM male KI mice, and to determine whether the associated responses to nutrient conditions or hormone stimulation were impacted by presence of the R458Q variant.

6.2 METHODS

6.2.1 Primary hepatocyte isolation

Primary hepatocytes were isolated from chow-fed male *CREBRF* R458Q gene variant mice (WT and HOM) aged 10 weeks, which were housed and maintained as described in section 2.1 of this thesis, using a two-step perfusion method. Mice were intraperitoneally injected with a ketamine and xylazine cocktail (125 mg/kg and 25 mg/kg respectively) to induce deep anaesthesia. The liver was exposed and perfused *in situ* via the inferior vena cava, outflow via the hepatic portal vein, with pre-warmed 1x Hanks Buffered Salt Solution (HBSS; 138 mM NaCl, 50 mM HEPES, 5.6 mM glucose, 5.4 mM KCl, 0.34 mM Na_2HPO_4, 0.44 mM KH_2PO_4, 4.17 mM $NaHCO_3$, pH 7.4, at 37°C) with 0.5 mM EGTA. After 15 mins perfusion at a flow rate of 5 mL/min, liver was perfused with 50 mL of 1 mg/mL collagenase H (Roche) in pre-warmed 1x HBSS supplemented with 2 mM $CaCl_2$. The digested liver was removed intact and placed in cold HBSS-$CaCl_2$. Hepatocytes were released by gentle teasing of the softened liver and filtered through a 100 μM cell strainer (BD Biosciences). Cells were then washed three times with ice-cold HBSS-$CaCl_2$ at 50 *g* for 3 min at 4°C and the supernatant discarded. The final cell pellet was resuspended in adherence medium (below) for plating.

6.2.2 Cell culture conditions

All cell culture was carried out in aseptic conditions in a sterile biohood. Cells were cultured in a 37°C, 5% CO_2 incubator. Hepatocytes were plated on collagen-coated 6-well plates (Type 2 rat collagen from tail, Gibco) in an adherence medium (5.5 mM glucose Dulbecco's Modified Eagle Medium [DMEM] supplemented with 1% penicillin/streptomycin, 1% v/v Bovine Albumin Fraction V [7.5% solution, Thermo Fisher], 100 nM dexamethasone, 100 nM insulin, 2% v/v FBS). After 4 hr attachment, media was changed to basal media as described below. All cells were used in subsequent experiments within 24 hr.

To test the possible influences of glucose content and/or amino acid composition, hepatocytes were cultured in either low- or high-glucose DMEM (D6046 and D6429 respectively, Sigma Aldrich), or in Medium 199 (M199; #11043, Gibco). Media were supplemented with 1% penicillin/streptomycin and 100 nM dexamethasone. To test the effects of highly lipotoxic FA treatment, chosen to potentiate more stressful conditions and prominent impairment of insulin signalling than is necessarily seen with mixed-FA

media (Montgomery *et al*., 2016), palmitic acid solutions prepared in absolute ethanol were diluted in low-glucose DMEM media containing 2% FA-free BSA (Sigma Aldrich) to concentrations of 250 μM or 750 μM palmitic acid, or vehicle (ethanol added at equivalent volumes). FA and vehicle media were conjugated for 2 hr at 55°C, filter-sterilised, and cooled to 37°C before addition to cells.

6.2.3 Molecular signalling in hepatocytes

To assess hormone-stimulated molecular signalling in hepatocytes after 16 hr incubation overnight as described above, hepatocytes were treated for 15 min with 100 nM insulin (Actrapid), 10 nM glucagon (Glucagen® Hypokit, Novo Nordisk), or insulin and glucagon coadministration (100 nM each; Mothe-Satney *et al*., 2004). For assessment of basal culture medium effects, hepatocytes were incubated for 24 hr without stimulation. Media was then removed, cells rapidly washed with cold phosphate-buffered saline (PBS), and collected using a cell scraper (Corning Inc., Corning, NY, USA) in 100 μl of ice-cold lysis buffer (50 mM HEPES, 150 mM NaCl, 10 mM EDTA, 1% nonidet NP-40, 10 mM $Na_4P_2O_7$, 1 mM β-glycerol phosphate) supplemented with protease and phosphatase inhibitors (100 mM NaF, 2 mM Na_3VO_4, 4 μg/mL leupeptin, 100 μg/mL PMSF, 4 μg/mL aprotinin, 1 μg/mL pepstatin, 30 μM ALLN). Wells were rinsed with an additional 100 μl of lysis buffer to ensure that all cell material was collected. Samples were kept on dry ice before storage at -80°C. Cells were mechanically homogenised by passing through a needle and lysates prepared for immunoblotting as per the methods described in sections 2.2.1-3. Phosphorylation was normalised by immunoblot analysis using antibodies to respective total proteins, with GAPDH and pan 14-3-3 (see Table 2.5) used as housekeepers.

6.2.4 Hepatocyte triglyceride measurements

To assess triglyceride accumulation in hepatocytes, cells were cultured as described above for 16 hr overnight. Cells were then washed with cold PBS and collected in 200 μl of ice-cold PBS. Protein was quantified as per the methods described in section 2.2.2 and lipids extracted and quantified using GPO-PAP reagent (Roche) using the protocol described in section 2.2.4.

6.2.5 Statistical analysis

Densitometry and triglyceride accumulation were analysed by ordinary two-way ANOVA with post-hoc testing of WT vs HOM by Sidak's multiple comparisons. Data

are presented as means ± SEM, with statistical significance accepted at $p < 0.05$. Sample size n represents biological replicates. Statistical analysis was performed in GraphPad Prism software (Prism 8, Version 8.0.2).

6.3 RESULTS

6.3.1 Nutrient-responsive protein expression

Examination of molecular signalling in an isolated hepatocyte model, free from influence of circulating hormones or substrates, allows narrower restriction of external confounding factors than is possible in an *in vivo* model. Nutrient provision impacts both hepatic metabolic function and CREBRF activity (Minster *et al.*, 2016; Tiebe *et al.*, 2019). We therefore clarified baseline effects of differential media composition on expression of selected proteins in hepatocytes isolated from male R458Q KI mice cultured for 24 hours under basal, unstimulated conditions, focusing on glucose and amino acid availability.

To provide preliminary control measures for hepatocyte response to glucose availability, we evaluated expression of known glucose-responsive proteins, glycogen synthase (GS) and thioredoxin-interacting protein (TXNIP). Basal levels of inhibitory phosphorylation of GS^{Ser641} in our hepatocyte model did not exhibit the expected glucose-induced increases in GS activity (Figure 6.1A). Under the high-glucose (25 mM) conditions only, HOM cells had significantly less GS^{Ser641} phosphorylation than WT. TXNIP expression, known to be upregulated in hyperglycaemia and degraded upon energy stress (Ma *et al.*, 2006; Wu *et al.*, 2013), was prominent in high-glucose and absent in low-glucose media (Figure 6.1A). There was no visible differentiation between WT and HOM cells.

Given the known hyperglycaemia-induced suppressive effects on the hepatic PI3K/PKB pathway (Cordero-Herrera *et al.*, 2014), comparative basal activity of PKB was assessed across the three media conditions. Phosphorylated PKB^{Ser473} and PKB^{Thr308} expression demonstrated the expected glucose-induced reductions, only faintly present in cells cultured in 25 mM glucose media (Figure 6.1A-B). Interestingly, phosphorylation was also promoted by culture in the more diverse amino acid conditions of M199 media, compared to either of the DMEM conditions. Expression of the phosphorylated proline-rich Akt substrate 40 kDa $(PRAS40)^{Thr246}$ protein, a canonical target of PKB kinase activity, appeared to mirror the glucose-induced repression patterns of PKB phosphorylation indicative of signal transduction (Figure 6.1B). The levels of PKB phosphorylation at both sites furthermore appeared to show a genotype-induced trend to reduced expression in HOM cells specifically in the low-glucose DMEM conditions. We therefore determined to focus primarily on hepatocytes cultured in this media to more thoroughly elucidate the potential genotype effect which was observed.

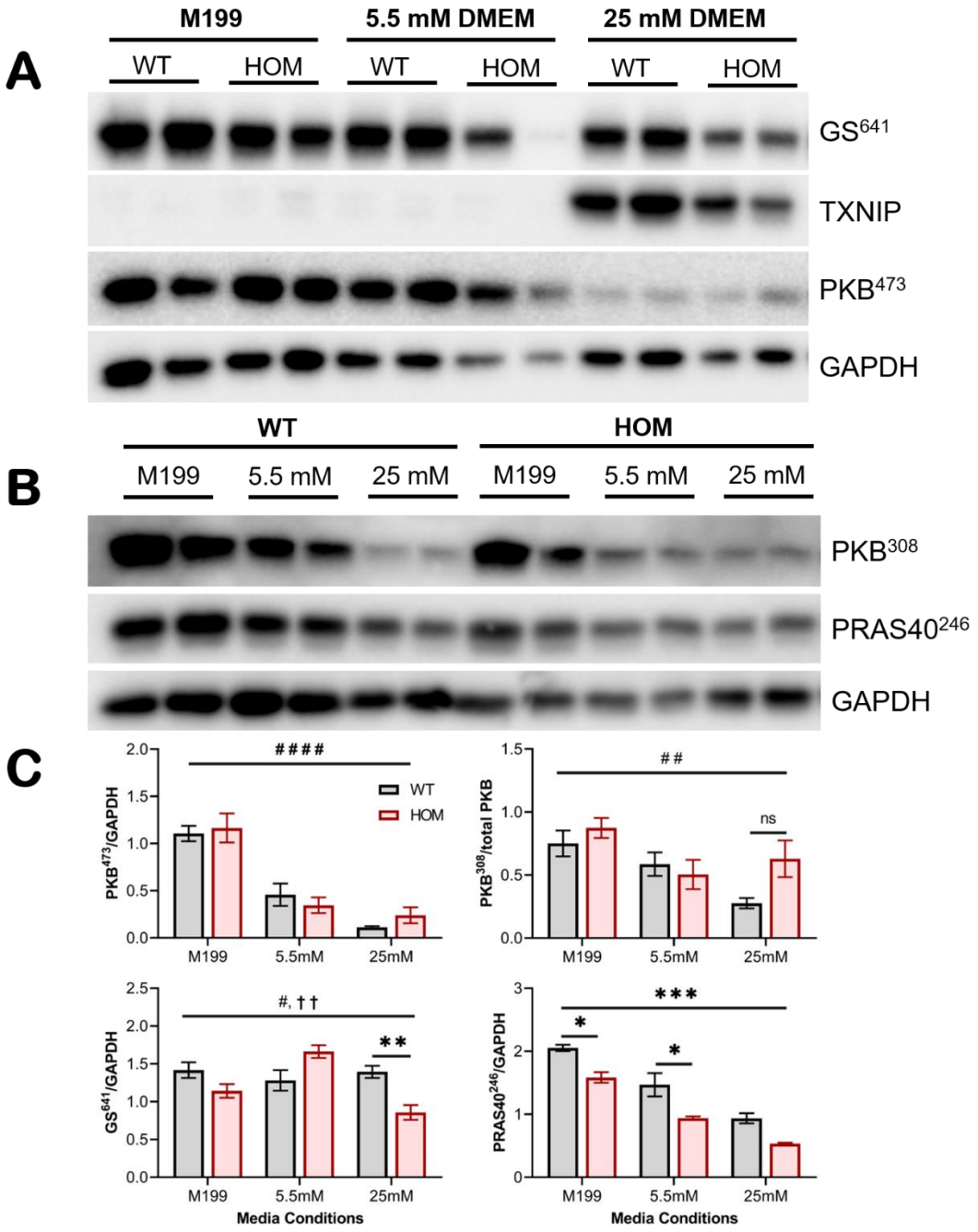

Figure 6.1: Basal nutrient-responsive signalling in R458Q primary hepatocytes. Hepatocytes isolated from WT and HOM male mice were cultured for 22 hours in M199 (5.5 mM glucose), low-glucose (5.5 mM) DMEM, and high-glucose (25 mM) DMEM conditions without treatment. Cell lysates were loaded at 30 µg/well and immunoblotted for expression of insulin signalling proteins, with GAPDH used as a housekeeper. Results are shown as (A-B) representative images and (C) quantification by densitometry analysis shown as mean ± SEM, n = 3-4. # $p < 0.05$, ## $p < 0.01$, #### $p < 0.0001$ main effect of media, †† $p = 0.0013$ interaction between media and genotype by ordinary two-way ANOVA; * $p < 0.05$, ** $p = 0.01$ HOM vs WT by Sidak's multiple comparisons test.

6.3.2 Insulin signalling

Given that the *CREBRF* variant had been associated with diabetes risk in humans (Minster *et al*., 2016; Krishnan *et al.*, 2018; Hanson *et al*., 2019; Krishnan *et al*., 2020), as well as with *in vivo* insulin tolerance in the mouse model (Figure 3.6), we investigated insulin signalling in isolated hepatocytes. Protein expression of phosphorylated PKB was utilised as the primary readout for the active insulin signalling pathway. Hepatocytes cultured overnight in low-glucose DMEM exhibited significantly lower levels of both PKB^{Ser473} and PKB^{Thr308} phosphorylation in insulin-treated HOM cells compared to WT (Figure 6.2). To provide a gauge for robustness of this genotype effect, the same measure was examined under different media conditions. Insulin-treated HOM hepatocytes reproduced the significantly stifled expression of phosphorylated PKB^{Ser473} when cultured in M199, with a trend towards the same effect seen in high-glucose conditions (Figures 6.3, 6.4).

To clarify any upstream source of the effects on PKB activity, protein expression of the active insulin receptor $(InsR)^{Tyr1150/1151}$ was assessed. Insulin-treated cells under low-glucose conditions did not show significant genotype differentiation (Figure 6.2). The HOM hepatocytes cultured in high-glucose media, in contrast, did demonstrate $InsR^{Tyr1150/1151}$ phosphorylation below WT levels, but this differentiation was not reflected in the comparatively minor reduction in PKB expression (Figure 6.3). Interestingly, the reduced PKB phosphorylation which was associated with presence of the missense variant following insulin stimulation was also a visible trend in the vehicle-treated cells. Prominence of this basal effect across media conditions largely mirrored insulin-stimulated expression levels of phosphorylated PKB: greatest with M199 and least with high-glucose media. The genotype effect therefore seemed to become statistically significant due to the magnification of activity levels by insulin, not only a consequence of hormone administration per se.

Possible functional relevance of this conserved genotype effect was therefore subsequently assessed in both low- and high-glucose conditions via the expression of key proteins representing distinct signalling pathways downstream of PKB. In the context of glycogen synthesis, phosphorylation of glycogen synthase kinase $(GSK)3\alpha^{Ser21}$ and $GSK3\beta^{Ser9}$ was not consistently or significantly different between WT and HOM hepatocytes cultured in any media condition despite the genotype-dependent expression of the responsible kinase (Figures 6.3, 6.4). This was not driven by a failure in signal

transduction, which was demonstrated in the expected increases to GSK3α/β$^{Ser21/Ser9}$ phosphorylation levels seen in insulin-treated WT cells. This stimulatory effect was most prominent in DMEM conditions but showed as a visibly more modest trend in M199-cultured cells. Expression of the phosphorylated PRAS40^{Thr246} in low-glucose conditions was likewise increased by insulin administration, but not significantly impacted by genotype in the stimulated cells when normalised to housekeeper (Figure 6.2). There was however a trend to variant-associated reduction in the basal state which reflected that seen for PKB and may therefore represent genotype-dependent signal transduction.

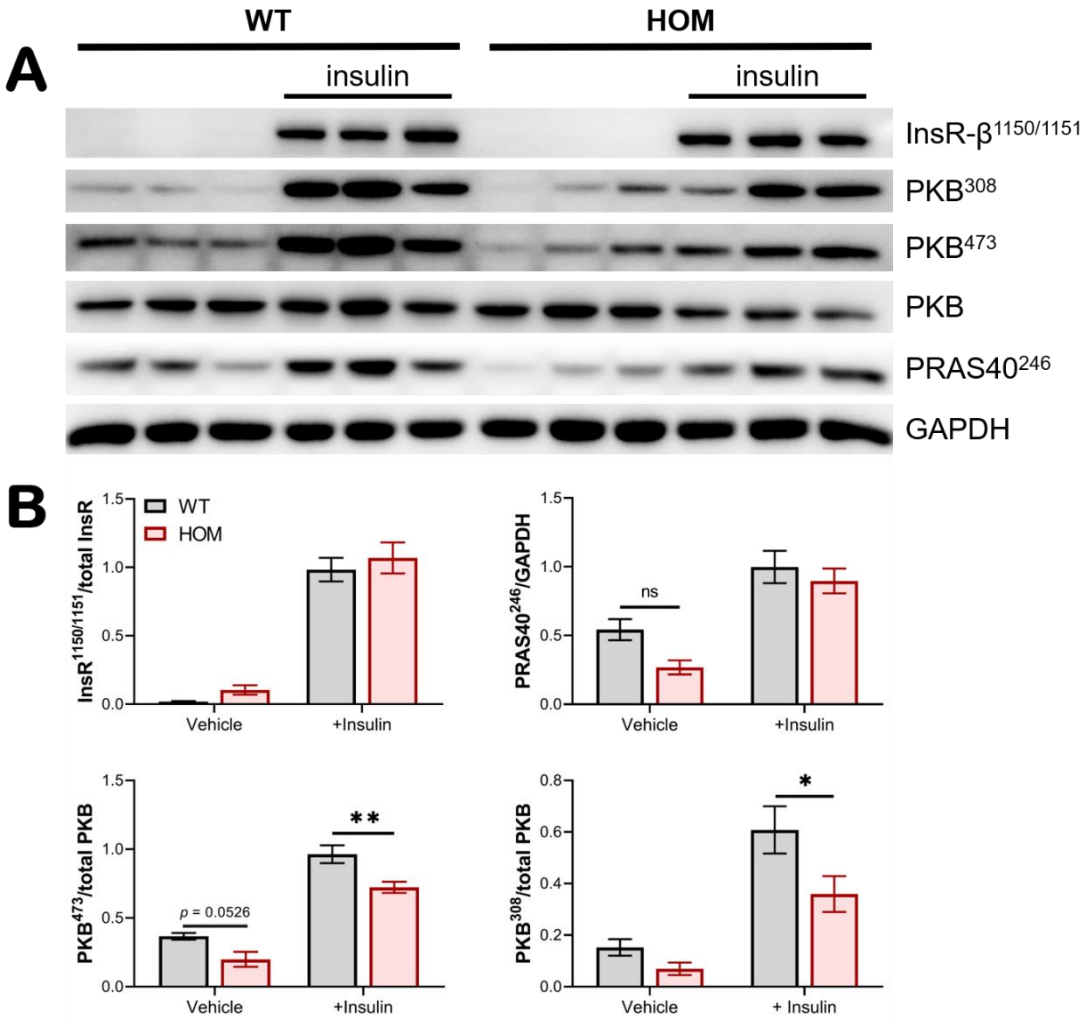

Figure 6.2: Insulin signalling in R458Q primary hepatocytes cultured in low-glucose DMEM.

Hepatocytes isolated from WT and HOM male mice were cultured overnight in 5.5 mM glucose DMEM and treated with vehicle or 100 nM insulin for 15 min. Cell lysates were loaded at 30 µg/well and immunoblotted for expression of insulin signalling proteins, with GAPDH used as a housekeeper. Results are shown as (A) representative images and (B) quantification by densitometry analysis shown as mean ± SEM, n = 3-6. Data were analysed by ordinary two-way ANOVA, ***** p = 0.0133, ** p = 0.0058 by Sidak's multiple comparisons test.

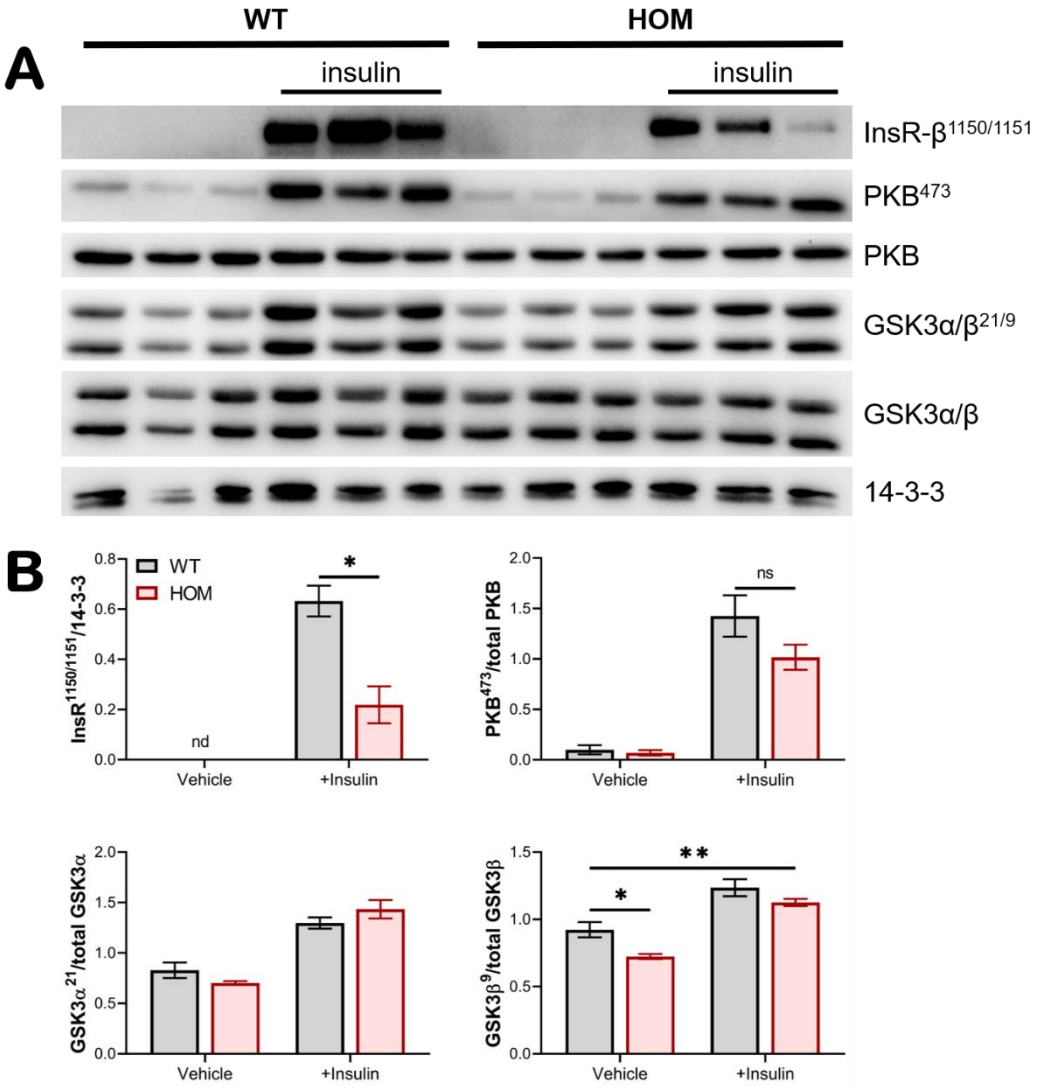

Figure 6.3: Insulin signalling in R458Q primary hepatocytes cultured in high-glucose DMEM.

Hepatocytes isolated from WT and HOM male mice were cultured overnight in 25 mM glucose DMEM and treated with vehicle or 100 nM insulin for 15 min. Cell lysates were loaded at 30 µg/well and immunoblotted for expression of insulin signalling proteins, with pan 14-3-3 used as a housekeeper. Results are shown as (A) representative images and (B) quantification by densitometry analysis shown as mean ± SEM, $n = 3$. ** $p < 0.01$ main effect of genotype by ordinary two-way ANOVA; * $p < 0.05$ by Sidak's multiple comparisons test.

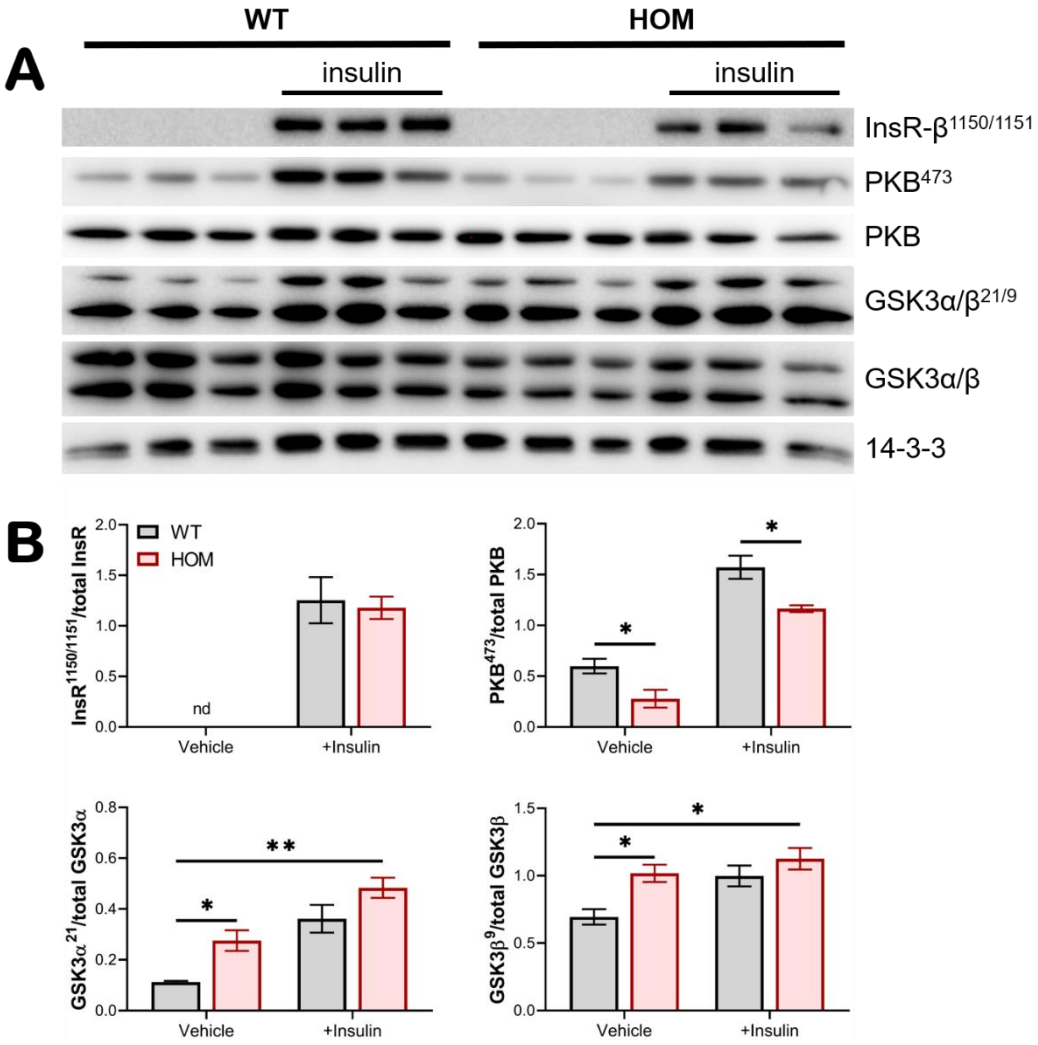

Figure 6.4: Insulin signalling in R458Q primary hepatocytes cultured in M199.
Hepatocytes isolated from WT and HOM male mice were cultured overnight in M199 and treated with vehicle or 100 nM insulin for 15 min. Cell lysates were loaded at 30 µg/well and immunoblotted for expression of insulin signalling proteins, with pan 14-3-3 used as a housekeeper. Results are shown as (A) representative images and (B) quantification by densitometry analysis shown as mean ± SEM, $n = 3$. * $p < 0.05$, ** $p < 0.01$ main effect of genotype by ordinary two-way ANOVA; ***** $p < 0.05$ by Sidak's multiple comparisons test.

6.3.3 Glucagon signalling

In order to supplement the analysis of hepatic insulin signalling, glucagon administration was used to develop a more complete image of pancreatic hormone signalling in our hepatocyte model. Given that, in physiological settings, periods of fasting are known to

induce both glucagon secretion and CREBRF expression, we investigated whether any elements of hepatic glucagon signalling might interact with presence of the *CREBRF* missense variant. Expression of phosphorylated CREB^{Ser133} protein, as an established gluconeogenic target of hepatic glucagon signalling, provides an important indicator of functional signal transduction in our hepatocyte model. In low-glucose DMEM media conditions, both WT and HOM glucagon-treated cells showed increased phosphorylation from basal levels, with no differentiation between the genotypes (Figure 6.5). β-catenin^{Ser552} phosphorylation can similarly be utilised as a readout of glucagon signalling (Chowdhury *et al.*, 2015). There were again no genotype differences in the significantly heightened expression which was induced by glucagon treatment in hepatocytes cultured in either low- or high-glucose DMEM media (Figures 6.5, 6.6).

In the context of hepatic lipid metabolism, inhibitory phosphorylation of the lipogenic ACC^{Ser79} was induced as expected by glucagon treatment (Figure 6.5). Expression levels in both vehicle- and glucagon-treated HOM cells suggested a shared trend to reduced phosphorylation, reflecting potentially greater activity irrespective of the hormone signal transduction, compared to WT. To further investigate specifically nutrient-responsive metabolism in our hepatocytes, we looked for the key growth- and survival-related protein mTOR. Phosphorylation at mTOR^{Ser2448}, typically taken as a marker of mTORC1 activation, was marginally induced by glucagon treatment and reflected a trend towards greater expression in HOM than WT cells which was present in both the basal and glucagon-stimulated conditions (Figure 6.5).

Protein expression of active PKB, which we had previously utilised primarily as an indicator of insulin signalling, was further examined in the context of glucagon stimulation. Hepatocytes cultured in low-glucose conditions showed that glucagon treatment induced PKB^{Ser473} phosphorylation in WT cells but was significantly less effective in HOM cells, where active PKB expression was only marginally greater than basal levels (Figure 6.5). The genotype differentiation represented in this measure was of greater magnitude than that seen with the equivalent insulin-stimulated conditions although the effect of glucagon was less. A similar trend to lesser HOM than WT expression of phosphorylated PKB^{Ser473} was present in hepatocytes cultured in both high-glucose DMEM and M199 media conditions, but this did not replicate the effect size (Figures 6.6, 6.7).

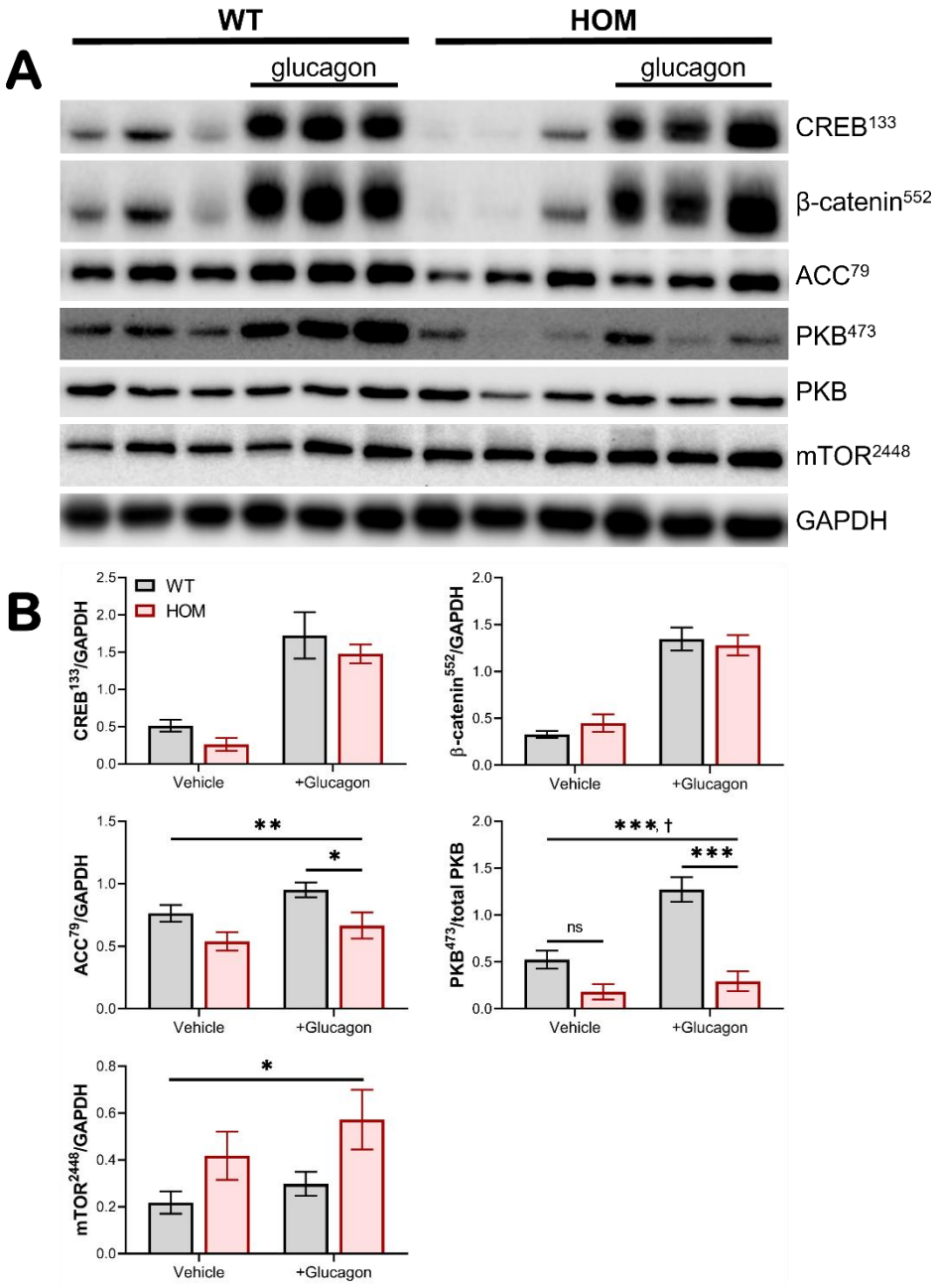

Figure 6.5: Glucagon signalling in R458Q primary hepatocytes cultured in low-glucose DMEM.

Hepatocytes isolated from WT and HOM male mice were cultured overnight in 5.5 mM glucose DMEM and treated with vehicle or 10 nM glucagon for 15 min. Cell lysates were loaded at 30 µg/well and immunoblotted for protein expression, with GAPDH used as a housekeeper. Results are shown as (A) representative images and (B) quantification by densitometry analysis shown as mean ± SEM, n = 3-4. ***** p = 0.0206, ** p = 0.0067, *** p = 0.0001 main effect of genotype, † p = 0.0170 interaction between treatment and genotype by ordinary two-way ANOVA; * p = 0.0467, *** p = 0.0002 by Sidak's multiple comparisons test.

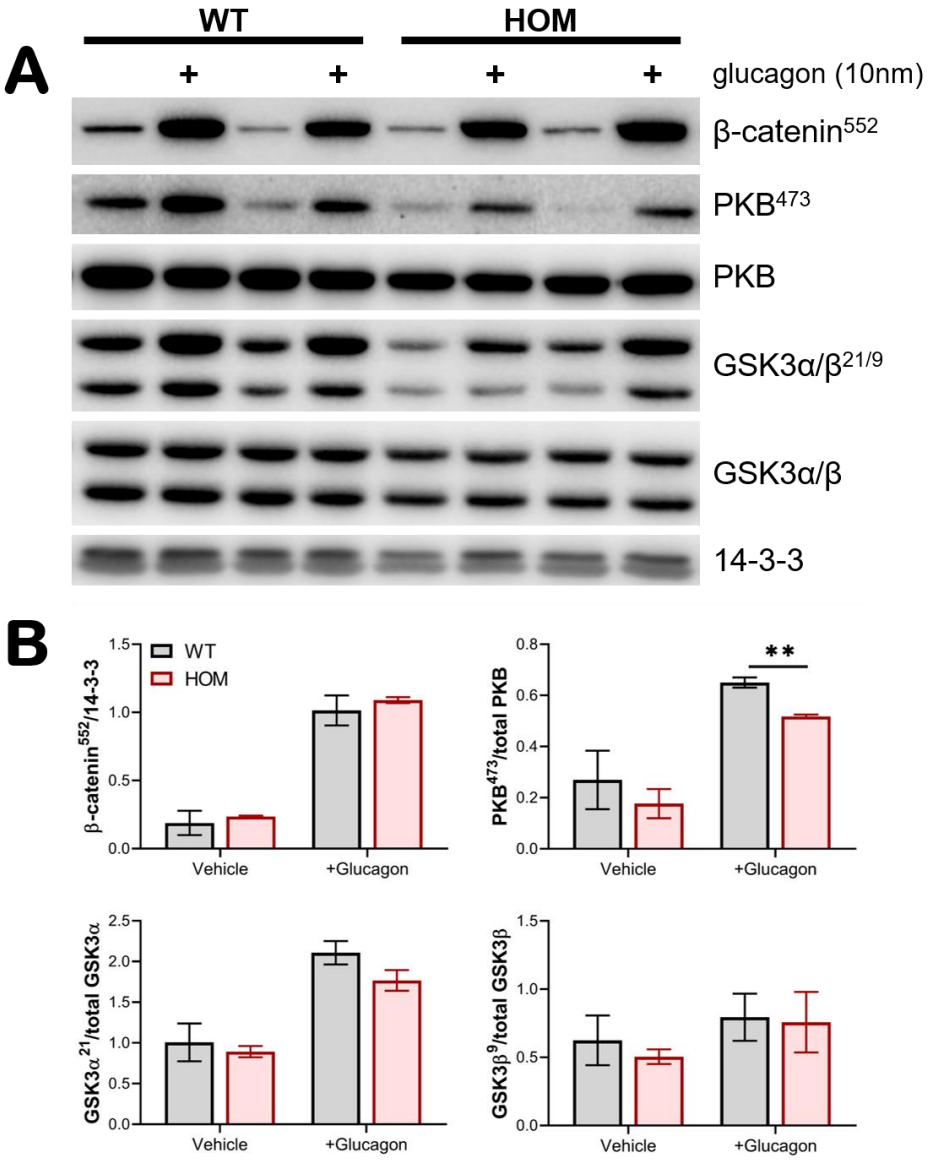

Figure 6.6: Glucagon signalling in R458Q primary hepatocytes cultured in high-glucose DMEM.

Hepatocytes isolated from WT and HOM male mice were cultured overnight in 25 mM glucose DMEM and treated with vehicle or 10 nM glucagon for 15 min. Cell lysates were loaded at 30 µg/well and immunoblotted for expression of insulin signalling proteins, with pan 14-3-3 used as a housekeeper. Results are shown as (A) representative images and (B) quantification by densitometry analysis shown as mean ± SEM, $n = 3$. $p = 0.0068$ HOM vs WT by multiple t-tests, corrected for multiple comparisons using the Holm-Sidak method.

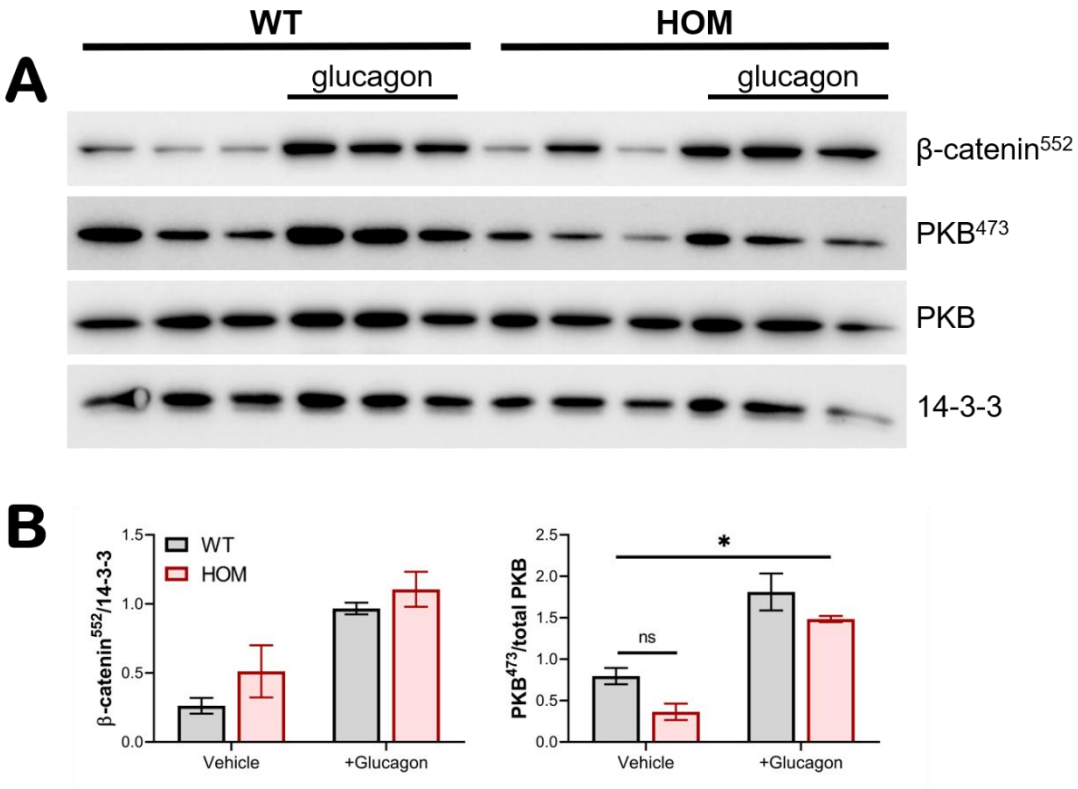

Figure 6.7: Glucagon signalling in R458Q primary hepatocytes cultured in M199. Hepatocytes isolated from WT and HOM male mice were cultured overnight in M199 and treated with vehicle or 10 nM glucagon for 15 min. Cell lysates were loaded at 30 µg/well and immunoblotted for expression of signalling proteins, with pan 14-3-3 used as a housekeeper. Results are shown as (A) representative images and (B) quantification by densitometry analysis shown as mean ± SEM, n = 3, ***** p = 0.0215 main effect of genotype by two-way ANOVA.

6.3.4 Insulin-glucagon crosstalk

Known crosstalk exists between the insulin and glucagon hepatic signalling networks, including specifically at the PKB junction; co-administration of the two hormones can, *in vivo*, stimulate greater activation of PKB than is induced by insulin alone (Kim *et al*., 2018). Given that we had identified PKB phosphorylation following glucagon stimulation, we therefore tested whether co-administration would produce this reported additive effect in our hepatocyte model, and whether this might show genotype differentiation.

In hepatocytes cultured under low-glucose media conditions, expression of phosphorylated PKB^{Ser473} protein was significantly elevated following insulin and glucagon co-administration compared to treatment with either vehicle or insulin alone (Figure 6.8). This reproduction of the apparent crosstalk effect was present in both WT and HOM cells. The genotype effect observed at this phosphorylation site with insulin treatment was furthermore partially retained in co-treated cells. Phosphorylation induced at the alternate PKB^{Thr308} site by co-treatment, in contrast, was not different between genotypes (Figure 6.8). Compared to the effects of insulin administration alone, the co-administered glucagon did not significantly alter PKB^{Thr308} in WT cells but induced mild increases in HOM cells.

Downstream of PKB, the insulin-induced phosphorylation of PRAS40^{Thr246} was not significantly further increased in cells co-treated with glucagon (Figure 6.8). The main effect of genotype visible in insulin-stimulated conditions was retained. Hormone-stimulated phosphorylated mTOR^{Ser2448} expression was significantly reduced in HOM compared to WT cells (Figure 6.8). The genotype effect appeared driven primarily by differentiated response to insulin treatment, which produced significantly increased phosphorylation in WT cells but strikingly had no discernible change from vehicle in HOM cells. There was however a repetition of the genotype trend in vehicle-treated cells, although this was not statistically significant, indicating some basal differentiation. Co-administered glucagon produced a further increase for both genotypes.

Signal transduction through the PKB-mTOR pathway, as evaluated here, displayed only mild cohesion. The additional phosphorylation of PKB which was observed in response to co-treatment did not seem to produce corresponding increases in the kinase activity directed at downstream substrates which were monitored here. The relationship between PRAS40 and mTOR, albeit not wholly interpretable solely from respective phosphorylation levels, was likewise not clearly correlated in the co-treatment context. The significant stimulatory effect of glucagon on β-catenin^{Ser552} expression in the co-treated cells (of both genotypes), absent in vehicle- and insulin only-treated cells, confirmed that the hormones acted as expected at the known target (Figure 6.8).

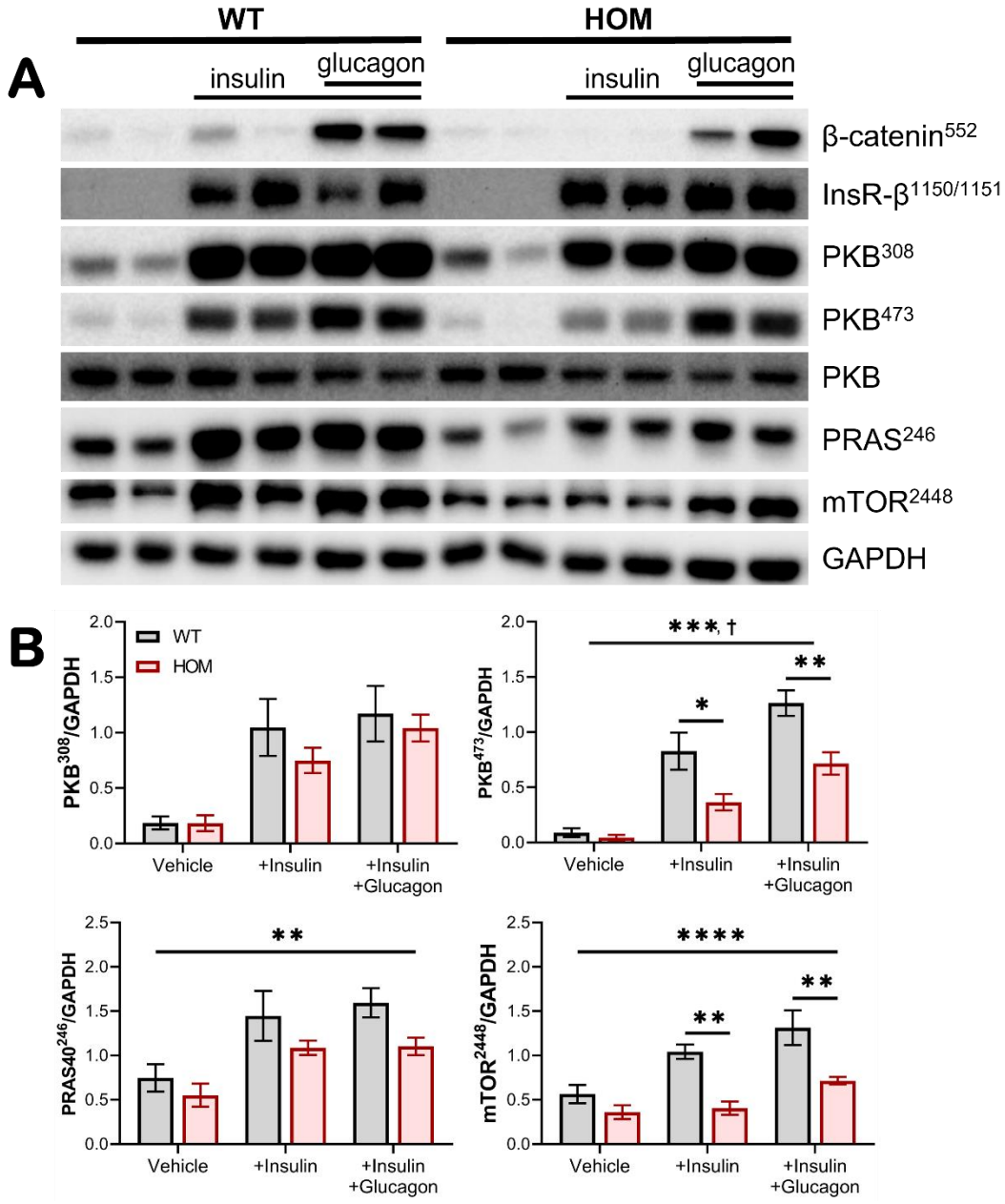

Figure 6.8: Insulin-glucagon signal crosstalk in R458Q primary hepatocytes.

Hepatocytes isolated from WT and HOM male mice were cultured overnight in 5.5 mM glucose DMEM and treated with vehicle, 100 nM insulin, or co-treated with 100 nM insulin and 100 nM glucagon for 15 min. Cell lysates were loaded at 30 µg/well and immunoblotted for expression of insulin signalling proteins, with GAPDH used as a housekeeper. Results are shown as (A) representative images and (B) quantification by densitometry analysis shown as mean ± SEM, n = 3-5. ** p = 0.0091, *** p = 0.0004, **** $p < 0.0001$ main effect of genotype, † p = 0.0392 interaction between treatment and genotype by two-way ANOVA; * $p < 0.05$, ** $p < 0.01$ HOM vs WT by Sidak's multiple comparisons test.

6.3.5 Triglyceride accumulation

Given that WT and variant CREBRF have been linked to lipid metabolism in published *in vitro* models (Minster *et al*., 2016; Tiebe *et al*., 2019), we assayed triglyceride content to determine possible R458Q variant protein involvement in the KI hepatocytes. Cells cultured in low- and high-glucose DMEM exhibited significantly lesser levels of triglyceride accumulation in HOM compared to WT hepatocytes (Figure 6.9A). This genotype effect was especially prominent in the low-glucose media. Glucose concentration did not itself have a significant impact on triglyceride despite a seemingly positive relationship between glucose and triglyceride in HOM hepatocytes only.

Hepatocytes were also cultured in a highly lipotoxic FA media to provide a crude mimicry of conditions observed with *in vivo* high fat feeding. Supplementation of low-glucose DMEM with palmitic acid consequently revealed a similar genotype differentiation in the FA-induced accumulation of triglyceride (Figure 6.9B). Provision of either 250 μM or 750 μM palmitic acid content in media significantly increased triglyceride levels above those seen in control conditions. Although WT cells showed a trend to further increases when cultured in the more concentrated palmitate medium, this was not observed in the HOM cells which demonstrated no significant differences in accumulated triglyceride between the two FA media conditions. The overall effect of lessened triglyceride content in hepatocytes isolated from mice carrying the *CREBRF* missense variant also reached statistical significance specifically in the 750 μM palmitic acid conditions.

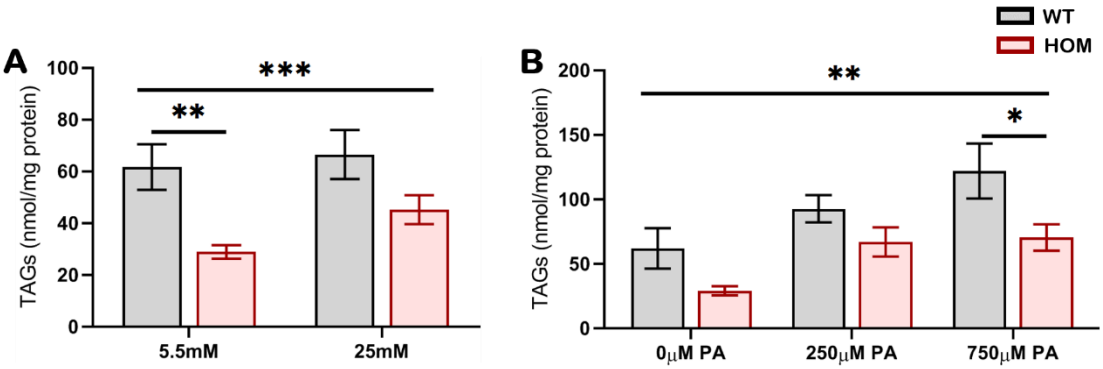

Figure 6.9: Triglyceride content in cultured hepatocytes isolated from R458Q mice. Accumulation of triglyceride in hepatocytes isolated from male 10-week-old variant mice and cultured overnight in **(A)** 5.5 mM and 25 mM glucose DMEM media (n = 5-7), or **(B)** low-glucose DMEM supplemented with 250 μM or 750 μM palmitic acid (PA), or vehicle (n = 3-5). Data are shown as mean ± SEM. ** p = 0.0015, *** p = 0.0005, main effect of genotype by two-way ANOVA. * p = 0.0216, ** p = 0.0038, HOM vs WT by Sidak's multiple comparisons test.

6.4 DISCUSSION

The liver is an essential organ involved in regulating the homeostatic response to nutrient state, mediated by the coordinated signalling actions of pancreatic hormones insulin and glucagon. Dysregulation of these hepatic networks is a contributor and consequence of metabolic perturbations found in, for example, insulin resistant conditions. The *CREBRF* R458Q missense variant is strongly associated with effects on growth and diabetes in human carriers but exploration of the metabolic phenotype has been largely restricted to the organismal scale (Minster *et al.*, 2016; Hanson *et al*., 2019; Carlson *et al*., 2020; Krishnan *et al*., 2020; Metcalfe *et al*., 2020; Arslanian *et al*., 2021). In the current *in vitro* study, primary hepatocytes isolated from male mice harbouring this missense variant showed a subdued signal at the PKB-mTOR axis in HOM compared to WT cells. This variant-induced trend would run contrary to a human phenotype more logically reflective of the opposite associations but persisted across cells exposed to differing pancreatic hormone and media nutrient conditions.

The current study examined PKB protein expression with the intent of providing a readout of insulin signalling in these hepatocytes. Activity at the insulin receptor did not, however, reflect differentiation in PKB phosphorylation between WT and HOM cells, suggesting that this effect was perhaps not driven by alterations to upstream insulin signal transduction per se. Indeed, the greater variant-induced impairment of PKB^{Ser473} phosphorylation which was produced in glucagon-stimulated HOM hepatocytes may suggest a closer interaction with CREBRF variant function than was presented by insulin. The nature of this R458Q interaction, revealed in PKB phosphorylation rather than total protein levels, seems to be mediated by upstream effector activity rather than changes to PKB gene transcription or protein degradation rates per se. The immediate kinases which act on PKB do not provide an obvious mechanistic basis: Thr308, phosphorylated by PDK1, and Ser473, phosphorylated by mTORC2, both showed reductions in HOM compared to WT cells.

In contrast to the well-established insulin signalling pathway stimulating both PDK1 and mTORC2 kinases, the mechanism by which glucagon induces hepatic PKB activity both *in vivo* and *in vitro* is underreported in literature (Kim *et al*., 2018; Sunilkumar *et al*., 2021). Although glucagon acutely stimulates insulin secretion *in vivo*, this has little effect on insulin clearance and furthermore cannot account for glucagon-stimulated effects in

isolated hepatocytes (Gelling *et al.*, 2009; Song *et al*., 2017). Sunilkumar *et al*. (2021) recently suggested that glucagon-induced increases to intracellular cAMP concentrations might trigger an Epac-mediated mechanism to stimulate mTORC2 and thereby PKB activity. Interference with this Epac pathway might explain the selectivity which left more conventional glucagon signalling targets, mediated instead by the PKA pathway, largely unaffected by the R458Q variant. Glucagon is not known to induce PDK1 action on PKB^{Thr308}, but some convergence of signal is feasible: genetic inhibition of hepatic mTORC2 activity can, for example, produce defects in insulin-stimulated phosphorylation of both PKB sites, not only its direct Ser473 target (Yuan *et al*., 2012). This proposal cannot fully explain the insulin-stimulated effects in R458Q hepatocytes but highlights mTORC2 as a stronger candidate for further investigation.

As shown here and elsewhere, coadministration of insulin and glucagon produces greater hepatic PKB activity than is achieved by either hormone alone (Kim *et al*., 2018). This additive effect implies distinct signalling pathways even downstream of the hormones' respective receptors. The increased PKB^{Ser473} activity following co-treatment in both WT and HOM hepatocytes, retaining but not enhancing the genotype effect, further proves that the R458Q variant did not impose an absolute ceiling on phosphorylation. Given that PKB phosphorylation was stifled in vehicle- as well as hormone-treated HOM cells, however, the variant-induced trend was perhaps not driven by hormone stimulation per se but brought into greater relief (and statistical significance) by the thusly heightened expression levels. This likely also holds for the comparatively mild genotype trend in cells cultured in 25 mM versus 5.5 mM glucose conditions, representing a consequence of the overall reduction in PKB expression induced by high glucose rather than any direct interaction between media and CREBRF variant function. The R458Q effect may therefore instead reflect a factor more consistently present in the kinase, cells, or culture conditions which has additional interaction with insulin- or glucagon-stimulated signalling. Phosphatase activity provides one feasible option, whereby the missense variant might induce greater removal of phosphorylation from PKB rather than limit upstream signal transduction. Beyond the potential to elucidate specific CREBRF variant protein interactions, identification of the relevant influence on PKB could also help to ascertain whether any other hepatic signalling pathways might likewise be impacted. Treatment of KI hepatocytes with alternate stimuli, or with inhibitors targeting either PKB-associated upstream molecules or phosphatases, could provide a more dedicated

interrogation. Mass spectrometric measurement of cellular contents would likewise provide broader knowledge, and thusly allow deeper insight into the variant-affected mechanism.

Alternate phosphorylation sites on PKB can indicate not only upstream signal origins but also downstream consequences. The kinase can be activated by Thr^{308} phosphorylation alone but reaches maximal activity following Ser^{473} phosphorylation. The balance between these sites can finetune PKB substrate specificity, gearing the hepatic response towards, for example, glucose or lipid metabolism (Kazyken *et al*., 2019; Kearney *et al*., 2019). Reductions to both Thr^{308} and Ser^{473} phosphorylation in vehicle- and insulin-treated hepatocytes might imply general stifling of PKB activity in these HOM cells, without overt direct impacts to substrate selection. PKB phosphorylation is, however, non-linearly related to its kinase substrates which can show near-maximal phosphorylation even following significant reductions in phosphorylated PKB levels, with different substrates exhibiting different sensitivities (Hoehn *et al*., 2008; Larance *et al*., 2010; Tan *et al*., 2012). The measure cannot therefore be interpreted to necessarily indicate variant-induced changes to functional downstream endpoints. The absence of consistent differences in GSK3α/$\beta^{Ser21/Ser9}$ phosphorylation between WT and HOM cells, for example, suggests that the missense variant may not directly impact this aspect of glucose metabolism. Given the important role of PKB signalling in glucose regulation, further clarification of variant (in)activity might involve analysis of cellular glucose uptake or output, or of gluconeogenic gene expression, to offer insight into downstream functional consequences. The consequences of lessened PKB signalling seem to instead flow to diminished $PRAS40^{Thr246}$ and $mTOR^{Ser2448}$ phosphorylation in insulin-stimulated HOM hepatocytes, indicating that any phenotypic impacts may more likely influence growth or proliferation outputs (Han *et al*., 2016; Saxton & Sabatini, 2017). Although this differentiation among these PKB substrate expression patterns may imply some variant-induced kinase selectivity, analysis of a broader range of PKB signalling targets, including functional metabolic assays, would elucidate any potential physiological relevance of these hepatic R458Q variant effects.

Phosphorylation of $mTOR^{Ser2448}$, although often taken as a proxy of mTOR activity, is nevertheless a debated and potentially inadequate measure. It has been variously reported as dependent on PKB activity or alternately as a target of p70S6K, itself an mTORC1

target, but is not necessarily indicative of mTOR catalytic activity (Chiang & Abraham, 2005; Figueiredo *et al.*, 2017). Indeed, both insulin and glucagon are elsewhere shown to induce mTOR^{Ser2448} (via PKB- and PKA-mediated pathways respectively) although only the former hormone will stimulate downstream mTORC1 targets 4E-BP1 and S6K1—an effect which is repressed by glucagon co-administration without change to Ser2448 expression levels (Kimball *et al*., 2004; Mothe-Satney *et al*., 2004; Baum *et al*., 2009). The R458Q variant-induced reduction in mTOR^{Ser2448} phosphorylation in KI hepatocytes seemed driven primarily by insulin stimulation, with the further increase in response to glucagon co-administration not significantly different between WT and HOM cells. This difference perhaps provides further indication that the CREBRF missense variant which we see in this model largely operates on the PKB-centric pathways and is selective in its flow-on effects. Sunilkumar *et al*. (2021) recently reported that glucagon transiently stimulated mTORC1 signalling followed by latent suppression of its downstream targets, a biphasic effect which was mediated by PKB, not additive with insulin, and may suggest further unaddressed complexities of the associated signalling networks. That mTOR expression in the glucagon-treated KI hepatocytes did not mirror PKB activity may further indicate context-specific influence of either variant or hormone signalling. Examination of other components of the mTOR complex(es), and/or of downstream signalling targets, would help determine CREBRF missense variant interactions.

Although phosphorylation at mTOR^{Ser2448} is reported in literature to be primarily found in mTORC1, with active mTORC2 instead dominated by autophosphorylation at mTOR^{Ser2481}, the distinction is not absolute (Copp *et al*., 2009). These two mTOR complexes possess disparate roles, operating either upstream or downstream of PKB, with their actions either distinct or feedback-linked depending on the stimulus (Julien *et al*., 2010; Tato *et al*., 2011; Saxton & Sabatini, 2017; Javary *et al*., 2018; Sunilkumar *et al*., 2021). Reduced mTOR expression could represent either cause or consequence of the reduced PKB activity seen in the HOM hepatocytes. More conclusive identification of the specific CREBRF variant-affected complex in this hepatocyte model would aid in confirming mechanistic interactions. The question is particularly relevant given the feedback loops involved: just as mTORC2 will impact PKB-mediated mTORC1 activation, so too can mTORC1 signalling inhibit mTORC2 phosphorylation of PKB (Julien *et al*., 2010). Implications of mTORC1 versus mTORC2 loss of function are not identical. Dysregulation of mTOR signalling is known to disrupt hepatocellular

homeostasis, provoking pathological consequences associated with metabolic disorders including obesity and diabetes (Cho *et al*., 2020). Identification of potentially functional consequences of the CREBRF missense variant in this context is therefore warranted.

Although the hepatic mTOR signalling pathway(s) impacted by the CREBRF R458Q variant remain to be conclusively defined, some theories can nevertheless be formed. Stressors such as energy or nutrient depletion, for example, can suppress the pro-growth mTORC1 activity and induce mTORC2 signalling (Ben-Sahra *et al*., 2013; Kazyken *et al*., 2019; Kowalsky *et al*., 2020). These same conditions promote CREBRF expression by means both dependent and independent of mTORC1 inhibition, facilitating the downstream transcriptional programme which acts as a metabolic brake (Tiebe *et al*., 2015; Minster *et al*., 2016; Tiebe *et al*., 2019). Consequent blunting of growth and proliferation, and promotion of cell survival, is perhaps not divorced from CREBRF-mediated degradation of CREB3, which is induced by and facilitates pro-growth mechanisms (Penney *et al*., 2018). If the CREBRF R458Q variant does suppress the signal from PKB to mTORC1 in the KI hepatocytes, perhaps partially via PRAS40, then in theory this might induce its own expression and/or help promote a cellular metabolic state leaning towards a fasting response. Lack of a viable CREBRF antibody has, however, hindered testing protein expression levels. Speculation of greater CREBRF (variant) activity in a context of reduced PKB signalling would run somewhat against earlier reports that silencing of the WT protein inhibited PKB in gastric cancer models (Han *et al*., 2018). Whether this might reflect an element of tissue or model specificity requires additional clarification.

Potential enhancement of the hepatic fasting response might typically incorporate heightened glycogenolysis, gluconeogenesis, or FAO. These pathways in the liver are at least partially stimulated by glucagon signalling (Longuet *et al*., 2008; Oh *et al.*, 2013; Pereira *et al*., 2020). Presence of the CREBRF variant appeared not, however, to influence (major) glucagon-induced changes to protein expression in the KI hepatocytes beyond (non-canonical) phosphorylation of PKB. The general lack of differentiation between WT and HOM hepatocytes in glucose-dependent protein expression likewise does not reflect significant genotype association with nutrient provision. Although PKB activity has elsewhere been identified to enhance cellular bioenergetics (Li *et al*., 2013a), perhaps influenced by nutrient state, the current R458Q hepatocyte model has not been explicitly

examined for mitochondrial substrate supply or catalytic efficiency. Future investigation of this aspect is perhaps warranted even independent of the PKB association, given the established involvement of CREBRF in both starvation and bioenergetics (Minster *et al*., 2016; Tiebe *et al*., 2019). Current work in this context cannot yet provide additional support for the theory that the R458Q variant might augment the hepatocyte fasting response. Cells were not, however, exposed to true starvation conditions. This perhaps hindered clarification of genotype-dependent hepatic signalling in response to bioenergetics or nutrient deprivation. Treatments such as rapamycin can induce mimicry of the fasting response and also provoke CREBRF expression (Minster *et al*., 2016; Tiebe *et al*., 2019). Implementation of different starvation conditions to model the KI hepatocyte response to nutrient scarcity vs sufficiency would permit more comprehensive interrogation of any R458Q interaction in this context.

Amino acids provide an additional contributor to culture medium composition. KI hepatocytes cultured in M199, irrespective of genotype, showed protein expression patterns which were distinct from low- or high-glucose DMEM-cultured cells even in unstimulated conditions. The composition of M199 differs from DMEM primarily by incorporating a more diverse range of AAs (including alanine, aspartic acid, glutamic acid, and proline, which are absent from the latter medium), but approximately half the total concentration. AAs comprise a major hepatic carbon fuel source and are considered to be essential elements in normalisation of the metabolic phenotype in hepatocytes (Boon *et al*., 2020). They can activate PKB at both phosphorylation sites, representing a stimulus independent of insulin with distinct downstream effects, as well as mTORC1 signalling (Findlay *et al*., 2007; Tato *et al*., 2011; Takahara *et al*., 2020). It is possible that the greater amino acid diversity in the M199 medium might facilitate AA-specific signals, producing the observed protein phosphorylation, despite the reduced quantity: supplementation of media with limited, specific AAs (e.g., glutamine, leucine, and proline) is sufficient to augment insulin-induced PKB phosphorylation (van Meijl *et al*., 2010). Although there was no clear genotype dependence of the M199 influence on hepatocyte protein expression, a more specific interrogation involving overload and/or starvation of amino acid content would likely help to conclusively define interaction with the R458Q variant.

Presence of the R458Q variant was associated with reduced triglyceride accumulation in isolated hepatocytes across multiple glucose and FA media conditions. The finding runs

contrary to Minster *et al*. (2016)'s adipocyte overexpression model in which the CREBRF missense variant promotes triglyceride accumulation even above the lipogenic effects of the WT protein. The disagreement may derive from differing models of variant protein transfected overexpression in immortalised cells versus transgenic knock-in in isolated primary cells. The protein may also have cell type-specific effects: knockdown of the CREBRF cofactor, Crebl2, inhibits lipogenesis in adipocytes but increases triglyceride levels in hepatocytes and myocytes (Ma *et al.*, 2011; Tiebe *et al*., 2019). If Crebl2 can be taken to reflect CREBRF activity, the murine R458Q variant may therefore enhance WT lipid metabolism activity in hepatocytes as was seen in the earlier adipocyte model. In providing a static image of lipid content, however, this measure has somewhat limited capacity to reflect potential variant-induced fluctuations in the dynamic intracellular lipid pool. It is unclear, for example, whether triglyceride storage in HOM (unlike WT) cells was not stimulated by greater palmitic acid supply due to inhibited FA uptake, inhibited triglyceride synthesis, or heightened lipid catabolism. Reduced pACC expression in HOM cells perhaps indicates a trend towards greater lipogenic activity, but carries the caveat that total levels could not be quantified. Although the variant effect is most pronounced following FA exposure, its presence in non-supplemented DMEM might imply partial contribution of glucose uptake and metabolism. Nor is it known how this altered triglyceride accumulation might consequently impact FA partitioning and accumulation of bioactive, potentially more deleterious, lipid species. These questions could be better answered by testing, for example, cellular fate of labelled palmitate or glucose substrates in order to elucidate a possible mechanism of action, as could not be sufficiently analysed in the present study (Parks & Hellerstein, 2006; Triebl & Wenk, 2018).

Altered triglyceride content suggests further-reaching effects of the R458Q variant influence on hepatocyte metabolism beyond the PKB-mTOR axis. The mutual stifling of these effects in HOM cells is perhaps unlikely to reflect a unanimous downregulation of cellular processes, given that total protein expression (and by implication activity) is not uniformly impacted. PKB-mTOR pathway inhibitors have, however, elsewhere been shown to reduce lipogenesis in primary hepatocytes, and it is possible that the subdued PKB signal in HOM hepatocytes might act similarly (Li *et al*., 2010; Han *et al*., 2015). Alternately, reduced mTORC2 activity has also been shown to inhibit hepatic lipogenesis both in consequence of and independent of its effects on PKB (Hagiwara *et al*., 2012;

Yuan *et al*., 2012). If reduced lipid storage implies fewer available energy reserves, this might pre-empt suppression of PKB-mediated growth processes. Given that KI hepatocytes were cultured in a lipid-rich environment, the absence of any overt response to this potential energy substrate source in the HOM cells could have broader implications for nutrient sensing or fuel selectivity. Regardless, the triglyceride measure serves to indicate that the apparent deterioration of insulin sensitivity in these R458Q hepatocytes was neither sparked nor facilitated by excess lipid accumulation.

Current literature provides no specific interrogation of hepatic molecular signalling in human CREBRF missense variant carriers. Of the pancreatic hormones, glucagon is wholly unmentioned. Although both Hanson *et al*. (2019) and Burden *et al*. (2021) report an association with greater insulin secretion in R457Q variant carriers, the effect appeared not to represent compensation for decreased peripheral sensitivity (such as that which seemed to be indicated in the KI hepatocytes). Indeed, hyperinsulinemic-euglycemic clamp measurements in the more recent human study indicate that the altered glucose-stimulated insulin release associated with the CREBRF variant is unaccompanied by any changes in insulin sensitivity (Burden *et al*., 2021). Responses within the hepatocyte may not strictly dictate organismal insulin signalling or sensitivity but are nevertheless key to homeostatic regulation. Rodent studies have elsewhere demonstrated that liver-specific deletion of PKB will produce whole-body insulin resistance, glucose intolerance, and hyperglycaemia (Lu *et al*., 2012). The CREBRF variant-associated deterioration of PKB activity in isolated hepatocytes, even if not seen only in insulin-treated conditions, could reasonably be expected to predispose R458Q carriers to more systemic insulin resistance (or to exacerbate such conditions). That these effects were continued in co-treated hepatocytes may moreover bear additional relevance to the diabetic condition, which human studies have associated with both hyperinsulinemia and hyperglucagonemia (Reaven *et al*., 1987; Demant *et al.*, 2018; Araujo *et al.*, 2019; Wewer Albrechtson *et al*., 2019). In light of this, further investigation of CREBRF variant function in human cohorts might also be benefited by a closer focus on pancreatic hormone signalling as well as secretion.

The links between hepatic hormone signalling and metabolic (dys)regulation invite a more deliberate study of insulin resistant or diabetic conditions. Culturing primary hepatocytes in high glucose conditions has elsewhere been typified by, for example,

significant suppression of insulin-stimulated PKB^{Thr308} phosphorylation and reduction in basal protein expression compared to low glucose-cultured cells (Cordero-Herrera *et al*., 2014; Chen *et al*., 2019). The lessened PKB expression which was displayed in the current study by hepatocytes cultured in 25 mM compared to 5.5 mM glucose media likely reflects partial induction of a similarly insulin resistant state. In this state, the CREBRF variant-induced decrease in PKB^{Ser473} phosphorylation seen in insulin- or glucagon-treated cells was of lesser magnitude but HOM cells were notably not protected from high glucose-induced reduction of insulin signalling. This contrasts the variant-associated protection against diabetes seen in human carriers (Minster *et al*., 2016; Krishnan *et al.*, 2018; Hanson *et al*., 2019; Krishnan *et al*., 2020), who are perhaps accordingly unlikely to share the liver-specific molecular signalling effects seen in the murine *in vitro* model reported here. Insulin-related discrepancies in human and murine variant phenotypes may indicate mistranslation of CREBRF variant function between species.

Any extrapolative effort to apply findings from this hepatocyte model to the whole-body context of the missense variant phenotype must consider tissue specificity. CREBRF has little literature to elucidate tissue-specific activities, but its cofactor Crebl2 has distinct effects on lipid and glucose metabolism across cell lines (Ma *et al*., 2011; Tiebe *et al*., 2019). Whole-body studies of the human R457Q missense variant focus on muscle mass and/or fat mass phenotypic effects without specific attention to liver. mTORC1/2 signalling is also differently regulated in liver compared to muscle, and although alterations to mTORC1 signalling in skeletal muscle or bone can impact whole-body metabolism, any systemic variant-induced changes similarly driven by other tissue or cell types would logically not be visible in a hepatic model (Naito *et al*., 2013; Guridi *et al*., 2016; Tangseefa *et al*., 2021). PKB-centric signalling in skeletal muscle promotes insulin-stimulated glucose uptake and is required for insulin/IGF1-mediated skeletal muscle growth (Jaiswal *et al*., 2019). Any reproduction in muscle of the hepatic CREBRF missense variant-induced stifling of PKB-mTOR signals, given the major contribution of skeletal muscle to whole-body glucose homeostasis and growth, might produce similarly weighted influence in variant carriers. Such a (theoretical) lessening of either glucose uptake or muscle mass would not align with the reported R457Q variant phenotype. The current hepatocyte model cannot be presumed to parallel variant effects in other tissues, which should be examined to extend our knowledge of genotype-dependent molecular signalling and relevance to the whole-body phenotype.

In conclusion, molecular signalling in primary hepatocytes isolated from male mice harbouring the *CREBRF* R458Q variant was most prominently affected by reduction of PKB activity. Origins of the baseline trend in HOM cells, seen irrespective of hormone or nutrient exposure, are unclear although its enhancement following hormone stimulation may indicate some immediate mechanistic convergence on mTORC2. Genotype-dependent stifling of signal through the PKB-mTORC1 axis, accompanied by altered triglyceride accumulation, may involve altered homeostatic response to nutrients reflecting known CREBRF functions as a starvation factor. Lessening of insulin or growth signalling would not, however, match the human CREBRF variant phenotype, and necessitates consideration of tissue specificity as well as species translatability. These results further invite more thorough cross-examination of response to nutrient conditions (especially mTORC1/2 signals) to understand the impacts of R458Q on molecular signalling.

CHAPTER 7: General Discussion

Obesity represents a public health concern of heightened significance to global contemporary populations, being increasingly prevalent and associated with substantial adverse metabolic conditions. Attention has been drawn to the search for genetic variants which might produce susceptibility to these comorbidities. The R457Q missense variant in the *CREBRF* gene is tightly restricted to Pacific Island (PI) populations, where it has been linked to excess body weight, increased height and fat-free mass, and paradoxical reductions in risk of type 2 and gestational diabetes (Minster *et al*., 2016; Naka *et al*., 2017; Krishnan *et al*., 2018; Arslanian *et al*., 2021). With published reports of the CREBRF R457Q variant thus far concentrating primarily on human population studies, the current project investigated missense variant function using a novel mouse model to facilitate closer *in vivo* and *in vitro* examination. This model knocked in the murine CREBRF R458Q variant to replace the endogenous CREBRF on an FVB/N background. We sought to characterise, firstly, the whole-body metabolic phenotype of this KI mouse model; and, secondly, any molecular pathways impacted by variant function.

The *in vivo* metabolic phenotypes of male and female R458Q KI mice were assessed from 8 to 20 weeks of age as described in Chapter 3. Changes in body weight and fat mass were not distinguishable between WT and HOM mice, but significant dose-dependent increases in total lean mass and naso-anal length were attributed to the missense variant in chow-fed male mice. Diabetes risk was not significantly diminished, with subdued response to insulin in male HOM mice, minimally altered glucose homeostasis, and unchanged basal glucose or insulin levels. Whole-body energy expenditure was not impacted, but tissue nutrient homeostasis implied potential exaggeration of fasting response in HOM mice. Overall, unlike the human CREBRF variant phenotype, the findings presented in this chapter demonstrate only mild differences between mice carrying either one or two copies of the knocked-in missense variant and their wildtype counterparts.

Chapter 4 interrogated the transcriptome of gastrocnemius and liver tissues taken from 20-week-old R458Q KI mice after metabolic characterisation. The results from this chapter demonstrated distinct sex- and tissue-specific impacts of the CREBRF missense variant on WT transcriptional action, illustrated in differential expression of both mRNA and ncRNA transcripts. GSEA revealed significant enrichment of biological processes or

pathways relating to protein synthesis, turnover, processing, and trafficking as well as cellular respiration and fuel metabolism. These variant-induced alterations broadly correlated to a catabolic transcriptional programme with a speculative role in bioenergetic homeostasis. Canonical transcriptional factors could not be unambiguously identified to mediate even half of the total differential expression, but associations were seen with CRE-binding, GRE-binding, and in particular FOXO TFs.

The fat-free mass phenotype identified in male carriers of the R458Q variant was more closely investigated in Chapter 5. Musculoskeletal characteristics of chow-fed WT and HOM male mice displayed only mild effects of genotype in this pilot cohort study. Skeletal muscle mass was slightly reduced in R458Q tibialis and EDL without visible effect on either larger hindlimb muscles. Hindlimb WT and HOM bones were only differentiated in femur width measurements. This chapter also saw no significant trends in muscle function for exercise endurance and forelimb grip strength parameters. Overall, muscle- and bone-specific effects of the murine R458Q variant were inconsistent across measures without strong genotype associations. The cohort did not recapitulate the genotype-dependent body composition effects seen in Chapter 1 and evidence of a muscle-driven lean mass effect could not be established.

The central goal of Chapter 6 was to perform *in vitro* characterisation of CREBRF R458Q variant effects on metabolic molecular pathways in primary hepatocytes isolated from WT and HOM male mice. The missense variant was associated with a subdued signal at the PKB-mTOR axis, an effect which was significantly amplified following stimulation by insulin and/or glucagon. Lipid accumulation was likewise subdued in HOM cells, and less responsive to fatty acid substrate provision. These results recapitulated the *in vivo* link to nutrient-sensitive function in isolated conditions, suggesting a potential molecular mechanism for its cellular transduction. The altered hormone response outlined in this chapter, which appeared to be pathway selective and persisted across different media conditions, also carried implications for missense variant-induced changes to *in vivo* insulin sensitivity and/or glucose homeostasis running counter to the human R457Q phenotype.

Major Phenotype

Overall, the current thesis finds that this novel CREBRF R458Q mouse model possesses a mild, sex-specific metabolic phenotype which, in the timeframe and conditions

assessed, showed only partial correlation and speculative parallels with the human R457Q variant phenotype. Given the somewhat preliminary nature of this work, the studies performed primarily sought to establish the new model without necessarily anticipating definitive mechanistic conclusions. The changed body composition seen in variant carriers is the most visible and therefore readily identifiable genotype effect in human populations; the significant alterations to body composition seen in the R458Q mouse model were sex-, diet-, and age-dependent and differed between animal cohorts and therefore also between chapters of this thesis. Total fat mass, for example, differed not between WT and HOM animals, but between Chapters 3 and 5; total lean mass had variant-induced increases in chow-fed males in the former but not the latter chapter. Although partially accounted for by natural biological variability independent of missense variant function *per se*, and exacerbated by limited sample sizes, inter-cohort differences highlight that the murine missense variant has only particularly minor effects. Potential restriction of phenotypic development to specific but largely unidentified contexts complexifies interpretation of missense variant function in this mouse model.

Despite the absence of any obesity phenotype in the R458Q mouse model, assessment of *in vivo* tissue triglyceride storage across these chapters might imply missense variant impacts to lipid metabolism on a smaller scale. The greater TG accumulation in male liver tissue taken from fasted HOM mice, reported in Chapter 3, might reflect the similarly enhanced circulating NEFA levels in these animals. In a similar vein, the R458Q-induced increases to male skeletal muscle TG content shown in Chapter 5, but absent in the larger cohort described in Chapter 3, might be partially due to the cross-cohort increase in total fat mass proportion. Such functional tissue-specific consequences could feasibly offer a partial reflection of the greater total or regional fat mass which has elsewhere been reported for the human (but not murine) missense variant phenotype (Minster *et al.*, 2016; Naka *et al*., 2017; Krishnan *et al*., 2018; Hawley *et al*., preprint). Any parallels drawn must, however, be considered with the caveats that CREBRF variant-associated adiposity in these population studies has not been assessed specifically in individual organs or tissues, disallowing any targeted analysis of possible ectopic distribution patterns. Given that the increased TG content in HOM liver and muscle did not significantly alter total endpoint mass of either individual tissue, unaltered adipose tissue mass could feasibly similarly mask smaller-scale changes. Indeed, this disjunction could thereby lend

speculative weight to the inconsistencies in human R457Q-associated adiposity (Krishnan *et al*., 2020; Lin *et al*., 2020; Hawley *et al*., preprint).

Rather than being taken to directly evidence steatotic or lipotoxic consequences on the organismal scale, the altered ectopic lipid accumulation in the KI mouse model may more accurately imply specific modulation of cellular metabolism. Although a targeted *in vitro* examination of affected pathways could typically facilitate the definition of molecular signalling, discrepancies between the *in vivo* results of Chapter 3 and the *in vitro* hepatocyte model described in Chapter 6 render such interpretation difficult. Presence of the CREBRF missense variant alters liver TG content in both contexts, but the *in vivo* increases and *in vitro* decreases seen in HOM male mice lack an overt common denominator to explicate the seeming contradiction. The greater *in vivo* TG content may superficially reflect enhanced hepatic FFA uptake and re-esterification in response to the heightened circulating NEFA levels in HOM mice. The failure of isolated HOM hepatocytes to likewise respond to greater FA media concentrations contrarily implies that the missense variant may impose a limit on one or both of these cellular processes. The differential expression of hepatic genes in fasted male mice, described in Chapter 4, lacks any clear transcriptional emphasis on either lipid deposition or oxidation processes. The results are not wholly irreconcilable. Circulating NEFAs may be heightened by reduced uptake as well as increased lipolysis, which may be a question better answered using a primary adipocyte model. Relative reductions in lipid storage as TGs may instead reflect greater oxidation for use in the TCA cycle or ketogenesis, or vice versa.

Alternately, the differentiation of these effects on lipid metabolism may be a consequence of nutrient conditions, with the missense variant potentially driven by acute adaptation to nutrient deprivation. Prolonged fasting is known to promote increased lipid deposition in tissues (Hashimoto *et al*., 2000; López-Soldado *et al*., 2020). On the molecular scale, lipid metabolism and deposition are mediated by nutrient-sensitive TFs including PPARs, BCL6, and ChREBP, which are affected in the R458Q variant transcriptome, as well as the mTOR complexes, which are also implicated in the hepatocyte model. The molecular processes underlying significant fasting-induced increases to NEFA and TG levels *in vivo*, exaggerated in the HOM males, are perhaps simply not stimulated, or even actively repressed, in the nutrient-replete conditions of the hepatocyte media. Indeed, reduced variant activity in overnutrition might reflect the greater lipid accumulation which was

induced in HFD-fed mice without genotype differentiation. Nutrient composition, in addition to quantity, can also influence cellular metabolism. Although FAs are known PPAR ligands, for example, polyunsaturated FAs are the more potent activators and disparity in stimulatory effect between different FAs has been demonstrated in primary hepatocytes (Pawar & Jump, 2003; Jump, 2008). The palmitic acid which was used to FA-treat the R458Q hepatocytes may have therefore had a milder effect on this lipid metabolic pathway than might be induced *in vivo*. These findings, taken together, may suggest that the missense variant could influence the flux through these pathways, balancing lipid accumulation and catabolism, in response to cues which presumably differ between systemic and isolated models.

In vivo increases to organismal growth, incorporating greater fat-free mass and naso-anal length, comprised the most significant alterations of total body composition phenotype in R458Q mice of the present study. Given that variant-induced lean mass and/or height has recently been likewise reported in multiple human population studies (Krishnan *et al*., 2018; Hanson *et al*., 2019; Carlson *et al*., 2020; Lin *et al*., 2020; Metcalfe *et al*., 2020; Arslanian *et al*., 2021; Oyama *et al*., 2021; Hawley *et al*., preprint), and indeed represents the sole strongest point of similarity between murine and human variant phenotypes, the functional basis underlying this effect becomes particularly pertinent. Interpretation can be somewhat complicated by the general lack of definitive evidence that the overall lean mass effect is driven by muscle, as is typically assumed by that measure; the current study's inability to attribute this to any specific tissue or organ might suggest a cumulative effect which, being subtler, is not readily defined. Lee *et al*. (preprint) have recently found lower circulating levels of myostatin in male variant carriers in an NZ population and present the depletion of this evolutionarily conserved negative regulator of musculoskeletal mass as a likely mediator of the CREBRF variant growth phenotype. The theorised mechanistic link to CREBRF is threefold: myostatin expression is induced by ER stress, by glucocorticoid signalling, and via a cAMP responsive element in the gene promoter (Ma *et al*., 2001; Nogalska *et al*., 2007; Grade *et al*., 2019). CREBRF activity can repress each of these factors (Audas *et al*., 2008; Martyn *et al*., 2012; Audas *et al*., 2016); although a direct causative link is unproven, missense variant-induced enhancement of these interactions may produce the *in vivo* myostatin reductions. These levels were not assessed in the current study, but the theorised association is no less plausible in the mouse model than in human populations.

Examination of possible transcriptional mechanisms underlying this lean mass phenotype, as described in Chapter 4, revealed instead a seemingly paradoxical shift towards atrophic or catabolic cellular processes in HOM gastrocnemius muscle. Although myostatin mRNA was not represented in these findings, the missense variant appeared to regulate other key mediators of muscle wasting and denervation in a manner not conducive to growth. Given that the transcriptional analysis in Chapter 4 was performed on tissues taken from the same animals which demonstrated the CREBRF variant growth phenotype in Chapter 3, this discrepancy cannot be relegated solely to biological variability. Although possible that the gastrocnemius transcriptome does not represent the cellular processes in other tissues, a stark opposition between muscle types would be necessitated to explain the overall difference. Muscle growth is driven by fibre number and size and individual muscles differing in fibre composition can experience fibre type- and thereby muscle-specific effects. Alternately, transcriptional changes in R458Q muscle were seen in animals which had been fasted overnight, perhaps representing missense variant interaction with the WT function as a starvation factor. Differentially expressed transcripts could undergo further mRNA processing without being fully translated to a correspondingly atrophic or dystrophic effect; a context-dependent driver of these changes could be active too briefly for visible constitutive changes to lean mass composition. The latter, indicating distinct susceptibility to external or environmental conditions, may partially explain why the cohort described in Chapter 5, unlike Chapter 3, did not exhibit variant-induced changes to total lean mass.

The catabolic transcriptional shift may not be wholly incompatible with increased total lean mass, despite the superficial contradictions, particularly in the context of applied pressures. Myostatin depletion, for example, illustrates similarly discrepant and not necessarily beneficial consequences for skeletal muscle form and function across multiple models. Excessive muscle growth following myostatin knockout or dysfunction can enhance bone mineral density and exercise-induced gains in bone strength (Montgomery *et al.*, 2005; Hamrick *et al.*, 2006), but can also compromise specific muscle force (Mendias *et al.*, 2006; Amthor *et al.*, 2007). This suggests that the trend to reduced grip strength and exercise endurance in HOM male mice described in Chapter 5, seen alongside greater femoral size, does not necessarily run counter to a pro-growth mechanism. More directly relevant, reduced myostatin inhibition of muscle hypertrophy does not protect against (and may associate with) the loss of muscle mass induced by

fasting, hindlimb suspension, exercise, or neuromuscular disease (McMahon *et al*., 2003; Baltusnikas *et al*., 2015; Mariot *et al*., 2017; Fokin *et al*., 2019). Curiously, myostatin deletion does inhibit glucocorticoid-induced proteolysis and atrophy (Gilson *et al*., 2007), implying additional pathway selectivity even within the bounds of acute muscle mass loss, which is perhaps instructive even if not strictly applicable to the present study. A more nuanced interpretation of CREBRF missense variant interactions in skeletal muscle might thereby integrate both constitutive increases to total growth and context-specific transcriptional atrophy programmes. Although findings from the current R458Q mouse model cannot constructively identify the molecular mechanisms inducing growth in variant carriers, they indicate likely transcriptional regulation which with further study might reveal details of a delicately balanced adaptive response facilitating skeletal muscle metabolism.

The defining metabolic characteristic of the human CREBRF missense variant is the significant reduced risk of type 2 and/or gestational diabetes (Minster *et al*., 2016; Krishnan *et al.*, 2018; Hanson *et al*., 2019; Krishnan *et al*., 2020). This protection has been associated with reduced fasting blood glucose levels and, independently, with greater compensatory insulin secretion or serum lipid content, but these potential causative factors are not consistently observed across the surveyed PI populations (Minster *et al*., 2016; Ohashi *et al*., 2018; Hanson *et al*., 2019; Krishnan *et al*., 2020; Lin *et al*., 2020; Burden *et al*., 2021; Russell *et al*, preprint). A current prevailing theory suggests that the increased height and lean mass in variant carriers, reflecting overall organismal growth including of the pancreas, is a key driver of improved glucose homeostasis and pancreatic hormone secretion (Metcalfe *et al*., 2020; Krishnan *et al*., 2020). This argument is persuasive in the human population, but distinctly not applicable to the current R458Q mouse model, given that glucose tolerance and insulin secretion were unchanged despite increased lean mass and length in the male HOM animals. Rather than being driven by glucose stimulation, the R458Q genotype differentiation in mice is instead observed in subdued peripheral sensitivity to insulin both *in vivo* and *in vitro*, significantly impairing systemic glucose clearance as well as PKB activity in isolated hepatocytes. This effect, seen in an isolated cell model, is logically not a product of organismal growth but does lead to further questions regarding possible tissue-specific effects of insulin stimulation. Murine variant carriers, seeming more likely to be

predisposed to insulin resistance than protected from metabolic syndrome, can in this regard offer little direct insight into the human phenotype.

Deterioration of insulin signalling has at least superficial links to metabolic ill-health but is not without ambiguities relating to the aetiology of metabolic syndrome. Excessive insulin signalling via the insulin receptor is also associated with developing resistance. Indeed, models of mildly defective glucose tolerance and/or mild IR, in contrast to total ablation of signalling, have been proposed to represent a protective mechanism during ageing (Holzenberger *et al*., 2003; Schulz *et al.*, 2007; Barzilai & Ferrucci, 2012; Lamming *et al*., 2012). Mice with partial impairment of peripheral insulin receptor expression were recently found to exhibit defects in glucose clearance during a GTT, but also protection from HFD-induced hepatic lipid accumulation (Merry *et al*., 2020). This metabolic phenotype was underlain by a hepatic energy deficit, accompanied by induction of AMPK and mitochondrial biogenesis. Merry *et al*. (2020) consequently suggest that the incomplete impairment of insulin signalling mimics caloric restriction during metabolic stress conditions. The link between these facets of metabolism may suggest a scenario through which to reconcile the R458Q-induced lessened response to insulin administration, the R457Q protection against diabetes, and the shared CREBRF influence on fasting nutrient homeostasis and physiological stress.

The subdued response to insulin administration in male murine variant carriers may not be straightforwardly applicable to *in vivo* diabetic or indeed physiological contexts. The disappearance of any significant insulin-induced genotype differentiation in glucose clearance upon HFD feeding *in vivo*, or in PKB expression upon high-glucose culturing of hepatocytes, shows an apparent restriction to conditions which are not likely to themselves induce insulin resistance. The potential for comparative protection against diet-induced deteriorations in sensitivity, being observed from uneven baselines, confers little practical advantage in the obesogenic conditions which are presumed to prevail among the human populations studied in this context (Minster *et al*., 2016). Nor did the reduction in insulin signalling in chow-fed HOM animals seem explicitly associated with altered circulating glucose or insulin levels in any *in vivo* context beyond the somewhat artificial design of the ITT. Diminished glucose uptake in high insulin and low (fasting) glucose conditions might be construed as avoidance of hypoglycaemia, but positing a genuine protective effect is perhaps too poorly evidenced. Postprandial secretion of

insulin, being less extreme than the dosages provided in either tolerance test or *in vitro* models, might well fail to induce notable genotype differentiation in these measures. Comparison to the hepatocyte model suggests a basal trend, magnified to statistical significance following pancreatic hormone stimulation. The nature or physiological circumstances of this stimulation, however, may not necessarily directly relate to diabetes aetiology despite the human variant phenotype. The hepatic PKB-mTOR molecular pathways affected *in vitro*, and indeed potentially the *in vivo* consequences, could suggest nutrient-responsive impacts to growth reminiscent of the likewise paradoxical catabolic transcriptome observed in muscle.

Interpretative Frameworks

The paradigm most commonly used in discussing CREBRF R457Q missense variant function is that of a thrifty metabolism, using a conception derived from Neel (1962)'s Thrifty Genotype Hypothesis (TGH). This theoretical framework positions the CREBRF variant at a bioenergetic pivot point, maximising energy storage and restricting energy expenditure to promote a more efficient energy balance. In a modern obesogenic environment, with increasing abundance of processed foods and declining physical activity, the evolutionary impetus is less applicable and such efficiency becomes less advantageous. The association was first drawn upon the discovery of the R457Q variant in Samoa and American Samoa, in alignment with greater BMI as well as increased lipid accumulation and decreased cellular respiration in the accompanying *in vitro* model (Minster *et al*., 2016). More recent studies of the R457Q genotype in other PI populations, however, have deemphasised the role of fat mass and thus cast some doubt on TGH applicability (Metcalfe *et al*., 2020; Krishnan *et al*., 2020; Lee *et al*., preprint). The mouse model described in the current thesis likewise cannot support this initially proposed framework, demonstrating neither increased total fat mass nor changed whole-body energy expenditure as might have been expected from a thrifty phenotype. This conceptual shift across both human and mouse studies may imply that the missense variant is not impervious to other environmental or ancestral factors, but the literature lacks obvious indications regarding the nature of such interference.

The driving evolutionary force behind the mutation and/or development of its contemporary phenotype likely does not directly mirror the thrifty model presented by Minster *et al*. (2016) but may reflect an offshoot of the controversial hypothesis. Studies

in *Drosophila*, for example, have recently demonstrated that the induction of metabolic thrift using high-protein environments predisposed animals to accumulate less triglyceride than controls, not more, when exposed to fattening high-carbohydrate foods (Gray *et al*., 2021). In contrast, *Drosophila* selected for starvation resistance typically develop significantly obese conditions compared to unselected animals, driven by altered nutrient response and catabolism, and exhibit metabolic trade-offs including low activity levels and disrupted sleeping patterns (Chippindale *et al*., 1996; Lee & Jang, 2014; Hardy *et al*., 2018). Similar models of adaptation to restricted nutrition can therefore demonstrably differ in development of maladaptation in comparatively nutrient-rich environments. It is possible that the varying body composition phenotypes in human and/or murine CREBRF missense variant carriers, driving increased total adiposity and/or total lean mass in different populations, may not disprove an evolutionary role in adaptation to nutrient conditions which may or may not induce metabolic thrift.

Given the canonical CREBRF role as a starvation factor, nutrient deprivation remains perhaps the most probable stimulus for the observation of any metabolic phenotype. These conditions are not explicitly examined in human populations beyond, for example, fasting blood glucose levels (Minster *et al*., 2016). The R458Q mouse model, however, showed some exaggeration of the fasting response in both tissue nutrient homeostasis and the tissue transcriptome, as outlined in Chapters 3 and 4. Fasting-induced changes in energy metabolism are not necessarily proof of metabolic thrift. Although greater decreases in energy expenditure during acute fasting are linked to the thrifty phenotype concept, Hollstein *et al*. (2020) have recently reattributed this finding to comparatively high expenditure during feeding conditions rather than to reduced fasting metabolic rate. The CREBRF variant-induced transcriptomic shift described in Chapter 4 towards reductions in oxidative phosphorylation and in energy-intensive processes such as protein synthesis and processing, and increased catabolism, nevertheless implies a certain conservation of energetic reserves reminiscent of survival-oriented thrift in male HOM mice. The subdued PKB-mTOR signalling and lipid accumulation seen in HOM primary hepatocytes could similarly suggest general reductions in cellular metabolic or anabolic activity, in this instance targeted to growth-centric pathways. It is accordingly possible that the absence of whole-body genotype impacts to energy expenditure and storage as fat mass, unchanged in the basal conditions examined, could be similarly context-dependent, able to reveal differentiation under more appropriate nutrient conditions.

An obesogenic diet may comprise a key determinant in metabolic syndrome aetiology, with or without the presence of obesity-linked gene variants. Deeper analysis shows that selective targeting of macronutrient composition produces distinctly varied consequences for energy storage and metabolic health. Experimental energy-dense or sugar-rich diet design in some mouse models of obesity, hindered by an unclear understanding of the healthy murine dietary and energy requirements which were addressed in the current study's HFD formulation, has elsewhere produced not only overfeeding but also malnutrition due to micronutrient deficiency (Bischoff & Volynets, 2016). High-fat diet overfeeding can lead to greater storage of excess energy and minimally altered substrate oxidation compared to lesser storage and progressively increased oxidation following isocaloric carbohydrate overfeeding (Horton *et al*., 1995). Metabolic outcomes differ between high-fat diets using medium-chain versus long-chain fatty acids, or between high-carbohydrate diets using resistant starch versus monosaccharide fructose-glucose mixtures (Turner *et al*., 2009; De Vogel-van den Bosch *et al*., 2011; Oliveira-de-Lira *et al*., 2018; Zicker *et al*., 2019; Ströher *et al*., 2020; Wali *et al*., 2021). That the introduction of a lard-based high-fat challenge did not introduce or exacerbate development of the CREBRF missense variant phenotype in the current study might not exclude the potential for interactions with gradations in macronutrient provision which were not evaluated in the R458Q mouse model.

Similar dietary considerations apply to consumption of protein. Severe dietary AA deficiency, for example, induces compensatory lowering of protein synthesis and heightened protein catabolism in muscle and liver (Roisné-Hamelin *et al*., 2021). The thematically similar but less pronounced transcriptomic changes seen in overnight fasted R458Q mice might also function in this setting. Greater dietary provision of AAs, in contrast, can improve lean tissue growth and muscle quality whereas (necessity-driven) increases in endogenous AA biosynthesis limits metabolic outputs including growth (Hou *et al*., 2016; Jang *et al*., 2021). Given that the presence of the R458Q missense variant was associated with enhancements to both lean mass and hepatic AA biosynthetic pathway activity in male mice, the intersection may suggest investigation of metabolic work rate in this context. AA signalling is also known to both stimulate and be facilitated by mTOR complex activity, and the variant-induced transcriptomic and *in vitro* changes associated with mTOR in this mouse model might further suggest feasible alterations in these pathways linked to AA or protein provision.

The presence of phenotypic differentiation between WT and HOM animals fed the standard chow diet could, however, suggest that the CREBRF missense variant might differentially impact nutrient handling even independent of the introduction of macronutrient-based interventions. Indeed, differential expression of carbohydrate interconversion and amino acid metabolism genes in HOM mice indicates potentially altered fluxes through these pathways. Development of increased lean mass, for example, depends on available energetic and protein resources which, if dietary provision *per se* does not differ, are presumably subject to altered utilisation if not accumulation. The variant phenotype may thusly be linked to theories of feed efficiency. This concept is often defined as a ratio of body weight gain per unit of feed consumed but can also be expressed as the cumulative metabolic efficiency with which dietary nutrients are utilised for growth and maintenance (Koch *et al.*, 1963; Patience *et al.*, 2015). Falling under general umbrella of thrifty metabolism, greater feed efficiency is associated with lower energy metabolic rate. It has been identified as potentially resulting from decreased protein turnover, increased expression of ETC components, and more efficient mitochondrial production of ATP in skeletal muscle, and enhanced ER protein processing in the liver (Kelly *et al.*, 2011; Cantalapiedra-Hijar *et al.*, 2018; McKenna *et al.*, 2021). Curiously, although these mechanisms were each associated with the R458Q transcriptome described in Chapter 4, variant-induced changes acted in the opposite directions, perhaps reflecting the interaction with fasted state in addition to genotype. Although the broader link to metabolic thriftiness in dietary intake and nutrient handling applies, greater focus on specific energy intake would be required for analysis of feed efficiency in human or murine variant carriers.

Mechanisms of Action and Molecular Pathways

The near-complete scarcity of published molecular studies to examine the CREBRF missense variant has left a similarly lacking understanding of its action on that (sub)cellular scale. For the wildtype protein, *in vitro* studies have primarily identified protein-protein interactions, regulating protein degradation of key transcription factors, via subcellular co-localisation (Audas *et al.*, 2008; Martyn *et al.*, 2012; Audas *et al.*, 2016). It may mediate transcriptional activity (Tiebe *et al.*, 2015, 2019), but beyond a putative transactivation region within the amino acid sequence, no evidence currently proves that CREBRF possesses direct DNA-binding or transcriptional function. The current R458Q mouse model likewise cannot offer any explicit indication of molecular

protein interactions, being a largely preliminary study on a broader phenotypic scale; any theorised implications are speculative. The variant-induced changes to muscle and liver tissue transcriptomes offer near-unequivocal evidence that CREBRF function is linked to gene expression. That these changes are relatively mild, largely failing to persist following FDR correction, implies that the R458Q mutation may impact transcription via its regulation of other factors. If the WT protein can indeed act as a TF, these functions may be retained by the variant protein without significant alteration.

Posttranscriptional and/or posttranslational regulation seem more likely targets of variant-induced changes, particularly given the ambiguous contributions of altered ribosomal transcript expression in HOM mice. Indeed, these male variant carriers shows limited correlation between gene and protein expression in key pathways including cellular stress responses. The metabolic phenotype similarly lacks overt overlaps in cellular and organismal processes, with decreased transcription of oxidative phosphorylation components not reflected in the unchanged whole-body energy expenditure measures. This variant-induced posttranscriptional regulation could not be identified in the current study. The moderate *in vivo* murine phenotype may be produced by similarly modest molecular changes or otherwise minimised by adaptive, compensatory mechanisms. Future evaluation of CREBRF protein interactions via co-immunoprecipitation and/or chromatin immunoprecipitation sequencing would be advisable to better identify affected proteins and DNA binding sites in both wildtype and missense variant contexts.

Review of the current literature pertaining to CREBRF and CREB3 highlights the physiological and cellular stress responses as potential molecular mechanisms influenced by missense variant activity. The former, mediated via GC signalling, represents perhaps the more overt functional link between CREBRF and the dual missense variant phenotype of body composition and diabetes protection. Loss of either CREBRF or CREB3 in mice produces developmental compensatory changes to HPA sensitivity and circulating corticosterone levels (Martyn *et al*., 2012; Penney *et al*., 2017; Frahm *et al*., 2020). Changes in GC signalling have in other models been linked to energy metabolism, including lipolytic and gluconeogenic pathways, appetite, and high-fat feeding, as well as adipose, muscle, and bone composition (Auvinen *et al*., 2012; Lawson *et al*., 2013; Harrell *et al*., 2016; Tanaka *et al*., 2017; Thuzar *et al*., 2018; Dassonvalle *et al*., 2020). Of particular note to the CREBRF variant phenotype, the maladaptive hypersecretion of

GCs provoked by chronic stress or similar environmental insult, including diet, can predispose an individual to metabolic "misprogramming" and risk of pathophysiological consequences (Ruiz *et al*., 2020; Sharma & Singh, 2020; Seal & Turner, 2021). That this disturbance of the HPA axis can also be induced by prenatal or early-life stressors bears clear thematic relevance to the TGH paradigm(s) used to frame the CREBRF missense variant phenotype in human populations (Seal & Turner, 2021). This was not, however, specifically examined within the current R458Q model and, despite mild transcriptomic associations with direct GC-linked gene expression, whole-body genotype effects are not attributable specifically or only to GC signalling.

Cellular ER and Golgi stress responses are each positively associated with CREB3 activity in a relationship which is negatively regulated by CREBRF. Dysregulation of this regulatory CREBRF-CREB3 counterbalance can suppress the cell stress response, compromising protein folding and cellular secretory capacity to produce greater protein burden and ER stress (Audas *et al*., 2008; Penney *et al*., 2018; Hu *et al*., 2019; Zhao *et al*., 2020). Its downregulation in the R458Q hepatic transcriptome described in Chapter 4, represented in UPR/ERAD, heat shock, and protein processing responses, offers perhaps the clearest manifestation of a possible stress-based interaction with missense variant function despite being unobserved in tissue protein expression. It is not without broader relevance to the CREBRF missense variant phenotype, having been linked in literature to the PKB-mTOR pathway, lipid metabolism, and development of IR and diabetes (Appenzeller-Herzog & Hall, 2012; Volmer & Ron, 2015; Song *et al*., 2016; Pinto *et al*., 2019; Fernandes-da-Silva *et al*., 2021). There are, however, weaknesses to any presumption of direct relevance. Although reduction of ER stress can improve metabolic defects in diet-induced obesity or diabetes (Ozcan *et al*., 2006; Zanotto *et al*., 2016; Wang *et al*., 2018), the downregulated hepatic gene expression seen in male HOM mice could also reflect a reduced ability to respond to proteotoxic stress and thus greater cellular disrepair. The stress response is moreover associated with wide-ranging physiological and pathophysiological conditions, beyond those which can be logically linked to variant function, including inflammation, NAFLD, autophagy, apoptosis, and chemoresistance (Verfaillie *et al*., 2013; Zhong *et al*., 2017; Wang *et al*., 2018; You *et al*., 2021). Cellular stress is likely at least tangentially involved with the R458Q variant phenotypic effect but cannot on the basis of current findings be identified as a primary mechanism.

Nutrient stress is likely to be the molecular signalling pathway most strongly correlated with theorised functions of the CREBRF missense variant. Previous studies indicated that CREBRF may act downstream of mTORC1, activated following starvation or rapamycin treatment to mediate an adaptive transcriptional programme which functions as a metabolic brake to promote cell survival (Tiebe *et al*., 2015; Minster *et al*., 2016; Tiebe *et al*., 2019). The current thesis implies that similar nutrient-sensitive adaptations may be exaggeratedly induced by the murine R458Q variant protein and could in theory also centre on the mTOR complex signalling network. Variant-induced alterations in mTORC1 regulatory factor mRNA expression, as well as potentially stifled mTOR complex activity represented by reduced $mTOR^{Ser2448}$ phosphorylation in primary hepatocytes, are suggestive even if not comprehensive. Subtle, context-dependent modulation of WT function would seem more appropriate to the mild *in vivo* phenotype observed in R458Q KI mice than a more dramatic constitutive abrogation or oversensitivity. Molecular drivers could be correspondingly difficult to detect. Chapters 4 and 6 suggest that the missense variant may heighten WT expression and/or activity but cannot determine from the current model whether this might reflect, for example, either cause or consequence of any heightened mTOR inhibition.

Mild genotype effects may indicate some degree of selectivity in missense variant interactions. The significantly lessened $mTOR^{Ser2448}$ phosphorylation in HOM compared to WT hepatocytes, for example, represents suppression of insulin-stimulated activation, an effect which is not similarly present in glucagon-treated cells. Specific context-dependence of this suppressive effect, like the catabolic programme discussed above, might help to reconcile it with theories of variant-induced growth. The broad range of mTOR complex functions could nevertheless potentially produce extensive impacts if indeed altered in variant carriers. In the context of metabolic features associated with the CREBRF missense variant, the mTOR complexes also have strong links to AA signalling, protein synthesis, cell and tissue growth, mitochondrial respiration, ER stress, and pancreatic hormone secretion (Mayer & Grummt, 2006; Song *et al*., 2016; Rosario *et al*., 2019; Ham *et al*., 2020a, 2020b; Rajak *et al*., 2021; Tabbaa *et al.*, 2021). Roles in diabetes further suggests that possible impacts on mTORC1/2 are also specifically relevant to the broader human CREBRF variant phenotype (Tuo & Xiang, 2019; Tsai *et al*., 2021). It is nevertheless possible, however, that the far-reaching mTORC1/2 regulatory influences on cellular and organismal metabolism might also give correlative associations a

misleadingly causative appearance. FOXO, which seems to share gene targets with the CREBRF ortholog in *Drosophila* in a TOR-associated pathway (Tiebe *et al*., 2015), is also linked to more than a quarter of the R458Q-affected genes described in Chapter 4 and could present another worthwhile investigative avenue for future study.

The distinct sexual dimorphism of this R458Q mouse model could presuppose biological sex-dependent mechanisms and thereby present a feasible exploratory avenue in future efforts to ascertain missense variant function. Development and sensitivity of the HPA axis and glucocorticoid stress response, for example, is sex-specific and crosstalk between glucocorticoid and sex steroid receptor signalling has recently been proposed to explain sex bias in stress-related metabolic disease risk (Oyola & Handa, 2017; Ruiz *et al*., 2020; Zuloaga *et al*., 2020; Moisan, 2021; Toews *et al*., 2021). The mTORC1/2 signalling networks likewise possess at least a degree of sex-dependence in both organismal and tissue metabolism. Inhibition of mTORC2 signalling impairs survival and reduces lifespan in male but not female mouse models (Lamming *et al*., 2014). Chronic rapamycin feeding likewise reveals greater sensitivity to hepatic mTORC1 inhibition in male compared to female mice (Drake *et al*., 2013). If the missense variant phenotype is indeed induced even partially via alterations to the wildtype CREBRF interactions downstream of mTORC1 inhibition, these male-dominant effects may explain broader organismal dimorphism. The mTORC1-related sex-dependence is curiously tissue-specific, with rapamycin-induced changes to skeletal muscle maintained across both sexes (Drake *et al*., 2013). This further level of regulation might differentially modulate any interaction with the CREBRF R458Q variant protein and thereby complexify murine phenotype manifestation and interpretation.

Sex-dependent interactions can produce organismal and developmental effects, including risks of (predisposition to) adverse metabolic conditions such as those which are associated with the human missense variant phenotype. Low circulating testosterone, for example, has been linked to male diabetes risk (Laaksonen *et al*., 2004; Pitteloud *et al*., 2005; Nna *et al*., 2019; Farooq *et al*., 2020); oestradiol can increase insulin sensitivity and protect against diet-induced glucose intolerance (Alonso *et al*., 2010; Stubbins *et al*., 2012). The latter may partially explain why female mice, unlike males, did not experience variant-induced deterioration of insulin response in the current study. A logical mechanistic basis for sex-specific CREBRF variant function is suggested by known

associations with sex steroid secretion, maternal behaviour, and fertility in CREBRF knockout models (Martyn *et al*., 2012; Yang *et al*., 2013b; Penney, 2017; Yang *et al*., 2018). Unlike the current mouse model, evidence for phenotypic disparity between human male and female CREBRF variant carriers is somewhat inconsistent, although effect size can differ between human sexes even without strict dimorphism. It is possible that whatever factor governs the murine sex-dependent interactions is absent or comparatively less dominant in human populations. Its identification might, therefore, aid the question of species translation as well as of murine dimorphism in the CREBRF context.

Model

The novel mouse model described in this thesis, although chosen with the aim to further understanding of the *CREBRF* R457Q variant phenotype in human carriers, bore limited correlation to published reports of that phenotype. As a model organism, mice are historically considered valuable tools in understanding biology and pathology for their phylogenetic relatedness and physiological similarities to humans, as well as ease of maintenance, breeding, and genetic manipulation (Perlman, 2016; Kottaisamy *et al*., 2021). In the context of the *CREBRF* missense variant, use of the R458Q mouse model can also facilitate closer and more invasive analyses of the metabolic effects than are currently performed in human population studies. The knock-in model, replacing rather than supplementing the endogenous CREBRF, provides a more accurate reflection of the human situation than might, for example, an overexpression model. Although the latter might magnify any phenotype, and indeed was used in Minster *et al*. (2016)'s *in vitro* adipocyte model to supplement the initial discovery of the human CREBRF variant, forced overexpression could invalidate any variant-induced effects on protein stability as seems indicated by the reduced hepatic *Crebrf* mRNA in the current model. The mild phenotype of the R458Q model, not wholly similar to human studies, nevertheless limits its explicative potential.

The CREBRF protein, which has more than 95% amino acid sequence identity between humans and mice, is perhaps therefore unlikely to comprise the direct cause of the species variation. The possible candidates which might drive altered interactions with the CREBRF variant protein, either directly or indirectly, are uncertain. The CREBRF variant could feasibly interact in humans with other gene variants, not independently identified,

but which could cooperatively promote the R457Q human phenotype. Effects on fat-free mass and height in human variant carriers, for example, might in this case represent augmentation of the known predisposition of PI populations to greater muscle and bone mass (Swinburn *et al*., 1999; Grant *et al*., 2005; Rush *et al*., 2009). Modulation of CREBRF alone, in mice lacking these other factors, might therefore limit development of the variant's full physiological effects. Although evolutionarily conserved biological processes are readily comparable between model species, the signalling networks underlying pathologies are more flexible, and mouse strains generated to simulate human genetic disease can often differ in phenotype between the two species (Elsea & Lucas, 2002; Perlman, 2016). Taking a broader view, species variation can be driven by the increased specific metabolic rate in mice compared to humans. This is characterised by anatomic, physiologic, and biochemical differences which are not limited to decreased organismal size, increased mitochondrial density, greater proportion of metabolically active tissues, and differently evolved dietary needs (Perlman, 2016). Given that each of these factors is implied to be at least partially influenced in the missense variant activity, the potential for its mistranslation across species could be partially endemic. Any straightforward simulation of the human phenotype may not be best served in a mouse line.

The transgenic mouse model herein established for the CREBRF R458Q missense variant had no published counterparts at the project's commencement. Two independent groups, based in the U.S.A and New Zealand, have since generated and provided preliminary (preprint) data for similar knock-in R458Q mouse models which further complexify interpretation of variant protein action (Kanshana *et al*., 2021; Lee *et al*., preprint). The earlier of these two models, using a C57BL/6J background, reported extensive characterisation of body composition and metabolic traits across nutritional conditions (Kanshana *et al*., 2021). Results of this assessment concluded that the R458Q variant had not influenced either energy or glucose homeostasis in mice fed either low- or high-fat diets, fasted or refed, or subjected to prolonged nutritional stress. Lee *et al*. (preprint), in contrast, tested missense variant KI mouse models on both C57BL/6J and FVB/NJ backgrounds. Interestingly, although this latter NZ study saw significant increases in relative lean mass of male R458Q variant carriers, aligned with both our current study and the human phenotype, the US model saw no changes to any measure of body composition. Grip strength and myostatin levels were similarly altered in the NZ but were

either not changed or not assessed in our or the US model. The disparity between these three KI mouse models demonstrates that manifestation of the variant phenotype can be disrupted not only by species translation but also by mouse strain, or potentially by a less tangible factor of handling, housing, study design, or location. The mild presentation of R458Q phenotype described in the current thesis, and indeed its apparent internal contradictions between whole-body, transcriptional, and *in vitro* effects, seems therefore an unsurprising development.

Environmental standardisation within and between studies or laboratories is a well-known weak point in reproducibility of experimental results, but the source of variation remains largely in question (Bailoo *et al*., 2020; Corrigan *et al*., 2020). In the context of these CREBRF variant mouse models, all of which were generated via similar CRISPR/Cas9 techniques, animal housing represents the most immediate point of difference. While Kanshana *et al*. (2021) set the temperature at 25C, both Lee *et al*. (preprint) and the current study used standard housing conditions of 22 ± 1-2°C. Room temperature has demonstrable influence on energy balance, which comprises a key element in the theorised activity of CREBRF and may therefore affect mouse metabolism differences here (Corrigan *et al*., 2020). The light/dark cycle, set at 14:10 hr and at 12:12 hr in the US-based and NZ-based studies respectively, might likewise influence phenotypic plasticity given potential CREBRF interaction with circadian rhythmicity. Whether these changes in laboratory conditions were sufficient to modulate the missense variant function so decisively as is observed between these models is uncertain, but they are a feasible contributor.

The US-based mouse model is also of especial relevance to the theorised molecular mechanisms underlying the CREBRF missense variant function. Grounded in the known literature associations with starvation and mTORC1 inhibition, as described above, Kanshana *et al*. (2021) evaluated the effects of not only extreme nutritional stress but also pharmacological mTORC1 inhibition. Both these conditions, and particularly the latter, have herein been argued to present feasible avenues in drawing out the murine missense variant phenotype. Kanshana *et al*. (2021) did not, however, observe a genotype-dependent effect on any of the body composition or metabolic measures assessed in their mouse model even when exposed to this more extreme nutrient deprivation. The absence of phenotype might seem to indicate against any involvement of the starvation response

and mTORC1 signalling in CREBRF variant function, running wholly counter to the theories linked to the current study's findings. By extension, there is little evidence that the reproduction of such an experimental design in our KI model would be effective in elucidating R458Q missense variant effects. Given the general lack of phenotypic corroboration between the differing R458Q models, however, it is possible that the extended nutrient deprivation would likewise produce varied interactions across these mouse lines. Indeed, such an examination may provide further answers regarding the molecular drivers of strain differentiation and therefore perhaps also species differentiation in variant carriers. The outstanding question might then become the robustness (or, perhaps, fragility) of starvation-induced genotype effects, particularly given that such effects were among the most significant actors in the current mouse model.

Future Directions

The largely preliminary nature of the current study, in seeking to establish basic metabolic characteristics of the novel R458Q mouse model, provides relatively broad scope for future efforts to elaborate upon the CREBRF missense variant phenotype. Modulation of *in vivo* experimental conditions as described in this thesis was limited to high-fat challenge, containing 45% kcal from lard, and to overnight fasting immediately prior to the endpoint; genotype effects were removed by the former and introduced by the latter. The utilisation of either more extreme or more diverse conditions might provoke CREBRF variant function and highlight differentiation between WT and HOM animals. In the context of nutritional adaptation, these conditions might include more prolonged starvation, or pharmacological inhibition of the underlying mTORC1 signalling pathway, as trialled by Kanshana *et al*. (2021). Diets with varied carbohydrate and/or protein composition could highlight preferential nutrient handling (Horton *et al*., 1995; Wali *et al*., 2021). Exacerbation of diet-induced metabolic deficiencies by greater fat content provision (e.g., 60% kcals), supplementation with greater sugar content (e.g., high fat: high fructose diet), or using fats sourced from coconut oil rather than lard to better mimic the traditional PI diet, might likewise differently reveal missense variant interactions (Zicker *et al*., 2019; Ströher *et al*., 2020).

Further exploration of the genotype effects which were identified in the current study could encompass interactions with muscle growth and atrophy, bone accretion, or insulin

sensitivity. Skeletal muscle atrophy, for example, can be induced by multiple stimuli including fasting, denervation, ageing, and immobilisation, leading to similar but distinct molecular alterations underlain by metabolic remodelling (McKinnell & Rudnicki, 2004; Bialek *et al*., 2011; Renzini *et al*., 2021). Differentiation between these in the CREBRF missense variant model, or of hypertrophic stimuli, might aid interpretation of the apparently contradictory transcriptional and organismal effects seen in this study. Tissue molecular response to insulin could be examined *in vivo* or *ex vivo*. Alternate physiological stressors, for example higher intensity exercise or restraint stress, might also elucidate possible effects on the canonical CREBRF interaction with the HPA axis and glucocorticoid signalling. The association with diabetes risk could perhaps also be explored in a more focused model, using streptozotocin or other pharmacological or genetic means to induce relevant metabolic dysfunction more strongly than the high-fat challenge in the current study.

The *in vitro* model described in Chapter 6 demonstrated specific molecular effects of the missense variant in isolated hepatocytes, free from confounding external influences. Extension of this study, given the *in vivo* tissue-specific genotype effects which were observed for R458Q mice, would logically entail examination of these molecular effects in different cell types. The association with muscle mass recommends myocyte isolation and culture; associations with obesity and circulating lipids suggests primary adipocyte culture; links to insulin secretion suggest pancreatic islet study. Sexual dimorphism of genotype effects, as discussed above, suggests analysis of steroidogenic or reproductive cells, which have elsewhere shown CREBRF-dependent interactions (Martyn *et al*., 2012; Yang *et al.*, 2013b; Penney, 2017; Yang *et al*., 2018). Given that these were seen primarily in female models, and particularly in the contexts of oestrous cycle, pregnancy, and reproductive tissue cell lines, it is possible that missense variant influence on female reproduction, cannot be discounted without a more appropriate experimental focus despite the otherwise male-specific phenotype. Further afield, current literature has linked CREBRF and/or CREB3 to neuronal and brain functions (Audas *et al.*, 2008; Ying *et al*., 2014, 2015a; Hasmatali *et al*., 2019; Oh-hashi *et al*., 2021b), thereby suggesting another possible site for variant interaction, less overtly implicated in the known phenotype. Analysis of these same tissues taken from *in vivo* cohorts would perhaps likewise present a feasible option.

Molecular characterisation of the CREBRF protein was beyond the scope and capacity of the current project. Efforts to determine, for example, any direct structural changes effected by the amino acid substitution may nevertheless provide one further means to gauge functional alterations. The replacement of arginine with glutamine, changing from charged and aliphatic to charge-neutral and polar, falls within a highly conserved region of the protein and evidently holds sufficient power to provoke organismal changes *in vivo*. If found to alter a defined binding or catalytic site, knowledge of the variant protein's altered interactions may be better defined. The three-dimensional structure of CREBRF, with or without the mutation, is however not yet known. Current literature likewise offers no theories regarding the effects of the amino acid substitution on localisation or half-life of the protein. This question is further complicated by the generally inconclusive nature of such examinations performed for the wildtype CREBRF, which has a short half-life and seems to localise dependent on cell type and experimental design (Audas *et al*., 2016; Tiebe *et al*., 2019; Oh-hashi *et al*., 2021b). Compounding these problems is the inability to procure any commercially available antibody selective for CREBRF protein (Tiebe *et al*., 2019), which has likewise limited efforts to examine its expression in the current thesis. Investigation along these lines could, however, provide a valuable insight into the regulation and/or interactions of the CREBRF variant.

Conclusion

The mild phenotype presented in the current *CREBRF* R458Q KI mouse model provides an imperfect mirror of the missense variant's major organismal effects as they manifest in human populations, or indeed in independently developed mouse models. Initial reports of the human R457Q variant in PI populations an increased obesity risk and reduced diabetes risk, but largely could not conclusively establish the mechanism mediating these effects (Minster *et al*., 2016; Naka *et al*., 2017; Ohashi *et al*., 2018). In seeking to establish a novel mouse model which might permit future elucidation of CREBRF variant action, this thesis found neither enhanced adiposity nor any benefit to insulin sensitivity or glucose tolerance in mice carrying the R458Q variant. The presence of the variant allele in these animals seems instead to mediate a whole-body growth phenotype, as well as speculative roles in energy homeostasis to produce an exaggerated adaptive response during periods of nutrient deprivation. These effects were sexually dimorphic and sensitive to environmental conditions including diet, suggesting a context-dependent modulation of phenotypic manifestation not overtly identified in human

variant carriers. Determining the nature of these potentially co-regulatory factors, which could cooperatively augment if not facilitate *CREBRF* variant activity, might enable future studies to draw out a more pronounced variant phenotype.

The feasible involvement of undefined genetic and/or environmental influences on phenotypic development, contributing to species mistranslation as well as inter-cohort variability, suggests a more potentially more malleable phenotype than was implied by earlier human studies. Indeed, as more studies are performed in PI populations, examining more metabolic traits with more exploratory study designs, the *in vivo* phenotype observed in human variant carriers is also becoming progressively more complex and at times contradictory. The significant impacts to PI population health which may result from presence of this human *CREBRF* R457Q missense variant reinforce the important public interests underpinning continued research into its function. The metabolic characterisation undertaken in this thesis, however, indicates that the variant allele contribution to body composition and metabolism in this R458Q KI mouse line cannot provide a wholly robust model of the human variant. Future utilisation of animal models may therefore require further (re)consideration of their explicative potential in the attempt to decipher the possible relationship between *CREBRF* missense variant function and resultant metabolic thrift and/or risk.

REFERENCES

Abu EO, Horner A, Kusec V, Triffitt JT & Compston JE (2000). The localisation of the functional glucocorticoid receptor α in human bone. *J Clin Endocrinol Metab* **85**, 883-889. doi: 10.1210/jcem.85.2.6365.

Agarwal P, Srivastava R, Srivastava AK, Ali S & Datta M (2013). miR-135a targets IRS2 and regulates insulin signalling and glucose uptake in the diabetic gastrocnemius skeletal muscle. *Biochim Biophys Acta* **1832**, 1294-1303. doi: 10.1016/j.bbadis.2013.03.021.

Agbim U, Carr RM, Pickett-Blakely O & Dagogo-Jack S (2019). Ethnic disparities in adiposity: focus on non-alcoholic fatty liver disease, visceral, and generalised obesity. *Curr Obes Rep* **8**, 243-254. doi: 10.1007/s13679-019-00349-x.

Agius L, Chachra SS & Ford BE (2020). The protective role of the carbohydrate response element binding protein in the liver: the metabolite perspective. *Front Endocrinol (Lausanne)* **11**, 594041. doi: 10.3389/fendo.2020.594041.

Ahmadi A, Sheikholeslami-Vatani D, Ghaeeni S & Baazm M (2021). The effects of different training modalities on monocarboxylate transporters MCT1 and MCT4, hypoxia inducible factor-1α (HIF-1α), and PGC-1α gene expression in rat skeletal muscles. *Mol Biol Rep* **48**, 2153-2161. doi: 10.1007/s11033-021-06224-0.

Ai Y, Sun Z, Peng C, Liu L, Xiao X & Li J (2017). Homocysteine induces hepatic steatosis involving ER stress response in high methionine diet-fed mice. *Nutrients* **9**, 346. doi: 10.3390/nu9040346.

AIN (1977). Report of the American Institute of Nurtition ad hoc Committee on standards for nutritional studies. *J Nutr* **107**, 1340-1348. doi: 10.1093/jn/107.7.1340.

Alabert C & Groth A (2012). Chromatin replication and epigenome maintenance. *Nat Rev Mol Cell Biol* **13**, 153-167. doi: 10.1038/nrm3288.

Aldridge S & Teichmann SA (2020). Single cell transcriptomics comes of age. *Nat Commun* **11**, 4307. doi: 10.1038/s41467-020-18158-5.

Alessi DR, Andjelkovic M, Caudwell B, Cron P, Morrice N, Cohen P, *et al*. (1996). Mechanism of activation of protein kinase B by insulin and IGF-1. *EMBO J* **15**, 6541-6551.

Alfadda AA, Masood A, Al-Naami MY, Chaurand P & Benabdelkamel H (2017). A proteomics based approach reveals differential regulation of visceral adipose tissue proteins between metabolically healthy and unhealthy obese patients. *Mol Cells* **40**, 685-695. doi: 10.14348/molcells.2017.0073.

AlOgayil N, Bauermeister K, Galvez JH, Venkatesh VS, Zhuang QK-W, Chang ML, *et al*. (2021). Distinct roles of androgen receptor, oestrogen receptor alpha, and BCL6 in the establishment of sex-biased DNA methylation in mouse liver. *Sci Rep* **11**, 13766. doi: 10.1038/s41598-021-93216-6.

Alonso A, González-Pardo H, Garrido P, Conejo NM, Llaneza P, Díaz F, *et al*. (2010). Acute effects of 17 β-estradiol and genistein on insulin sensitivity and spatial memory in aged ovariectomised female rats. *Age (Dordr)* **32**, 421-434. doi: 10.1007/s11357-010-9148-6.

Al-Qahtani SM, Bryzgalova G, Valladolid-Acebes I, Korach-André M, Dahlman-Wright K, Efendić S, *et al*. (2017). 17β-estradiol suppresses visceral adipogenesis and activates brown adipose tissue-specific gene expression. *Horm Mol Biol Clin Investig* **29**, 13-26. doi: 10.1515/hmbci-2016-0031.

Amaral PP, Dinger ME & Mattick JS (2013). Non-coding RNAs in homeostasis, disease and stress responses: an evolutionary perspective. *Brief Funct Genomics* **12**, 254-278. doi: 10.1093/bfgp/elt016.

Amthor H, Macharia R, Navarrete R, Schuelke M, Brown SC, Otto A, *et al*. (2007). Lack of myostatin results in excessive muscle growth but impaired force generation. *Proc Natl Acad Sci U S A* **104**, 1835-1840. doi: 10.1073/pnas.0604893104.

Andreasen CH, Stender-Petersen KL, Mogensen MS, Torekov SS, Wegner L, Andersen G, *et al*. (2008). Low physical activity accentuates the effect of the FTO rs9939609 polymorphism on body fat accumulation. *Diabetes* **57**(1), 95-101. doi: 10.2337/db07-0910.

Andrews B, Carroll J, Ding S, Fearnley IM & Walker JE (2013). Assembly factors for the membrane arm of human complex I. *PNAS* **110**, 18934-18939. doi: 10.1073/pnas.1319247110.

Anthonisen EH, Berven L, Holm S, Nygård M, Nebb HI & Grønning-Wang LM (2010). Nuclear receptor liver X receptor is *O*-GlcNAc-modified in response to glucose. *J Biol Chem* **285**, 1607-1615. doi: 10.1074/jbc.M109.082685.

Anunciado-Koza RP, Zhang J, Ukropec J, Bajpeyi S, Koza RA, Rogers RC, Cefalu WT, Mynatt RL, *et al*. (2011). Inactivation of the mitochondrial carrier SLC25A25

(ATP-MG^{2+}/P_i transporter) reduces physical endurance and metabolic efficiency in mice. *J Biol Chem* **286**, 11659-11671. doi: 10.1074/jbc.M110.203000.

Appenzeller-Herzog C & Hall MN (2012). Bidirectional crosstalk between endoplasmic reticulum stress and mTOR signalling. *Trends Cell Biol* **22**, 274-282. doi: 10.1016/j.tcb.2012.02.006.

Appleton SL, Seaborn CJ, Visvanathan R, Hill CL, Gill TK, Taylor AW, *et al*. (2013). Diabetes and cardiovascular disease outcomes in the metabolically healthy obese phenotype: a cohort study. *Diabetes Care* **36**, 2388-2394. doi: 10.2337/dc12-1971.

Araujo TR, da Silva JA, Vettorazzi JF, Freitas IN, Lubaczeuski C, Magalhães EA, *et al*. (2019). Glucose intolerance in monosodium glutamate obesity is linked to hyperglucagonemia and insulin resistance in α cells. *J Cell Physiol* **234**, 7019-7031. doi: 10.1002/jcp.27455.

Argilés JM, Campos N, Lopez-Pedrosa JM, Rueda R & Rodriguez-Mañas L (2016). Skeletal muscle regulates metabolism via interorgan crosstalk: roles in health and disease. *J Am Med Dir Assoc* **17**, 789-796. doi: 10.1016/j.jamda.2016.04.019.

Arias J, Alberts AS, Brindle P, Claret FX, Smeal T, Karin M, *et al*. (1994). Activation of cAMP and mitogen responsive genes relies on a common nuclear factor. *Nature* **370**, 226-229. doi: 10.1038/370226a0.

Arimoto K-I, Takahashi H, Hishiki T, Konishi H, Fujita T & Shimotohno K (2007). Negative regulation of the RIG-I signalling by the ubiquitin ligase RNF125. *Proc Natl Acad Sci U S A* **104**, 7500-7505. doi: 10.1073/pnas.0611551104.

Arner P & Spalding KL (2010). Fat cell turnover in humans. *Biochem Biophys Res Commun* **396**(1), 101-104. doi: 10.1016/j.bbrc.2010.02.165.

Arora S & Golemis EA (2015). A new strategy to ERADicate HER2-positive breast tumours? *Sci Signal* **8**, fs11. doi: 10.1126/scisignal.aac4746.

Arslanian KJ, Fidow UT, Atanoa T, Unasa-Apelu F, Naseri T, Wetzel AI, *et al*. (2021). A missense variant in CREBRF, rs373863828, is associated with fat-free mass, not fat mass in Samoan infants. *Int J Obes (Lond)* **45,** 45-55. doi: 10.1038/s41366-020-00659-4.

Ashburner M, Ball CA, Blake JA, Botstein D, Butler H, Cherry JM, *et al*. (2000). Gene ontology: tool for the unification of biology. The Gene Ontology Consortium. *Nat Genet* **25**, 25-29. doi: 10.1038/75556.

Ashby R, Adams J, Roberts SA, Mughal MZ & Ward KA (2011). The muscle-bone unit of peripheral and central skeletal sites in children and young adults. *Osteoporos Int* **22**, 121-132. doi: 10.1007/s00198-010-1216-3.

Audas TE, Hardy-Smith PW, Penney J, Taylor T & Lu R (2016). Characterisation of nuclear foci-targeting of Luman/CREB3 recruitment factor (LRF/CREBRF) and its potential role in inhibition of herpes simplex virus-1 replication. *Eur J Cell Biol* **95**, 611-622. doi: 10.1016/j.ejcb.2016.10.006.

Audas TE, Li Y, Liang G & Lu R (2008). A novel protein, Luman/CREB3 recruitment factor, inhibits luman activation of the unfolded protein response. *Mol Cell Biol* **28**, 3952-3966. doi: 10.1128/MCB.01439-07.

Australian Institute of Health and Welfare (2013). Diabetes expenditure in Australia 2009-09. AIHW: Canberra.

Australian Institute of Health and Welfare (2017). A picture of overweight and obesity in Australia. AIHW: Canberra.

Australian Institute of Health and Welfare (2018). Australia's health 2018. AIHW: Canberra.

Auvinen HE, Romijn JA, Biermasz NR, Pijl H, Havekes LM, Smit JWA, *et al*. (2012). The effects of high fat diet on the basal activity of the hypothalamus-pituitary-adrenal axis in mice. *J Endocrinol* **214**, 191-197. doi: 10.1530/JOE-12-0056.

Ayub Q, Moutsianas L, Chen Y, Panoutsopoulou K, Colonna V, Pagani L, *et al*. (2014). Revisiting the thrifty gene hypothesis via 65 loci associated with susceptibility to type 2 diabetes. *Am J Hum Genet* **94**, 176-185. doi: 10.1016/j.ajhg.2013.12.010..

Azzout-Marniche D, Bécard D, Guichard C, Foretz M, Ferré P & Foufelle F (2000). Insulin effects on sterol regulatory-element-binding protein-1c (SREBP-1c) transcriptional activity in rat hepatocytes. *Biochem J* **350**, 389-393.

Bacchi E, Negri C, Zanolin ME, Milanese C, Faccioli N, Trombetta M, *et al*. (2012). Metabolic effects of aerobic training and resistance training in type 2 diabetic subjects: a randomised controlled trial (the RAED2 study). *Diabetes Care* **35**, 676-682. doi: 10.2337/dc11-1655.

Back SH & Kaufman RJ (2012). Endoplasmic reticulum stress and type 2 diabetes. *Annu Rev Biochem* **81**, 767-793. doi: 10.1146/annurev-biochem-072909-095555.

Baehr LM, Hughes DC, Lynch SA, Van Haver D, Maia TM, Marshall AG, *et al*. (2021). Identification of the MuRF1 skeletal muscle ubiquitylome through quantitative proteomics. *Function (Oxf)* **2**, zqab029. doi: 10.1093/function/zqab029.

Baig U, Belsare P, Watve M & Jog M (2011). Can thrifty gene(s) or predictive foetal programming for thriftiness lead to obesity? *Journal of Obesity* **2011**, 861049. doi: 10.1155/2011/861049.

Bailoo JD, Voelkl B, Varholick J, Novak J, Murphy E, Rosso M, *et al*. (2020). Effects of weaning age and housing conditions on phenotypic differences in mice. *Sci Rep* **10**, 11684. doi: 10.1038/s41598-020-68549-3.

Baldini L, Charpentier B & Labialle S (2021). Emerging data on the diversity of molecular mechanisms involving C/D snoRNAs. *Noncoding RNA* **7**, 30. doi: 10.3390/ncrna7020030.

Ballard JWO, Melvin RG & Simpson SJ (2008). Starvation resistance is positively correlated with body lipid proportion in five wild caught *Drosophila simulans* populations. *J Insect Physiol* **54**, 1371-1376. doi: 10.1016/j.jinsphys.2008.07.009.

Baltusnikas J, Kilikevicius A, Venckunas T, Fokin A, Bünger L, Lionikas A, *et al*. (2015). Myostatin dysfunction impairs force generation in extensor digitorum longus muscle and increases exercise-induced protein efflux from extensor digitorum longus and soleus muscles. *Appl Physiol Nutr Metab* **40**, 817-821. doi: 10.1139/apnm-2014-0513.

Barba-Aliaga M, Alepuz P & Pérez-Ortín JE (2021). Eukaryotic RNA polymerases: the many ways to transcribe a gene. *Front Mol Biosci* **8**, 663209. doi: 10.3389/fmolb.2021.663209.

Bar-Peled L, Schweitzer LD, Zoncu R & Sabatini DM (2012). Ragulator is a GEF for the rag GTPases that signal amino acid levels to mTORC1. *Cell* **150**, 1196-1208. doi: 10.1016/j.cell.2012.07.032.

Barzilai N & Ferrucci L (2012). Insulin resistance and aging: a cause or a protective response? *J Gerontol A Biol Sci Med Sci* **67**, 1329-1331. doi: 10.1093/gerona/gls145.

Bassett DR, Rosenblatt G, Moellering RC Jr & Hartwell AS (1966). Cardiovascular disease, diabetes mellitus, and anthropometric evaluation of Polynesian males on the island of Niihau-1963. *Circulation* **34**, 1088-1097. doi: 10.1161/01.cir.34.6.1088.

Batista TM, Garcia-Martin R, Cai W, Konishi M, O'Neill BT, Sakaguchi M, *et al*. (2019). Multi-dimensional transcriptional remodelling by physiological insulin *in vivo*. *Cell Rep* **26**, 3429-3443.e3. doi: 10.1016/j.celrep.2019.02.081.

Baum JI, Kimball SR & Jefferson LS (2009). Glucagon acts in a dominant manner to repress insulin-induced mammalian target of rapamycin complex 1 signalling in perfused rat liver. *Am J Physiol Endocrinol Metab* **297**, E410-E415. doi: 10.1152/ajpendo.00042.2009.

Baumann CT, Ma H, Wolford R, Reyes JC, Maruvada P, Lim C, Yen PM, Stallcup MR & Hager GL (2001). The glucocorticoid receptor interacting protein 1 (GRIP1) localises in discrete nuclear foci that associate with ND10 bodies and are enriched in components of the 26S proteasome. *Mol Endocrinol* **15**, 485-500. doi: 10.1210/mend.15.4.0618.

Bazhan N, Jakovleva T, Feofanova N, Denisova E, Dubinina A, Sitnikova N, *et al*. (2019). Sex differences in liver, adipose tissue, and muscle transcriptional response to fasting and refeeding in mice. *Cells* **8**, 1529. doi: 10.3390/cells8121529.

Ben-Sahra I, Dirat B, Laurent K, Puissant A, Auberger P, Budanov A, *et al*. (2013). Sestrin2 integrates Akt and mTOR signalling to protect cells against energetic stress-induced death. *Cell Death Differ* **20**, 611-619. doi: 10.1038/cdd.2012.157.

Bentzinger CF, Lin S, Romanino K, Castets P, Guridi M, Summermatter S, *et al*. (2013). Differential response of skeletal muscles to mTORC1 signalling during atrophy and hypertrophy. *Skelet Muscle* **3**, 6. doi: 10.1186/2044-5040-3-6.

Berglund ED, Lee-Young RS, Lustig DG, Lynes SE, Donahue EP, Camacho RC, *et al*. (2009). Hepatic energy state is regulated by glucagon receptor signalling in mice. *J Clin Invest* **119**, 2412-2422. doi: 10.1172/jci38650.

Bergman BC & Goodpaster BH (2020). Exercise and muscle lipid content, composition, and localisation: influence on muscle insulin sensitivity. *Diabetes* **69**, 848-858. doi: 10.2337/dbi18-0042.

Bergman RN & Iyer MS (2017). Indirect regulation of endogenous glucose production by insulin: the single gateway hypothesis revisited. *Diabetes* **66**, 1742-1747. doi: 10.2337/db16-1320.

Berry SD, Walker CG, Ly K, Snell RG, Atatoa Carr PE, Bandara D, *et al*. (2018). Widespread prevalence of a CREBRF variant amongst Māori and Pacific children is associated with weight and height in early childhood. *Int J Obes (Lond)* **42**, 603-607. doi: 10.1038/ijo.2017.230.

Berry SE, Valdes AM, Drew DA, Asnicar F, Mazidi M, Wolf J, *et al*. (2020). Human postprandial responses to food and potential for precision nutrition. *Nat Med* **26**, 964-973. doi: 10.1038/s41591-020-0934-0.

Beverly MC & Evans MJ (1986). Bone mineral content in Polynesian and white New Zealand women. *Br Med J (Clin Res Ed)* **293**, 204. doi: 10.1136/bmj.293.6540.204-b.

Bhat SS, Ali R & Khanday FA (2019). Syntrophins entangled in cytoskeletal network: helping to hold it all together. *Cell Prolif* **52**, e12562. doi: 10.1111/cpr.12562.

Bhattacharya A (2019). Endoplasmic reticulum associated degradation (ERAD) in the liver. PhD dissertation, Cornell University, New York, USA. doi: 10.7298/k4gs-zj35.

Bhattacharya A, Sun S, Wang H, Liu M, Long Q, Yin L, *et al*. (2018). Hepatic Sel1L-Hrd1 ER-associated degradation (ERAD) manages FGF21 levels and systemic metabolism via CREBH. *EMBO J* **37**, e99277. doi: 10.15252/embj.201899277.

Bhatti GK, Khullar N, Sidhu IS, Navik US, Reddy AP, Reddy PH, *et al*. (2021). Emerging role of non-coding RNA in health and disease. *Metab Brain Dis* **36**, 1119-1134. doi: 10.1007/s11011-021-00739-y.

Bhopal RS & Rafnsson SB (2009). Could mitochondrial efficiency explain the susceptibility to adiposity, metabolic syndrome, diabetes and cardiovascular diseases in South Asian populations? *Int J Epidemiol* **38**, 1072-1081. doi: 10.1093/ije/dyp202.

Bialek P, Morris C, Parkington J, St Andre M, Owens J, Yaworsky P, *et al*. (2011). Distinct protein degradation profiles are induced by different disuse models of skeletal muscle atrophy. *Physiol Genomics* **43**, 1075-1086. doi: 10.1152/physiolgenomics.00247.2010.

Biddinger SB, Hernandez-Ono A, Rask-Madsen C, Haas JT, Alemán JO, Suzuki R, *et al*. (2008). Hepatic insulin resistance is sufficient to produce dyslipidemia and susceptibility to atherosclerosis. *Cell Metab* **7**, 125-134. doi: 10.1016/j.cmet.2007.11.013.

Bienvenu T, Lebrun N, Clarke J, Duriez P, Gorwood P & Ramoz N (2020). De novo deleterious variants that may alter the dopaminergic reward pathway are associated with anorexia nervosa. *Eat Weight Disord* **25**, 1643-1650. doi: 10.1007/s40519-019-00802-9.

Bindesbøll C, Fan Q, Nørgaard RC, MacPherson L, Ruan H-B, Wu J, *et al*. (2015). Liver X receptor regulates hepatic nuclear O-GlcNAc signalling and

carbohydrate responsive element-binding protein activity. *J Lipid Res* **56**, 771-785. doi: 10.1194/jlr.M049130.

Bischoff SC & Volynets V (2016). Nutritional influences of overfeeding on experimental outcomes in laboratory mice: consequences for gut microbiota and other functional studies. *Int J Med Microbiol* **306**, 328-333. doi: 10.1016/j.ijmm.2016.05.018.

Bisgaard Bengtsen M & Møller N (2021). Mini-review: glucagon responses in type 1 diabetes – a matter of complexity. *Physiol Rep* **9**, e15009. doi: 10.14814/phy2.15009.

Bloks VW, Bakker-Van Waarde WM, Verkade HJ, Kema IP, Wolters H, Vink E, *et al*. (2004). Down-regulation of hepatic and intestinal Abcg5 and Abcg8 expression associated with altered sterol fluxes in rats with streptozotocin-induced diabetes. *Diabetologia* **47**, 104-112. doi: 10.1007/s00125-003-1261-y.

Blot G, Lopez-Vergès S, Treand C, Kubat NJ, Delcroix-Genête D, Emiliani S, *et al.* (2006). Luman, a new partner of HIV-1 TMgp41, interferes with Tat-mediated transcription of the HIV-1 LTR. *J Mol Biol* **364**, 1034-1047. doi: 10.1016/j.jmb.2006.09.080.

Blüher M (2020). Metabolically healthy obesity. *Endocr Rev* **41**, 405-420. doi: 10.1210/endrev/bnaa004.

Bohnsack MT & Sloan KE (2018). Modifications in small nuclear RNAs and their roles in spliceosome assembly and function. *Biol Chem* **399**, 1265-1276. doi: 10.1515/hsz-2018-0205.

Bonds DE, Larson JC, Schwartz AV, Strotmeyer ES, Robbins J, Rodriguez BL, *et al*. (2006). Risk of fracture in women with type 2 diabetes: the Women's Health Initiative Observational Study. *J Clin Endocrinol* **91**, 3404-3410. doi: 10.1210/jc.2006-0614.

Bone RN, Oyebamiji O, Talware S, Selvaraj S, Krishnan P, Syed F, Wu H & Evans-Molina C (2020). A computational approach for defining a signature of β-cell Golgi stress in diabetes. *Diabetes* **69,** 2364-2376. doi: 10.2337/db20-0636.

Bonhoure N, Praz V, Moir RD, Willemin G, Mange F, Moret C, *et al*. (2020). MAF1 is a chronic repressor of RNA polymerase III transcription in the mouse. *Sci Rep* **10**, 11956. doi: 10.1038/s41598-020-68665-0.

Boon R, Kumar M, Tricot T, Elia I, Ordovas L, Jacobs F, *et al*. (2020). Amino acid levels determine metabolism and CYP450 function of hepatocytes and hepatoma cell lines. *Nat Commun* **11**, 1393. doi: 10.1038/s41467-020-15058-6.

Borrmann H, McKeating JA & Zhuang X (2021). The circadian clock and viral infections. *J Biol Rhythms* **36**, 9-22. doi: 10.1177/0748730420967768.

Bouchard C (2007). The biological predisposition to obesity: beyond the thrifty genotype scenario. *Int J Obes* **31**, 1337-1339. doi: 10.1038/sj.ijo.0803610.

Bourguignon A, Rameau A, Toullec G, Romestaing C & Roussel D (2017). Increased mitochondrial energy efficiency in skeletal muscle after long-term fasting: its relevance to animal performance. *J Exp Biol* **220**, 2445-2451. doi: 10.1242/jeb.159087.

Bozadjiema Kramer N, Lubaczeuski C, Blandino-Rosano M, Barker G, Gittes GK, Caicedo A, *et al*. (2021). Glucagon resistance and decreased susceptibility to diabetes in a model of chronic hyperglucagonemia. *Diabetes* **70**, 477-491. doi: 10.2337/db20-0440.

Briassoulis G, Keil MF, Naved B, Liu S, Starost MF, Nesterova M, *et al*. (2016). Studies of mice with cyclic AMP-dependent protein kinase (PKA) defects reveal the critical role of PKA's catalytic subunits in anxiety. *Behav Brain Res* **307**, 1-10. doi: 10.1016/j.bbr.2016.03.001.

Britto FA, Cortade F, Belloum Y, Blaquière M, Gallot YS, Docquier A, *et al*. (2018). Glucocorticoid-dependent REDD1 expression reduces muscle metabolism to enable adaptation under energetic stress. *BMC Biol* **16**, 65. doi: 10.1186/s12915-018-0525-4.

Brohée S & van Helden J (2006). Evaluation of clustering algorithms for protein-protein interaction networks. *BMC Bioinformatics* **7**, 488. doi: 10.1186/1471-2105-7-488.

Brosnan JT (2000). Glutamate, at the interface between amino acid and carbohydrate metabolism. *J Nutr* **130**, 988S-990S. doi: 10.1093/jn/130.4.988S.

Brown LS & Doyle FJ 3rd (2020). A dual-feedback loop model of the mammalian circadian clock for multi-input control of circadian phase. *PLoS Comput Biol* **16**, e1008459. doi: 10.1371/journal.pcbi.1008459.

Bugge A, Feng D, Everett LJ, Briggs ER, Mullican SE, Wang F, *et al*. (2012). Rev-erbα and Rev-erbβ coordinately protect the circadian clock and normal metabolic function. *Genes Dev* **26**, 657-667. doi: 10.1101/gad.186858.112.

Burden HJ, Adams S, Kulatea B, Wright-McNaughton M, Sword D, Ormsbee JJ, *et al*. (2021). The CREBRF diabetes-protective rs373863828-A allele is associated with enhanced early insulin release in men of Māori and Pacific ancestry. *Diabetologia* doi: 10.1007/s00125-021-05552-x.

Cadzow M, Merriman TR, Boocock J, Dalbeth N, Stamp LK, Black MA, *et al*. (2016). Lack of direct evidence for natural selection at the candidate thrifty gene locus, *PPARGC1A*. *BMC Med Genet* **17**, 80. doi: 10.1186/s12881-016-0341-z.

Cagen LM, Deng X, Wilcox HG, Park EA, Raghow R & Elam MB (2005). Insulin activates the rat sterol-regulatory-element-binding protein 1c (SREBP-1c) promoter through the combinatorial actions of SREBP, LXR, Sp-1 and NF-Y cis-acting elements. *Biochem J* **385**, 207-216. doi: 10.1042/BJ20040162.

Campbell JE, Fediuc S, Hawke TJ & Riddell MC (2009). Endurance exercise training increases adipose tissue glucocorticoid exposure: adaptations that facilitate lipolysis. *Metabolism* **58**, 651-660. doi: 10.1016/j.metabol.2009.01.002.

Cantalapiedra-Hijar G, Abo-Ismail M, Carstens GE, Guan LL, Hegarty R, Kenny DA, *et al*. (2018). Review: Biological determinants of between-animal variation in feed efficiency of growing beef cattle. *Animal* **12**, s321-s335. doi: 10.1017/S1751731118001489.

Capulli M, Ponzetti M, Maurizi A, Gemini-Piperni S, Berger T, Mak TW, *et al*. (2018). A complex role for lipocalin 2 in bone metabolism: global ablation in mice induces osteopenia caused by an altered energy metabolism. *J Bone Miner Res* **33**, 1141-1153. doi: 10.1002/jbmr.3406.

Caratti G, Iqbal M, Hunter L, Kim D, Wang P, Vonslow RM, *et al*. (2018). REVERBa couples the circadian clock to hepatic glucocorticoid action. *J Clin Invest* **128**, 4454-4471. doi: 10.1172/JCI96138.

Cardellach F, Martí MJ, Fernández-Solá J, Marín C, Hoek JB, Tolosa E, *et al*. (1993). Mitochondrial respiratory chain activity in skeletal muscle from patients with Parkinson's disease. *Neurology* **43**, 2258-2262. doi: 10.1212/wnl.43.11.2258.

Carissimo G, Chan Y-H, Utt A, Chua T-K, Bakar FA, Merits A, *et al*. (2019). VCP/p97 is a proviral host factor for replication of chikungunya virus and other alphaviruses. *Front Microbiol* **10**, 2236. doi: 10.3389/fmicb.2019.02236.

Carlson JC, Rosenthal SL, Russell EM, Hawley NL, Sun G, Cheng H, *et al*. (2020). A missense variant in *CREBRF* is associated with taller stature in Samoans. *Am J Hum Biol* **32**, e23414. doi: 10.1002/ajhb.23414.

Casale M, von Hurst PR, Beck KL, Shultz S, Kruger MC, O'Brien W, *et al*. (2016). Lean mass and body fat percentage are contradictory predictors of bone mineral density in pre-menopausal Pacific Island women. *Nutrients* **8**, 470. doi: 10.3390/nu8080470.

Castro AA & Garland T Jr (2018). Evolution of hindlimb bone dimensions and muscle masses in house mice selectively bred for high voluntary wheel-running behaviour. *J Morphol* **279**, 766-779. doi: 10.1002/jmor.20809.

Celis-Morales C, Marsaux CFM, Livingstone KM, Navas-Carretero S, San-Cristobal R, O'Donovan CB, *et al*. (2016). Physical activity attenuates the effect of the FTO genotype on obesity traits in European adults: the Food4Me study. *Obesity (Silver Spring)* **24**(4), 962-969. doi: 10.1002/oby.21422.

Cetinus E, Buyukbese MA, Uzel M, Ekerbicer H & Karaoguz A (2005). Hand grip strength in patients with type 2 diabetes mellitus. *Diabetes Res Clin Pract* **70**, 278-286. doi: 10.1016/j.diabres.2005.03.028.

Chaillou T, Kirby TJ & McCarthy JJ (2014). Ribosome biogenesis: emerging evidence for a central role in the regulation of skeletal muscle mass. *J Cell Physiol* **229**, 1584-1594. doi: 10.1002/jcp.24604.

Chakravarthy MV & Booth FW (2004). Eating, exercise, and "thrifty" genotypes: connecting the dots toward an evolutionary understanding of modern chronic diseases. *J Appl Physiol (1985)* **96**, 3-10. doi: 10.1152/japplphysiol.00757.2003.

Chakravorty A, Jetto CT & Manjithaya R (2019). Dysfunctional mitochondria and mitophagy as drivers of Alzheimer's disease pathogenesis. *Front Aging Neurosci* **11**, 311. doi: 10.3389/fnagi.2019.00311.

Chanda D, Kim DK, Li T, Kim YH, Koo SH, Lee CH, *et al*. (2011). Cannabinoid receptor type 1 (CB1R) signalling regulates hepatic gluconeogenesis via induction of endoplasmic reticulum-bound transcription factor cAMP-responsive element-binding protein H (CREBH) in primary hepatocytes. *J Biol Chem* **286**, 27971-27979. doi: 10.1074/jbc.M111.224352.

Chanda D, Kim YH, Li T, Misra J, Kim DK, Kim JR, *et al*. (2013). Hepatic cannabinoid receptor type 1 mediates alcohol-induced regulation of bile acid enzyme genes expression via CREBH. *PLoS One* **8**, e68845. doi: 10.1371/journal.pone.0068845.

Chao LC, Zhang Z, Pei L, Saito T, Tontonoz P & Pilch PE (2007). Nur77 coordinately regulates expression of genes linked to glucose metabolism in skeletal muscle. *Mol Endocrinol* **21**, 2152-2163. doi: 10.1210/me.2007-0169.

Chavez JA & Summers SA (2012). A ceramide-centric view of insulin resistance. *Cell Metab* **15**(5), 585-594. doi: 10.1016/j.cmet.2012.04.002.

Cheetham SW, Faulkner GJ & Dinger ME (2020). Overcoming challenges and dogmas to understand the functions of pseudogenes. *Nat Rev Genet* **21**, 191-201. doi: 10.1038/s41576-019-0196-1.

Chen L, Sun F, Yang X, Jin Y, Shi M, Wang L, *et al*. (2017). Correlation between RNA-Seq and microarrays results using TCGA data. *Gene* **628**, 200-204. doi: 10.1016/j.gene.2017.07.056.

Chen X, McClusky R, Chen J, Beaven SW, Tontonoz P, Arnold AP, *et al.* (2012). The number of X chromosomes causes sex differences in adiposity in mice. *PLoS Genet* **8**, e1002709. doi: 10.1371/journal.pgen.1002709.

Chen X, Shen J & Prywes R (2002). The luminal domain of ATF6 sense endoplasmic reticulum (ER) stress and causes translocation of ATF6 from the ER to the Golgi. *J Biol Chem* **277**, 13045-13052. doi: 10.1074/jbc.M110636200.

Chen X, Wu M, Liang N, Lu J, Qu S & Chen H (2021). Thyroid hormone-regulated expression of Period2 promotes liver urate production. *Front Cell Dev Biol* **9**, 636802. doi: 10.3389/fcell.2021.636802.

Chen Y, Liu H, Wang Y, Yang S, Yu M, Jiang T, *et al*. (2019). Glycosaminoglycan from Apostichopus japonicus inhibits hepatic glucose production via activating Akt/FoxO1 and inhibiting PKA/CREB signalling pathways in insulin resistant hepatocytes. *Food Funct* **10**, 7565-7575. doi: 10.1039/c9fo01444f.

Cheng D, Xu X, Simon T, Boudyguina E, Deng Z, VerHague M, *et al*. (2016). Very low density lipoprotein assembly is required for cAMP-responsive element-binding protein H processing and hepatic apolipoprotein A-IV expression. *J Biol Chem* **291**, 23793-23803. doi: 10.1074/jbc.M116.749283.

Cheng KKY, Iglesias MA, Lam KSL, Wang Y, Sweeney G, Zhu W, *et al*. (2009). APPL1 potentiates insulin-mediated inhibition of hepatic glucose production and alleviates diabetes via Akt activation in mice. *Cell Metab* **9**, 417-427. doi: 10.1016/j.cmet.2009.03.013.

Cheng Z & White MF (2011). Targeting Forkhead box O1 from the concept to metabolic diseases: lessons from mouse models. *Antioxid Redox Signal* **14**, 649-661. doi: 10.1089/ars.2010.3370.

Cheng Z, Mugler CF, Keskin A, Hodapp S, Chan LY-L, Weis K, *et al*. (2019). Small and large ribosomal subunit deficiencies lead to distinct gene expression signatures that reflect cellular growth rate. *Mol Cell* **73**, 36-47.e10. doi: 10.1016/j.molcel.2018.10.032.

Chiang GG & Abraham RT (2005). Phosphorylation of mammalian target of rapamycin (mTOR) at Ser-2448 is mediated by p70S6 kinase. *J Biol Chem* **280**, 25485-25490. doi: 10.1074/jbc.M501707200.

Chiavaroli V, Gibbins JD, Cutfield WS & Derraik JGB (2019). Childhood obesity in New Zealand. *World J Pediatr* **15**, 322-331. doi: 10.1007/s12519-019-00261-3/

Chin K, Evans MC, Cornish J, Cundy T & Reid IR (1997). Differences in hip axis and femoral neck length in premenopausal women of Polynesian, Asian and European origin. *Osteoporos Int* **7**, 344-347. doi: 10.1007/BF01623775.

Chippindale AK, Chu TJF & Rose MR (1996). Complex trade-offs and the evolution of starvation resistance in *Drosophila melanogaster*. *Evolution* **50**, 753-766. doi: 10.1111/j.1558-5646.1996.tb03885.x.

Chiu YH, Schwarz E, Li D, Xu Y, Sheu TR, Li J, *et al*. (2017). Dendritic cell-specific transmembrane protein (DC-STAMP) regulates osteoclast differentiation via the Ca^{2+}/NFATc1 axis. *J Cell Physiol* **232**, 2538-2549. doi: 10.1002/jcp.25638.

Chiurazzi M, Cozzolino M, Orsini RC, Di Maro M, Di Minno MND & Colantuoni A (2020). Impact of genetic variations and epigenetic mechanisms on the risk of obesity. *Int J Mol Sci* **21**, 9035. doi: 10.3390/ijms21239035.

Cho C-S, Kowalsky AH & Lee JH (2020). Pathological consequences of hepatic mTORC1 dysregulation. *Genes (Basel)* **11**, 896. doi: 10.3390/genes11080896.

Choi J-A & Song C-H (2020). Insights into the role of endoplasmic reticulum stress in infectious diseases. *Front Immunol* **10**, 3147. doi: 10.3389/fimmu.2019.03147.

Choquet H & Meyre D (2011). Genetics of obesity: what have we learned? *Curr Genomics* **12**(3), 169-179. doi: 10.2174/138920211795677895.

Chowdhury MKH, Montgomery MK, Morris MJ, Cognard E, Shepherd PR & Smith GC (2015). Glucagon phosphorylates serine 552 of β-catenin leading to increased expression of cyclin D1 and c-Myc in the isolated rat liver. *Arch Physiol Biochem* **121**, 88-96. doi: 10.3109/13813455.2015.1048693.

Choy CC, Wang D, Naseri T, Soti-Ulberg C, Reupena MS, Duckham RL, *et al*. (2020). Longitudinal assessment of childhood dietary patterns: associations with body mass index z-score among children in the Samoan *Ola Tuputupua'e* (Growing Up) cohort. *Child Obes* **16**, 534-543. doi: 10.1089/chi.2020.0058.

Chrivia JC, Kwok RP, Lamb N, Hagiwara M, Montminy MR & Goodman RH (1993). Phosphorylated CREB binds specifically to the nuclear protein CBP. *Nature* **365**, 855-859. doi: 10.1038/365855a0.

Church C, Lee S, Bagg EAL, McTaggart JS, Deacon R, Gerken T, *et al*. (2009). A mouse model for the metabolic effects of the human fat mass and obesity associated *FTO* gene. *PLoS Genet* **5**(8), e1000599. doi: 10.1371/journal.pgen.1000599.

Chutkow WA, Patwari P, Yoshioka J & Lee RT (2008). Thioredoxin-interacting protein (Txnip) is a critical regulator of hepatic glucose production. *J Biol Chem* **283**, 2397-2406. doi: 10.1074/jbc.M708169200.

Clayton JA (2018). Applying the new SABV (sex as a biological variable) policy to research and clinical care. *Physiol Behav* **187**, 2-5. doi: 10.1016/j.physbeh.2017.08.012.

Clifford AJ, Riumallo JA, Baliga BS, Munro HN & Brown PR (1972). Liver nucleotide metabolism in relation to amino acid supply. *Biochim Biophys Acta* **277**, 443-458. doi: 10.1016/0005-2787(72)90087-1.

Cnop M, Foufelle F & Velloso LA (2012). Endoplasmic reticulum stress, obesity and diabetes. *Trends Mol Med* **18**, 59-68. doi: 10.1016/j.molmed.2011.07.010.

Conley KE, Kemper WF & Crowther GJ (2001). Limits to sustainable muscle performance: interaction between glycolysis and oxidative phosphorylation. *J Exp Biol* **204**, 3189-3194.

Contreras AV, Torres N & Tovar AR (2013). PPAR-α as a key nutritional and environmental sensor for metabolic adaptation. *Adv Nutr* **4**, 439-452. doi: 10.3945/an.113.003798.

Cooper MS, Seibel MJ & Zhou H (2016). Glucocorticoids, bone and energy metabolism. *Bone* **82**, 64-68. doi: 10.1016/j.bone.2015.05.038.

Copp J, Manning G & Hunter T (2009). TORC-specific phosphorylation of mammalian target of rapamycin (mTOR): phospho-Ser2481 is a marker for intact mTOR signalling complex 2. *Cancer Res* **69**, 1821-1827. doi: 10.1158/0008-5472.CAN-08-3014.

Cordero-Herrera I, Martín MA, Goya L & Ramos S (2014). Cocoa flavonoids attenuate high glucose-induced insulin signalling blockade and modulate glucose uptake and production in human HepG2 cells. *Food Chem Toxicol* **64**, 10-19. doi: 10.1016/j.fct.2013.11.014.

Corrigan JK, Ramachandran D, He Y, Palmer CJ, Jurczak MJ, Chen R, *et al*. (2020). A big-data approach to understanding metabolic rate and response to obesity in laboratory mice. *Elife* **9**, e53560. doi: 10.7554/eLife.53560.

Cortez-Toledo O, Schnair C, Sangngern P, Metzger D & Chao LC (2017). Nur77 deletion impairs muscle growth during developmental myogenesis and muscle regeneration in mice. *PLoS One* **12**, e0171268. doi: 10.1371/journal.pone.0171268.

Cousin MA, Lando D & Moguilewsky M (1982). Ornithine decarboxylase induction by glucocorticoids in brain and liver of adrenalectomized rats. *J Neurochem* **38**, 1296-1304. doi: 10.1111/j.1471-4159.1982.tb07904.x.

Crawford AA, Bankier S, Altmaier E, Barnes CLK, Clark DW, Ermel R, *et al*. (2021). Variation in the SERPINA6/SERPINA1 locus alters morning plasma cortisol, hepatic corticosteroid binding globulin expression, gene expression in peripheral tissues, and risk of cardiovascular disease. *J Hum Genet* **66**, 625-636. doi: 10.1038/s10038-020-00895-6.

Cundy T, Cornish J, Evans MC, Gamble G, Stapleton J & Reid IR (1995). Sources of interracial variation in bone mineral density. *J Bone Miner Res* **10**, 368-373. doi: 10.1002/jbmr.5650100306.

Cypess AM, Lehman S, Williams G, Tal I, Rodman D, Goldfine AB, *et al*. (2009). Identification and importance of brown adipose tissue in adult humans. *N Engl J Med* **360**, 1509-1517. doi: 10.1056/NEJMoa0810780.

Dai W, Panserat S, Plagnes-Juan E, Seiliez I & Skiba-Cassy S (2015). Amino acids attenuate insulin action on gluconeogenesis and promote fatty acid biosynthesis via mTORC1 signalling pathway in trout hepatocytes. *Cell Physiol Biochem* **36**, 1084-1100. doi: 10.1159/000430281.

Daitoku H, Hatta M, Matsuzaki H, Aratani S, Ohshima T, Miyagishi M, *et al*. (2004). Silent information regulator 2 potentiates Foxo1-mediated transcription through its deacetylase activity. *Proc Natl Acad Sci USA* **101**, 10042-10047. doi: 10.1073/pnas.0400593101.

Dalise S, Azzollini V & Chisari C (2020). Brain and muscle: how central nervous system disorders can modify the skeletal muscle. *Diagnostics (Basel)* **10**, 1047. doi: 10.3390/diagnostics10121047.

Danaei G, Finucane MM, Lu Y, Singh GM, Cowan MJ, Paciorek CJ, *et al*. (2011). National, regional, and global trends in fasting plasma glucose and diabetes prevalence since 1980: systematic analysis of health examination surveys and epidemiological studies with 370 country-years and 2.7 million participants. *Lancet* **378**, 31-40. doi: 10.1016/S0140-6736(11)60679-X.

Dang F, Sun X, Ma X, Wu R, Zhang D, Chen Y, *et al*. (2016). Insulin post-transcriptionally modulates Bmal1 protein to affect the hepatic circadian clock. *Nat Commun* **7**, 12696. doi: 10.1038/ncomms12696.

Dassonvalle J, Díaz-Castro F, Donoso-Barraza C, Sepúlveda C, Pino-de la Fuente F, Pino P, *et al*. (2020). Moderate aerobic exercise training prevents the augmented hepatic glucocorticoid response induced by high fat diet in mice. *Int J Mol Sci* **21**, 7582. doi: 10.3390/ijms21207582.

De Bock K, Richter EA, Russell AP, Eijnde BO, Derave W, Ramaekers M, *et al*. (2005). Exercise in the fasted state facilitates fibre type-specific intramyocellular lipid breakdown and stimulates glycogen resynthesis in humans. *J Physiol* **564**, 649-660. doi: 10.1113/jphysiol.2005.083170.

De Bono JP, Adlam D, Paterson DJ & Channon KM (2006). Novel quantitative phenotypes of exercise training in mouse models. *Am J Physiol Regul Integr Comp Physiol* **290**, R926-R934. doi: 10.1152/ajpregu.00694.2005.

de Klerk E & 't Hoen PAC (2015). Alternative mRNA transcription, processing, and translation: insights from RNA sequencing. *Trends Genet* **31**, 128-139. doi: 10.1016/j.tig.2015.01.001.

de Lange P, Moreno M, Silvestri E, Lombardi A, Gogli F & Lanni A (2007). Fuel economy in food-deprived skeletal muscle: signalling pathways and regulatory mechanisms. *FASEB J* **21**, 3431-3441. doi: 10.1096/fj.07-8527rev.

De Souza CJ, Eckhardt M, Gagen K, Dong M, Chen W, Laurent D, *et al.* (2001). Effects of pioglitazone on adipose tissue remodelling within the setting of obesity and insulin resistance. *Diabetes* **50**, 1863-1871. doi: 10.2337/diabetes.50.8.1863.

De Vogel-van den Bosch J, van den Berg SAA, Bijland S, Voshol PJ, Havekes LM, Romijn HA, *et al*. (2011). High-fat diets rich in medium- versus long-chain fatty acids induce distinct patterns of tissue specific insulin resistance. *J Nutr Biochem* **22**, 366-371. doi: 10.1016/j.jnutbio.2010.03.004.

Dean ED, Li M, Prasad N, Wisniewski SN, Von Deylen A, Spaeth J, *et al*. (2017). Interrupted glucagon signalling reveals hepatic α cell axis and role for L-glutamine in α cell proliferation. *Cell Metab* **25**, 1362-1373. doi: 10.1016/j.cmet.2017.05.011.

DeBalsi KL, Wong KE, Koves TR, Slentz DH, Seiler SE, Wittmann AH, *et al*. (2014). Targeted metabolomics connects thioredoxin-interacting protein (TXNIP) to

mitochondrial fuel selection and regulation of specific oxidoreductase enzymes in skeletal muscle. *J Biol Chem* **289**, 8106-8120. doi: 10.1074/jbc.M113.511535.

Defay R, Jaussent I, Lacroux A & Fontbonne A (2007). Relationships between glycaemic abnormalities, obesity and insulin resistance in nondiabetic Polynesians of New Caledonia. *Int J Obes (Lond)* **31**, 109-113. doi: 10.1038/sj.ijo.0803384.

DeFronzo RA, Gunnarsson R, Björkman O, Olsson M & Wahren J (1985). Effects of insulin on peripheral and splanchnic glucose metabolism in noninsulin-dependent (type II) diabetes mellitus. *J Clin Invest* **76**, 149-155. doi: 10.1172/JCI111938.

Delfin F, Myles S, Choi Y, Hughes D, Illek R, van Oven M, *et al*. (2012). Bridging near and remote Oceania: mtDNA and NRY variation in the Solomon Islands. *Mol Biol Evol* **29**, 545-564. doi: 10.1093/molbev/msr186.

Della Torre S, Mitro N, Meda C, Lolli F, Pedretti S, Barcella M, *et al*. (2018). Short-term fasting reveals amino acid metabolism as a major sex-discriminating factor in the liver. *Cell Metab* **28**, 256-267. doi: 10.1016/j.cmet.2018.05.021.

Demant M, Bagger JI, Suppli MP, Lund A, Gyldenløve M, Hansen KB, *et al*. (2018). Determinants of fasting hyperglucagonemia in patients with type 2 diabetes and nondiabetic control subjects. *Metab Syndr Relat Disord* **16**, 530-536. doi: 10.1089/met.2018.0066.

Demerath EW, Sun SS, Rogers N, Lee M, Reed D, Choh AC, *et al*. (2007). Anatomical patterning of visceral adipose tissue: race, sex, and age variation. *Obesity (Silver Spring)* **15**, 2984-2993. doi: 10.1038/oby.2007.356.

DenBoer LM, Iyer A, McCluggage ARR, Li Y, Martyn AC & Lu R (2013). JAB1/CSN5 inhibits the activity of Luman/CREB3 by promoting its degradation. *Biochim Biophys Acta* **1829**, 921-929. doi: 10.1016/j.bbagrm.2013.04.001.

Dentin R, Pégorier J-P, Benhamed F, Foufelle F, Ferré P, Fauveau V, *et al*. (2004). Hepatic glucokinase is required for the synergisitic action of ChREBP and SREBP-1c on glycolytic and lipogenic gene expression. *J Biol Chem* **279**, 20314-20326. doi: 10.1074/jbc.M312475200.

Deurenberg P, Weststrate JA & Seidell JC (1991). Body mass index as a measure of body fatness: age- and sex-specific prediction formulas. *Br J Nutr* **65**, 105-114. doi: 10.1079/bjn19910073.

Dias Junior AG, Sampaio NG & Rehwinkel J (2019). A balancing act: MDA5 in antiviral immunity and autoinflammation. *Trends Microbiol* **27**, 75-85. doi: 10.1016/j.tim.2018.08.007.

Diaz EC, Børsheim E, Shankar K, Cleves MA & Andres A (2019). Prepregnancy fat free mass and associations to glucose metabolism before and during pregnancy. *J Clin Endocrinol Metab* **104**, 1394-1403. doi: 10.1210/jc.2018-01381.

DiBello JR, McGarvey ST, Kraft P, Goldberg R, Campos H, Quested C, *et al*. (2009). Dietary patterns are associated with metabolic syndrome in adult Samoans. *J Nutr* **139**, 1933-1943. doi: 10.3945/jn.109.107888.

Dina C, Meyre D, Gallina S, Durand E, Körner A, Jacobson P, *et al*. (2007). Variation in *FTO* contributes to childhood obesity and severe adult obesity. *Nat Genet* **39**(6), 724-726. doi: 10.1038/ng2048.

Donnelly KL, Margosian MR, Sheth SS, Lusis AJ & Parks EJ (2004). Increased lipogenesis and fatty acid reesterification contribute to hepatic triacylglycerol stores in hyperlipidemic Txnip-/- mice. *J Nutr* **134**, 1475-1480. doi: 10.1093/jn/134.6.1475.

Drake AJ, Livingstone DEW, Andrew R, Seckl JR, Morton NM & Walker BR (2005). Reduced adipose glucocorticoid reactivation and increased hepatic glucocorticoid clearance as an early adaptation to high-fat feeding in Wistar rats. *Endocrinology* **146**, 913-919. doi: 10.1210/en.2004-1063.

Drake JC, Peelor FF 3rd, Biela LM, Watkins MK, Miller RA, Hamilton KL, *et al*. (2013). Assessment of mitochondrial biogenesis and mTORC1 signalling during chronic rapamycin feeding in male and female mice. *J Gerontol A Biol Sci Med Sci* **68**, 1493-1501. doi: 10.1093/gerona/glt047.

Dreher LS & Hoppe T (2018). Hepatic ERAD takes control of the organism. *EMBO J* **37**, e100676. doi: 10.15252/embj.2018100676.

Duclos M, Gouarne C, Martin C, Rocher C, Mormède P & Letellier T (2004). Effects of corticosterone on muscle mitochondria identifying different sensitivity to glucocorticoids in Lewis and Fischer rats. *Am J Physiol Endocrinol Metab* **286**, E159-E167. doi: 10.1152/ajpendo.00281.2003.

Duclos M, Martin C, Malgat M, Mazat JP, Chaouloff F, Mormède P, *et al*. (2001). Relationships between muscle mitochondrial metabolism and stress-induced corticosterone variations in rats. *Pflugers Arch* **443**, 218-226. doi: 10.1007/s004240100675.

Duggan AT, Evans B, Friedlaender FR, Friedlaender JS, Koki G, Merriwether DA, *et al*. (2014). Maternal history of Oceania from complete mtDNA genomes: contrasting ancient diversity with recent homogenisation due to the Austronesian expansion. *Am J Hum Genet* **94**, 721-733. doi: 10.1016/j.ajhg.2014.03.014.

Dulloo AG (2008). Thrifty energy metabolism in catch-up growth trajectories to insulin and leptin resistance. *Best Pract Res Clin Endocrinol Metab* **22**, 155-171. doi: 10.1016/j.beem.2007.08.001.

Dulloo AG, Jacquet J, Seydoux J & Montani J-P (2006). The thrifty 'catch-up fat' phenotype: its impact on insulin sensitivity during growth trajectories to obesity and metabolic syndrome. *Int J Obes (Lond)* **30 Suppl 4**, S23-S35. doi: 10.1038/sj.ijo.0803516.

Eason RJ, Pada J, Wallace R, Henry A & Thornton R (1987). Changing patterns of hypertension, diabetes, obesity and diet among Melanesians and Micronesians in the Solomon Islands. *Med J Aust* **146**, 465-469. doi: 10.5694/j.1326-5377.1987.tb120359.x.

Ebert SM, Dyle MC, Kunkel SD, Bullard SA, Bongers KS, Fox DK, *et al*. (2012). Stress-induced skeletal muscle Gadd45a expression reprograms myonuclei and causes muscle atrophy. *J Biol Chem* **287**, 27290-27301. doi: 10.1074/jbc.M112.374777.

Ebrahimi KH, Howie D, Rowbotham JS, McCullagh J, Armstrong FA & James WS (2020). Viperin, through its radical-SAM activity, depletes cellular nucleotide pools and interferes with mitochondrial metabolism to inhibit viral replication. *FEBS Lett* **594**, 1624-1630. doi: 10.1002/1873-3468.13761.

Eckel N, Meidtner K, Kalle-Uhlmann T, Stefan N & Schulze MB (2016). Metabolically healthy obesity and cardiovascular events: a systematic review and meta-analysis. *Eur J Prev Cardiol* **23**, 956-966. doi: 10.1177/2047487315623884.

Eckstein SS, Weigart C & Lehmann R (2017). Divergent roles of IRS (insulin receptor substrate) 1 and 2 in liver and skeletal muscle. *Curr Med Chem* **24**, 1827-1852. doi: 10.2174/0929867324666170426142826.

Edgerton DS, Lautz M, Scott M, Everett CA, Stettler KM, Neal DW, *et al*. (2006). Insulin's direct effects on the liver dominate the control of hepatic glucose production. *J Clin Invest* **116**, 521-527. doi: 10.1172/JCI27073.

Egan B & Zierath JR (2013). Exercise metabolism and the molecular regulation of skeletal muscle adaptation. *Cell Metab* **17**, 162-184. doi: 10.1016/j.cmet.2012.12.012.

Ehmsen JT, Kawaguchi R, Kaval D, Johnson AE, Nachun D, Coppola G, *et al*. (2021). GADD45A is a protective modifier of neurogenic skeletal muscle atrophy. *JCI Insight* **6**, 149381. doi: 10.1172/jci.insight.149381.

Eisenstein AB, Strack I & Steiner A (1974). Glucagon stimulation of hepatic gluconeogenesis in rats fed a high-protein, carbohydrate-free diet. *Metabolism* **23**, 15-23. doi: 10.1016/0026-0495(74)90099-7.

Eleveld-Trancikova D, Sanecka A, van Hout-Kuijer MA, Looman MW, Hendriks IA, Jansen BJ, *et al*. (2010). DC-STAMP interacts with ER-resident transcription factor LUMAN which becomes activated during DC maturation. *Mol Immunol* **47**, 1963-1973. doi: 10.1016/j.molimm.2010.04.019.

Eliasson B, Smith U, Mullen S, Cushman SW, Sherman AS & Yang J (2014). Amelioration of insulin resistance by rosiglitazone is associated with increased adipose cell size in obese type 2 diabetic patients. *Adipocyte* **3**, 314-321. doi: 10.4161/adip.34425.

Elsea SH & Lucas RE (2002). The mousetrap: what we can learn when the mouse model does not mimic the human disease. *ILAR J* **43**, 66-79. doi: 10.1093/ilar.43.2.66.

Emmanuel N, Ragunathan S, Shan Q, Wang F, Giannakou A, Huser N, *et al*. (2017). Purine nucleotide availability regulates mTORC1 activity through the Rheb GTPase. *Cell Rep* **19**, 2665-2680. doi: 10.1016/j.celrep.2017.05.043.

Engelking LJ, Liang G, Hammer RE, Takaishi K, Kuriyama H,Evers BM, *et al*. (2005). Schoenheimer effect explained – feedback regulation of cholesterol synthesis in mice mediated by Insig proteins. *J Clin Invest* **115**, 2489-2498. doi: 10.1172/JCI25614.

Eriksson KF, Saltin B & Lindgärde F (1994). Increased skeletal muscle capillary density precedes diabetes development in men with impaired glucose tolerance. A 15-year follow-up. *Diabetes* **43**, 805-808. doi: 10.2337/diab.43.6.805.

Eura Y, Yanamoto H, Arai Y, Okuda T, Miyata T & Kokame K (2012). Derlin-1 deficiency is embryonic lethal, Derlin-3 deficiency appears normal, and Herp deficiency is intolerant to glucose load and ischemia in mice. *PLoS One* **7**, e34298. doi: 10.1371/journal.pone.0034298.

Fabbrini E, Yoshino J, Yoshino M, Magkos F, Tiemann Luecking C, Samovski D, *et al.* (2015). Metabolically normal obese people are protected from adverse effects following weight gain. *J Clin Invest* **125**, 787-795. doi: 10.1172/JCI78425.

Farhat R, Séron K, Ferlin J, Fénéant L, Belouzard S, Goueslain L, *et al*. (2016). Identification of class II ADP-ribosylation factors as cellular factors required for hepatitis C virus replication. *Cell Microbiol* **18**, 1121-1133. doi: 10.1111/cmi.12572.

Farooq R, Bhat MH, Majid S & Mir MM (2021). Association between T2DM and the lowering of testosterone levels among Kashmiri males. *Arch Endocrinol Metab* **64**, 528-532. doi: 10.20945/2359-3997000000288.

Fazeli PK, Zhang Y, O'Keefe J, Pesaresi T, Lun M, Lawney B & Steinhauser ML (2020). Prolonged fasting drives a program of metabolic inflammation in human adipose tissue. *Mol Metab* **42**, 101082. doi: 10.1016/j.molmet.2020.101082.

Feng S, Liu N, Chen X, Liu Y & An J (2020). Long non-coding RNA NEAT1/miR-338-3p axis impedes the progression of acute myeloid leukemia via regulating CREBRF. *Cancer Cell Int* **20**, 112. doi: 10.1186/s12935-020-01182-2.

Fernandes-da-Silva A, Miranda CS, Santana-Oliveira DA, Oliveira-Cordeiro B, Rangel-Azevedo C, Silva-Veiga FM, *et al*. (2021). Endoplasmic reticulum stress as the basis of obesity and metabolic diseases: focus on adipose tissue, liver, and pancreas. *Eur J Nutr* **60**, 2949-2960. doi: 10.1007/s00394-021-02542-y.

Ferron M, McKee MD, Levine RL, Ducy P & Karsenty G (2012). Intermittent injections of osteocalcin improve glucose metabolism and prevent type 2 diabetes in mice. *Bone* **50**, 568-575. doi: 10.1016/j.bone.2011.04.017.

Figueiredo VC, Markworth JF & Cameron-Smith D (2017). Considerations on mTOR regulation at serine 2448: implications for muscle metabolism studies. *Cell Mol Life Sci* **74**, 2537-2545. doi: 10.1007/s00018-017-2481-5.

Findlay GM, Yan L, Procter J, Mieulet V & Lamb RF (2007). A MAP4 kinase related to Ste20 is a nutrient-sensitive regulator of mTOR signalling. *Biochem J* **403**, 13-20. doi: 10.1042/BJ20061881.

Fingeret M, Marques-Vidal P & Vollenweider P (2018). Incidence of type 2 diabetes, hypertension, and dyslipidemia in metabolically healthy obese and non-obese. *Nutr Metab Cardiovasc Dis* **28**, 1036-1044. doi: 10.1016/j.numecd.2018.06.011.

Finucane MM, Stevens GA, Cowan MJ, Danaei G, Lin JK, Paciorek CJ, *et al*. (2011). National, regional, and global trends in body-mass index since 1980: systematic analysis of health examination surveys and epidemiological studies with 960 country-years and 9.1 million participants. *Lancet* **377**, 557-567. doi: 10.1016/S0140-6736(10)62037-5.

Fisher E, Schulze MB, Stefan N, Häring HU, Döring F, Joost HG, *et al*. (2012). Association of the *FTO* rs9939609 single nucleotide polymorphism with C-reactive protein levels. *Obesity (Silver Spring)* **17**(2), 330-334. doi: 10.1038/oby.2008.465.

Fokin A, Minderis P, Venckunas T, Lionikas A, Kvedaras M & Ratkevicius A (2019). Myostatin dysfunction does not protect from fasting-induced loss of muscle mass in mice. *J Musculoskelet Neuronal Interact* **19**, 342-353.

Fonseca V (2003). Effect of thiazolidinediones on body weight in patients with diabetes mellitus. *Am J Med* **115**, 42S-48S. doi: 10.1016/j.amjmed.2003.09.005.

Foretz M, Pacot C, Dugail I, Lemarchand P, Guichard C, Le Lièpvre X, *et al*. (1999). ADD1/SREBP-1c is required in the activation of hepatic lipogenic gene expression by glucose. *Mol Cell Biol* **19**, 3760-3768. doi: 10.1128/MCB.19.5.3760.

Formentini L, Ryan AJ, Gálvez-Santisteban M, Carter L, Taub P, Lapek JD Jr, *et al*. (2017). Mitochondrial H+-ATP synthase in human skeletal muscle: contribution to dyslipidaemia and insulin resistance. *Diabetologia* **60**, 2052-2065. doi: 10.1007/s00125-017-4379-z.

Frahm KA, Williams AA, Wood AN, Ewing MC, Mattila PE, Chuan BW, *et al*. (2020). Loss of CREBRF reduces anxiety-like behaviours and circulating glucocorticoids in male and female mice. *Endocrinology* **161**, bqaa163. doi: 10.1210/endocr/bqaa163.

Francisco AB, Singh R, Li S, Vani AK, Yang L, Munroe RJ, *et al*. (2010). Deficiency of suppressor enhancer Lin12 1 like (SEL1L) in mice leads to systemic endoplasmic reticulum stress and embryonic lethality. *J Biol Chem* **285**, 13694-13703. doi: 10.1074/jbc.M109.085340.

Francisco AB, Singh R, Sha H, Yan X, Qi L, Lei X, *et al*. (2011). Haploid insufficiency of suppressor enhancer Lin12 1-like (SEL1L) protein predisposes mice to high fat diet-induced hyperglycaemia. *J Biol Chem* **286**, 22275-22282. doi: 10.1074/jbc.M111.239418.

Frayling TM, Timpson NJ, Weedon MN, Zeggini E, Freathy RM, Lindgren CM, *et al*. (2007). A common variant in the *FTO* gene is associated with body mass index and predisposes to childhood and adult obesity. *Science* **316**(5826), 889-894. doi: 10.1126/science.1141634.

Freathy RM, Timpson NJ, Lawlor DA, Pouta A, Ben-Shlomo Y, Ruokonen A, *et al*. (2008). Common variation in the *FTO* gene alters diabetes-related metabolic

traits to the extent expected, given its effect on BMI. *Diabetes* **57**(5), 1419-1426. doi: 10.2337/db07-1466.

Friedlaender JS, Friedlaender FR, Reed FA, Kidd KK, Kidd JR, Chambers GK, *et al*. (2008). The genetic structure of Pacific Islanders. *PLOS Genetics* **4**, e19. doi: 10.1371/journal.pgen.0040019.

Fujita Y, Makishima M & Bhawal UK (2016). Differentiated embryo chondrocyte 1 (DEC1) is a novel negative regulator of hepatic fibroblast growth factor 21 (FGF21) in aging mice. *Biochem Biophys Res Commun* **469**, 477-482. doi: 10.1016/j.bbrc.2015.12.045.

Fuller SE, Huang T-Y, Simon J, Batdorf HM, Essajee NM, Scott MC, *et al*. (2019). Low-intensity exercise induces acute shifts in liver and skeletal muscle substrate metabolism but not chronic adaptations in tissue oxidative capacity. *J Appl Physiol (1985)* **127**, 143-156. doi: 10.1152/japplphysiol.00820.2018.

Fun XH & Thibault G (2020). Lipid bilayer stress and proteotoxic stress-induced unfolded protein response deploy divergent transcriptional and non-transcriptional programmes. *Biochim Biophys Acta Mol Cell Biol Lipids* **1865**, 158449. doi: 10.1016/j.bbalip.2019.04.009.

Furusawa T, Naka I, Yamauchi T, Natsuhara K, Kimura R, Nakazawa M, *et al*. (2011). The serum leptin level and body mass index in Melanesian and Micronesian Solomon Islanders: focus on genetic factors and urbanisation. *Am J Hum Biol* **23**, 435-444. doi: 10.1002/ajhb.21124.

Galber C, Carissimi S, Baracca A & Giorgio V (2021). The ATP synthase deficiency in human diseases. *Life (Basel)* **11**, 325. doi: 10.3390/life11040325.

Galicia-Garcia U, Benito-Vicente A, Jebari S, Larrea-Sebal A, Siddiqi H, Uribe KB, *et al*. (2020). Pathophysiology of type 2 diabetes mellitus. *Int J Mol Sci* **21**, 6275. doi: 10.3390/ijms21176275.

Galsgaard KD (2020). The vicious circle of hepatic glucagon resistance in non-alcoholic fatty liver disease. *J Clin Med* **9**, 4049. doi: 10.3390/jcm9124049.

Ganda OP (2000). Lipoatrophy, lipodystrophy, and insulin resistance. *Ann Intern Med* **133**, 304-306. doi: 10.7326/0003-4819-133-4-200008150-00017.

Garduño-Espinosa J, Ávila-Montiel D, Quezada-García AG, Merelo-Arias CA, Torres-Rodríguez V & Muñoz-Hernández O (2019). Obesity and thrifty genotype: biological and social determinism versus free will. *Bol Med Hosp Infant Mex* **76**, 106-112. doi: 10.24875/BMHIM.19000159.

Gavrilova O, Marcus-Samuels B, Graham D, Kim JK, Shulman GI, Castle AL, *et al*. (2000). Surgical implantation of adipose tissue reverses diabetes in lipoatrophic mice. *J Clin Invest* **105**, 271-278. doi: 10.1172/JCI7901.

Geer EB & Shen W (2009). Gender differences in insulin resistance, body composition, and energy balance. *Gend Med* **6**, 60-75. doi: 10.1016/j.genm.2009.02.002.

Gelling RW, Du XQ, Dichmann DS, Romer J, Huang H, Cui L, *et al*. (2003). Lower blood glucose, hyperglucagonemia, and pancreatic alpha cell hyperplasia in glucagon receptor knockout mice. *Proc Natl Acad Sci U S A* **100**, 1438-1443. doi: 10.1073/pnas.0237106100.

Gelling RW, Vuguin PM, Du XQ, Cui L, Rømer J, Pederson RA, *et al*. (2009). Pancreatic beta-cell overexpression of the glucagon receptor gene results in enhanced beta-cell function and mass. *Am J Physiol Endocrinol Metab* **297**, E695-E707. doi: 10.1152/ajpendo.00082.2009.

Genders AJ, Holloway GP & Bishop DJ (2020). Are alterations in skeletal muscle mitochondria a cause or consequence of insulin resistance? *Int J Mol Sci* **21**, 6948. doi: 10.3390/ijms21186948.

Genuth NR & Barna M (2018). The discovery of ribosome heterogeneity and its implications for gene regulation and organismal life. *Mol Cell* **71**, 364-374. doi: 10.1016/j.molcel.2018.07.018.

Gesta S, Bluher M, Yamamoto Y, Norris AW, Berndt J, Kralisch S, *et al*. (2006). Evidence for a role of developmental genes in the origin of obesity and body fat distribution. *Proc Natl Acad Sci USA* **103**, 6676-6681. doi: 10.1073/pnas.0601752103.

Ghachem A, Lagacé J-C, Brochu M & Dionne IJ (2019). Fat-free mass and glucose homeostasis: is greater fat-free mass an independent predictor of insulin resistance? *Aging Clin Exp Res* **31**, 447-454. doi: 10.1007/s40520-018-0993-y.

Ghanemi A, Yoshioka M & St-Amand J (2021). Obesity as a neuroendocrine reprogramming. *Medicina (Kaunas)* **57**, 66. doi: 10.3390/medicina57010066.

Gilad VH, Rabey JM, Kimiagar Y & Gilad GM (2001). The polyamine stress response: tissue-, endocrine-, and developmental-dependent regulation. *Biochem Pharmacol* **61**, 207-213. doi: 10.1016/s0006-2952(00)00517-7.

Gilson H, Schakman O, Combaret L, Lause P, Grobet L, Attaix D, *et al*. (2007). Myostatin gene deletion prevents glucocorticoid-induced muscle atrophy. *Endocrinology* **148**, 452-460. doi: 10.1210/en.2006-0539.

Goodman CA, Hornberger TA & Robling AG (2015). Bone and skeletal muscle: key players in mechanotransduction and potential overlapping mechanisms. *Bone* **80**, 24-36. doi: 10.1016/j.bone.2015.04.014.

Goodpaster BH, Thaete FL, Simoneau JA & Kelley DE (1997). Subcutaneous abdominal fat and thigh muscle composition predict insulin sensitivity independently of visceral fat. *Diabetes* **46**, 1579-1585. doi: 10.2337/diacare.46.10.1579.

Goossens GH (2017). The metabolic phenotype in obesity: fat mass, body fat distribution, and adipose tissue function. *Obes Facts* **10**(3), 207-215. doi: 10.1159/000471488.

Gosling AL, Buckley HR, Matisoo-Smith E & Merriman TR (2015). Pacific populations, metabolic disease and 'Just-So Stories': a critique of the 'thrifty genotype' hypothesis in Oceania. *Ann Hum Genet* **79**, 470-480. doi: 10.1111/ahg.12132.

Gotoh T, Chowdhury S, Takiguchi M & Mori M (1997). The glucocorticoid-responsive gene cascade. Activation of the rat arginase gene through induction of C/EBPbeta. *J Biol Chem* **272**, 3694-3698. doi: 10.1074/jbc.272.6.3694.

Gouspillou G, Godin R, Piquereau J, Picard M, Mofarrahi M, Mathew J, *et al*. (2018). Protective role of Parkin in skeletal muscle contractile and mitochondrial function. *J Physiol* **596**, 2565-2579. doi: 10.1113/JP275604.

Grade CVC, Mantovani CS & Alvares LE (2019). Myostatin gene promoter: structure, conservation and importance as a target for muscle modulation. *J Anim Sci Biotechnol* **10**, 32. doi: 10.1186/s40104-019-0338-5.

Grant AM, Gordon FK, Ferguson EL, Williams SM, Henry TE, Toafa VM, *et al.* (2005). Do young New Zealand Pacific Island and European children differ in bone size or bone mineral? *Calcif Tissue Int* **76**, 397-403. doi: 10.1007/s00223-004-0156-3.

Gray LJ, Sokolowski MB & Simpson SJ (2021). Drosophila as a useful model for understanding the evolutionary physiology of obesity resistance and metabolic thrift. *Fly (Austin)* **15**, 47-59. doi: 10.1080/19336934.2021.1896960.

Grimaldi B, Bellet MM, Katada S, Astarita G, Hirayama J, Amin RH, *et al*. (2010). PER2 controls lipid metabolism by direct regulation of PPARγ. *Cell Metab* **12**, 509-520. doi: 10.1016/j.cmet.2010.10.005.

Gu Y, Lee W & Shen J (2014). Site-2 protease responds to oxidative stress and regulates oxidative injury in mammalian cells. *Sci Rep* **4**, 6268. doi: 10.1038/srep06268.

Guerrero N, Bunout D, Hirsch S, Barrera G, Leiva L, Henríquez S, *et al*. (2016). Premature loss of muscle mass and function in type 2 diabetes. *Diabetes Res Clin Pract* **117**, 32-38. doi: 10.1016/j.diabres.2016.04.011.

Guglielmi V & Sbraccia P (2018). Obesity phenotypes: depot-differences in adipose tissue and their clinical implications. *Eat Weight Disord* **23**, 3-14. doi: 10.1007/s40519-017-0467-9.

Gulfo J, Castel R, Ledda A, Romero MDM, Esteve M & Grasa M (2019). Corticosteroid-binding globulin is expressed in the adrenal gland and its absence impairs corticosterone synthesis and secretion in a sex-dependent manner. *Sci Rep* **9**, 14018. doi: 10.1038/s41598-019-50355-1.

Guo L, Lee AA, Rizvi TA, Ratner N & Kirschner LS (2013). The protein kinase A regulatory subunit R1A (Prkar1a) plays critical roles in peripheral nerve development. *J Neurosci* **33**, 17967-17975. doi: 10.1523/JNEUROSCI.0766-13.2013.

Guo S, Dunn SL & White MF (2006). The reciprocal stability of FOXO1 and IRS2 creates a regulatory circuit that controls insulin signalling. *Mol Endocrinol* **20**, 3389-3399. doi: 10.1210/me.2006-0092.

Guridi M, Kupr B, Romanino K, Lin S, Falcetta D, Tintignac L, *et al*. (2016). Alterations to mTORC1 signalling in the skeletal muscle differentially affect whole-body metabolism. *Skelet Muscle* **6**, 13. doi: 10.1186/s13395-016-0084-8.

Haas JT, Miao J, Chanda D, Wang Y, Zhao E, Haas ME, *et al*. (2012). Hepatic insulin signalling is required for obesity-dependent expression of SREBP-1c mRNA but not for feeding-dependent expression. *Cell Metab* **15**, 873-884. doi: 10.1016/j.cmet.2012.05.002.

Hacker B, Schultheiß C, Döring M & Kurzik-Dumke U (2018). Molecular partners of hNOT/ALG3, the human counterpart of the Drosophila NOT and yeast ALG3 gene, suggest its involvement in distinct cellular processes relevant to congenital disorders of glycosylation, cancer, neurodegeneration and a variety of further pathologies. *Hum Mol Genet* **27**, 1858-1878. doi: 10.1093/hmg/ddy087.

Hagiwara A, Cornu M, Cybulski N, Polak P, Betz C, Trapani F, *et al*. (2012). Hepatic mTORC2 activates glycolysis and lipogenesis through Akt, glucokinase, and SREBP1c. *Cell Metab* **15**, 725-738. doi: 10.1016/j.cmet.2012.03.015.

Hales CN & Barker DJ (2001). The thrifty phenotype hypothesis. *Br Med Bull* **60**, 5-20. doi: 10.1093/bmb/60.1.5.

Ham AS, Chojnowska K, Tintignac LA, Lin S, Schmidt A, Ham DJ, *et al*. (2020a). mTORC1 signalling is not essential for the maintenance of muscle mass and function in adult sedentary mice. *J Cachexia Sarcopenia Muscle* **11**, 259-273. doi: 10.1002/jcsm.12505.

Ham DJ, Börsch A, Lin S, Thürkauf M, Weihrauch M, Reinhard JR, *et al*. (2020b). The neuromuscular junction is a focal point of mTORC1 signalling in sarcopenia. *Nat Commun* **11**, 4510. doi: 10.1038/s41467-020-18140-1.

Hamel FG, Bennett RG, Upward JL & Duckworth WC (2001). Insulin inhibits peroxisomal fatty acid oxidation in isolated rat hepatocytes. *Endocrinology* **142**, 2702-2706. doi: 10.1210/endo.142.6.8178.

Hamrick MW, Samaddar T, Pennington C & McCormick J (2006). Increased muscle mass with myostatin deficiency improves gains in bone strength with exercise. *J Bone Miner Res* **21**, 477-483. doi: 10.1359/JBMR.051203.

Han C, Wei S, He F, Liu D, Wan H, Liu H, *et al*. (2015). The regulation of lipid deposition by insulin in goose liver cells is mediated by the PI3K-AKT-mTOR signalling pathway. *PLoS One* **10**, e0098759. doi: 10.1371/journal.pone.0098759.

Han C, Wei S, Song Q, He F, Xiong X, Wan H, *et al*. (2016). Insulin stimulates goose liver cell growth by activating PI3K-AKT-mTOR signal pathway. *Cell Physiol Biochem* **38**, 558-570. doi: 10.1159/000438650.

Han F, Zhong C, Li W, Wang R, Zhang C, Yang X, *et al*. (2020). *hsa_circ_0001947* suppresses acute myeloid leukemia progression via targeting *hsa-miR-329-5p/CREBRF* axis. *Epigenomics* **12**, 935-953. doi: 10.2217/epi-2019-0352.

Han J, Zhang L, Zhang J, Jiang Q, Tong D, Wang X, *et al*. (2018). CREBRF promotes the proliferation of human gastric cancer cells via the AKT signalling pathway. *Cell Mol Biol (Noisy-le-grand)* **64**, 40-45.

Han TS, Al-Gindan YY, Govan L, Hankey CR & Lean MEJ (2019). Associations of BMI, waist circumference, body fat, and skeletal muscle with type 2 diabetes in adults. *Acta Diabetologia* **56**, 947-954. doi: 10.1007/s00592-019-01328-3.

Hanson RL, Safabakhsh S, Curtis JM, Hsueh WC, Jones LI, Aflague TF, *et al*. (2019). Association of CREBRF variants with obesity and diabetes in Pacific Islanders from Guam and Saipan. *Diabetologia* **62**, 1647-1652. doi: 10.1007/s00125-019-4932-z.

Haramizu S, Nagasawa A, Ota N, Hase T, Tokimitsu I & Murase T (2009). Different contribution of muscle and liver lipid metabolism to endurance capacity and obesity susceptibility of mice. *J Appl Physiol (1985)* **106**, 871-879. doi: 10.1152/japplphysiol.90804.2008.

Hardy CM, Burke MK, Everett LJ, Han MV, Lantz KM & Gibbs AG (2018). Genome-wide analysis of starvation-selected Drosophila melanogaster-A genetic model of obesity. *Mol Biol Evol* **35**, 50-65. doi: 10.1093/molbev/msx254.

Hargreaves M & Spriet LL (2020). Skeletal muscle energy metabolism during exercise. *Nat Metab* **2**, 817-828. doi: 10.1038/s42255-020-0251-4.

Harrell CS, Gillespie CF & Neigh GN (2016). Energetic stress: the reciprocal relationship between energy availability and the stress response. *Physiol Behav* **166**, 43-55. doi: 10.1016/j.physbeh.2015.10.009.

Harvey NR, Voisin S, Lea RA, Yan X, Benton MC, Papadimitriou ID, *et al*. (2020). Investigating the influence of mtDNA and nuclear encoded mitochondrial variants on high intensity interval training outcomes. *Sci Rep* **10**, 11089. doi: 10.1038/s41598-020-67870-1.

Hashimoto T, Cook WS, Qi C, Yeldandi AV, Reddy JK & Rao MS (2000). Defect in peroxisome proliferator-activated receptor alpha-inducible fatty acid oxidation determines the severity of hepatic steatosis in response to fasting. *J Biol Chem* **275**, 28918-28928. doi: 10.1074/jbc.M910350199.

Hasmatali JCD, De Guzman J, Zhai R, Yang L, McLean NA, Hutchinson C, *et al*. (2019). Axotomy induces phasic alterations in Luman/CREB3 expression and nuclear localisation in injured and contralateral uninjured sensory neurons: correlation with intrinsic axon growth capacity. *J Neuropathol Exp Neurol* **78**, 348-364. doi: 10.1093/jnen/nlz008.

Haupt A, Thamer C, Staiger H, Tschritter O, Kirchhoff K, Machicao F, *et al*. (2009). Variation in the FTO gene influences food intake but not energy expenditure. *Exp Clin Endocrinol Diabetes* **117**(4), 194-197. doi: 10.1055/s-0028-1087176.

Hawley NL & McGarvey ST (2015). Obesity and diabetes in Pacific Islanders: the current burden and the need for urgent action. *Curr Diab Rep* **15**, 29. doi: 10.1007/s11892-015-0594-5.

Hawley NL, Duckham RL, Carlson JC, Naseri T, Reupena MS, Lameko V, *et al*. (preprint). The association of *CREBRF* variant rs373863828 with body composition in adult Samoans. https://doi.org/10.1101/2021.02.11.21251582. [posted 12 Feb 2021]

Hayashi Y & Seino Y (2018). Regulation of amino acid metabolism and α cell proliferation by glucagon. *J Diabetes Investig* **9**, 464-472. doi: 10.1111/jdi.12797.

He D, Fu M, Miao S, Hotta K & Chandak GR (2014). *FTO* gene variant and risk of hypertension: a meta-analysis of 57,464 hypertensive cases and 41,256 controls. *Metabolism* **63**(5), 633-639. doi: 10.1016/j.metabol.2014.02.008.

Hearris MA, Hammond KM, Fell JM & Morton JP (2018). Regulation of muscle glycogen metabolism during exercise: implications for endurance performance and training adaptations. *Nutrients* **10**, 298. doi: 10.3390/nu10030298.

Henkel AS, LeCuyer B, Olivares S & Green RM (2017). Endoplasmic reticulum stress regulates hepatic bile acid metabolism in mice. *Cell Mol Gastroenterol Hepatol* **3**, 261-271. doi: 10.1016/j.jcmgh.2016.11.006.

Henry Y, Overgaard J & Colinet H (2020). Dietary nutrient balance shapes phenotypic traits of Drosophila melanogaster in interaction with gut microbiota. *Comp Biochem Physiol A Mol Integr Physiol* **241**, 110626. doi: 10.1016/j.cbpa.2019.110626.

Hildebrandt AL & Neufer PD (2000). Exercise attenuates the fasting-induced transcriptional activation of metabolic genes in skeletal muscle. *Am J Physiol Endocrinol Metab* **278**, E1078-E1086. doi: 10.1152/ajpendo.2000.278.6.E1078.

Hildebrandt AL, Pilegaard H & Neufer PD (2003). Differential transcriptional activation of select metabolic genes in response to variations in exercise intensity and duration. *Am J Physiol Endocrinol Metab* **285**, E1021-E1027. doi: 10.1152/ajpendo.00234.2003.

Hill JO, Wyatt HR & Peters JC (2012). Energy balance and obesity. *Circulation* **126**, 126-132. doi: 10.1161/CIRCULATIONAHA.111.087213.

Hodge AM, Dowse GK, Toelupe P, Collins VR, Imo T & Zimmet PZ (1994). Dramatic increase in the prevalence of obesity in western Samoa over the 13 year period 1978-1991. *Int J Obes Relat Metab Disord* **18**, 419-428.

Hoehn LK, Hohnen-Behrens C, Cederberg A, Wu LE, Turner N, Yuasa T, *et al*. (2008). IRS1-independent defects define major nodes of insulin resistance. *Cell Metab* **7**, 421-433. doi: 10.1016/j.cmet.2008.04.005.

Holloszy JO (2009). Skeletal muscle "mitochondrial deficiency" does not mediate insulin resistance. *Am J Clin Nutr* **89**, 463S-466S. doi: 10.3945/ajcn.2008.26717C.

Holloway KL, De Abreu LLF, Hans D, Kotowicz MA, Sajjad MA, Hyde NK, *et al*. (2018). Trabecular bone score in men and women with impaired fasting glucose and diabetes. *Calcif Tissue Int* **102**, 32-40. doi: 10.1007/s00223-017-0330-z.

Hollstein T, Basolo A, Ando T, Votruba SB, Walter M, Krakoff J, *et al*. (2020). Recharacterising the metabolic state of energy balance in thrifty and spendthrift phenotypes. *J Clin Endocrinol Metab* **105**, 1375-1392. doi: 10.1210/clinem/dgaa098.

Holzenberger M, Dupont J, Ducos B, Leneuve P, Géloën A, Even PC, *et al*. (2003). IGF-1 receptor regulates lifespan and resistance to oxidative stress in mice. *Nature* **421**, 182-187. doi: 10.1038/nature01298.

Ho-Pham LT & Nguyen TV (2019). Association between trabecular bone score and type 2 diabetes: a quantitative update of evidence. *Osteoporos Int* **30**, 2079-2085. doi: 10.1007/s00198-019-05053-z.

Horton TJ, Drougas H, Brachey A, Reed GW, Peters JC & Hill JO (1995). Fat and carbohydrate overfeeding in humans: different effects on energy storage. *Am J Clin Nutr* **62**, 19-29. doi: 10.1093/ajcn/62.1.19.

Horton TJ, Pagliasotti MJ, Hobbs K & Hill JO (1998). Fuel metabolism in men and women during and after long-duration exercise. *J Apply Physiol* **85**, 1823-1832. doi: 10.1152/jappl.1998.85.5.1823.

Hou Y, Yao K, Yin Y & Wu G (2016). Endogenous synthesis of amino acids limits growth, lactation, and reproduction in animals. *Adv Nutr* **7**, 331-342. doi: 10.3945/an.115.010850.

Housley MP, Udeshi ND, Rodgers JT, Shabanowitz J, Puigserver P, Hunt DF, *et al*. (2009). A PGC-1alpha-O-GlcNAc transferase complex regulates FoxO transcription factor activity in response to glucose. *J Biol Chem* **284**, 5148-5157. doi: 10.1074/jbc.M808890200.

Howley BV, Link LA, Grelet S, El-Sabban M & Howe PH (2018). A CREB3-regulated ER-Golgi trafficking signature promotes metastatic progression in breast cancer. *Oncogene* **37**, 1308-1325. doi: 10.1038/s41388-017-0023-0.

Hoxhaj G, Hughes-Hallett J, Timson RC, Ilagan E, Yuan M, Asara JM, *et al*. (2017). The mTORC1 signalling network senses changes in cellular purine nucleotide levels. *Cell Rep* **21**, 1331-1346. doi: 10.1016/j.celrep.2017.10.029.

Hu Y, Chu L, Liu J, Yu L, Song SB, Yang H, *et al*. (2019). Knockdown of *CREB3* activates endoplasmic reticulum stress and induces apoptosis in glioblastoma. *Aging (Albany NY)* **11**, 8156-8168. doi: 10.18632/aging.102310.

Huang J & Manning BD (2009). A complex interplay between Akt, TSC2 and the two mTOR complexes. *Biochem Soc Trans* **37**, 217-222. doi: 10.1042/BST0370217.

Hubacek JA, Bohuslavova R, Kuthanova L, Kubinova R, Peasey A, Pikhart H, *et al*. (2008). The *FTO* gene and obesity in a large Eastern European population sample: the HAPIEE study. *Obesity* **16**(12), 2764-2766. doi: 10.1038/oby.2008.421.

Hudjashov G, Endicott P, Post H, Nagle N, Ho SYW, Lawson DJ, *et al*. (2018). Investigating the origins of eastern Polynesians using genome-wide data from the Leeward Society Isles. *Sci Rep* **8**, 1823. doi: 10.1038/s41598-018-20026-8.

Hummel KP, Dickie MM & Coleman DL (1966). Diabetes, a new mutation in the mouse. *Science* **153**, 1127-1128. doi: 10.1126/science.153.3740.1127.

Humphrey SJ, Azimifar SB & Mann M (2015). High-throughput phosphoproteomics reveals in vivo insulin signalling dynamics. *Nat Biotechnol* **33**(9), 990-995. doi: 10.1038/nbt.3327.

Hwang J & Qi L (2018). Quality control in the endoplasmic reticulum: crosstalk between ERAD and UPR pathways. *Trends Biochem Sci* **43**, 593-605. doi: 10.1016/j.tibs.2018.06.005.

Hwang S-Y, Sarna LK, Siow YL & O K (2013). High-fat diet stimulates hepatic cystathionine β-synthase and cystathionine γ-lyase expression. *Can J Physiol Pharmacol* **91**, 913-919. doi: 10.1139/cjpp-2013-0106.

Hyatt H, Deminice R, Yoshihara T & Powers SK (2019). Mitochondrial dysfunction induces muscle atrophy during prolonged inactivity: a review of the causes and effects. *Arch Biochem Biophys* **662**, 49-60. doi: 10.1016/j.abb.2018.11.005.

Hydes T, Alam U & Cuthbertson DJ (2021). The impact of macronutrient intake on non-alcoholic fatty liver disease (NAFLD): too much fat, too much carbohydrate, or just too many calories? *Front Nutr* **8**, 640557. doi: 10.3389/fnut.2021.640557.

Iaea DB, Spahr ZR, Singh RK, Chan RB, Zhou B, Bareja R, *et al*. (2020). Stable reduction of STARD4 alters cholesterol regulation and lipid homeostasis. *Biochim Biophys Acta Mol Cell Biol Lipids* **1865**, 158609. doi: 10.1016/j.bbalip.2020.158609.

Ibebunjo C, Chick JM, Kendall T, Eash JK, Li C, Zhang Y, *et al*. (2013). Genomic and proteomic profiling reveals reduced mitochondrial function and disruption of the neuromuscular junction driving sarcopenia. *Mol Cell Biol* **33**, 194-212. doi: 10.1128/MCB.01036-12.

Ibrahim M, Wasselin T, Challet E, Van Dorsselaer A, Le Maho Y, Raclot T, *et al*. (2020). Transcriptional changes involved in atrophying muscles during prolonged fasting in rats. *Int J Mol Sci* **21**, 5984. doi: 10.3390/ijms21175984.

Ijzerman TH, Schaper NC, Melai T, Meijer K, Willems PJB & Savelberg HHCM (2012). Lower extremity muscle strength is reduced in people with type 2 diabetes, with and without polyneuropathy, and is associated with impaired mobility and reduced quality of life. *Diabetes Res Clin Pract* **95**, 345-351. doi: 10.1016/j.diabres.2011.10.026.

Ikeda R, Tsuchiya Y, Koike N, Umemura Y, Inokawa H, Ono R, *et al*. (2019). REV-ERBα and REV-ERBβ function as key factors regulating mammalian circadian output. *Sci Rep* **9**, 10171. doi: 10.1038/s41598-019-46656-0.

Ingalls AM, Dickie MM & Snell GD (1950). Obese, a new mutation in the house mouse. *J Hered* **41**, 317-318. doi: 10.1093/oxfordjournals.jhered.a106073.

Intihar TA, Martinez EA & Gomez-Pastor R (2019). Mitochondrial dysfunction in Huntington's disease; interplay between HSF1, p53 and PGC-1α transcription factors. *Front Cell Neurosci* **13**, 103. doi: 10.3389/fncel.2019.00103.

Iozzo P, Geisler F, Oikonen V, Mäki M, Takala T, Solin O, *et al*. (2003). Insulin stimulates liver glucose uptake in humans: an 18F-FDG PET study. *J Nucl Med* **44**, 682-689.

Iso T, Haruyama H, Sunaga H, Matsui H, Matsui M, Tanaka R, *et al*. (2018). CD36 is indispensable for nutrient homeostasis and endurance exercise capacity during prolonged fasting. *Physiol Rep* **6**, e13884. doi: 10.14814/phy2.13884.

Iso T, Haruyama H, Sunaga H, Matsui M, Matsui H, Tanaka R, *et al*. (2019). Exercise endurance capacity is markedly reduced due to impaired energy homeostasis during prolonged fasting in FABP4/5 deficient mice. *BMC Physiol* **19**, 1. doi: 10.1186/s12899-019-0038-6.

Isshiki M, Naka I, Watanabe Y, Nishida N, Kimura R, Furusawa T, *et al*. (2020). Admixture and natural selection shaped genomes of an Austronesian-speaking population in the Solomon Islands. *Sci Rep* **10**, 6872. doi: 10.1038/s41598-020-62866-3.

Issiki M, Naka I, Kimura R, Furusawa T, Natsuhara K, Yamauchi T, *et al*. (2018). Mitochondrial DNA variations in Austronesian-speaking populations living in the New Georgia Islands, the Western Province of the Solomon Islands. *J Hum Genet* **63**, 101-104. doi: 10.1038/s10038-017-0372-0.

Jacinto E, Loewith R, Schmidt A, Lin S, Rüegg MA, Hall A, *et al*. (2004). Mammalian TOR complex 2 controls the actin cytoskeleton and is rapamycin insensitive. *Nat Cell Biol* **6**, 1122-1128. doi: 10.1038/ncb1183.

Jackson AS, Stanforth PR, Gagnon J, Rankinen T, Leon AS, Rao DC, *et al*. (2002). The effect of sex, age and race on estimating percentage body fat from body mass index: the Heritage Family Study. *Int J Obes Relat Metab Disord* **26**, 789-796. doi: 10.1038/sj.ijo.0802006.

Jacobs RL, House JD, Brosnan ME & Brosnan JT (1998). Effects of streptozotocin-induced diabetes and of insulin treatment on homocysteine metabolism in the rat. *Diabetes* **47**, 1967-1970. doi: 10.2337/diabetes.47.12.1967.

Jafari M, Seese RR, Babayan AH, Gall CM & Lauterborn JC (2012). Glucocorticoid receptors are localised to dendritic spines and influence local actin signalling. *Mol Neurobiol* **46**, 304-315. doi: 10.1007/s12035-012-8288-3.

Jaiswal N, Gavin MG, Quinn WJ 3rd, Luongo TS, Gelfer RG, Baur JA, *et al*. (2019). The role of skeletal muscle Akt in the regulation of muscle mass and glucose homeostasis. *Mol Metab* **28**, 1-13. doi: 10.1016/j.molmet.2019.08.001.

Jakob A & Diem S (1974). Activation of glycogenolysis in perfused rat livers by glucagon and metabolic inhibitors. *Biochim Biophys Acta* **362**, 469-479. doi: 10.1016/0304-4165(74)90142-1.

James DE, Stöckli J & Birnbaum MJ (2021). The aetiology and molecular landscape of insulin resistance. *Nat Rev Mol Cell Biol* doi: 10.1038/s41580-021-00390-6.

Janah L, Kjeldsen S, Galsgaard KD, Winther-Sørensen M, Stojanovska E, Pedersen J, *et al*. (2019). Glucagon receptor signalling and glucagon resistance. *Int J Mol Sci* **20**, 3314. doi: 10.3390/ijms20133314.

Jang J, Park S, Kim Y, Jung J, Lee J, Chang Y, *et al*. (2021). Myostatin inhibition-induced increase in muscle mass and strength was amplified by resistance exercise training, and dietary essential amino acids improved muscle quality in mice. *Nutrients* **13**, 1508. doi: 10.3390/nu13051508.

Jang SW, Kim YS, Kim YR, Sung HJ & Ko J (2007a). Regulation of human LZIP expression by NF-kappaB and its involvement in monocyte cell migration induced by Lkn-1. *J Biol Chem* **282**, 11092-11100. doi: 10.1074/jbc.M607962200.

Jang SW, Kim YS, Lee YH & Ko J (2007b). Role of human LZIP in differential activation of the NF-kappaB pathway that is induced by CCR1-dependent chemokines. *J Cell Physiol* **211**, 630-637. doi: 10.1002/jcp.20968.

Jang SY, Jang S-W & Ko J (2012). Regulation of ADP-ribosylation factor 4 expression by small leucine zipper protein and involvement in breast cancer cell migration. *Cancer Lett* **314**, 185-197. doi: 10.1016/j.canlet.2011.09.028.

Janssens S, Pulendran B & Lambrecht BN (2014). Emerging functions of the unfolded protein response in immunity. *Nat Immunol* **15**, 910-919. doi: 10.1038/ni.2991.

Jaspers RT, Zillikens MC, Friesema ECH, delli Paoli G, Bloch W, Uitterlinden AG, *et al*. (2017). Exercise, fasting, and mimetics: toward beneficial combinations? *FASEB J* **31**, 14-28. doi: 10.1096/fj.201600652R.

Javary J, Allain-Courtois N, Saucisse N, Costet P, Heraud C, Benhamed F, *et al*. (2018). Liver reptin/RUVBL2 controls glucose and lipid metabolism with opposite actions on mTORC1 and mTORC2 signalling. *Gut* **67**, 2192-2203. doi: 10.1136/gutjnl-2017-314208.

Jensen TL, Kiersgaard MK, Sørensen DB & Mikkelsen LF (2013). Fasting of mice: a review. *Lab Anim* **47**, 225-240. doi: 10.1177/0023677213501659.

Ji H, Wang H, Ji Q, Luo X, Wang J, Chai Z, *et al*. (2020). Differential expression profile of microRNA in yak skeletal muscle and adipose tissue during development. *Genes Genomics* **42**, 1347-1359. doi: 10.1007/s13258-020-00988-8.

Ji Y, Yiorkas AM, Frau F, Mook-Kanamori D, Staiger H, Thomas EL, *et al*. (2019). Genome-wide and abdominal MRI data provide evidence that a genetically determined favourable adiposity phenotype is characterised by lower ectopic liver fat and lower risk of type 2 diabetes, heart disease, and hypertension. *Diabetes* **68**, 207-219. doi: 10.2337/db18-0708.

Jia W-H, Wang N-Q, Yin L, Chen X, Hou B-Y, Qiang G-F, *et al*. (2019). Effect of skeletal muscle phenotype and gender on fasting-induced myokine expression in mice. *Biochem Biophys Res Commun* **514**, 407-414. doi: 10.1016/j.bbrc.2019.04.155.

Jia X, Zhou H, Wu C, Wu Q, Ma S, Wei C, *et al*. (2017). The ubiquitin ligase RNF125 targets innate immune adaptor protein TRIM14 for ubiquitination and degradation. *J Immunol* **198**, 4652-4658. doi: 10.4049/jimmunol.1601322.

Jindrich K & Degnan BM (2016). The diversification of the basic leucine zipper family in eukaryotes correlates with the evolution of multicellularity. *BMC Evol Biol* **16**, 28. doi: 10.1186/s12862-016-0598-z.

Jo J, Gavrilova O, Pack S, Jou W, Mullen S, Sumner AE, *et al*. (2009). Hypertrophy and/or hyperplasia: dynamics of adipose tissue growth. *PLoS Comput Biol* **5**(3), e1000324. doi: 10.1371/journal.pcbi.1000324.

Johannsen DL, Tchoukalova Y, Tam CS, Covington JD, Xie W, Schwarz JM, *et al.* (2014). Effect of 8 weeks of overfeeding on ectopic fat deposition and insulin sensitivity: testing the "adipose tissue expandability" hypothesis. *Diabetes* **37**, 2789-2797. doi: 10.2337/dc14-0761.

Johnson RJ, Stenvinkel P, Martin SL, Jani A, Sanchez-Lozada LG, Hill JO, *et al*. (2013). Redefining metabolic syndrome as a fat storage condition based on studies of comparative physiology. *Obesity (Silver Spring)* **21**, 659-664. doi: 10.1002/oby.20026.

Johnson TA, Paakinaho V, Kim S, Hager GL & Presman DM (2021). Genome-wide binding potential and regulatory activity of the glucocorticoid receptor's monomeric and dimeric forms. *Nat Comm* **12**, 1987. doi: 10.1038/s41467-021-22234-9..

Joseph R, Poschmann J, Sukarieh R, Too PG, Julien SG, Xu F, *et al*. (2015). ACSL1 is associated with fetal programming of insulin sensitivity and cellular lipid content. *Mol Endocrinol* **29**, 909-920. doi: 10.1210/me.2015-1020.

Julien L-A, Carriere A, Moreau J & Roux PP (2010). mTORC1-activated S6K1 phosphorylates Rictor on threonine 1135 and regulates mTORC2 signalling. *Mol Cell Biol* **30**, 908-921. doi: 10.1128/MCB.00601-09.

Jump DB (2008). N-3 polyunsaturated fatty acid regulation of hepatic gene transcription. *Curr Opin Lipidol* **19**, 242-247. doi: 10.1097/MOL.0b013e3282ffaf6a.

Kalsotra A & Cooper TA (2011). Functional consequences of developmentally regulated alternative splicing. *Nat Rev Genet* **12**, 715-729. doi: 10.1038/nrg3052.

Kalvisa A, Siersbæk MS, Præstholm SM, Christensen LJL, Nielsen R, Stohr O, *et al*. (2018). Insulin signalling and reduced glucocorticoid receptor activity attenuate postprandial gene expression in liver. *PLoS Biol* **16**, e2006249. doi: 10.1371/journal.pbio.2006249.

Kamei Y, Miura S, Suzuki M, Kai Y, Mizukami J, Taniguchi T, *et al*. (2004). Skeletal muscle FOXO1 (FKHR) transgenic mice have less skeletal muscle mass, down-regulated type I (slow twitch/red muscle) fibre genes, and impaired glycaemic control. *J Biol Chem* **279**, 41114-41123. doi: 10.1074/jbc.M400674200.

Kanehisa M, Furumichi M, Tanabe M, Sato Y & Morishima K (2017). KEGG: new perspectives on genomes, pathways, diseases and drugs. *Nucleic Acids Res* **45**, D353-D361. doi: 10.1093/nar/gkw1092.

Kanemoto S, Kobayashi Y, Yamashita T, Miyamoto T, Cui M, Asada R, *et al*. (2015). Luman is involved in osteoclastogenesis through the regulation of DC-STAMP expression, stability and localisation. *J Cell Sci* **128**, 4353-4365. doi: 10.1242/jcs.176057.

Kang H, Kim YS & Ko J (2009). A novel isoform of human LZIP negatively regulates the transactivation of the glucocorticoid receptor. *Mol Endocrinol* **23**, 1746-1757. doi: 10.1210/me.2009-0009.

Kang M, Han SK, Kim S, Park S, Jo Y, Kang H, *et al*. (2020). Role of small leucine zipper protein in hepatic gluconeogenesis and metabolic disorder. *J Mol Cell Biol* **13**, 361-373. doi: 10.1093/jmcb/mjaa069.

Kang M, Kim J, An HT & Ko J (2017). Human leucine zipper protein promotes hepatic steatosis *via* induction of apolipoprotein A-IV. *FASEB* **31**, 2548-2561. doi: 10.1096/fj.201601227R.

Kanshana JS, Mattila PE, Ewing MC, Wood AN, Schoiswohl G, Meyer AC, *et al*. (2021). A murine model of the human CREBRF^{R457Q} obesity-risk variant does not influence energy or glucose homeostasis in response to nutritional stress. *PLoS One* **16**, e0251895. doi: 10.1371/journal.pone.0251895.

Karasik D & Kiel D (2008). Genetics of the musculoskeletal system: a pleiotropic approach. *J Bone Miner Res* **23**, 788-802. doi: 10.1359/jbmr.080218.

Karns R, Viali S, Tuitele J, Sun G, Cheng H, Weks DE, *et al*. (2012). Common variants in *FTO* are not significantly associated with obesity-related phenotypes among Samoans of Polynesia. *Ann Hum Genet* **76**(1), 17-24. doi: 10.1111/j.1469-1809.2011.00686.x.

Karpe F & Pinnick KE (2015). Biology of upper-body and lower-body adipose tissue - link to whole-body phenotypes. *Nat Rev Endocrinol* **11**, 90-100. doi: 10.1038/nrendo.2014.185.

Kawamoto R, Ninomiya D, Kasai Y, Kusunoki T, Ohtsuka N, Kumagi T, *et al*. (2016). Handgrip strength is associated with metabolic syndrome among middle-aged and elderly community-dwelling persons. *Clin Exp Hypertens* **38**, 245-251. doi: 10.3109/10641963.2015.1081232.

Kayser M, Brauer S, Cordaux R, Casto A, Lao O, Zhivotovsky LA, *et al*. (2006). Melanesian and Asian origins of Polynesians: mtDNA and Y chromosome

gradients across the Pacific. *Mol Biol Evol* **23**, 2234-2244. doi: 10.1093/molbev/msl093.

Kayser M, Choi Y, van Oven M, Mona S, Brauer S, Trent RJ, *et al*. (2008). The impact of the Austronesian expansion: evidence from mtDNA and Y chromosome diversity in the Admiralty Islands of Melanesia. *Mol Biol Evol* **25**, 1362-1374. doi: 10.1093/molbev/msn078.

Kazyken D, Magnuson B, Bodur C, Acosta-Jaquez HA, Zhang D, Tong X, *et al*. (2019). AMPK directly activates mTORC2 to promote cell survival during acute energetic stress. *Sci Signal* **12**, eaav3249. doi: 10.1126/scisignal.aav3249.

Kearney AL, Cooke KC, Norris DM, Zadoorian A, Krycer JR, Fazakerley DJ, *et al*. (2019). Serine 474 phosphorylation is essential for maximal Akt2 kinase activity in adipocytes. *J Biol Chem* **294**, 16729-16739. doi: 10.1074/jbc.RA119.010036.

Kelly AK, Waters SM, McGee M, Fonseca RG, Carberry C & Kenny DA (2011). mRNA expression of genes regulating oxidative phosphorylation in the muscle of beef cattle divergently ranked on residual feed intake. *Physiol Genomics* **43**, 12-23. doi: 10.1152/physiolgenomics.00213.2009.

Kelly SA, Czech PP, Wight JT, Blank KM & Garland T Jr (2006). Experimental evolution and phenotypic plasticity of hindlimb bones in high-activity house mice. *J Morphol* **267**, 360-374. doi: 10.1002/jmor.10407.

Kerr TA, Saeki S, Schneider M, Schaefer K, Berdy S, Redder T, *et al*. (2002). Loss of nuclear receptor SHP impairs but does not eliminate negative feedback regulation of bile acid synthesis. *Dev Cell* **2**, 713-720. doi: 10.1016/s1534-5807(02)00154-5.

Kersten S, Mandard S, Escher P, Gonzalez FJ, Tafuri S, Desvergne B, *et al*. (2001). The peroxisome proliferator-activated receptor alpha regulates amino acid metabolism. *FASEB J* **15**, 1971-1978. doi: 10.1096/fj.01-0147com.

Kessaram T, McKenzie J, Girin N, Roth A, Vivili P, Williams G, *et al*. (2015). Noncommunicable diseases and risk factors in adult populations of several Pacific Islands: results from the WHO STEPwise approach to surveillance. *Aust N Z J Public Health* **39**, 336-343. doi: 10.1111/1753-6405.12398.

Khan MM, Strack S, Wild F, Hanashima A, Gasch A, Brohm K, *et al*. (2014). Role of autophagy, SQSTM1, SH3GLB1, and TRIM63 in the turnover of nicotinic acetylcholine receptors. *Autophagy* **10**, 123-136. doi: 10.4161/auto.26841.

Kilikevicius A, Bunger L & Lionikas A (2016). Baseline muscle mass is a poor predictor of functional overload-induced gain in the mouse model. *Front Physiol* **7**, 534. doi: 10.3389/fphys.2016.00534.

Kilpeläinen TO, Qi L, Brage S, Sharp SJ, Sonestedt E, Demerath E, *et al*. (2011). Physical activity attenuates the influence of *FTO* variants on obesity risk: a meta-analysis of 218,166 adults and 19,268 children. *PLoS Med* **8**(11), e1001116. doi: 10.1371/journal.pmed.1001116.

Kim C, Dabelea D, Kalyani RR, Christophi CA, Bray GA, Pi-Sunyer X, *et al*. (2017a). Changes in visceral adiposity, subcutaneous adiposity, and sex hormones in the diabetes prevention program. *J Clin Endocrinol Metab* **102**, 3381-3389. doi: 10.1210/jc.2017-00967.

Kim H, Wei J, Song Z, Mottillo E, Samavati L, Zhang R, *et al*. (2021a). Regulation of hepatic circadian metabolism by the E3 ubiquitin ligase HRD1-controlled CREBH/PPARα transcriptional program. *Mol Metab* **49**, 101192. doi: 10.1016/j.molmet.2021.101192.

Kim H, Zheng Z, Walker PD, Kapatos G & Zhang K (2017c). CREBH maintains circadian glucose homeostasis by regulating hepatic glycogenolysis and gluconeogenesis. *Mol Cell Biol* **37**, e00048-17. doi: 10.1128/MCB.00048-17.

Kim HC, Choi KC, Choi HK, Kang HB, Kim MJ, Lee YH, *et al.* (2010a). HDAC3 selectively represses CREB3-mediated transcription and migration of metastatic breast cancer cells. *Cell Mol Life Sci* **67**, 3499-3510. doi: 10.1007/s00018-010-0388-5.

Kim J & Ko J (2014). A novel PPARγ_2 modulator sLZIP controls the balance between adipogenesis and osteogenesis during mesenchymal stem cell differentiation. *Cell Death Differ* **21**, 1642-1655. doi: 10.1038/cdd.2014.80.

Kim J, Okamoto H, Huang Z, Anguiano G, Chen S, Liu Q, *et al*. (2017b). Amino acid transporter Slc38a5 controls glucagon receptor inhibition-induced pancreatic α cell hyperplasia in mice. *Cell Metab* **25**, 1348-1361. doi: 10.1016/j.cmet.2017.05.006.

Kim JI, Huh JY, Sohn JH, Choe SS, Lee YS, Lim CY, *et al.* (2015a). Lipid-overloaded enlarged adipocytes provoke insulin resistance independent of inflammation. *Mol Cell Biol* **35**, 1686-1699. doi: 10.1128/MCB.01321-14.

Kim JK, Gavrilova O, Chen Y, Reitman ML & Shulman GI (2000). Mechanism of insulin resistance in A-ZIP/F-1 fatless mice. *J Biol Chem* **275**, 8456-8460. doi: 10.1074/jbc.275.12.8456.

Kim MS, Pak YK, Jang PG, Namkoong C, Choi YS, Won JC, *et al*. (2006). Role of hypothalamic Foxo1 in the regulation of food intake and energy homeostasis. *Nat Neurosci* **9**, 901-906. doi: 10.1038/nn1731.

Kim S, Kang M & Ko J (2021b). Small leucine zipper protein promotes the metastasis of castration-resistant prostate cancer through transcriptional regulation of matrix metalloproteinase-13. *Carcinogenesis* **42**, 1089-1099. doi: 10.1093/carcin/bgab045.

Kim S, Kim Y, Lee J & Chung J (2010b). Regulation of FOXO1 by TAK1-Nemo-like kinase pathway. *J Biol Chem* **285**, 8122-8129. doi: 10.1074/jbc.M110.101824.

Kim S, Park S, Kang M & Ko J (2020). The role of small leucine zipper protein in osteoclastogenesis and its involvement in bone remodelling. *Biochim Biophys Acta Mol Cell Res* **1867**, 118827. doi: 10.1016/j.bbamcr.2020.118827.

Kim T, Holleman CL, Nason S, Arble DM, Ottaway N, Chabenne J, *et al*. (2018). Hepatic glucagon receptor signalling enhances insulin-stimulated glucose disposal in rodents. *Diabetes* **67**, 2157-2166. doi: 10.2337/db18-0068.

Kim TN, Park MS, Yang SJ, Yoo HJ, Kang HJ, Song W, *et al*. (2010c). Prevalence and determinant factors of sarcopenia in patients with type 2 diabetes: the Korean Sarcopenic Obesity Study (KSOS). *Diabetes Care* **33**, 1497-1499. doi: 10.2337/dc09-2310.

Kim Y, Kim J, Jang S-W & Ko J (2015b). The role of sLZIP in cyclin D3-mediated negative regulation of androgen receptor transactivation and its involvement in prostate cancer. *Oncogene* **34**, 226-236. doi: 10.1038/onc.2013.538.

Kimball SR, Siegfried BA & Jefferson LS (2004). Glucagon represses signalling through the mammalian target of rapamycin in rat liver by activating AMP-activated protein kinase. *J Biol Chem* **279**, 54103-54109. doi: 10.1074/jbc.M410755200.

King H, Finch C, Collins A, King LF, Zimmet P, Koki G, *et al*. (1989). Glucose tolerance in Papua New Guinea: ethnic differences, association with environmental and behavioural factors and the possible emergence of glucose intolerance in a highland community. *Med J Aust* **151**, 204-210. doi: 10.5694/j.1326-5377.1989.tb115991.x.

King H, Taylor R, Zimmet P, Pargeter K, Raper LR, Beriki T, *et al*. (1984). Non-insulin-dependent diabetes (NIDDM) in a newly independent Pacific nation: the Republic of Kiribati. *Diabetes Care* **7**, 409-415. doi: 10.2337/diacare.7.5.409.

Kinouchi K, Magnan C, Ceglia N, Liu Y, Cervantes M, Pastore N, *et al*. (2018). Fasting imparts a switch to alternative daily pathways in liver and muscle. *Cell Rep* **25**, 3299-3314.e6. doi: 10.1016/j.celrep.2018.11.077.

Kirn-Safran CB, Oristian DS, Focht RJ, Parker SG, Vivian JL & Carson DD (2007). Global growth deficiencies in mice lacking the ribosomal protein HIP/RPL29. *Dev Dyn* **236**, 447-460. doi: 10.1002/dvdy.21046.

Klemm SL, Shipony Z & Greenleaf WJ (2019). Chromatin accessibility and the regulatory epigenome. *Nat Rev Genet* **20**, 207-220. doi: 10.1038/s41576-018-0089-8.

Kmita K, Wirth C, Warnau J, Guerrero-Castillo S, Hunte C, Hummer G, *et al*. (2015). Accessory NUMM (NDUFS6) subunit harbours a Zn-binding site and is essential for biogenesis of mitochondrial complex I. *PNAS* **112**, 5685-5690. doi: 10.1073/pnas.1424353112.

Ko J, Jang SW, Kim YS, Kim IS, Sung HJ, Kim HH, *et al*. (2004). Human LZIP binds to CCR1 and differentially affects the chemotactic activities of CCR1-dependent chemokines. *FASEB J* **18**, 890-892. doi: 10.1096/fj.03-0867fje.

Kobayashi A, Azuma K, Ikeda K & Inoue S (2020). Mechanisms underlying the regulation of mitochondrial respiratory chain complexes by nuclear steroid receptors. *Int J Mol Sci* **21**, 6683. doi: 10.3390/ijms21186683.

Koch RM, Swiger LA, Chambers D & Gregory KE (1963). Efficiency of feed use in beef cattle. *J Anim Sci* **22**, 486-494. doi: 10.2527/jas1963.222486x.

Kodani N & Nakae J (2020). Tissue-specific metabolic regulation of FOXO-binding protein: FOXO does not act alone. *Cells* **9**, 702. doi: 10.3390/cells9030702.

Koh X-H, Liu X & Teo Y-Y (2014). Can evidence from genome-wide association studies and positive natural selection surveys be used to evaluate the thrifty gene hypothesis in East Asians? *PLoS ONE* **9**, e110974. doi: 10.1371/journal.pone.0110974.

Kondo S, Saito A, Asada R, Kanemoto S & Imaizumi K (2011). Physiological unfolded protein response regulated by OASIS family members, transmembrane bZIP transcription factors. *IUBMB Life* **63**, 233-239. doi: 10.1002/iub.433.

Koo S-H, Flechner L, Qi L, Zhang X, Screaton RA, Jeffries S, *et al*. (2005). The CREB coactivator TORC2 is a key regulator of fasting glucose metabolism. *Nature* **437**, 1109-1111. doi: 10.1038/nature03967.

Korenfeld N, Finkel M, Buchshtab N, Bar-Shimon M, Charni-Natan M & Goldstein I (2021). Fasting hormones synergistically induce amino acid catabolism genes to promote gluconeogenesis. *Cell Mol Gastroenterol Hepatol* doi: 10.1016/j.jcmgh.2021.04.017.

Kottaisamy CPD, Raj DS, Kumar VP & Sankaran U (2021). Experimental animal models for diabetes and its related complications—a review. *Lab Anim Res* **37**, 23. doi: 10.1186/s42826-021-00101-4.

Kovacs WJ, Tape KN, Shackelford JE, Wikander TM, Richards MJ, Fliesler SJ, *et al*. (2009). Peroxisome deficiency causes a complex phenotype because of hepatic SREBP/Insig dysregulation associated with endoplasmic reticulum stress. *J Biol Chem* **284**, 7232-7245. doi: 10.1074/jbc.M809064200.

Kowalsky AH, Namkoong S, Mettetal E, Park H-W, Kazyken D, Fingar DC, *et al*. (2020). The GATOR2-mTORC2 axis mediates Sestrin2-induced AKT Ser/Thr kinase activation. *J Biol Chem* **295**, 1769-1780. doi: 10.1074/jbc.RA119.010857.

Kraegen EW, Clark PW, Jenkins AB, Daley EA, Chisholm DJ & Storlien LH (1991). Development of muscle insulin resistance after liver insulin resistance in high-fat-fed rats. *Diabetes* **40**(11), 1397-1403. doi: 10.2337/diab.40.11.1397.

Kramer CK, Zinman B & Retnakaran R (2013). Are metabolically healthy overweight and obesity benign conditions?: A systematic review and meta-analysis. *Ann Intern Med* **159**, 758-769. doi: 10.7326/0003-4819-159-11-201312030-00008.

Kranendonk ME, van Herwaarden JA, Stupkova T, de Jager W, Vink A, Moll FL, *et al*. (2015). Inflammatory characteristics of distinct abdominal adipose tissue depots relate differently to metabolic risk factors for cardiovascular disease: distinct fat depots and vascular risk factors. *Atherosclerosis* **239**, 419-427. doi: 10.1016/j.atherosclerosis.2015.01.035.

Krempler F, Esterbauer H, Weitgasser R, Ebenbichler C, Patsch JR, Miller K, *et al*. (2002). A functional polymorphism in the promoter of UCP2 enhances obesity risk but reduces type 2 diabetes risk in obese middle-aged humans. *Diabetes* **51**, 3331-3335. doi: 10.2337/diabetes.51.11.3331..

Krishnaiah SY, Wu G, Altman BJ, Growe J, Rhoades SD, Coldren F, *et al*. (2017). Clock regulation of metabolites reveals coupling between transcription and metabolism. *Cell Metab* **25**, 961-974.e4. doi: 10.1016/j.cmet.2017.03.019.

Krishnan M, Major TJ, Topless RK, Dewes O, Yu L, Thompson JMD, *et al*. (2018). Discordant association of the *CREBRF* rs373863828 A allele with increased

BMI and protection from type 2 diabetes in Māori and Pacific (Polynesian) people living in Aotearoa/New Zealand. *Diabetologia* **61**, 1603-1613. doi: 10.1007/s00125-018-4623-1.

Krishnan M, Murphy R, Okesene-Gafa KAM, Ji M, Thompson JMD, Taylor RS, *et al*. (2020). The Pacific-specific CREBRF rs373863828 allele protects against gestational diabetes mellitus in Māori and Pacific women with obesity. *Diabetologia* **63**, 2169-2176. doi: 10.1007/s00125-020-05202-8.

Kristensen CM, Jessen H, Ringholm S & Pilegaard H (2018). Muscle PGC-1α in exercise and fasting-induced regulation of hepatic UPR in mice. *Acta Physiol (Oxf)* **224**, e13158. doi: 10.1111/apha.13158.

Kroon J, Koorneef LL, van den Heuvel JK, Verzijl CRC, van de Velde NM, Mol IM, *et al*. (2018). Selective glucocorticoid receptor antagonist CORT125281 activates brown adipose tissue and alters lipid distribution in male mice. *Endocrinology* **159**, 535-546. doi: 10.1210/en.2017-00512.

Kruglov E, Gautam S, Guerra MT & Nathanson MH (2011). Type 2 inositol 1,4,5-triphosphate receptor modulates bile salt export pump activity in rat hepatocytes. *Hepatology* **54**, 1790-1799. doi: 10.1002/hep.24548.

Krumm CS, Xu X, Bare CJ, Holman CD, Kersten S, Dow LE, *et al*. (2021). Inducible hepatic expression of CREBH mitigates diet-induced obesity, insulin resistance and hepatic steatosis in mice. *J Biol Chem* (in press). doi: 10.1016/j.jbc.2021.100815.

Kuo T, Lew MJ, Mayba O, Harris CA, Speed TP & Wang J-C (2012). Genome-wide analysis of glucocorticoid receptor-binding sites in myotubes identifies gene networks modulating insulin signalling. *Proc Natl Acad Sci U S A* **109**, 11160-11165. doi: 10.1073/pnas.1111334109.

Kurano M, Tsukamoto K, Shimizu T, Kassai H, Nakao K, Aiba A, *et al*. (2020). Protection against insulin resistance by apolipoprotein M/sphingosine-1-phosphate. *Diabetes* **69**, 867-881. doi: 10.2337/db19-0811.

Kvedaras M, Minderis P, Fokin A, Ratkevicius A, Venckunas T & Lionikas A (2017). Forced running endurance is influenced by gene(s) on mouse chromosome 10. *Front Physiol* **8**, 9. doi: 10.3389/fphys.2017.00009.

Laatsch A, Merkel M, Talmud PJ, Grewal T, Beisiegel U & Heeren J (2009). Insulin stimulates hepatic low density lipoprotein receptor-related protein 1 (LRP1) to increase postprandial lipoprotein clearance. *Atherosclerosis* **204**, 105-111. doi: 10.1016/j.atherosclerosis.2008.07.046.

Lacasa D, Le Liepvre X, Ferre P & Dugail I (2001). Progesterone stimulates adipocyte determination and differentiation 1/sterol regulatory element-binding protein 1c gene expression. potential mechanism for the lipogenic effect of progesterone in adipose tissue. *J Biol Chem* **276**, 11512-11516. doi: 10.1074/jbc.M008556200.

Lamming DW, Mihaylova MM, Katajisto P, Baar EL, Yilmaz OH, Hutchins A, *et al*. (2014). Depletion of Rictor, an essential protein component of mTORC2, decreases male lifespan. *Aging Cell* **13**, 911-917. doi: 10.1111/acel.12256.

Lamming DW, Ye L, Katajisto P, Goncalves MD, Saitoh M, Stevens DM, *et al*. (2012). Rapamycin-induced insulin resistance is mediated by mTORC2 loss and uncoupled from longevity. *Science* **335**, 1638-1643. doi: 10.1126/science.1215135.

Lang F, Aravamudhan S, Nolte H, Türk C, Hölper S, Müller S, *et al*. (2017). Dynamic changes in the mouse skeletal muscle proteome during denervation-induced atrophy. *Dis Model Mech* **10**, 881-896. doi: 10.1242/dmm.028910.

Larance M, Rowland AF, Hoehn KL, Humphreys DT, Preiss T, Guilhaus M, *et al*. (2010). Global phosphoproteomics identifies a major role for AKT and 14-3-3 in regulating EDC3. *Mol Cell Proteomics* **9**, 682-694. doi: 10.1074/mcp.M900435-MCP200.

Larson S, Arrazola A, Parra R, Morrissey K, Faulkner T, Jafarikia M, *et al*. (in press). Genetic variation in *LUMAN/CREB3* and association with stress and meat quality traits in Yorkshire pigs. *Can J Anim Sci* doi: 10.1139/CJAS-2020-0156.

Lau-Corona D, Suvorov A & Waxman DJ (2017). Feminisation of male mouse liver by persistent growth hormone stimulation: activation of sex-biased transcriptional networks and dynamic changes in chromatin states. *Mol Cell Biol* **37**, e00301-e00317. doi: 10.1128/MCB.00301-17.

Lawson EA, Holsen LM, Desanti R, Santin M, Meenaghan E, Herzog DB, *et al*. (2013). Increased hypothalamic-pituitary-adrenal drive is associated with decreased appetite and hypoactivation of food-motivation neurocircuitry in anorexia nervosa. *Eur J Endocrinol* **169**, 639-647. doi: 10.1530/EJE-13-0433.

Lear SA, Humphries KH, Kohli S & Birmingham CL (2007). The use of BMI and waist circumference as surrogates of body fat differs by ethnicity. *Obesity (Silver Spring)* **15**, 2817-2824. doi: 10.1038/oby.2007.334.

Leavens KF & Birnbaum MJ (2011). Insulin signalling to hepatic lipid metabolism in health and disease. *Crit Rev Biochem Mol Biol* **46**, 200-215. doi: 10.3109/10409238.2011.562481.

Lecker SH, Jagoe RT, Gilbert A, Gomes M, Baracos V, Bailey J, *et al*. (2004). Multiple types of skeletal muscle atrophy involve a common program of changes in gene expression. *FASEB J* **18**, 39-51. doi: 10.1096/fj.03-0610com.

LeCroy MN, Hua S, Kaplan RC, Sotres-Alvarez D, Qi Q, Thyagarajan B, *et al*. (2021). Associations of changes in fat free mass with risk for type 2 diabetes: Hispanic community health study/study of Latinos. *Diabetes Res Clin Pract* **171**, 108557. doi: 10.1016/j.diabres.2020.108557.

Lee GY, Jang H, Lee JH, Huh JY, Choi S, Chung J, *et al.* (2014). PIASy-mediated sumoylation of SREBP1c regulates hepatic lipid metabolism upon fasting signalling. *Mol Cell Biol* **34**, 926-938. doi: 10.1128/MCB.01166-13.

Lee HS & Hwang JS (2020). Impact of type 2 diabetes mellitus and antidiabetic medications on bone metabolism. *Curr Diab Rep* **20**, 78. doi: 10.1007/s11892-020-01361-5.

Lee K, Vakili S, Burden HJ, Adams S, Smith GC, Kulatea B, *et al*. (preprint). The minor allele of the CREBRF rs373863828 p.R457Q coding variant is associated with reduced levels of myostatin in males: implications for body composition. https://doi.org/10.1101/2021.07.13.21260462. [posted 15 Jul 2021]

Lee KP & Jang T (2014). Exploring the nutritional basis of starvation resistance in *Drosophila melanogaster*. *Functional Ecology* **28**, 1144-1155. doi: 10.1111/1365-2435.12247.

Lee MJ, Wu Y & Fried SK (2013). Adipose tissue heterogeneity: implication of depot differences in adipose tissue for obesity complications. *Mol Aspects Med* **34**, 1-11. doi: 10.1016/j.mam.2012.10.001.

Lee MW, Chanda D, Yang J, Oh H, Kim SS, Yoon YS, *et al*. (2010). Regulation of hepatic gluconeogenesis by an ER-bound transcription factor, CREBH. *Cell Metab* **11**, 331-339. doi: 10.1016/j.cmet.2010.02.01.

Lee NK & Karsenty G (2008). Reciprocal regulation of bone and energy metabolism. *Trends Endocrinol Metab* **19**, 161-166. doi: 10.1016/j.tem.2008.02.006.

Lee NK, Sowa H, Hinoi E, Ferron M, Ahn JD, Confavreux C, *et al*. (2007). Endocrine regulation of energy metabolism by the skeleton. *Cell* **130**, 456-469. doi: 10.1016/j.cell.2007.05.047.

Lee Y, Wang M-Y, Du ZQ, Charron MJ & Unger RH (2011). Glucagon receptor knockout prevents insulin-deficient type 1 diabetes in mice. *Diabetes* **60**, 391-397. doi: 10.2337/db10-0426.

Lee YH, Wang M-Y, Yu X-X & Unger RH (2016). Glucagon is the key factor in the development of diabetes. *Diabetologia* **59**, 1372-1375. doi: 10.1007/s00125-016-3965-9.

Lerch JK, Alexander JK, Madalena KM, Motti D, Quach T, Dhamija A, *et al*. (2017). Stress increases peripheral axon growth and regeneration through glucocorticoid receptor-dependent transcriptional programs. *eNeuro* **4**, ENEURO.0246-17.2017. doi: 10.1523/ENEURO.0246-17.2017.

Lewis MT, Kasper JD, Bazil JN, Frisbee JC & Wiseman RW (2019). Quantification of mitochondrial oxidative phosphorylation in metabolic disease: application to type 2 diabetes. *Int J Mol Sci* **20**, 5271. doi: 10.3390/ijms20215271.

Li C, Li Y, He L, Agarwal AR, Zeng N, Cadenas E, *et al*. (2013a). PI3K/AKT signalling regulates bioenergetics in immortalised hepatocytes. *Free Radic Biol Med* **60**, 29-40. doi: 10.1016/j.freeradbiomed.2013.01.013.

Li M, Fan P & Wang Y (2015a). Lipidomics in health and diseases – beyond the analysis of lipids. *J Glycomics Lipidomics* **5**, 126. doi: 10.4172/2153-0637.100012.

Li M-D, Ruan H-B, Hughes ME, Lee J-S, Singh JP, Jones SP, *et al*. (2013b). O-GlcNAc signalling entrains the circadian clock by inhibiting BMAL1/CLOCK ubiquitination. *Cell Metab* **17**, 303-310. doi: 10.1016/j.cmet.2012.12.015.

Li P, Ruan X, Yang L, Kiesewetter K, Zhao Y, Luo H, *et al*. (2015b). A liver-enriched long non-coding RNA, lncLSTR, regulates systemic lipid metabolism in mice. *Cell Metab* **21**, 455-467. doi: 10.1016/j.cmet.2015.02.004.

Li S, Brown MS & Goldstein JL (2010). Bifurcation of insulin signalling pathway in rat liver: mTORC1 required for stimulation of lipogenesis, but not inhibition of gluconeogenesis. *Proc Natl Acad Sci USA* **107**, 3441-3446. doi: 10.1073/pnas.0914798107.

Li X, Lin P, Chen F, Wang N, Zhao F, Wang A, *et al.* (2016). Luman recruiting factor is involved in stromal cell proliferation during decidualisation in mice. *Cell Tissue Res* **365**, 437-447. doi: 10.1007/s00441-016-2392-z.

Li Y, Ding H, Dong J, Rahman SU, Feng S, Wang X, *et al*. (2019). Glucagon attenuates lipid accumulation in cow hepatocytes through AMPK signalling pathway activation. *J Cell Physiol* **234**, 6054-6066. doi: 10.1002/jcp.27258.

Liang G, Audas TE, Li Y, Cockram GP, Dean JD, Martyn AC, *et al*. (2006). Luman/CREB3 induces transcription of the endoplasmic reticulum (ER) stress

response protein Herp through an ER stress response element. *Mol Cell Biol* **26**, 7999-8010. doi: 10.1128/MCB.01046-06.

Lim U, Monroe KR, Buchthal S, Fan B, Cheng I, Kristal BS, *et al*. (2019). Propensity for intra-abdominal and hepatic adiposity varies among ethnic groups. *Gastroenterology* **156**, 966-975. doi: 10.1053/j.gastro.2018.11.021.

Lin M, Caberto C, Wan P, Li Y, Lum-Jones A, Tiirikainen M, *et al*. (2020). Population-specific reference panels are crucial for genetic analyses: an example of the CREBRF locus in Native Hawaiians. *Hum Mol Genet* **29**, 2275-2284. doi: 10.1093/hmg/ddaa083.

Lin S, Naseri T, Linhart C, Morrell S, Taylor R, McGarvey ST, *et al*. (2017). Trends in diabetes and obesity in Samoa over 35 years, 1978-2013. *Diabet Med* **34**, 654-661. doi: 10.1111/dme.13197.

Listerman I, Bledau AS, Grishina I & Neugebauer KM (2007). Extragenic accumulation of RNA polymerase II enhances transcription by RNA polymerase III. *PLoS Genet* **3**, e212. doi: 10.1371/journal.pgen.0030212.

Liu G, Zhu H, Lagou V, Gutin B, Stallmann-Jorgensen IS, Treiber FA, *et al*. (2010). *FTO* variant rs9939609 is associated with body mass index and waist circumference, but not with energy intake or physical activity in European- and African-American youth. *BMC Med Genet* **11**, 57. doi: 10.1186/1471-2350-11-57.

Liu H-Y, Han J, Cao SY, Hong T, Zhuo D, Shi J, *et al*. (2009). Hepatic autophagy is suppressed in the presence of insulin resistance and hyperinsulinemia: inhibition of FoxO1-dependent expression of key autophagy genes by insulin. *J Biol Chem* **284**, 31484-31492. doi: 10.1074/jbc.M109.033936.

Liu J, Peng Y, Wang X, Fan Y, Qin C, Shi L, *et al*. (2016). Mitochondrial dysfunction launches dexamethasone-induced skeletal muscle atrophy via AMPK/FOXO3 signalling. *Mol Pharm* **13**, 73-84. doi: 10.1021/acs.molpharmaceut.5b00516.

Liu Q, Yang X, Long G, Hu Y, Gu Z, Boisclair YR, *et al*. (2020). ERAD deficiency promotes mitochondrial dysfunction and transcriptional rewiring in human hepatic cells. *J Biol Chem* **295**, 16743-16753. doi: 10.1074/jbc.RA120.013987.

Liu W, Cao H, Ye C, Chang C, Lu M, Jing Y, *et al*. (2014). Hepatic miR-378 targets p110α and controls glucose and lipid homeostasis by modulating hepatic insulin signalling. *Nat Commun* **5**, 5684. doi: 10.1038/ncomms6684.

Llewellyn C & Wardle J (2015). Behavioural susceptibility to obesity: gene-environment interplay in the development of weight. *Physiol Behav* **152**(Pt B), 494-501. doi: 10.1016/j.physbeh.2015.07.006.

Llewellyn CH & Fildes A (2017). Behavioural susceptibility theory: Professor Jane Wardle and the role of appetite in genetic risk of obesity. *Curr Obes Rep* **6**(1), 38-45. doi: 10.1007/s13679-017-0247-x.

Longo SK, Guo MG, Ji AL & Khavari PA (2021). Integrating single-cell and spatial transcriptomics to elucidate intercellular tissue dynamics. *Nat Rev Genet* (in press) doi: 10.1038/s41576-021-00370-8.

Longuet C, Sinclair EM, Maida A, Baggio LL, Maziarz M, Charron MJ, *et al*. (2008). The glucagon receptor is required for the adaptive metabolic response to fasting. *Cell Metab* **8**, 359-371. doi: 10.1016/j.cmet.2008.09.008.

Loos RJF (2016). *CREBRF* variant increases obesity risk and protects against diabetes in Samoans. *Nat Genet* **48**, 976-978. doi: 10.1038/ng.3653.

Loos RJF, Lindgren CM, Li S, Wheeler E, Zhao JH, Prokopenko I, *et al*. (2008). Common variants near *MCR4* are associated with fat mass, weight and risk of obesity. *Nat Genet* **40**(6), 768-775. doi: 10.1038/ng.140.

López-Maury L, Marguerat S & Bähler J (2008). Tuning gene expression to changing environments: from rapid responses to evolutionary adaptation. *Nat Rev Genet* **9**, 583-593. doi: 10.1038/nrg2398.

López-Soldado I, Bertini A, Adrover A, Duran J & Guinovart JJ (2020). Maintenance of liver glycogen during long-term fasting preserves energy state in mice. *FEBS Lett* **594**, 1698-1710. doi: 10.1002/1873-3468.13770.

Lu M, Wan M, Leavens KF, Chu Q, Monks BR, Fernandez S, *et al*. (2012). Insulin regulates liver metabolism in the absence of hepatic Akt and Foxo1. *Nat Med* **18**, 388-395. doi: 10.1038/nm.2686.

Lu R & Misra V (2000). Potential role for Luman, the cellular homologue of herpes simplex virus VP16 (a gene *trans*-inducing factor) in Herpesvirus latency. *J Virol* **74**, 934-943. doi: 10.1128/jvi.74.2.934-943.2000.

Lu R, Yang P, O'Hare P & Misra V (1997). Luman, a new member of the CREB/ATF family, binds to herpes simplex virus VP16-associated host cellular factor. *Mol Cell Biol* **17**, 5117-5126. doi: 10.1128/MCB.17.9.5117.

Lu R, Yang P, Padmakumar S & Misra V (1998). The Herpesvirus transactivator VP16 mimics a human basic domain leucine zipper protein, Luman, in its interaction with HCF. *J Virol* **72**, 6291-6297. doi: 10.1128/JVI.72.8.6291-6297.1998.

Lv S, Qiu X, Li J, Liang J, Li W, Zhang C, *et al*. (2017). Glucagon-induced extracellular cAMP regulates hepatic lipid metabolism. *J Endocrinol* **234**, 73-87. doi: 10.1530/JOE-16-0649.

Lydic TA & Goo YH (2018). Lipidomics unveils the complexity of the lipidome in metabolic diseases. *Clin Transl Med* **7**, 4. doi: 10.1186/s40169-018-0182-9.

Ma K, Mallidis C, Artaza J, Taylor W, Gonzalez-Cadavid N & Bhasin S (2001). Characterisation of 5'-regulatory region of human myostatin gene: regulation by dexamethasone in vitro. *Am J Physiol Endocrinol Metab* **281**, E1128-E1136. doi: 10.1152/ajpendo.2001.281.6.E1128.

Ma L, Robinson LN & Towle HC (2006). ChREBP*Mlx is the principal mediator of glucose-induced gene expression in the liver. *J Biol Chem* **281**, 28721-28730. doi: 10.1074/jbc.M601576200.

Ma M, Duan R, Shen L, Liu M, Ji Y, Zhou H, *et al*. (2020). The lncRNA Gm15622 stimulates SREBP-1c expression and hepatic lipid accumulation by sponging the miR-742-3p in mice. *J Lipid Res* **61**, 1052-1064. doi: 10.1194/jlr.RA120000664.

Ma X, Zhang H, Yuan L, Jing H, Thacker P & Li D (2011). CREBL2, interacting with CREB, induces adipogenesis in 3T3-L1 adipocytes. *Biochem J* **439**(1), 27-38. doi: 10.1042/BJ20101475.

Maga A, De Courten M, Dan L, Uele F, Macdonald N, Lili'o L, *et al*. (2007). *American Samoa NCD risk factors STEPS report: A collaborative effort between the Department of Health, World Health Organization and Monash University, Australia, supported by the Australian Agency for International Development*. Manila (PHL): WHO. Available from: https://www.who.int/ncds/surveillance/steps/Printed_STEPS_Report_American_Samoa.pdf.

Magnusson I, Rothman DL, Gerard DP, Katz LD & Shulman GI (1995). Contribution of hepatic glycogenolysis to glucose production in humans in response to a physiological increase in plasma glucagon concentration. *Diabetes* **44**, 185-189. doi: 10.2337/diab.44.2.185.

Mahmoud TN, Lin PF, Chen FL, Zhou JH, Wang XG, Wang N, *et al.* (2015). Expression and localisation of Luman/CREB3 in mouse embryos during the pre-implantation period. *Genet Mol Res* **14**, 13595-13602. doi: 10.4238/2015.

Majaw T & Sharma R (2015). Arginase I expression is upregulated by dietary restriction in the liver of mice as a function of age. *Mol Cell Biochem* **407**, 1-7. doi: 10.1007/s11010-015-2448-5.

Manczak M, Park BS, Jung Y & Reddy PH (2004). Differential expression of oxidative phosphorylation genes in patients with Alzheimer's disease: implications for early mitochondrial dysfunction and oxidative damage. *Neuromolecular Med* **5**, 147-162. doi: 10.1385/NMM:5:2:147.

Manolescu D-C, Sima A & Bhat PV (2010). All-trans retinoic acid lowers serum retinol-binding protein 4 concentrations and increases insulin sensitivity in diabetic mice. *J Nutr* **140**, 311-316. doi: 10.3945/jn.109.115147.

Manolopoulos KN, Karpe F & Frayn KN (2010). Gluteofemoral body fat as a determinant of metabolic health. *Int J Obes (Lond)* **34**, 949-959. doi: 10.1038/ijo.2009.286.

Mao L, Fang Y, Campbell M & Southerland WM (2017). Population differentiation in allele frequencies of obesity-associated SNPs. *BMC Genomics* **18**(1), 861. doi: 10.1186/s12864-017-4262-9.

Mao Z & Zhang W (2018). Role of mTOR in glucose and lipid metabolism. *Int J Mol Sci* **19**, 2043. doi: 10.3390/ijms19072043.

Mårin P, Andersson B, Krotkiewski M & Björntorp P (1994). Muscle fiber composition and capillary density in women and men with NIDDM. *Diabetes Care* **17**, 382-386. doi: 10.2337/diacare.17.5.382.

Mariot V, Joubert R, Hourdé C, Féasson L, Hanna M, Muntoni F, *et al*. (2017). Downregulation of myostatin pathway in neuromuscular diseases may explain challenges of anti-myostatin therapeutic approaches. *Nat Commun* **8**, 1859. doi: 10.1038/s41467-017-01486-4.

Martin LJ & Tremblay JJ (2008). Glucocorticoids antagonise cAMP-induced Star transcription in Leydig cells through the orphan nuclear receptor NR4A1. *J Mol Endocrinol* **41**, 165-175. doi: 10.1677/JME-07-0145.

Martos-Moreno GÁ, Martínez-Villanueva J, González-Leal R, Barrios V, Sirvent S, Hawkins F, *et al*. (2020). Ethnicity strongly influences body fat distribution determining serum adipokine profile and metabolic derangement in childhood obesity. *Front Pediatr* **8**, 551103. doi: 10.3389/fped.2020.551103.

Martyn AC, Choleris E, Gillis DJ, Armstrong JN, Amor TR, McCluggage ARR, *et al*. (2012) Luman/CREB3 recruitment factor regulates glucocorticoid receptor

activity and is essential for prolactin-mediated maternal instinct. *Mol Cell Biol* **32**, 5140-5150. doi: 10.1128/MCB.01142-12.

Maskarinec G, Garber AK, Wong MC, Kelly N, Kazemi L, Buchthal SD, *et al*. (2020). Predictors of liver fat among children and adolescents from five different ethnic groups. *Obes Sci Pract* **7**, 53-62. doi: 10.1002/osp4.459.

Massa ML, Gagliardino JJ & Francini F (2011). Liver glucokinase: an overview on the regulatory mechanisms of its activity. *IUBMB Life* **63**, 1-6. doi: 10.1002/iub.411.

Massart R, Freyburger M, Suderman M, Paquete J, El Helou J, Belanger-Nelson E, *et al*. (2014). The genome-wide landscape of DNA methylation and hydroxymethylation in response to sleep deprivation impacts on synaptic plasticity genes. *Transl Psychiatry* **4**, e347. doi: 10.1038/tp.2013.120.

Massett MP, Courtney SM, Kim SK & Avila JJ (2019). Contribution of chromosome 14 to exercise capacity and training responses in mice. *Front Physiol* **10**, 1165. doi: 10.3389/fphys.2019.01165.

Matsuhisa K, Saito A, Cai L, Kaneko M, Okamoto T, Sakaue F, *et al.* (2020). Production of BBF2H7-derived small peptide fragments via endoplasmic reticulum stress-dependent regulated intramembrane proteolysis. *FASEB J* **34**, 865-880. doi: 10.1096/fj.201901748R.

Matsuzaki H, Daitoku H, Hatta M, Aoyama H, Yoshimochi K & Fukamizu A (2005). Acetylation of Foxo1 alters its DNA-binding ability and sensitivity to phosphorylation. *Proc Natl Acad Sci USA* **102**, 11278-11283. doi: 10.1073/pnas.0502738102.

Matsuzaki H, Daitoku H, Hatta M, Tanaka K & Fukamizu A (2003). Insulin-induced phosphorylation of FKHR (Foxo1) targets to proteasomal degradation. *Proc Natl Acad Sci U S A* **100**, 11285-11290. doi: 10.1073/pnas.1934283100.

Mattos GE, Heinzmann J-M, Norkowski S, Helbling J-C, Minni AM, Moisan M-P, *et al*. (2013). Corticosteroid-binding globulin contributes to the neuroendocrine phenotype of mice selected for extremes in stress reactivity. *J Endocrinol* **219**, 217-229. doi: 10.1530/JOE-13-0255.

Mayer C & Grummt I (2006). Ribosome biogenesis and cell growth: mTOR coordinates transcription by all three classes of nuclear RNA polymerases. *Oncogene* **25**, 6384-6391. doi: 10.1038/sj.onc.1209883.

McAteer JB, Prudente S, Bacci S, Lyon HN, Hirschhorn JN, Trischitta V, *et al*. (2008). The ENPP1 K121Q polymorphism is associated with type 2 diabetes in

European populations: evidence from an updated meta-analysis in 42,042 subjects. *Diabetes* **57**(4), 1125-1130. doi: 10.2337/db07-1336.

McAuley KA, Williams SM, Mann JI, Goulding A & Murphy E (2002). Increased risk of type 2 diabetes despite same degree of adiposity in different racial groups. *Diabetes Care* **25**, 2360-2361. doi: 10.2337/diacare.25.12.2360.

McGarvey ST (1991). Obesity in Samoans and a perspective on its aetiology in Polynesians. *Am J Clin Nutr* **53**, 1586S-1594S. doi: 10.1093/ajcn/53.6.1586S.

McKenna C, Keogh K, Porter RK, Waters SM, Cormican P & Kenny DA (2021). An examination of skeletal muscle and hepatic tissue transcriptomes from beef cattle divergent for residual feed intake. *Sci Rep* **11**, 8942. doi: 10.1038/s41598-021-87842-3.

McKinnell IW & Rudnicki MA (2004). Molecular mechanisms of muscle atrophy. *Cell* **119**, 907-910. doi: 10.1016/j.cell.2004.12.007.

McLaughlin T, Lamendola C, Coghlan N, Liu TC, Lerner K, Sherman A, *et al.* (2014). Subcutaneous adipose cell size and distribution: relationship to insulin resistance and body fat. *Obesity (Silver Spring)* **22**, 673-680. doi: 10.1002/oby.20209.

McLaughlin T, Lamendola C, Liu A & Abbasi F (2011). Preferential fat deposition in subcutaneous *versus* visceral depots is associated with insulin sensitivity. *J Clin Endocrinol Metab* **96**, E1756-E1760. doi: 10.1210/jc.2011-0615..

McLaughlin T, Sherman A, Tsao P, Gonzalez O, Yee G, Lamendola C, *et al.* (2007). Enhanced proportion of small adipose cells in insulin-resistant vs insulin-sensitive obese individuals implicates impaired adipogenesis. *Diabetologia* **50**, 1707-1715. doi: 10.1007/s00125-007-0708-y.

McMahon CD, Popovic L, Oldham JM, Jeanplong F, Smith HK, Kambadur R, *et al*. (2003). Myostatin-deficient mice lose more skeletal muscle mass than wild-type controls during hindlimb suspension. *Am J Physiol Endocrinol Metab* **285**, E82-E87. doi: 10.1152/ajpendo.00275.2002.

McMillin M, Frampton G, Quinn M, Divan A, Grant S, Patel N, *et al*. (2015). Suppression of the HPA axis during cholestasis can be attributed to hypothalamic bile acid signalling. *Mol Endocrinol* **29**, 1720-1730. doi: 10.1210/me.2015-1087.

Mears HV & Sweeney TR (2018). Better together: the role of IFIT protein-protein interactions in the antiviral response. *J Gen Virol* **99**, 1463-1477. doi: 10.1099/jgv.0.001149.

Meex RCR, Schrauwen-Hinderling VB, Moonen-Kornips E, Schaart G, Mensink M, Phielix E, *et al*. (2010). Restoration of muscle mitochondrial function and metabolic flexibility in type 2 diabetes by exercise training in paralleled by increased myocellular fat storage and improved insulin sensitivity. *Diabetes* **59**, 572-579. doi: 10.2337/db09-1322.

Meikle PJ & Summers SA (2017). Sphingolipids and phospholipids in insulin resistance and related metabolic disorders. *Nat Rev Endocrinol* **13**, 79-91. doi: 10.1038/nrendo.2016.169.

Mendias CL, Marcin JE, Calerdon DR & Faulkner JA (2006). Contractile properties of EDL and soleus muscles of myostatin-deficient mice. *J Appl Physiol (1985)* **101**, 898-905. doi: 10.1152/japplphysiol.00126.2006.

Meng J & Ferguson SM (2018). GATOR1-dependent recruitment of FLCN-FNIP to lysosomes coordinates Rag GTPase heterodimer nucleotide status in response to amino acids. *J Cell Biol* **217**, 2765-2776. doi: 10.1083/jcb.201712177.

Merchant RA, Chan YH, Lim JY & Morley JE (2020). Prevalence of metabolic syndrome and association with grip strength in older adults: findings from the HOPE study. *Diabetes Metab Syndr Obes* **13**, 2677-2686. doi: 10.2147/DMSO.S260544.

Meroni M, Dongiovanni P, Longo M, Carli F, Baselli G, Rametta R, *et al*. (2020). Mboat7 down-regulation by hyper-insulinemia induces fat accumulation in hepatocytes. *EBioMedicine* **52**, 102658. doi: 10.1016/j.ebiom.2020.102658.

Merry TL, Hedges CP, Masson SW, Laube B, Pöhlmann D, Wueest S, *et al*. (2020). Partial impairment of insulin receptor expression mimics fasting to prevent diet-induced fatty liver disease. *Nat Commun* **11**, 2080. doi: 10.1038/s41467-020-15623-z.

Metcalfe LK, Krishnan M, Turner N, Yaghootkar H, Merry TL, Dewes O, *et al*. (2020). The Māori and Pacific specific CREBRF variant and adult height. *Int J Obes (Lond)* **44**, 748-752. doi: 10.1038/s41366-019-0437-6.

Meyre D, Bouatia-Naji N, Tounian A, Samson C, Lecoeur C, Vatin V, *et al*. (2005). Variants of *ENPP1* are associated with childhood and adult obesity and increase the risk of glucose intolerance and type 2 diabetes. *Nat Genet* **37**(8), 863-867. doi: 10.1038/ng1604.

Mihaylova MM, Vasquez DS, Ravnskjaer K, Denechaud PD, Yu RT, Alvarez JG, *et al*. (2011). Class IIa histone deacetylases are hormone-activated regulators of

FOXO and mammalian glucose homeostasis. *Cell* **145**, 607-621. doi: 10.1016/j.cell.2011.03.043.

Minster RL, Hawley NL, Su CT, Sun G, Kershaw EE, Cheng H, *et al*. (2016). A thrifty variant in *CREBRF* strongly influences body mass index in Samoans. *Nat Genet* **48**, 1049-1054. doi: 10.1038/ng.3620.

Mirzoev TM (2020). Skeletal muscle recovery from disuse atrophy: protein turnover signaling and strategies for accelerating muscle regrowth. *Int J Mol Sci* **21**, 7940. doi: 10.3390/ijms21217940.

Misra J, Chanda D, Kim DK, Cho SR, Koo SH, Lee CH, Back SH & Choi HS (2014). Orphan nuclear receptor Errγ induces C-reactive protein gene expression through induction of ER-bound Bzip transmembrane transcription factor CREBH. *PLoS One* **9**, e86342. doi: 10.1371/journal.pone.0086342.

Mittendorfer B, Horowitz JF & Klein S (2002). Effect of gender on lipid kinetics during endurance exercise of moderate intensity in untrained subjects. *Am J Physiol Endocrinol Metab* **283**, E58-E65. doi: 10.1152/ajpendo.00504.2001.

Miyamoto T (2006). The dendritic cell-specific transmembrane protein DC-STAMP is essential for osteoclast fusion and osteoclast bone-resorbing activity. *Mod Rheumatol* **16**, 341-342. doi: 10.1007/s10165-006-0524-0.

Mizokami A, Yasutake Y, Higashi S, Kawakubo-Yasukochi T, Chishaki S, Takahashi I, *et al*. (2014). Oral administration of osteocalcin improves glucose utilisation by stimulating glucagon-like peptide-1 secretion. *Bone* **69**, 68-79. doi: 10.1016/j.bone.2014.09.006.

Moisan MP & Castanon N (2016). Emerging role of corticosteroid-binding globulin in glucocorticoid-driven metabolic disorders. *Front Endocrinol (Lausanne)* **7**, 160. doi: 10.3389/fendo.2016.00160.

Moisan M-P (2021). Sexual dimorphism in glucocorticoid stress response. *Int J Mol Sci* **22**, 3139. doi: 10.3390/ijms22063139.

Monternier P-A, Fongy A, Hervant F, Drai J, Collin-Chavagnac D, Rouanet J-L, *et al*. (2015). Skeletal muscle phenotype affects fasting-induced mitochondrial oxidative phosphorylation flexibility in cold-acclimated ducklings. *J Exp Biol* **218**, 2427-2434. doi: 10.1242/jeb.122671.

Montgomery E, Pennington C, Isales CM & Hamrick MW (2005). Muscle-bone interactions in dystrophin-deficient and myostatin-deficient mice. *Anat Rec A Discov Mol Cell Evol Biol* **286**, 814-822. doi: 10.1002/ar.a.20224.

Montgomery MK, Brown SHJ, Lim XY, Fiveash CE, Osborne B, Bentley NL, *et al*. (2016). Regulation of glucose homeostasis and insulin action by ceramide acyl-chain length: a beneficial role for very long-chain sphingolipid species. *Biochim Biophys Acta* **1861**, 1828-1839. doi: 10.1016/j.bbalip.2016.08.016.

Montgomery MK, Hallahan NL, Brown SH, Liu M, Mitchell TW, Cooney GJ, *et al*. (2013). Mouse strain-dependent variation in obesity and glucose homeostasis in response to high-fat feeding. *Diabetologia* **56**, 1129-1139. doi: 10.1007/s00125-013-2846-8.

Morais P, Adachi H & Yu Y-T (2021). Spliceosomal snRNA epitranscriptomics. *Front Genet* **12**, 652129. doi: 10.3389/fgene.2021.652129.

Morita M, Gravel S-P, Chénard V, Sikström K, Zheng L, Alain T, *et al*. (2013). mTORC1 controls mitochondrial activity and biogenesis through 4E-BP-dependent translational regulation. *Cell Metab* **18**, 698-711. doi: 10.1016/j.cmet.2013.10.001.

Mosialou I, Shikhel S, Liu J-M, Maurizi A, Luo N, He Z, *et al*. (2017). MC4R-dependent suppression of appetite by bone-derived lipocalin 2. *Nature* **543**, 385-390. doi: 10.1038/nature21697.

Mothe-Satney I, Gautier N, Hinault C, Lawrence JC Jr & Van Obberghen E (2004). In rat hepatocytes glucagon increases mammalian target of rapamycin phosphorylation on serine 2448 but antagonises the phosphorylation of its downstream targets induced by insulin and amino acids. *J Biol Chem* **279**, 42628-42637. doi: 10.1074/jbc.M405173200.

Motyl KJ, McCabe LR & Schwartz AV (2010). Bone and glucose metabolism: a two-way street. *Arch Biochem Biophys* **503**, 2-10. doi: 10.1016/j.abb.2010.07.030.

Mueller KM, Hartmann K, Kaltenecker D, Vettorazzi S, Bauer M, Mauser L, *et al*. (2017). Adipocyte glucocorticoid receptor deficiency attenuates aging- and HFD-induced obesity and impairs the feeding-fasting transition. *Diabetes* **66**, 272-286. doi: 10.2337/db16-0381.

Muller FL, Song W, Jang YC, Liu Y, Sabia M, Richardson A, *et al*. (2007). Denervation-induced skeletal muscle atrophy is associated with increased mitochondrial ROS production. *Am J Physiol Regul Integr Comp Physiol* **293**, R1159-R1168. doi: 10.1152/ajpregu.00767.2006.

Müller WA, Faloona GR & Unger RH (1973). Hyperglucagonemia in diabetic ketoacidosis. Its prevalence and significance. *Am J Med* **54**, 52-57. doi: 10.1016/0002-9343(73)90083-1.

Müller-Nedebock AC, Brennan RR, Venter M, Pienaar IS, van der Westhuizen FH, Elson JL, *et al*. (2019). The unresolved role of mitochondrial DNA in Parkinson's disease: an overview of published studies, their limitations, and future prospects. *Neurochem Int* **129**, 104495. doi: 10.1016/j.neuint.2019.104495.

Murach KA, McCarthy JJ, Peterson CA & Dungan CM (2020). Making mice mighty: recent advances in translational models of load-induced muscle hypertrophy. *J Appl Physiol (1985)* **129**, 516-521. doi: 10.1152/japplphysiol.00319.2020.

Myles S, Hradetzky E, Engelken J, Lao O, Nürnberg P, Trent RJ, *et al*. (2007). Identification of a candidate genetic variant for the high prevalence of type II diabetes in Polynesians. *Eur J Hum Genet* **15**, 584-589. doi: 10.1038/sj.ejhg.5201793.

Myles S, Lea RA, Ohashi J, Chambers GK, Weiss JG, Hardouin E, *et al*. (2011). Testing the thrifty gene hypothesis: the Gly482Ser variant in *PPARGC1A* is associated with BMI in Tongans. *BMC Med Genet* **12**, 10. doi: 10.1186/1471-2350-12-10.

Nabuurs CI, Choe CU, Veltien A, Kan HE, van Loon LJC, Rodenburg RJT, *et al*. (2013). Disturbed energy metabolism and muscular dystrophy caused by pure creatine deficiency are reversible by creatine intake. *Journal of Physiology* **591**, 571-592. doi: 10.1113/jphysiol.2012.241760.

Nadanaka S, Okada T, Yoshida H & Mori K (2007). Role of disulphide bridges formed in the luminal domain of ATF6 in sensing endoplasmic reticulum stress. *Mol Cell Biol* **27**, 1027-1043. doi: 10.1128/MCB.00408-06.

Naito T, Kuma A & Mizushima N (2013). Differential contribution of insulin and amino acids to the mTORC1-autophagy pathway in the liver and muscle. *J Biol Chem* **288**, 21074-21081. doi: 10.1074/jbc.M113.456228.

Naka I, Furusawa T, Kimura R, Natsuhara K, Yamauchi T, Nakazawa M, *et al*. (2017). A missense variant, rs373863828-A (p.Arg457Gln), of *CREBRF* and body mass index in Oceanic populations. *J Hum Genet* **62**, 847-849. doi: 10.1038/jhg.2017.44.

Nakao R, Abe T, Yamamoto S & Oishi K (2019). Ketogenic diet induces skeletal muscle atrophy via reducing muscle protein synthesis and possibly activating proteolysis in mice. *Sci Rep* **9**, 19652. doi: 10.1038/s41598-019-56166-8..

Nason SR, Kim T, Antipenko JP, Finan B, DiMarchi R, Hunter CS & Habegger KM (2020). Glucagon-receptor signalling reverses hepatic steatosis independent of

leptin receptor expression. *Endocrinology* **161**, bqz013. doi: 10.1210/endocr/bqz013.

Natera-Naranjo O, Kar AN, Aschrafi A, Gervasi NM, Macgibeny MA, Gioio AE & Kaplan BB (2012). Local translation of ATP synthase subunit 9 mRNA alters ATP levels and the production of ROS in the axon. *Mol Cell Neurosci* **49**, 263-270. doi: 10.1016/j.mcn.2011.12.006.

National Institutes of Health (2015). Consideration of sex as a biological variable in NIH-funded research. Available at: https://grants.nih.gov/grants/guide/notice-files/NOT-OD-15-102.html.

Nazare J-A, Smith JD, Borel A-L, Haffner SM, Balkau B, Ross R, *et al*. (2012). Ethnic influences on the relations between abdominal subcutaneous and visceral adiposity, liver fat, and cardiometabolic risk profile: the International Study of Prediction of Intra-Abdominal Adiposity and Its Relationship with Cardiometabolic Risk/Intrabdominal Adiposity. *Am J Clin Nutr* **96**, 714-726. doi: 10.3945/ajcn.112.035758.

Nazarov PV, Muller A, Kaoma T, Nicot N, Maximo C, Birembaut P, *et al*. (2017). RNA sequencing and transcriptome arrays analyses show opposing results for alternative splicing in patient derived samples. *BMC Genomics* **18**, 443. doi: 10.1186/s12864-017-3819-y.

Neel JV (1962). Diabetes Mellitus: a "thrifty" genotype rendered detrimental by "progress"? *Am J Hum Genet* **14**, 353-362.

Neel JV (1999). The 'thrifty genotype' in 1998. *Nut Rev* **57**, S2-S9.

Nielsen S, Guo Z, Albu JB, Klein S, O'Brien PC & Jensen MD (2003). Energy expenditure, sex, and endogenous fuel availability in humans. *J Clin Invest* **111**, 981-988. doi: 10.1172/JCI16253.

Nikitina TV, Tischenko LI & Schulz WA (2011). Recent insights into regulation of transcription by RNA polymerase III and the cellular functions of its transcripts. *Biol Chem* **392**, 395-404. doi: 10.1515/BC.2011.049.

Nna VU, Bakar ABA, Ahmad A & Mohamed M (2019). Down-regulation of steroidogenesis-related genes and its accompanying fertility decline in streptozotocin-induced diabetic male rats: ameliorative effect of metformin. *Andrology* **7**, 110-123. doi: 10.1111/andr.12567.

Noblet B, Benhamed F, O-Sullivan I, Zhang W, Filhoulaud G, Montagner A, *et al*. (2021). Dual regulation of TxNIP by ChREBP and FoxO1 in liver. *iScience* **24**, 102218. doi: 10.1016/j.isci.2021.102218.

Nogalska A, Wojcik S, Engel WK, McFerrin J & Askanas V (2007). Endoplasmic reticulum stress induces myostatin precursor protein and NF-kappaB in cultured human muscle fibers: relevance to inclusion body myositis. *Exp Neurol* **204**, 610-618. doi: 10.1016/j.expneurol.2006.12.014.

Noguchi R, Kubota H, Yugi K, Toyoshima Y, Komori Y, Soga T, *et al*. (2013). The selective control of glycolysis, gluconeogenesis and glycogenesis by temporal insulin patterns. *Mol Syst Biol* **9**, 664. doi: 10.1038/msb.2013.19.

Noshiro M, Usui E, Kawamoto T, Kubo H, Fujimoto K, Furukawa M, *et al*. (2007). Multiple mechanisms regulate circadian expression of the gene for cholesterol 7alpha-hydroxylase (Cyp7a), a key enzyme in hepatic bile acid biosynthesis. *J Biol Rhythms* **22**, 299-311. doi: 10.1177/0748730407302461.

O'Rahilly S & Farooqi IS (2008). Human obesity: a heritable neurobehavioural disorder that is highly sensitive to environmental conditions. *Diabetes* **57**(11), 2905-2910. doi: 10.2337/db08-0210.

Oberbach A, Bossenz Y, Lehmann S, Niebauer J, Adams V, Paschke R, *et al*. (2006). Altered fiber distribution and fiber-specific glycolytic and oxidative enzyme activity in skeletal muscle of patients with type 2 diabetes. *Diabetes Care* **29**, 895-900. doi: 10.2337/diacare.29.04.06.dc05-1854.

Obrochta KM, Krois CR, Campos B & Napoli JL (2015). Insulin regulates retinol dehydrogenase expression and all-trans-retinoic acid biosynthesis through FoxO1. *J Biol Chem* **290**, 7259-7268. doi: 10.1074/jbc.M114.609313.

Oh K-J, Han H-S, Kim M-J & Koo S-H (2013). CREB and FoxO1: two transcription factors for the regulation of hepatic gluconeogenesis. *BMB Rep* **46**, 567-574. doi: 10.5483/bmbrep.2013.46.12.248.

Ohainle M, Kim K, Keceli SK, Felton A, Campbell E, Luban J, *et al*. (2020). TRIM34 restricts HIV-1 and SIV capsids in a TRIM5α-dependent manner. *PLoS Pathog* **16**, e1008507. doi: 10.1371/journal.ppat.1008507.

Ohashi J, Naka I, Furusawa T, Kimura R, Natsuhara K, Yamauchi T, *et al*. (2018). Association study of CREBRF missense variant (rs373863828:G > A; p.Arg457Gln) with levels of serum lipid profile in the Pacific populations. *Ann Hum Biol* **45**, 215-219. doi: 10.1080/03014460.2018.1461928.

Ohashi J, Naka I, Kimura R, Natsuhara K, Yamauchi T, Furusawa T, *et al*. (2007). *FTO* polymorphisms in oceanic populations. *J Hum Genet* **52**(12)**,** 1031-1035. doi: 10.1007/s10038-007-0198-2.

Ohashi J, Naka I, Tokunaga K, Inaoka T, Ataka Y, Nakazawa M, *et al*. (2006). Brief communication: mitochondrial DNA variation suggests extensive gene flow from Polynesian ancestors to indigenous Melanesians in the northwestern Bismarck Archipelago. *Am J Phys Anthropol* **130**, 551-556. doi: 10.1002/ajpa.20383.

Oh-Hashi K, Hasegawa T, Mizutani Y, Takahashi K & Hirata Y (2021a). Elucidation of brefeldin A-induced ER and Golgi stress responses in Neuro2a cells. *Mol Cell Biochem* doi: 10.1007/s11010-021-04187-1.

Oh-Hashi K, Hasegawa T, Naruse Y & Hirata Y (2021b). Molecular characterisation of mouse CREB3 regulatory factor in Neuro2a cells. *Mol Biol Rep* **48**, 5411-5420. doi: 10.1007/s11033-021-06543-2.

Oh-hashi K, Soga A, Naruse Y, Takahashi K, Kazutoshi K & Hirata Y (2018). Elucidating post-translational regulation of mouse CREB3 in Neuro2a cells. *Mol Cell Biochem* **448**, 287-297. doi: 10.1007/s11010-018-3333-9.

Oh-Hashi K, Takahashi K & Hirata Y (2019). Regulation of the ER-bound transcription factor Luman/CREB3 in HEK293 cells. *FEBS Lett* **593**, 2771-2778. doi: 10.1002/1873-3468.13535.

Oh-Hashi K, Yamamoto A, Murase R & Hirata Y (2021c). Comparative analysis of CREB3 and CREB3L2 protein expression in HEK293 cells. *Int J Mol Sci* **22**, 2767. doi: 10.3390/ijms22052767.

Oishi K, Amagai N, Shirai H, Kadota K, Ohkura N & Ishida N (2005). Genome-wide expression analysis reveals 100 adrenal gland-dependent circadian genes in the mouse liver. *DNA Res* **12**, 191-202. doi: 10.1093/dnares/dsi003.

Okada Y, Kubo M, Ohmiya H, Takahashi A, Kumasaka N, Hosono N, *et al*. (2012). Common variants at CDKAL1 and KLF9 are associated with body mass index in east Asian populations. *Nat Genet* **44**(3), 302-306. doi: 10.1038/ng.1086.

Okun JG, Conway S, Schmidt KV, Schumacher J, Wang X, de Guia R, *et al*. (2015). Molecular regulation of urea cycle function by the liver glucocorticoid receptor. *Mol Metab* **4**, 732-740. doi: 10.1016/j.molmet.2015.07.006.

Okun JG, Rusu PM, Chan AY, Wu Y, Yap YW, Sharkie T, *et al*. (2021). Liver alanine catabolism promotes skeletal muscle atrophy and hyperglycaemia in type 2 diabetes. *Nat Metab* **3**, 394-409. doi: 10.1038/s42255-021-00369-9.

Oliveira-de-Lira L, Santos EMC, de Souza RF, Matos RJB, da Silva MC, Oliveira LDS, *et al*. (2018). Supplementation-dependent effects of vegetable oils with varying

fatty acid compositions on anthropometric and biochemical parameters in obese women. *Nutrients* **10**, 932. doi: 10.3390/nu10070932.

Orlando G, Balducci S, Bazzucchi I, Pugliese G & Sacchetti M (2017). Muscle fatigability in type 2 diabetes. *Diabetes Metab Res Rev* **33**, e2821. doi: 10.1002/dmrr.2821.

Ostbye T, Welby TJ, Prior IA, Salmond CE & Stokes YM (1989). Type 2 (non-insulin-dependent) diabetes mellitus, migration and westernisation: the Tokelau Island migrant study. *Diabetologia* **32**, 585-590. doi: 10.1007/BF00285332.

Ostler JE, Maurya SK, Dials J, Roof SR, Devor ST, Ziolo MT, *et al*. (2014). Effects of insulin resistance on skeletal muscle growth and exercise capacity in type 2 diabetic mouse models. *Am J Physiol Endocrinol Metab* **306**, E592-E605. doi: 10.1152/ajpendo.00277.2013.

Otero YF, Stafford JM & McGuinness OP (2014). Pathway-selective insulin resistance and metabolic disease: the importance of nutrient flux. *J Biol Chem* **289**, 20462-20469. doi: 10.1074/jbc.R114.576355.

Oyama S, Duckham RL, Arslanian KJ, Kershaw EE, Strayer JA, Fidow UT, *et al*. (2021). Body size and composition of Samoan toddlers aged 18-25 months in 2019. *Ann Hum Biol*. doi: 10.1080/03014460.2021.1951351.

Oyola MG & Handa RJ (2017). Hypothalamic-pituitary-adrenal and hypothalamic-pituitary-gonadal axes: sex differences in regulation of stress responsivity. *Stress* **20**, 476-494. doi: 10.1080/10253890.2017.1369523.

Ozcan L, Wong CCL, Li G, Xu T, Pajvani U, Park SKR, *et al*. (2012). Calcium signalling through CaMKII regulates hepatic glucose production in fasting and obesity. *Cell Metab* **15**, 739-751. doi: 10.1016/j.cmet.2012.03.002.

Ozcan U, Yilmaz E, Ozcan L, Furuhashi M, Vaillancourt E, Smith RO, *et al*. (2006). Chemical chaperones reduce ER stress and restore glucose homeostasis in a mouse model of type 2 diabetes. *Science* **313**, 1137-1140. doi: 10.1126/science.1128294.

Paek J, Kalocsay M, Staus DP, Wingler L, Pascolutti R, Paulo JA, *et al*. (2017). Multidimensional tracking of GPCR signalling via peroxidase-catalysed proximity labelling. *Cell* **169**, 338-349.e11. doi: 10.1016/j.cell.2017.03.028.

Pandak WM, Bohdan P, Franklund C, Mallonee DH, Eggertsen G, Björkhem I, *et al*. (2001). Expression of sterol 12alpha-hydroxylase alters bile acid pool composition in primary rat hepatocytes and in vivo. *Gastroenterology* **120**, 1801-1809. doi: 10.1053/gast.2001.24833.

Park JH, Lee NK & Lee SY (2017a). Current understanding of RANK signalling in osteoclast differentiation and maturation. *Mol Cells* **40**, 706-713. doi: 10.14348/molcells.2017.0225.

Park J-L, Lee Y-S, Kunkeaw N, Kim S-Y, Kim I-H & Lee YS (2017b). Epigenetic regulation of noncoding RNA transcription by mammalian RNA polymerase III. *Epigenomics* **9**, 171-187. doi: 10.2217/epi-2016-0108.

Park SW, Goodpaster BH, Lee JS, Kuller LH, Boudreau R, de Rekeneire N, *et al*. (2009). Excessive loss of skeletal muscle mass in older adults with type 2 diabetes. *Diabetes Care* **32,** 1993-1997. doi: 10.2337/dc09-0264.

Park SW, Goodpaster BH, Strotmeyer ES, de Rekeneire N, Harris TB, Schwartz AV, *et al*. (2006). Decreased muscle strength and quality in older adults with type 2 diabetes. *Diabetes* **55**, 1813-1818. doi: 10.2337/db05-1183.

Parkash R & Aggarwal DD (2012). Trade-off of energy metabolites as well as body colour phenotypes for starvation and desiccation resistance in montane populations of Drosophila melanogaster. *Comp Biochem Physiol A Mol Integr Physiol* **161**, 102-113. doi: 10.1016/j.cbpa.2011.09.010.

Parks EJ & Hellerstein MK (2006). Thematic review series: patient-oriented research. Recent advances in liver triacylglycerol and fatty acid metabolism using stable isotope labelling techniques. *J Lipid Res* **47**, 1651-1660. doi: 10.1194/jlr.R600018-JLR200.

Patel K, Foretz M, Marion A, Campbell DG, Gourlay R, Boudaba N, *et al*. (2014). The LKB1-salt-inducible kinase pathway functions as a key gluconeogenic suppressor in the liver. *Nature Communications* **5**, 4535. doi: 10.1038/ncomms5535.

Pathak P & Chiang JYL (2019). Sterol 12α-hydroxylase aggravates dyslipidemia by activating the ceramide/mTORC1/SREBP-1c pathway via FGF21 and FGF15. *Gene Expr* **19**, 161-173. doi: 10.3727/105221619X15529371970455.

Patience JF, Rossoni-Serão MC & Gutiérrez NA (2015). A review of feed efficiency in swine: biology and application. *J Anim Sci Biotechnol* **6**, 33. doi: 10.1186/s40104-015-0031-2.

Paul BD, Snyder SH & Kashfi K (2021). Effects of hydrogen sulfide on mitochondrial function and cellular bioenergetics. *Redox Biol* **38**, 101772. doi: 10.1016/j.redox.2020.101772.

Pawar A & Jump DB (2003). Unsaturated fatty acid regulation of peroxisome proliferator-activated receptor alpha activity in rat primary hepatocytes. *J Biol Chem* **278**, 35931-35939. doi: 10.1074/jbc.M306238200.

Pearen MA, Myers SA, Raichur S, Ryall JG, Lynch GS & Muscat GEO (2008). The orphan nuclear receptor, NOR-1, a target of beta-adrenergic signalling, regulates gene expression that controls oxidative metabolism in skeletal muscle. *Endocrinology* **149**, 2853-2865. doi: 10.1210/en.2007-1202.

Pedersen SB, Kristensen K, Hermann PA, Katzenellenbogen JA & Richelsen B (2004). Estrogen controls lipolysis by up-regulating alpha2A-adrenergic receptors directly in human adipose tissue through the estrogen receptor alpha. Implications for the female fat distribution. *J Clin Endocrinol Metab* **89**, 1869-1878. doi: 10.1210/jc.2003-031327.

Pederson BA, Cope CR, Schroeder JM, Smith MW, Irimia JM, Thurberg BL, *et al*. (2005). Exercise capacity of mice genetically lacking muscle glycogen synthase: in mice, muscle glycogen is not essential for exercise. *J Biol Chem* **280**, 17260-17265. doi: 10.1074/jbc.M410448200.

Penney J (2017). Characterisation of the potential role of Luman as a novel regulator of animal stress responses. PhD thesis, University of Guelph, Ontario, Canada.

Penney J, Mendell A, Zeng M, Tran K, Lymer J, Turner PV, *et al*. (2017). LUMAN/CREB3 is a key regulator of glucocorticoid-mediated stress responses. *Mol Cell Endocrinol* **439**, 95-104. doi:10.1016/j.mce.2016.10.022.

Penney J, Taylor T, MacLusky N & Lu R (2018). LUMAN/CREB3 plays a dual role in stress responses as a cofactor of the glucocorticoid receptor and a regulator of secretion. *Front Mol Neurosci* **11**, 352. doi: 10.3389/fnmol.2018.00352.

Pereira MJ, Thombare K, Sarsenbayeva A, Kamble PG, Almby K, Lundqvist M, *et al*. (2020). Direct effects of glucagon on glucose uptake and lipolysis in human adipocytes. *Mol Cell Endocrinol* **503**, 110696. doi: 10.1016/j.mce.2019.110696.

Perlman RL (2016). Mouse models of human disease. *Evol Med Public Health* **2016**, 170-176. doi: 10.1093/emph/eow014.

Perry RJ, Zhang D, Guerra MT, Brill AL, Goedeke L, Nasiri AR, *et al*. (2020). Glucagon stimulates gluconeogenesis by INSP3R1-mediated hepatic lipolysis. *Nature* **579**, 279-283. doi: 10.1038/s41586-020-2074-6.

Petersen KF, Laurent D, Rothman DL, Cline GW & Shulman GI (1998). Mechanism by which glucose and insulin inhibit net hepatic glycogenolysis in humans. *J Clin Invest* **101**, 1203-1209. doi: 10.1172/JCI579.

Petersen MC & Shulman GI (2017). Roles of diacylglycerols and ceramides in hepatic insulin resistance. *Trends Pharmacol Sci* **38**, 649-665. doi: 10.1016/j.tips.2017.04.004.

Pilegaard H, Osada T, Andersen LT, Helge JW, Saltin B & Neufer PD (2005). Substrate availability and transcriptional regulation of metabolic genes in human skeletal muscle during recovery from exercise. *Metabolism* **54**, 1048-1055. doi: 10.1016/j.metabol.2005.03.008.

Pino MF, Stephens NA, Eroshkin AM, Yi F, Hodges A, Cornnell HH, *et al*. (2019). Endurance training remodels skeletal muscle phospholipid composition and increases intrinsic mitochondrial respiration in men with type 2 diabetes. *Physiol Genomics* **51**, 586-595. doi: 10.1152/physiolgenomics.00014.2019.

Pinto BAS, França LM, Laurindo FRM & Paes AMA (2019). Unfolded protein response: cause or consequence of lipid and lipoprotein metabolism disturbances? *Adv Exp Med Biol* **1127**, 67-82. doi: 10.1007/978-3-030-11488-6_5.

Pitteloud N, Mootha VK, Dwyer AA, Hardin M, Lee H, Eriksson K-F, *et al*. (2005). Relationship between testosterone levels, insulin sensitivity, and mitochondrial function in men. *Diabetes Care* **28**, 1636-1642. doi: 10.2337/diacare.28.7.1636.

Plochocki JH, Rivera JP, Zhang C & Ebba SA (2008). Bone modelling response to voluntary exercise in the hindlimb of mice. *J Morphol* **269**, 313-318. doi: 10.1002/jmor.10587.

Poulsen Ll, Siersbæk M & Mandrup S (2012). PPARs: fatty acid sensors controlling metabolism. *Semin Cell Dev Biol* **23**, 631-639. doi: 10.1016/j.semcdb.2012.01.003.

Powers SK, Wiggs MP, Duarte JA, Zergeroglu AM & Demirel HA (2012). Mitochondrial signalling contributes to disuse muscle atrophy. *Am J Physiol Endocrinol Metab* **303**, E31-E39. doi: 10.1152/ajpendo.00609.2011.

Priante E, Verlato G, Giordano G, Stocchero M, Visentin S, Mardegan V, *et al*. (2019). Intrauterine growth restriction: new insight from the metabolomic approach. *Metabolites* **9**, 267. doi: 10.3390/metabo9110267.

Primeau V, Coderre L, Karelis AD, Brochu M, Lavoie ME, Messier V, *et al*. (2011). Characterizing the profile of obese patients who are metabolically healthy. *Int J Obes (Lond)* **35**, 971-981. doi: 10.1038/ijo.2010.216.

Proctor D, Melton L, Khosla S, Crowson CS, O'Connor MK & Riggs BL (2000). Relative influence of physical activity, muscle mass and strength on bone density. *Osteoporos Int* **11**, 944-952. doi: 10.1007/s001980070033.

Proud CG (2006). Regulation of protein synthesis by insulin. *Biochem Soc Trans* **34**, 213-216. doi: 10.1042/BST20060213.

Pugach I, Duggan AT, Merriwether DA, Friedlaender FR, Friedlaender JS & Stoneking M (2018). The gateway from near into remote Oceania: new insights from genome-wide data. *Mol Biol Evol* **35**, 871-886. doi: 10.1093/molbev/msx333.

Qasim A, Turcotte M, de Souza RJ, Samaan MC, Champredon D, Dushoff J, *et al*. (2018). On the origin of obesity: identifying the biological, environmental and cultural drivers of genetic risk among human populations. *Obes Rev* **19**, 121-149. doi: 10.1111/obr.12625.

Qi L, Kraft P, Hunter DJ & Hu FB (2008). The common obesity variant near *MC4R* gene is associated with higher intakes of total energy and dietary fat, weight change and diabetes risk in women. *Hum Mol Genet* **17**(22), 3502-3508. doi: 10.1093/hmg/ddn242.

Qi M, Lei T, Zhou L, Chen XD, Long H, Long QQ, *et al*. (2009). Cloning, characterisation, chromosomal mapping and tissue transcription analysis of porcine CREB2 and CREB3 genes. *Folia Biol (Praha)* **55**, 137-144.

Qi Q, Downer MK, Kilpeläinen TO, Taal HR, Barton SJ, Ntalla I, *et al*. (2015). Dietary intake, FTO genetic variants, and adiposity: a combined analysis of over 16,000 children and adolescents. *Diabetes* **64**(7), 2467-2476. doi: 10.2337/db14-1629.

Qin W, Pan J, Qin Y, Lee DN, Bauman WA & Cardozo C (2014). Identification of functional glucocorticoid response elements in the mouse FoxO1 promoter. *Biochem Biophys Res Commun* **450**, 979-983. doi: 10.1016/j.bbrc.2014.06.080.

Quagliarini F, Mir AA, Balazs K, Wierer M, Dyar KA, Jouffe C, *et al*. (2019). Cistromic reprogramming of the diurnal glucocorticoid hormone response by high-fat diet. *Mol Cell* **76**, 531-545. doi: 10.1016/j.molcel.2019.10.007.

Quy PN, Kuma A, Pierre P & Mizushima N (2013). Proteasome-dependent activation of mammalian target of rapamycin complex 1 (mTORC1) is essential for autophagy suppression and muscle remodelling following denervation. *J Biol Chem* **288**, 1125-1134. doi: 10.1074/jbc.M112.399949.

Raggo C, Rapin N, Stirling J, Gobeil P, Smith-Windsor E, O'Hare P, *et al*. (2002). Luman, the cellular counterpart of herpes simplex virus VP16, is processed by

regulated intramembrane proteolysis. *Mol Cell Biol* **22**, 5639-5649. doi: 10.1128/MCB.22.16.5639-5649.2002.

Rajak S, Xie S, Tewari A, Raza S, Wu Y, Bay B-H, *et al*. (2021). MTORC1 inhibition drives crinophagic degradation of glucagon. *Mol Metab* **53**, 101286. doi: 10.1016/j.molmet.2021.101286.

Ramirez ME, McMurry MP, Wiebke GA, Felten KJ, Ren K, Meikle AW, *et al*. (1997). Evidence for sex steroid inhibition of lipoprotein lipase in men: comparison of abdominal and femoral adipose tissue. *Metabolism* **46**, 179-185. doi: 10.1016/s0026-0495(97)90299-7.

Ratnam S, Wijekoon EP, Hall B, Garrow TA, Brosnan ME & Brosnan JT (2006). Effects of diabetes and insulin on betaine-homocysteine S-methyltransferase expression in rat liver. *Am J Physiol Endocrinol Metab* **290**, E933-E939. doi: 10.1152/ajpendo.00498.2005.

Rauch A, Seitz S, Baschant U, Schilling AF, Illing A, Stride B, *et al*. (2010). Glucocorticoids suppress bone formation by attenuating osteoblast differentiation via the monomeric glucocorticoid receptor. *Cell Metab* **11**, 517-531. doi: 10.1016/j.cmet.2010.05.005.

Reales G, Rovaris DL, Jacovas VC, Hünemeier T, Sandoval JR, Salazar-Granara A, *et al*. (2017). A tale of agriculturalists and hunter-gatherers: exploring the thrifty genotype hypothesis in native South Americans. *Am J Phys Anthropol* **163**, 591-601. doi: 10.1002/ajpa.23233.

Reaven GM, Chen YD, Golay A, Swislocki AL & Jaspan JB (1987). Documentation of hyperglucagonemia throughout the day in nonobese and obese patients with noninsulin-dependent diabetes mellitus. *J Clin Endocrinol Metab* **64**, 106-110. doi: 10.1210/jcem-64-1-106.

Rebrin K, Steil GM, Getty L & Bergman RN (1995). Free fatty acid as a link in the regulation of hepatic glucose output by peripheral insulin. *Diabetes* **44**, 1038-1045. doi: 10.2337/diab.44.9.1038.

Reddy AB, Maywood ES, Karp NA, King VM, Inoue Y, Gonzalez FJ, *et al*. (2007). Glucocorticoid signalling synchronises the liver circadian transcriptome. *Hepatology* **45**, 1478-1488. doi: 10.1002/hep.21571.

Reeves PG (1989). AIN-76 diet: should we change the formulation? *J Nutr* **119**, 1081-1082. doi: 10.1093/jn/119.8.1081.

Regitz-Zagrosek V, Lehmkuhl E & Mahmoodzadeh S (2007). Gender aspects of the role of the metabolic syndrome as a risk factor for cardiovascular disease. *Gend Med* **4**, S162-S177. doi: 10.1016/s1550-8579(07)80056-8.

Reid IR, Mackie M & Ibbertson HK (1986). Bone mineral content in Polynesian and white New Zealand women. *Br Med J (Clin Res Ed)* **292**, 1547-1548. doi: 10.1136/bmj.292.6535.1547.

Reiling JH, Olive AJ, Sanyal S, Carette JE, Brummelkamp TR, Ploegh HL, *et al*. (2013). A CREB3-ARF4 signalling pathway mediates the response to Golgi stress and susceptibility to pathogens. *Nat Cell Biol* **15**, 1473-1485. doi: 10.1038/ncb2865..

Rennert C, Vlaic S, Marbach-Breitrück E, Thiel C, Sales S, Shevchenko A, *et al*. (2018). The diurnal timing of starvation differently impacts murine hepatic gene expression and lipid metabolism – a systems biology analysis using self-organising maps. *Front Physiol* **9**, 1180. doi: 10.3389/fphys.2018.01180.

Renzini A, Riera CS, Minic I, D'Ercole C, Lozanoska-Ochser B, Cedola A, *et al*. (2021). Metabolic remodelling in skeletal muscle atrophy as a therapeutic target. *Metabolites* **11**, 517. doi: 10.3390/metabo11080517.

Reue K (2017). Sex differences in obesity: X chromosome dosage as a risk factor for increased food intake, adiposity and co-morbidities. *Physiol Behav* **176**, 174-182. doi: 10.1016/j.physbeh.2017.02.040.

Reusch JEB, Kumar TR, Regensteiner JG, Zeitler PS & Conference Participants (2018). Identifying the critical gaps in research on sex differences in metabolism across the life span. *Endocrinology* **159**, 9-19. doi: 10.1210/en.2017-03019.

Ricoult SJH & Manning BD (2013). The multifaceted role of mTORC1 in the control of lipid metabolism. *EMBO Rep* **14**, 242-251. doi: 10.1038/embor.2013.5.

Rion S & Kawecki TJ (2007). Evolutionary biology of starvation resistance: what we have learned from Drosophila. *J Evol Biol* **20**, 1655-1664. doi: 10.1111/j.1420-9101.2007.01405.x.

Rocha M, Diaz-Morales N, Rovira-Llopis S, Escribano-Lopez I, Bañuls C, Hernandez-Mijares A, *et al*. (2016). Mitochondrial dysfunction and endoplasmic reticulum stress in diabetes. *Curr Pharm Des* **22**, 2640-2649. doi: 10.2174/1381612822666160209152033.

Rochlani Y, Pothineni NV & Mehta JL (2015). Metabolic syndrome: does it differ between women and men? *Cardiovasc Drugs Ther* **29**, 329-338. doi: 10.1007/s10557-015-6593-6.

Röhrl C & Stangl H (2018). Cholesterol metabolism – physiological regulation and pathophysiological deregulation by the endoplasmic reticulum. *Wien Med Wochenschr* **168**, 280-285. doi: 10.1007/s10354-018-0626-2.

Roisné-Hamelin G, Moro J, Delhaye N, Calvez J, Chaumontet C, Even P, *et al*. (2021). Lower synthesis and higher catabolism of liver and muscle protein compensate for amino acid deficiency in severely protein-restricted growing rat. *Curr Dev Nutr* **5**, 518. doi: 10.1093/cdn/nzab041_033.

Rolfe DF & Brown GC (1997). Cellular energy utilisation and molecular origin of standard metabolic rate in mammals. *Physiol Rev* **77**, 731-758. doi: 10.1152/physrev.1997.77.3.731.

Romanello V, Guadagnin E, Gomes L, Roder I, Sandri C, Petersen Y, *et al*. (2010). Mitochondrial fission and remodelling contributes to muscle atrophy. *EMBO J* **29**, 1774-1785. doi: 10.1038/emboj.2010.60.

Romanski SA, Nelson RM & Jensen MD (2000). Meal fatty acid uptake in adipose tissue: gender effects in nonobese humans. *Am J Physiol Endocrinol Metab* **279**, E455-E462. doi: 10.1152/ajpendo.2000.279.2.E455.

Romieu I, Dossus L, Barquera S, Blottière HM, Franks PW, Gunter M, *et al*. (2017). Energy balance and obesity: what are the main drivers? *Cancer Causes Control* **28**, 247-258. doi: 10.1007/s10552-017-0869-z.

Rosa EF, Alves GA, Luz J, Silva SMA, Suchecki D, Pesquero JB, *et al*. (2014). Activation of HPA axis and remodelling of body chemical composition in response to an intense and exhaustive exercise in C57BL/6 mice. *Physiol Res* **63**, 605-613. doi: 10.33549/physiolres.932562.

Rosario FJ, Gupta MB, Myatt L, Powell TL, Glenn JP, Cox L, *et al*. (2019). Mechanistic target of rapamycin complex 1 promotes the expression of genes encoding electron transport chain proteins and stimulates oxidative phosphorylation in primary human trophoblast cells by regulating mitochondrial biogenesis. *Sci Rep* **9**, 246. doi: 10.1038/s41598-018-36265-8.

Rose AJ, Díaz MB, Reimann A, Klement J, Walcher T, Krones-Herzig A, *et al*. (2011). Molecular control of systemic bile acid homeostasis by the liver glucocorticoid receptor. *Cell Metab* **14**, 123-130. doi: 10.1016/j.cmet.2011.04.010.

Roussel D, Boël M & Romestaing C (2018). Fasting enhances mitochondrial efficiency in duckling skeletal muscle by acting on the substrate oxidation system. *J Exp Biol* **221**, jeb172213. doi: 10.1242/jeb.172213.

Rozance PJ, Jones AK, Bourque SL, D'Alessandro A, Hay WW Jr, Brown LD, *et al*. (2020). Effects of chronic hyperinsulinemia on metabolic pathways and insulin signalling in the fetal liver. *Am J Physiol Endocrinol Metab* **319**, E721-E733. doi: 10.1152/ajpendo.00323.2020.

Ruan X, Li P, Cangelosi A, Yang L & Cao H (2016). A long non-coding RNA, lncLGR, regulates hepatic glucokinase expression and glycogen storage during fasting. *Cell Rep* **14**, 1867-1875. doi: 10.1016/j.celrep.2016.01.062.

Rudolf R, Bogomolovas J, Strack S, Choi K-R, Khan MM, Wagner A, *et al*. (2013a). Regulation of nicotinic acetylcholine receptor turnover by MuRF1 connects muscle activity to endo-lysosomal and atrophy pathways. *Age (Dordr)* **35**, 1663-1674. doi: 10.1007/s11357-012-9468-9.

Rudolf R, Khan MM, Lustrino D, Labeit S, Kettelhut IC & Navegantes LCC (2013b). Alterations of cAMP-dependent signalling in dystrophic skeletal muscle. *Front Physiol* **4**, 290. doi: 10.3389/fphys.2013.00290.

Rui L (2014). Energy metabolism in the liver. *Compr Physiol* **4**, 177-197. doi: 10.1002/cphy.c130024.

Ruiz D, Padmanabhan V & Sargis RM (2020). Stress, sex, and sugar: glucocorticoids and sex-steroid crosstalk in the sex-specific misprogramming of metabolism. *J Endocr Soc* **4**, bvaa087. doi: 10.1210/jendso/bvaa087.

Rush EC, Freitas I & Plank LD (2009). Body size, body composition and fat distribution: comparative analysis of European, Maori, Pacific Island and Asian Indian adults. *Br J Nutr* **102**, 632-641. https://doi.org/10.1017/S0007114508207221.

Russell AP, Ghobrial L, Wright CR, Lamon S, Brown EL, Kon M, Skelton MR & Snow RJ (2014). Creatine transporter (SLC6A8) knockout mice display an increased capacity for *in vitro* creatine biosynthesis in skeletal muscle. *Front Physiol* **5**, 314. doi: 10.3389/fphys.2014.00314.

Russell EM, Carlson JC, Krishnan M, Hawley NL, Sun G, Cheng H, *et al*. (preprint). *CREBRF* missense variant rs373863828 has both direct and indirect effects on type 2 diabetes and fasting glucose in Polynesians living in Samoa and Aotearoa New Zealand. https://doi.org/10.1101/2021.02.15.21251768. [posted 19 Feb 2021]

Russell-Jones DL, Hoskins P, Kearney E, Morris R, Katoaga S, Slavin B, *et al*. (1990). Rural/urban differences of diabetes—impaired glucose tolerance, hypertension,

obesity, glycosylated haemoglobin, nutritional proteins, fasting cholesterol and apolipoproteins in Fijian Melanesians over 40. *Q J Med* **74**, 75-81.

Sabaratnam K, Renner M, Paesen G, Harlos K, Nair V, Owens RJ, *et al*. (2019). Insights from the crystal structure of the chicken CREB3 bZIP suggest that members of the CREB3 subfamily transcription factors may be activated in response to oxidative stress. *Protein Sci* **28**, 779-787. doi: 10.1002/pro.3573.

Sabarneh A, Ereqat S, Cauchi S, AbuShamma O, Abdelhafez M, Ibrahim M, *et al*. (2018). Common FTO rs9939609 variant and risk of type 2 diabetes in Palestine. *BMC Med Genet* **19**(1), 156. doi: 10.1186/s12881-018-0668-8.

Sailer C, Schmid V, Fritsche L, Gerter T, Machicao F, Niess A, *et al*. (2016). FTO genotype interacts with improvement in aerobic fitness on body weight loss during lifestyle intervention. *Obes Facts* **9**(3), 174-181. doi: 10.1159/000444145.

Saltiel AR & Kahn CR (2001). Insulin signalling and the regulation of glucose and lipid metabolism. *Nature* **414**(6865), 799-806. doi: 10.1038/414799a.

Samocha-Bonet D, Chisholm DJ, Tonks K, Campbell LV & Greenfield JR (2012). Insulin-sensitive obesity in humans – a 'favorable fat' phenotype? *Trends Endocrinol Metab* **23**, 116-124. doi: 10.1016/j.tem.2011.12.005.

Sampieri L, Di Giusto P & Alvarez C (2019). CREB3 transcription factors: ER-Golgi stress transducers as hubs for cellular homeostasis. *Front Cell Dev Biol* **7**, 123. doi: 10.3389/fcell.2019.00123.

Sanecka A, Ansems M, van Hout-Kuijer MA, Looman MWG, Prosser AC, Welten S, *et al*. (2012). Analysis of genes regulated by the transcription factor LUMAN identifies ApoA4 as a target gene in dendritic cells. *Mol Immunol* **50**, 66-73. doi: 10.1016/j.molimm.2011.12.003.

Satoh A, Han S-I, Araki M, Nakagawa Y, Ohno H, Mizunoe Y, *et al*. (2020). CREBH improves diet-induced obesity, insulin resistance, and metabolic disturbances by FGF21-dependent and FGF21-independent mechanisms. *iScience* **23**, 100930. doi: 10.1016/j.isci.2020.100930.

Saxton RA & Sabatini DM (2017). mTOR signalling in growth, metabolism, and disease. *Cell* **168**, 960-976. doi: 10.1016/j.cell.2017.02.004.

Schoenau E (2005). From mechanostat theory to development of the "Functional Muscle-Bone-Unit". *J Musculoskelet Neuronal Interact* **5**, 232-238.

Schönau E, Werhahn E, Schiedermaier U, Mokow E, Schiessl H, Scheidhauer K, *et al*. (1996). Influence of muscle strength on bone strength during childhood and adolescence. *Horm Res* **45 Suppl 1**, 63-66. doi: 10.1159/000184834.

Schreiner PJ, Terry JG, Evans GW, Hinson WH, Crouse JR III & Heiss G (1996). Sex-specific associations of magnetic resonance imaging-derived intra-abdominal and subcutaneous fat areas with conventional anthropometric indices. The Atherosclerosis Risk in Communities Study. *Am J Epidemiol* **144**, 335-345. doi: 10.1093/oxfordjournals.aje.a008934.

Schulz TJ, Zarse K, Voigt A, Urban N, Birringer M & Ristow M (2007). Glucose restriction extends Caenorhabditis elegans life span by inducing mitochondrial respiration and increasing oxidative stress. *Cell Metab* **6**, 280-293. doi: 10.1016/j.cmet.2007.08.011.

Schulze RJ, Schott MB, Casey CA, Tuma PL & McNiven MA (2019). The cell biology of the hepatocyte: a membrane trafficking machine. *J Cell Biol* **218**, 2096-2112. doi: 10.1083/jcb.201903090.

Schutz Y (2011). Protein turnover, ureagenesis and gluconeogenesis. *Int J Vitam Nutr Res* **81**, 101-107. doi: 10.1024/0300-9831/a000064.

Scuteri A, Sanna S, Chen WM, Uda M, Albai G, Strait J, *et al*. (2007). Genome-wide association scan shows genetic variants in the *FTO* gene are associated with obesity-related traits. *PLoS Genetics* **3**(7), e115. doi: 10.1371/journal.pgen.0030115.

Seal SV & Turner JD (2021). The 'Jekyll and Hyde' of gluconeogenesis: early life adversity, later life stress, and metabolic disturbances. *Int J Mol Sci* **22**, 3344. doi: 10.3390/ijms22073344.

Senagolage MD, Sommars MA, Ramachandran K, Futtner CR, Omura Y, Allred AL, *et al*. (2018). Loss of transcriptional repression by BCL6 confers insulin sensitivity in the setting of obesity. *Cell Rep* **25**, 3283-3298.e6. doi: 10.1016/j.celrep.2018.11.074.

Senefeld JW, Harmer AR & Hunter SK (2020a). Greater lower limb fatigability in people with prediabetes than controls. *Med Sci Sports Exerc* **52**, 1176-1186. doi: 10.1249/MSS.0000000000002238.

Senefeld JW, Keenan KG, Ryan KS, D'Astice SE, Negro F & Hunter SK (2020b). Greater fatigability and motor unit discharge variability in human type 2 diabetes. *Physiol Rep* **8**, e14503. doi: 10.14814/phy2.14503.

Senefeld JW, Singh-Peters LA, Kenno KA, Hunter SK & Jakobi JM (2020c). Greater fatigue resistance of dorsiflexor muscles in people with prediabetes than type 2 diabetes. *J Electromyogr Kinesiol* **54**, 102458. doi: 10.1016/j.jelekin.2020.102458.

Sha H, Sun S, Francisco AB, Ehrhardt N, Xue Z, Liu L, *et al*. (2014). The ER-associated degradation adaptor protein Sel1L regulates LPL secretion and lipid metabolism. *Cell Metab* **20**, 458-470. doi: 10.1016/j.cmet.2014.06.015.

Sharma VK & Singh TG (2020). Chronic stress and diabetes mellitus: interwoven pathologies. *Curr Diabetes Rev* **16**, 546-556. doi: 10.2174/1573399815666191111152248.

Shen C, Lu J, Xu Z, Xu Y & Yang Y (2020). Association between handgrip strength and the risk of new-onset metabolic syndrome: a population-based cohort study. *BMJ Open* **10**, e041384. doi: 10.1136/bmjopen-2020-041384.

Shen L, Pearson KJ, Xiong Y, Lo CM, Tso P, Woods SC, *et al.* (2008). Characterisation of apolipoprotein A-IV in brain areas involved in energy homeostasis. *Physiol Behav* **95**, 161-7.

Shi Y, Lam SM, Liu H, Luo G, Zhang J, Yao S, *et al*. (2020). Comprehensive lipidomics in apoM-/- mice reveals an overall state of metabolic distress and attenuated hepatic lipid secretion into the circulation. *J Genet Genomics* **47**, 523-534. doi: 10.1016/j.jgg.2020.08.003.

Shi Z, Fujii K, Kovary KM, Genuth NR, Röst HL, Teruel MN, *et al*. (2017). Heterogeneous ribosomes preferentially translate distinct subpools of mRNAs genome-wide. *Mol Cell* **67**, 71-83. doi: 10.1016/j.molcel.2017.05.021.

Shimba A & Ikuta K (2020a). Glucocorticoids regulate circadian rhythm of innate and adaptive immunity. *Front Immunol* **11**, 2143. doi: 10.3389/fimmu.2020.02143.

Shimizu N, Maruyama T, Yoshikawa N, Matsumiya R, Ma Y, Ito N, *et al*. (2015). A muscle-liver-fat signalling axis is essential for central control of adaptive adipose remodelling. *Nat Commun* **6**, 6693. doi: 10.1038/ncomms7693.

Shirai T, Obara T & Takemasa T (2021). Effect of endurance exercise duration on muscle hypertrophy induced by functional overload. *FEBS Open Bio* **11**, 85-94. doi: 10.1002/2211-5463.13028.

Shoffner JM, Watts RL, Juncos JL, Torroni A & Wallace DC (1991). Mitochondrial oxidative phosphorylation defects in Parkinson's disease. *Ann Neurol* **30**, 332-339. doi: 10.1002/ana.410300304.

Simmons D, Thompson CF & Volklander D (2001). Polynesians: prone to obesity and type 2 diabetes mellitus but not hyperinsulinaemia. *Diabet Med* **18**, 193-198. doi: 10.1046/j.1464-5491.2001.00435.x.

Sims EAH (2001). Are there persons who are obese, but metabolically healthy? *Metabolism* **50**, 1499-1504. doi: 10.1053/meta.2001.27213.

Singh BK, Tripathi M, Sandireddy R, Tikno K, Zhou J & Yen PM (2020). Decreased autophagy and fuel switching occur in a senescent hepatic cell model system. *Aging (Albany NY)* **12**, 13958-13978. doi: 10.18632/aging.103740.

Singh N, Joshi R & Komurov K (2015). HER2-mTOR signalling-driven breast cancer cells require ER-associated degradation to survive. *Sci Signal* **8**, ra52. doi: 10.1126/scisignal.aaa6922.

Singh R, Artaza JN, Taylor WE, Braga M, Yuan X, Gonzalez-Cadavid NF, *et al*. (2006). Testosterone inhibits adipogenic differentiation in 3T3-L1 cells: nuclear translocation of androgen receptor complex with beta-catenin and T-cell factor 4 may bypass canonical Wnt signaling to down-regulate adipogenic transcription factors. *Endocrinology* **147**, 141-154. doi: 10.1210/en.2004-1649.

Sinha RA, Singh BK & Yen PM (2018). Direct effects of thyroid hormones on hepatic lipid metabolism. *Nat Rev Endocrinol* **14**, 259-269. doi: 10.1038/nrendo.2018.10.

Skoglund P, Posth C, Sirak K, Spriggs M, Valentin F, Bedford S, *et al*. (2016). Genomic insights into the peopling of the Southwest Pacific. *Nature* **538**, 510-513. doi: 10.1038/nature19844.

Smirnov A, Entelis N, Martin RP & Tarassov I (2011). Biological significance of 5S rRNA import into human mitochondria: role of ribosomal protein MRP-L18. *Genes Dev* **25**, 1289-1305. doi: 10.1101/gad.624711.

Snijder MB, Visser M, Dekker JM, Goodpaster BH, Harris TB, Kritchevsky SB, *et al*. (2005) Low subcutaneous thigh fat is a risk factor for unfavourable glucose and lipid levels, independently of high abdominal fat. The Health ABC study. *Diabetologia* **48**, 301-308. doi: 10.1007/s00125-004-1637-7.

Soeters MR, Soeters PB, Schooneman MG, Houten SM & Romijn JA (2012). Adaptive reciprocity of lipid and glucose metabolism in human short-term starvation. *Am J Physiol Endocrinol Metab* **303**, E1397-E1407. doi: 10.1152/ajpendo.00397.2012.

Sokolović M, Sokolović A, Wehkamp D, van Themaat EVL, de Waart DR, Gilhuijs-Pederson LA, *et al*. (2008). The transcriptomic signature of fasting murine liver. *BMC Genomics* **9**, 528. doi: 10.1186/1471-2164-9-528.

Solloway MJ, Madjidi A, Gu C, Eastham-Anderson J, Clarke HJ, Kljavin N, *et al*. (2015). Glucagon couples hepatic amino acid catabolism to mTOR-dependent regulation of α-cell mass. *Cell Rep* **12**, 495-510. doi: 10.1016/j.celrep.2015.06.034.

Sols A, Salas M & Viñuela E (1964). Induced biosynthesis of liver glucokinase. *Adv Enzyme Regul* **2**, 177-188. doi: 10.1016/s0065-2571(64)80012-1.

Sommars MA, Ramachandran K, Senagolage MD, Futtner CR, Germain DM, Allred AL, *et al*. (2019). Dynamic repression by BCL6 controls the genome-wide liver response to fasting and steatosis. *Elife* **8**, e43922. doi: 10.7554/eLife.43922.

Song G, Pacini G, Ahrén B & D'Argenio DZ (2017). Glucagon increases insulin levels by stimulating insulin secretion without effect on insulin clearance in mice. *Peptides* **88**, 74-79. doi: 10.1016/j.peptides.2016.12.012.

Song K-H, Lee K & Choi H-S (2002). Endocrine disrupter bisphenol a induces orphan nuclear receptor Nur77 gene expression and steroidogenesis in mouse testicular Leydig cells. *Endocrinology* **143**, 2208-2215. doi: 10.1210/endo.143.6.8847.

Song Q, Han CC, Xiong XP, He F, Gan W, Wei SH, *et al*. (2016). PI3K-Akt-mTOR signal inhibition affects expression of genes related to endoplasmic reticulum stress. *Genet Mol Res* **15**. doi: 10.4238/gmr.15037868.

Sørensen A, Mayntz D, Raubenheimer D & Simpson SJ (2008). Protein-leverage in mice: the geometry of macronutrient balancing and consequences for fat deposition. *Obesity (Silver Spring)* **16**, 566-571. doi: 10.1038/oby.2007.58.

Southam L, Soranzo N, Montgomery SB, Frayling TM, McCarthy MI, Barroso I, *et al*. (2009). Is the thrifty genotype hypothesis supported by evidence based on confirmed type 2 diabetes- and obesity-susceptibility variants? *Diabetologia* **52**, 1846-1851. doi: 10.1007/s00125-009-1419-3.

Sparks LM, Johannsen NM, Church TS, Earnest CP, Moonen-Kornips E, Moro C, *et al*. (2013). Nine months of combined training improves ex vivo skeletal muscle metabolism in individuals with type 2 diabetes. *J Clin Endocrinol Metab* **98**, 1694-1702. doi: 10.1210/jc.2012-3874.

Sparrer KMJ, Gableske S, Zurenski MA, Parker ZM, Full F, Baumgart GJ, *et al*. (2017). TRIM23 mediates virus-induced autophagy via activation of TBK1. *Nat Microbiol* **2**, 1543-1557. doi: 10.1038/s41564-017-0017-2.

Speakman JR & Westerterp KR (2013). A mathematical model of weight loss under total starvation: evidence against the thrifty-gene hypothesis. *Dis Model Mech* **6**, 236-251. doi: 10.1242/dmm.010009.

Speakman JR (2008). Thrifty genes for obesity, an attractive but flawed idea, and an alternative perspective: the 'drifty gene' hypothesis. *Int J Obes (Lond)* **32**, 1611-1617. doi: 10.1038/ijo.2008.161.

Speakman JR, Rance KA & Johnstone AM (2008). Polymorphisms of the *FTO* gene are associated with variation in energy intake, but not energy expenditure. *Obesity* **16**(8), 1961-1965. doi: 10.1038/oby.2008.318.

Speliotes EK, Willer CJ, Berndt SI, Monda KL, Thorleifsson G, Jackson AU, *et al*. (2010). Association analyses of 249,796 individuals reveal 18 new loci associated with body mass index. *Nat Genet* **42**(11), 937-948. doi: 10.1038/ng.686.

Staiano AE & Katzmarzyk PT (2012). Ethnic and sex differences in body fat and visceral and subcutaneous adiposity in children and adolescents. *Int J Obes (Lond)* **36**, 1261-1269. doi: 10.1038/ijo.2012.95.

Staiano AE, Broyles ST, Gupta AK & Katzmarzyk PT (2013a). Ethnic and sex differences in visceral, subcutaneous, and total body fat in children and adolescents. *Obesity (Silver Spring)* **21**, 1251-1255. doi: 10.1002/oby.20210.

Staiano AE, Broyles ST, Gupta AK, Malina RM & Katzmarzyk PT (2013b). Maturity-associated variation in total and depot-specific body fat in children and adolescents. *Am J Hum Biol* **25**, 473-479. doi: 10.1002/ajhb.22380.

Stannard SR & Johnson NA (2004). Insulin resistance and elevated triglyceride in muscle: more important for survival than "thrifty" genes? *J Physiol* **554**, 595-607. doi: 10.1113/jphysiol.2003.053926.

Stark R, Grzelak M & Hadfield J (2019). RNA sequencing: the teenage years. *Nat Rev Genet* **20**, 631-656. doi: 10.1038/s41576-019-0150-2.

Starup-Linde J, Hygum K & Langdahl BL (2018). Skeletal fragility in type 2 diabetes mellitus. *Endocrinol Metab (Seoul)* **33**, 339-351. doi: 10.3803/EnM.2018.33.3.339.

Stefan N, Haring HU, Hu FB & Schulze MB (2013). Metabolically healthy obesity: epidemiology, mechanisms, and clinical implications. *Lancet Diabetes Endocrinol* **1**, 152-162. doi: 10.1016/S2213-8587(13)70062-7.

Steinhauser ML, Olenchock BA, O'Keefe J, Lun M, Pierce KA, Lee H, *et al*. (2018). The circulating metabolome of human starvation. *JCI Insight* **3**, e121434. doi: 10.1172/jci.insight.121434.

Steinthorsdottir V, Thorleifsson G, Reynisdottir I, Benediktsson R, Jonsdottir T, Walters GB, *et al*. (2007). A variant in CDKAL1 influences insulin response and risk of type 2 diabetes. *Nat Genet* **39**(6), 770-775. doi: 10.1038/ng2043.

Steinthorsdottir V, Thorleifsson G, Sulem P, Helgason H, Grarup N, Sigurdsson A, *et al*. (2014). Identification of low-frequency and rare sequence variants associated with elevated or reduced risk of type 2 diabetes. *Nat Genet* **46**, 294-298. doi: 10.1038/ng.2882.

Steneberg P, Sykaras AG, Backlund F, Straseviciene J, Söderström I & Edlund H (2015). Hyperinsulinemia enhances hepatic expression of the fatty acid transporter Cd36 and provokes hepatosteatosis and hepatic insulin resistance. *J Biol Chem* **290**, 19034-19043. doi: 10.1074/jbc.M115.640292.

Stöger R (2008). The thrifty epigenotype: an acquired and heritable predisposition for obesity and diabetes? *Bioessays* **30**, 156-166. doi: 10.1002/bies.20700.

Stride P (2016). Polynesian bones. *Br J Med Med Res* **16**, 1-9.

Ströher DJ, de Oliveira MF, Martinez-Oliveira P, Pilar BC, Cattelan MDP, Rodrigues E, *et al*. (2020). Virgin coconut oil associated with high-fat diet induces metabolic dysfunctions, adipose inflammation, and hepatic lipid accumulation. *J Med Food* **23**, 689-698. doi: 10.1089/jmf.2019.0172.

Stubbins RE, Najjar K, Holcomb VB, Hong J & Núñez NP (2012). Oestrogen alters adipocyte biology and protects female mice from adipocyte inflammation and insulin resistance. *Diabetes Obes Metab* **14**, 58-66. doi: 10.1111/j.1463-1326.2011.01488.x.

Suchacki KJ, Roberts F, Lovdel A, Farguharson C, Morton NM, MacRae VE, *et al*. (2017). Skeletal energy homeostasis: a paradigm of endocrine discovery. *J Endocrinol* **234**, R67-R79. doi: 10.1530/JOE-17-0147.

Summers SA (2006). Ceramides in insulin resistance and lipotoxicity. *Prog Lipid Res* **45**(1), 42-72. doi: 10.1016/j.plipres.2005.11.002.

Sun F, Liao Y, Qu X, Xiao X, Hou S, Chen Z, *et al*. (2020). Hepatic DNAJB9 drives anabolic biasing to reduce steatosis and obesity. *Cell Rep* **30**, 1835-1847. doi: 10.1016/j.celrep.2020.01.043.

Sun H, Lin M, Russell EM, Minster RL, Chan TF, Dinh BL, *et al*. (2021). The impact of global and local Polynesian genetic ancestry on complex traits in Native Hawaiians. *PLoS Genet* **17**, e1009273. doi: 10.1371/journal.pgen.1009273.

Sun S, Shi G, Han X, Francisco AB, Ji Y, Mendonça N, *et al*. (2014). Sel1L is indispensable for mammalian endoplasmic reticulum-associated degradation, endoplasmic reticulum homeostasis, and survival. *Proc Natl Acad Sci U S A* **111**, E582-E591. doi: 10.1073/pnas.1318114111.

Sun S, Shi G, Sha H, Ji Y, Han X, Shu X, *et al*. (2015a). IRE1α is an endogenous substrate of endoplasmic-reticulum-associated degradation. *Nat Cell Biol* **17**, 1546-1555. doi: 10.1038/ncb3266.

Sun X, Dang F, Zhang D, Yuan Y, Zhang C, Wu Y, *et al*. (2015b). Glucagon-CREB/CRTC2 signalling cascade regulates hepatic BMAL1 protein. *J Biol Chem* **290**, 2189-2197. doi: 10.1074/jbc.M114.612358.

Sung HJ, Kim YS, Kang H & Ko J (2008). Human LZIP induces monocyte CC chemokine receptor 2 expression leading to enhancement of monocyte chemoattractant protein 1/CCL2-induced cell migration. *Exp Mol Med* **40**, 332-338. doi: 10.3858/emm.2008.40.3.332.

Sunilkumar S, Kimball SR & Dennis MD (2021). Glucagon transiently stimulates mTORC1 by activation of an EPAC/Rap1 signalling axis. *Cell Signal* doi: 10.1016/j.cellsig.2021.110010.

Suppli MP, Bagger JI, Lund A, Demant M, van Hall G, Strandberg C, *et al*. (2020). Glucagon resistance at the level of amino acid turnover in obese subjects with hepatic steatosis. *Diabetes* **69**, 1090-1099. doi: 10.2337/db19-0715.

Suppli MP, Lund A, Bagger JI, Vilsbøll T & Knop FK (2016). Involvement of steatosis-induced glucagon resistance in hyperglucagonemia. *Med Hypotheses* **86**, 100-103. doi: 10.1016/j.mehy.2015.10.029.

Suzuki A, Minamide M, Iwaya C, Ogata K & Iwata J (2020). Role of metabolism in bone development and homeostasis. *Int J Mol Sci* **21**, 8992. doi: 10.3390/ijms21238992.

Swinburn BA, Ley SJ, Carmichael HE & Plank LD (1999). Body size and composition in Polynesians. *Int J Obes Relat Metab Disord* **23**, 1178-1183. doi: 10.1038/sj.ijo.0801053.

Szklarczyk D, Gable AL, Lyon D, Junge A, Wyder S, Huerta-Cepas J, *et al*. (2019). STRING v11: protein-protein association networks with increased coverage,

supporting functional discovery in genome-wide experimental datasets. *Nucleic Acids Res* **47**, D607-D613. doi: 10.1093/nar/gky1131.

Tabbaa M, Gomez TR, Campelj DG, Gregorevic P, Hayes A & Goodman CA (2021). The regulation of polyamine pathway proteins in models of skeletal muscle hypertrophy and atrophy: a potential role for mTORC1. *Am J Physiol Cell Physiol* **320**, C987-C999. doi: 10.1152/ajpcell.00078.2021.

Takahara T, Amemiya Y, Sugiyama R, Maki M & Shibata H (2020). Amino acid-dependent control of mTORC1 signalling: a variety of regulatory modes. *J Biomed Sci* **27**, 87. doi: 10.1186/s12929-020-00679-2.

Talmadge RJ, Otis JS, Rittler MR, Garcia ND, Spencer SR, Lees SJ, *et al*. (2004). Calcineurin activation influences muscle phenotype in a muscle-specific fashion. *BMC Cell Biol* **5**, 28. doi: 10.1186/1471-2121-5-28.

Tan S-X, Ng Y, Meoli CC, Kumar A, Khoo P-S, Fazakerley DJ, *et al*. (2012). Amplification and demultiplexing in insulin-regulated Akt protein kinase pathway in adipocytes. *J Biol Chem* **287**, 6128-6138. doi: 10.1074/jbc.M111.318238.

Tanaka H, Shimizu N & Yoshikawa N (2017). Role of skeletal muscle glucocorticoid receptor in systemic energy homeostasis. *Exp Cell Res* **360**, 24-26. doi: 10.1016/j.yexcr.2017.03.049.

Tang X, Wen X, Li Z, Wen D, Lin L, Liu J, *et al*. (2021). Has_circ_0102171 aggravates the progression of cervical cancer through targeting miR-4465/CREBRF axis. *J Cell Physiol* **236**, 4973-4984. doi: 10.1002/jcp.30210.

Tangseefa P, Martin SK, Chin PY, Breen J, Mah CY, Baldock PA, *et al*. (2021). The mTORC1 complex in pre-osteoblasts regulates whole-body energy metabolism independently of osteocalcin. *Bone Res* **9**, 10. doi: 10.1038/s41413-020-00123-z.

Taniguchi CM, Emanuelli B & Kahn CR (2006). Critical nodes in signalling pathways: insights into insulin action. *Nat Rev Mol Cell Biol* **7**(2), 85-96. doi: 10.1038/nrm1837.

Taniguchi M & Yoshida H (2017). TFE3, HSP47, and CREB3 pathways of the mammalian Golgi stress response. *Cell Struct Funct* **42**, 27-36. doi: 10.1247/csf.16023.

Tarnopolsky MA (2000). Gender differences in substrate metabolism during endurance exercise. *Can J Appl Physiol* **25**, 312-327. doi: 10.1139/h00-024.

Tata DA & Anderson BJ (2010). The effects of chronic glucocorticoid exposure on dendritic length, synapse numbers and glial volume in animal models: implications for hippocampal volume reductions in depression. *Physiol Behav* **99**, 186-193. doi: 10.1016/j.physbeh.2009.09.008.

Tato I, Bartrons R, Ventura F & Rosa JL (2011). Amino acids activate mammalian target of rapamycin complex 2 (mTORC2) via PI3K/Akt signalling. *J Biol Chem* **286**, 6128-6142. doi: 10.1074/jbc.M110.166991.

Taylor R & Zimmet P (1981a). The influence of variation in obesity in the sex difference in the prevalence of abnormal glucose tolerance in Tuvalu. *N Z Med J* **94**, 176-178.

Taylor R, Bennett P, Uili R, Joffres M, Germain R, Levy S, *et al*. (1985). Diabetes in Wallis Polynesians: a comparison of residents of Wallis Island and first generation migrants to Noumea, New Caledonia. *Diabetes Res Clin Pract* **1**, 169-178. doi: 10.1016/s0168-8227(85)80007-3.

Taylor R, Levy S, Jalaludin B, Montaville B, Gee K & Sladden T (1991). Prevalence of diabetes, hypertension and obesity at different levels of urbanisation in Vanuatu. *Med J Aust* **155**, 86-90. doi: 10.5694/j.1326-5377.1991.tb142133.x.

Taylor RJ & Zimmet PZ (1981b). Obesity and diabetes in Western Samoa. *Int J Obes* **5**, 367-376.

Taylor RJ, Bennett PH, LeGonidec G, Lacoste J, Combe D, Joffres M, *et al*. (1983). The prevalence of diabetes mellitus in a traditional-living Polynesian population: the Wallis Island survey. *Diabetes Care* **6**, 334-340. doi: 10.2337/diacare.6.4.334.

Taylor TE (2018). Luman potentially regulates metabolism through modulation of the hypothalamic-pituitary-adrenal axis. Masters thesis, University of Guelph, Ontario, Canada.

Tchkonia T, Thomou T, Zhu Y, Karagiannides I, Pothoulakis C, Jensen MD, *et al*. (2013). Mechanisms and metabolic implications of regional differences among fat depots. *Cell Metab* **17**, 644-656. doi: 10.1016/j.cmet.2013.03.008.

Teleman AA, Kietakangas V, Sayadian AC & Cohen SM (2008). Nutritional control of protein biosynthetic capacity by insulin via Myc in Drosophila. *Cell Metab* **7**, 21-32. doi: 10.1016/j.cmet.2007.11.010.

Tepavčević V (2021). Oligodendroglial energy metabolism and (re)myelination. *Life (Basel)* **11**, 238. doi: 10.3390/life11030238.

Thuzar M, Phillip Law W, Ratnasingam J, Jang C, Dimeski G & Ho KK (2018). Glucocorticoids suppress brown adipose tissue function in humans: a double-blind placebo-controlled study. *Diabetes Obes Metab* **20**, 840-848. doi: 10.1111/dom.13157.

Tian J, Goldstein JL & Brown MS (2016). Insulin induction of SREBP-1c in rodent liver requires LXRα-C/EBPβ complex. *Proc Natl Acad Sci U S A* **113**, 8182-8187. doi: 10.1073/pnas.1608987113.

Tian J, Wu J, Chen X, Guo T, Chen ZJ, Goldstein JL, *et al*. (2018). BHLHE40, a third transcription factor required for insulin induction of SREBP-1c mRNA in rodent liver. *Elife* **7**, e36826. doi: 10.7554/eLife.36826.

Tiebe M, Lutz M, De La Garza A, Buechling T, Boutros M & Teleman AA (2015). REPTOR and REPTOR-BP regulate organismal metabolism and transcription downstream of TORC1. *Dev Cell* **33**, 272-284. doi: 10.1016/j.devcel.2015.03.013.

Tiebe M, Lutz M, Tiebe DS & Teleman AA (2019). Crebl2 regulates cell metabolism in muscle and liver cells. *Sci Rep* **9**, 19869. doi: 10.1038/s41598-019-56407-w.

Titchenell PM, Chu Q, Monks BR & Birnbaum MJ (2015). Hepatic insulin signalling is dispensable for suppression of glucose output by insulin *in vivo*. *Nat Commun* **6**, 7078. doi: 10.1038/ncomms8078.

Titchenell PM, Lazar MA & Birnbaum MJ (2017). Unravelling the regulation of hepatic metabolism by insulin. *Trends Endocrinol Metab* **28**, 497-505. doi: 10.1016/j.tem.2017.03.003.

Toews JNC, Hammond GL & Viau V (2021). Liver at the nexus of rat postnatal HPA axis maturation and sexual dimorphism. *J Endocrinol* **248**, R1-R17. doi: 10.1530/JOE-20-0286.

Tong X, Li P, Zhang D, VanDommelen K, Gupta N, Rui L, *et al*. (2016). E4BP4 is an insulin-induced stabiliser of nuclear SREBP-1c and promotes SREBP-1c-mediated lipogenesis. *J Lipid Res* **57**, 1219-1230. doi: 10.1194/jlr.M067181.

Tontonoz P, Cortez-Toledo O, Wroblewski K, Hong C, Lim L, Carranza R, *et al*. (2015). The orphan nuclear receptor Nur77 is a determinant of myofiber size and muscle mass in mice. *Mol Cell Biol* **35**, 1125-1138. doi: 10.1128/MCB.00715-14.

Torres-Odio S, Key J, Hoepken HH, Canet-Pons J, Valek L, Roller B, *et al*. (2017). Progression of pathology in PINK1-deficient mouse brain from splicing via

ubiquitination, ER stress, and mitophagy changes to neuroinflammation. *J Neuroinflammation* **14**, 154. doi: 10.1186/s12974-017-0928-0.

Triebl A & Wenk MR (2018). Analytical considerations of stable isotope labelling in lipidomics. *Biomolecules* **8**, 151. doi: 10.3390/biom8040151.

Troncoso R, Paredes F, Parra V, Gatica D, Vásquez-Trincado C, Quiroga C, *et al*. (2014). Dexamethasone-induced autophagy mediates muscle atrophy through mitochondrial clearance. *Cell Cycle* **13**, 2281-2295. doi: 10.4161/cc.29272.

Tsai K, Tullis B, Jensen T, Graff T, Reynolds P & Arroyo J (2021). Differential expression of mTOR related molecules in the placenta from gestational diabetes mellitus (GDM), intrauterine growth restriction (IUGR) and preeclampsia patients. *Reprod Biol* **21**, 100503. doi: 10.1016/j.repbio.2021.100503.

Tsatsoulis A & Paschou SA (2020). Metabolically healthy obesity: criteria, epidemiology, controversies, and consequences. *Curr Obes Rep* **9**, 109-120. doi: 10.1007/s13679-020-00375-0.

Tschritter O, Preissl H, Yokoyama Y, Machicao F, Häring H-U & Fritsche A (2007). Variation in the *FTO* gene locus is associated with cerebrocortical insulin resistance in humans. *Diabetologia* **50**(12), 2602-2603. doi: 10.1007/s00125-007-0839-1.

Tsun Z-Y, Bar-Peled L, Chantranupong L, Zoncu R, Wang T, Kim C, *et al*. (2013). The folliculin tumour suppressor is a GAP for the RagC/D GTPases that signal amino acid levels to mTORC1. *Mol Cell* **52**, 495-505. doi: 10.1016/j.molcel.2013.09.016.

Tuo Y & Xiang M (2019). mTOR: a double-edged sword for diabetes. *J Leukoc Biol* **106**, 385-395. doi: 10.1002/JLB.3MR0317-095RR.

Turner N, Bruce CR, Beale SM, Hoehn KL, So T, Rolph MS, *et al*. (2007). Excess lipid availability increases mitochondrial fatty acid oxidative capacity in muscle: evidence against a role for reduced fatty acid oxidation in lipid-induced insulin resistance in rodents. *Diabetes* **56**, 2085-2092. Doi: 10.2337/db07-0093.

Turner N, Hariharan K, TidAng J, Frangioudakis G, Beale SM, Wright LE, *et al*. (2009). Enhancement of muscle mitochondrial oxidative capacity and alterations in insulin action are lipid species dependent: potent tissue-specific effects of medium-chain fatty acids. *Diabetes* **58**, 2547-2554. doi: 10.2337/db09-0784.

Turner N, Kowalski GM, Leslie SJ, Risis S, Yang C, Lee-Young RS, *et al*. (2013). Distinct patterns of tissue-specific lipid accumulation during the induction of

insulin resistance in mice by high-fat feeding. *Diabetologia* **56**(7), 1638-1648. doi: 10.1007/s00125-013-2913-1.

Tyagi N, Sedoris KC, Steed M, Ovechkin AV, Moshal KS & Tyagi SC (2005). Mechanisms of homocysteine-induced oxidative stress. *Am J Physiol Heart Circ Physiol* **289**, H2649-H2656. doi: 10.1152/ajpheart.00548.2005.

Unger RH & Cherrington AD (2012). Glucagonocentric restructuring of diabetes: a pathophysiologic and therapeutic makeover. *J Clin Invest* **122**, 4-12. doi: 10.1172/JCI60016.

Unger RH, Aguilar-Parada E, Müller WA & Eisentraut AM (1970). Studies of pancreatic alpha cell function in normal and diabetic subjects. *J Clin Invest* **49**, 837-848. doi: 10.1172/JCI106297.

Uno K, Yamada T, Ishigaki Y, Imai J, Hasegawa Y, Sawada S, *et al*. (2015). A hepatic amino acid/mTOR/S6K-dependent signalling pathway modulates systemic lipid metabolism via neuronal signals. *Nat Commun* **6**, 7940.

Uranga AP, Levine J & Jensen M (2005). Isotope tracer measures of meal fatty acid metabolism: reproducibility and effects of the menstrual cycle. *Am J Physiol Endocrinol Metab* **288**, E547-E555.

van den Berghe G (1991). The role of the liver in metabolic homeostasis: implications for inborn errors of metabolism. *J Inherit Metab Dis* **14**, 407-420. doi: 10.1007/BF01797914.

Van der Heide LP & Smidt MP (2005). Regulation of FoxO activity by CBP/p300-mediated acetylation. *Trends Biochem Sci* **30**, 81-86. doi: 10.1016/j.tibs.2004.12.002.

Van Meijl LEC, Popeijus HE & Mensink RP (2010). Amino acids stimulate Akt phosphorylation, and reduce IL-8 production and NF-κB activity in HepG2 liver cells. *Mol Nutr Food Res* **54**, 1568-1573. doi: 10.1002/mnfr.200900438.

Van Proeyen K, Szlufcik K, Nielens H, Ramaekers M & Hespel P (2011). Beneficial metabolic adaptations due to endurance exercise training in the fasted state. *J Appl Physiol (1985)* **110**, 236-245. doi: 10.1152/japplphysiol.00907.2010.

Van Tienen FHJ, Praet SFE, de Feyter HM, van den Broek NM, Lindsey PJ, Schoonderwoerd KGC, *et al*. (2012). Physical activity is the key determinant of skeletal muscle mitochondrial function in type 2 diabetes. *J Clin Endocrinol Metab* **97**, 3261-3269. doi: 10.1210/jc.2011-3454.

Vander Haar E, Lee S-I, Bandhakavi S, Griffin TJ & Kim D-H (2007). Insulin signalling to mTOR mediated by the Akt/PKB substrate PRAS40. *Nat Cell Biol* **9**, 316-323. doi: 10.1038/ncb1547.

Vecchi C, Montosi G, Zhang K, Lamberti I, Duncan SA, Kaufman RJ & Pietrangelo A (2009). ER stress controls iron metabolism through induction of hepcidin. *Science* **325**, 877-880. doi: 10.1126/science.1176639.

Vega A, Martinot E, Baptissart M, De Haze A, Saru J-P, Baron S, *et al*. (2015). Identification of the link between the hypothalamic-pituitary axis and the testicular orphan nuclear receptor NR0B2 in adult male mice. *Endocrinology* **156**, 660-669. doi: 10.1210/en.2014-1418.

Vellers HL, Kleeberger SR & Lightfoot JT (2018). Inter-individual variation in adaptations to endurance and resistance exercise training: genetic approaches towards understanding a complex phenotype. *Mamm Genome* **29**, 48-62. doi: 10.1007/s00335-017-9732-5.

Venneri MA, Hasenmajer V, Fiore D, Sbardella E, Pofi R, Graziadio C, *et al*. (2018). Circadian rhythm of glucocorticoid administration entrains clock genes in immune cells: a DREAM trial ancillary study. *J Clin Endocrinol Metab* **103**, 2998-3009. doi: jc.2018-00346.

Venniyoor A (2020). PTEN: a thrifty gene that causes disease in times of plenty? *Front Nutr* **7**, 81. doi: 10.3389/fnut.2020.00081.

Venz R, Korosteleva A, Jongsma E & Ewald CY (2020). Combining auxin-induced degradation and RNAi screening identifies novel genes involved in lipid bilayer stress sensing in *Caenorhabditis elegans*. *G3 (Bethesda)* **10**, 3921-3928. doi: 10.1534/g3.120.401635

Verfaillie T, Garg AD & Agostinis P (2013). Targeting ER stress induced apoptosis and inflammation in cancer. *Cancer Lett* **332**, 249-264. doi: 10.1016/j.canlet.2010.07.016.

VerHague MA, Cheng D, Weinberg RB & Shelness GS (2013). Apolipoprotein A-IV expression in mouse liver enhances triglyceride secretion and reduces hepatic lipid content by promoting very low density lipoprotein particle expression. *Arterioscler Thromb Vasc Biol* **33**, 2501-2508. doi: 10.1161/ATVBAHA.113.301948.

Vijgen GH, Bouvy ND, Teule GJ, Brans B, Schrauwen P & van Marken Lichtenbelt WD (2011). Brown adipose tissue in morbidly obese subjects. *PLoS One* **6**, e17247. doi: 10.1371/journal.pone.0017247.

Virtanen KA, Lidell ME, Orava J, Heglind M, Westergren R, Niemi T, *et al*. (2009). Functional brown adipose tissue in healthy adults. *N Engl J Med* **360**, 1518-1525. doi: 10.1056/NEJMoa0808949.

Vishram JKK, Borglykke A, Andreasen AH, Jeppesen J, Ibsen H, Jørgensen T, *et al*. (2014). Impact of age and gender on the prevalence and prognostic importance of the metabolic syndrome and its components in Europeans. The MORGAM prospective cohort project. *PLoS ONE* **10**, e0128848. doi: 10.1371/journal.pone.0107294.

Volmer R & Ron D (2015). Lipid-dependent regulation of the unfolded protein response. *Curr Opin Cell Biol* **33**, 67-73. doi: 10.1016/j.ceb.2014.12.002.

Von Meyenn F, Porstmann T, Gasser E, Selevsek N, Schmidt A, Aebersold R & Stoffel M (2013). Glucagon-induced acetylation of Foxa2 regulates hepatic lipid metabolism. *Cell Metab* **17**, 436-447. doi: 10.1016/j.cmet.2013.01.014.

Waddell DS, Baehr LM, van den Brandt J, Johnsen SA, Reichardt HM, Furlow JD, *et al*. (2008). The glucocorticoid receptor and FOXO1 synergistically activate the skeletal muscle atrophy-associated MuRF1 gene. *Am J Physiol Endocrinol Metab* **295**, E785-E797. doi: 10.1152/ajpendo.00646.2007.

Wagenmakers AJ (1998). Muscle amino acid metabolism at rest and during exercise: role in human physiology and metabolism. *Exerc Sport Sci Rev* **26**, 287-314.

Wagner R, Tabák ÁG, Fehlert E, Fritsche L, Jaghutriz BA, Bánhegyi RJ, *et al*. (2017). Excessive fuel availability amplifies the FTO-mediated obesity risk: results from the TUEF and Whitehall II studies. *Sci Rep* **7**(1), 15486. doi: 10.1038/s41598-017-15744-4.

Wali JA, Solon-Biet SM, Freire T & Brandon AE (2021). Macronutrient determinants of obesity, insulin resistance and metabolic health. *Biology (Basel)* **10**, 336. doi: 10.3390/biology10040336.

Wang D, Hawley NL, Thompson AA, Lameko V, Reupena MS, McGarvey ST, *et al*. (2017). Dietary patterns are associated with metabolic outcomes among adult Samoans in a cross-sectional study. *J Nutr* **147**, 628-635. doi: 10.3945/jn.116.243733.

Wang G & Speakman JR (2016). Analysis of positive selection at single nucleotide polymorphisms associated with body mass index does not support the “thrifty gene” hypothesis. *Cell Metab* **24**, 531-541. doi: 10.1016/j.cmet.2016.08.014.

Wang H, Zhao M, Sud N, Christian P, Shen J, Song Y, *et al*. (2016). Glucagon regulates hepatic lipid metabolism via cAMP and Insig-2 signalling: implication for the

pathogenesis of hypertriglyceridemia and hepatic steatosis. *Sci Rep* **6**, 32246. doi: 10.1038/srep32246.

Wang J, Mitsche MA, Lütjohann D, Cohen JC, Xie X-S & Hobbs HH (2015a). Relative roles of ABCG5/ABCG8 in liver and intestine. *J Lipid Res* **56**, 319-330. doi: 10.1194/jlr.M054544.

Wang L, Chen J, Ning C, Lei D & Ren J (2018). Endoplasmic reticulum stress related molecular mechanisms in nonalcoholic fatty liver disease (NAFLD). *Curr Drug Targets* **19**, 1087-1094. doi: 10.2174/1389450118666180516122517.

Wang L, Lee Y-K, Bundman D, Han Y, Thevananther S, Kim CS, *et al*. (2002). Redundant pathways for negative feedback regulation of bile acid production. *Dev Cell* **2**, 721-731. doi: 10.1016/s1534-5807(02)00187-9.

Wang L, Lu M, Zhang R, Guo W, Lin P, Yang D, *et al*. (2019). Inhibition of Luman/CREB3 expression leads to the upregulation of testosterone synthesis in mouse Leydig cells. *J Cell Physiol* **234**, 15257-15269. doi: 10.1002/jcp.28171.

Wang L, Meng Q, Yang L, Yang D, Guo W, Lin P, *et al*. (2021). Luman/CREB3 knock-down inhibit hCG induced MLTC-1 apoptosis. *Theriogenology* **161**, 140-150. doi: 10.1016/j.theriogenology.2020.11.010.

Wang L, Zhao Y, Bao X, Kwok YK-Y, Sun K, Chen X, *et al*. (2015b). LncRNA Dum interacts with Dnmts to regulate Dppa2 expression during myogenic differentiation and muscle regeneration. *Cell Res* **25**, 335-350. doi: 10.1038/cr.2015.21.

Wang N, Liu Y, Ma Y & Wen D (2018). Hydroxytyrosol ameliorates insulin resistance by modulating endoplasmic reticulum stress and prevents hepatic steatosis in diet-induced obesity mice. *J Nutr Biochem* **57**, 180-188. doi: 10.1016/j.jnutbio.2018.03.018.

Wang Y, Nakajima T, Gonzalez FJ & Tanaka N (2020). PPARs as metabolic regulators in the liver: lessons from liver-specific PPAR-null mice. *Int J Mol Sci* **21**, 2061. doi: 10.3390/ijms21062061.

Wardle J & Carnell S (2009). Appetite is a heritable phenotype associated with adiposity. *Ann Behav Med* **38**(Suppl 1), S25-30. doi: 10.1007/s12160-009-9116-5.

Wasserman DH & Cherrington AD (1991). Hepatic fuel metabolism during muscular work: role and regulation. *Am J Physiol* **260**, E811-E824. doi: 10.1152/ajpendo.1991.260.6.E811.

Webb AE, Kundaje A & Brunet A (2016). Characterisation of the direct targets of FOXO transcription factors throughout evolution. *Aging Cell* **15**, 673-685. doi: 10.1111/acel.12479.

Weber K, Brück P, Mikes Z, Küpper J-H, Klingenspor M & Wiesner RJ (2002). Glucocorticoid hormone stimulates mitochondrial biogenesis specifically in skeletal muscle. *Endocrinology* **143**, 177-184. doi: 10.1210/endo.143.1.8600.

Wei D, Tao R, Zhang Y, White MF & Dong XC (2011). Feedback regulation of hepatic gluconeogenesis through modulation of SHP/Nr0b2 gene expression by Sirt1 and FoxO1. *Am J Physiol Endocrinol Metab* **300**, E312-E320. doi: 10.1152/ajpendo.00524.2010.

Wei J, Chen L, Li F, Yuan Y, Wang Y, Xia W, *et al*. (2018). HRD1-ERAD controls production of the hepatokine FGF21 through CREBH polyubiquitination. *EMBO J* **37**, e98942. doi: 10.15252/embj.201898942.

Wei Y, Tsang CK & Zheng XFS (2009). Mechanisms of regulation of RNA polymerase III-dependent transcription by TORC1. *EMBO J* **28**, 2220-2230. doi: 10.1038/emboj.2009.179.

Weinstein S, Sedlak-Weinstein E, Taylor R & Zimmet P (1981). The high prevalence of impaired glucose tolerance and diabetes mellitus in an isolated Polynesian population, Manihiki, Cook Islands. *N Z Med J* **94**, 411-413.

Wells JCK (2006). The evolution of human fatness and susceptibility to obesity: an ethological approach. *Biol Rev Camb Philos Soc* **81**, 183-205. doi: 10.1017/S1464793105006974.

Wells JCK (2007a). Sexual dimorphism of body composition. *Best Pract Res Clin Endocrinol Metab* **21**, 415-430. doi: 10.1016/j.beem.2007.04.007.

Wells JCK (2007b). The thrifty phenotype as an adaptive maternal effect. *Biol Rev Camb Philos Soc* **82**, 143-172. doi: 10.1111/j.1469-185X.2006.00007.x.

Wells JCK (2011). The thrifty phenotype: an adaptation in growth or metabolism? *Am J Hum Biol* **23**, 65-75. doi: 10.1002/ajhb.21100.

Wells JCK (2017). Body composition and susceptibility to type 2 diabetes: an evolutionary perspective. *Eur J Clin Nutr* **71**, 881-889. doi: 10.1038/ejcn.2017.31.

Wewer Albrechtson NJ, Pedersen J, Galsgaard KD, Winther-Sørensen M, Suppli MP, Janah L, *et al*. (2019). The liver-α-cell axis and type 2 diabetes. *Endocr Rev* **40**, 1353-1366. doi: 10.1210/er.2018-00251.

Weyer C, Foley JE, Bogardus C, Tataranni PA & Pratley RE (2000). Enlarged subcutaneous abdominal adipocyte size, but not obesity itself, predicts type II diabetes independent of insulin resistance. *Diabetologia* **43**, 1498-1506. doi: 10.1007/s001250051560.

Wiemerslage L, Nilsson EK, Dahlberg LS, Ence-Eriksson F, Castillo S, Larsen AL, *et al*. (2016). An obesity-associated risk allele within the *FTO* gene affects brain activity for areas important for emotion, impulse control, and reward in response to food images. *Eur J Neurosci* **43**(9), 1173-1180. doi: 10.1111/ejn.13177.

Wijesekara N, Konrad D, Eweida M, Jefferies C, Liadis N, Giacca A, *et al*. (2005). Muscle-specific Pten deletion protects against insulin resistance and diabetes. *Mol Cell Biol* **25**, 1135-1145. doi: 10.1128/MCB.25.3.1135-1145.2005.

Willis IM, Moir RD & Hernandez N (2018). Metabolic programming a lean phenotype by deregulation of RNA polymerase III. *Proc Natl Acad Sci U S A* **115**, 12182-12187. doi: 10.1073/pnas.1815590115.

Wing SS & Goldberg AL (1993). Glucocorticoids activate the ATP-ubiquitin-dependent proteolytic system in skeletal muscle during fasting. *Am J Physiol* **264**, E668-E676. doi: 10.1152/ajpendo.1993.264.4.E668.

Winther-Sørensen M, Galsgaard KD, Santos A, Trammell SAJ, Sulek K, Kuhre RE, *et al*. (2020). Glucagon acutely regulates hepatic amino acid catabolism and the effect may be disturbed by steatosis. *Mol Metab* **42**, 101080. doi: 10.1016/j.molmet.2020.101080.

Wolfrum C, Asilmaz E, Luca E, Friedman JM & Stoffel M (2004). Foxa2 regulates lipid metabolism and ketogenesis in the liver during fasting and in diabetes. *Nature* **432**, 1027-1032. doi: 10.1038/nature03047.

Woller A, Duez H, Staels B & Lefranc M (2016). A mathematical model of the liver circadian clock linking feeding and fasting cycles to clock function. *Cell Rep* **17**, 1087-1097. doi: 10.1016/j.celrep.2016.09.060.

Wollstein A, Lao O, Becker C, Brauer S, Trent RJ, Nürnberg P, *et al*. (2010). Demographic history of Oceania inferred from genome-wide data. *Curr Biol* **20**, 1983-1992. doi: 10.1016/j.cub.2010.10.040.

Wondisford AR, Xiong L, Chang E, Meng S, Meyers DJ, Li M, *et al*. (2014). Control of *Foxo1* gene expression by co-activator p300. *J Biol Chem* **289**, 4326-4333. doi: 10.1074/jbc.M113.540500.

Wong JT, Kim PTW, Peacock JW, Yau TY, Mui AL-F, Chung SW, *et al*. (2007). Pten (phosphatase and tensin homologue gene) haploinsufficiency promotes insulin hypersensitivity. *Diabetologia* **50**, 395-403. doi: 10.1007/s00125-006-0531-x.

Woolley CS, Gould E & McEwen BS (1990). Exposure to excess glucocorticoids alters dendritic morphology of adult hippocampal pyramidal neurons. *Brain Res* **531**, 225-231. doi: 10.1016/0006-8993(90)90778-a.

Wu K, Huang J, Xu T, Ye Z, Jin F, Li N, *et al*. (2019a). MicroRNA-181b blocks ginsenoside Rg3-mediated tumour suppression of gallbladder carcinoma by promoting autophagy flux via CREBRF/CREB3 pathway. *Am J Transl Res* **11**, 5776-5787.

Wu KC, Reisman SA & Klaassen CD (2020a). Tissue distribution, hormonal regulation, ontogeny, diurnal expression, and induction of mouse cystine transporters Slc3a1 and Slc7a9. *Free Radic Res* **54**, 525-534. doi: 10.1080/10715762.2020.1812597.

Wu N, Kim KH, Zhou Y, Lee JM, Kettner NM, Mamrosh JL, *et al*. (2016). Small heterodimer partner (NR0B2) coordinates nutrient signalling and the circadian clock in mice. *Mol Endocrinol* **30**, 988-995. doi: 10.1210/me.2015-1295.

Wu N, Zheng B, Shaywitz A, Dagon Y, Tower C, Bellinger G, *et al*. (2013). AMPK-dependent degradation of TXNIP upon energy stress leads to enhanced glucose uptake via GLUT1. *Mol Cell* **49**, 1167-1175. doi: 10.1016/j.molcel.2013.01.035..

Wu R, Dang F, Li P, Wang P, Xu Q, Liu Z, *et al*. (2019b). The circadian protein Period2 suppresses mTORC1 activity via recruiting Tsc1 to mTORC1 complex. *Cell Metab* **29**, 653-667.e6. doi: 10.1016/j.cmet.2018.11.006.

Wu Y, Pan Q, Yan H, Zhang K, Guo X, Xu Z, *et al*. (2018). Novel mechanism of Foxo1 phosphorylation in glucagon signalling in control of glucose homeostasis. *Diabetes* **67**, 2167-2182. doi: 10.2337/db18-0674.

Wu Y, Xie Z, Chen J, Chen J, Ni W, Ma Y, *et al*. (2019c). Circular RNA circTADA2A promotes osteosarcoma progression and metastasis by sponging miR-203a-3p and regulating CREB3 expression. *Mol Cancer* **18**, 73. doi: 10.1186/s12943-019-1007-1.

Wu Y, Zhou A, Tang L, Lei Y, Tang B & Zhang L (2020b). Bile acids: key regulators and novel treatment targets for type 2 diabetes. *J Diabetes Res* **2020**, 6138438. doi: 10.1155/2020/6138438.

Xiao J, Xiong Y, Yang L-T, Wang J-Q, Zhou Z-M, Dong L-W, *et al*. (2021). POST1/C12ORF49 regulates the SREBP pathway by promoting site-1 protease maturation. *Protein Cell* **12**, 279-296. doi: 10.1007/s13238-020-00753-3.

Xiao Y, Yan W, Zhou K, Cao Y & Cai W (2016). Glucocorticoid treatment alters systemic bile acid homeostasis by regulating the biosynthesis and transport of bile salts. *Dig Liver Dis* **48**, 771-779. doi: 10.1016/j.dld.2016.03.022.

Xie J, Ponuwei GA, Moore CE, Willars GB, Tee AR & Herbert TP (2011). cAMP inhibits mammalian target of rapamycin complex-1 and -2 (mTORC1 and 2) by promoting complex dissociation and inhibiting mTOR kinase activity. *Cell Signal* **23**, 1927-1935. doi: 10.1016/j.cellsig.2011.06.025.

Xu M, Chen X, Chen D, Yu B & Huang Z (2017). FoxO1: a novel insight into its molecular mechanisms in the regulation of skeletal muscle differentiation and fibre type specification. *Oncotarget* **8**, 10662-10674. doi: 10.18632/oncotarget.12891.

Xu X, Park J-G, So J-S, Hur KY & Lee A-H (2014). Transcriptional regulation of apolipoprotein A-IV by the transcription factor CREBH. *J Lipid Res* **55**, 850-859. doi: 10.1194/jlr.M045104.

Xue H, Yuan G, Guo X, Liu Q, Zhang J, Gao X, *et al*. (2016a). A novel tumour-promoting mechanism of IL6 and the therapeutic efficacy of tocilizumab: hypoxia-induced IL6 is a potent autophagy initiator in glioblastoma via the pSTAT3-*MIR155-3p*-CREBRF pathway. *Autophagy* **12**, 1129-1152. doi: 10.1080/15548627.2016.1178446.

Xue H, Zhang J, Guo X, Wang J, Li J, Gao X, *et al*. (2016b). CREBRF is a potent tumour suppressor of glioblastoma by blocking hypoxia-induced autophagy via the CREB3/ATG5 pathway. *Int J Oncol* **49**, 519-528. doi: 10.3892/ijo.2016.3576.

Xue S & Barna M (2012). Specialised ribosomes: a new frontier in gene regulation and organismal biology. *Nat Rev Mol Cell Biol* **13**, 355-369. doi: 10.1038/nrm3359.

Yadavalli T, Suryawanshi R, Koganti R, Hopkins J, Ames J, Koujah L, *et al*. (2020). Standalone or combinatorial phenylbutyrate therapy shows excellent antiviral activity and mimics CREB3 silencing. *Sci Adv* **6**, eabd9443. doi: 10.1126/sciadv.abd9443.

Yaghootkar H, Lotta LA, Tyrrell J, Smit RAJ, Jones SE, Donnelly L, *et al*. (2016). Genetic evidence for a link between favourable adiposity and lower risk of type

2 diabetes, hypertension and heart disease. *Diabetes* **65**, 2448-2460. doi: 10.2337/db15-1671.

Yajnik CS, Janipalli CS, Bhaskar S, Kulkarni SR, Freathy RM, Prakash S, *et al*. (2009). *FTO* gene variants are strongly associated with Type 2 Diabetes but only weakly with obesity in South Asian Indians. *Diabetologia* **52**(2), 247-252. doi: 10.1007/s00125-008-1186-6.

Yam P, Albright J, VerHague M, Gertz ER, de Villena FP-M & Bennett BJ (2020). Genetic background shapes phenotypic response to diet for adiposity in the Collaborative Cross. *Front Genet* **11**, 615012. doi: 10.3389/fgene.2020.615012.

Yamamoto M, Yamauchi M & Sugimoto T (2019). Prevalent vertebral fracture is dominantly associated with spinal microstructural deterioration rather than bone mineral density in patients with type 2 diabetes mellitus. *PLoS One* **14**, e0222571. doi: 10.1371/journal.pone.0222571.

Yang D, Jiang T, Liu J, Zhang B, Lin P, Chen H, *et al*. (2018). CREB3 regulatory factor-mTOR-autophagy regulates goat endometrial function during early pregnancy. *Biol Reprod* **98**, 713-721. doi: 10.1093/biolre/ioy044.

Yang X, Chen Q, Sun L, Zhang H, Yao L, Cui X, *et al*. (2017). KLF10 transcription factor regulates hepatic glucose metabolism in mice. *Diabetologia* **60**, 2443-2452. doi: 10.1007/s00125-017-4412-2.

Yang X, Jansson PA, Nagaev I, Jack MM, Carvalho E, Sunnerhagen KS, *et al.* (2004). Evidence of impaired adipogenesis in insulin resistance. *Biochem Biophys Res Commun* **317**, 1045-1051. doi: 10.1016/j.bbrc.2004.03.152.

Yang Y, Jin Y, Lin P, Hu L, Cui C, Li X, *et al.* (2013a). The expression and localisation of LRF in the female reproductive tract of cycling mice throughout the estrous cycle. *J Immunoassay Immunochem* **34**, 313-322. doi: 10.1080/15321819.2012.732169.

Yang Y, Jin Y, Martyn AC, Lin P, Song Y, Chen F, *et al.* (2013b). Expression pattern implicates a potential role for luman recruitment factor in the process of implantation in uteri and development of preimplantation embryos in mice. *J Reprod Dev* **59**, 245-251. doi: 10.1262/jrd.2012-137.

Yang Z, Roth K, Agarwal M, Liu W & Petriello MC (2021). The transcription factors CREBH, PPARa, and FOXO1 as critical hepatic mediators of diet-induced metabolic dysregulation. *J Nutr Biochem* **95**, 108633. doi: 10.1016/j.jnutbio.2021.108633.

Yao S, Zhang J, Zhan Y, Shi Y, Yu Y, Zheng L, *et al*. (2020). Insulin resistance in apolipoprotein M knockout mice is mediated by the protein kinase Akt signalling pathway. *Endocr Metab Immune Disord Drug Targets* **20**, 771-780. doi: 10.2174/1871530319666191023125820.

Yasrebi A, Rivera JA, Krumm EA, Yang JA & Roepke TA (2017). Activation of estrogen response element-independent ERα signalling protects female mice from diet-induced obesity. *Endocrinology* **158**, 319-334. doi: 10.1210/en.2016-1535.

Yecies JL, Zhang HH, Menon S, Liu S, Yecies D, Lipovsky AI, *et al*. (2011). Akt stimulates hepatic SREBP1c and lipogenesis through parallel mTORC1-dependent and independent pathways. *Cell Metab* **14**, 21-32. doi: 10.1016/j.cmet.2011.06.002.

Yellaturu CR, Deng X, Cagen LM, Wilcox HG, Mansbach CM, Siddiqi SA, *et al*. (2009a). Insulin enhances post-translational processing of nascent SREBP-1c by promoting its phosphorylation and association with COPII vesicles. *J Biol Chem* **284**, 7518-7532. doi: 10.1074/jbc.M805746200.

Yellaturu CR, Deng X, Park EA, Raghow R & Elam MB (2009b). Insulin enhances the biogenesis of nuclear sterol regulatory element-binding protein (SREBP)-1c by posttranscriptional down-regulation of Insig-2A and its dissociation from SREBP cleavage-activating protein (SCAP)·SREBP-1c complex. *J Biol Chem* **284**, 31726-31734. doi: 10.1074/jbc.M109.050914.

Ying Z, Misra V & Verge VMK (2014). Sensing nerve injury at the axonal ER: activated Luman/CREB3 serves as a novel axonally synthesised retrograde regeneration signal. *Proc Natl Acad Sci U.S.A.* **111**, 16142-16147. doi: 10.1073/pnas.1407462111.

Ying Z, Zhai R, McLean NA, Johnston JM, Misra V & Verge VMK (2015a). The unfolded protein response and cholesterol biosynthesis link Luman/CREB3 to regenerative axon growth in sensory neurons. *J Neurosci* **35**, 14557-14570. doi: 10.1523/JNEUROSCI.0012-15.2015.

Ying Z, Zhang R, Verge VMK & Misra V (2015b). Cloning and characterisation of rat Luman/CREB3, a transcription factor highly expressed in nervous system tissue. *J Mol Neurosci* **55**, 347-354. doi: 10.1007/s12031-014-0330-7.

Yokokawa T, Mori R, Suga T, Isaka T, Hayashi T & Fujita S (2020). Muscle denervation reduces mitochondrial biogenesis and mitochondrial translation factor expression in mice. *Biochem Biophys Res Commun* **527**, 146-152. doi: 10.1016/j.bbrc.2020.04.062.

Yoshihara E (2020). TXNIP/TBP-2: a master regulator for glucose homeostasis. *Antioxidants (Basel)* **9**, 765. doi: 10.3390/antiox9080765.

You Z, He L & Yan N (2021). Tunicamycin-induced endoplasmic reticulum stress promotes breast cancer cell MDA-MB-231 apoptosis through inhibiting Wnt/β-catenin signalling pathway. *J Healthc Eng* **2021**, 6394514. doi: 10.1155/2021/6394514.

Yuan M, Pino E, Wu L, Kacergis M & Soukas AA (2012). Identification of Akt-independent regulation of hepatic lipogenesis by mammalian target of rapamycin (mTOR) complex 2. *J Biol Chem* **287**, 29579-29588. doi: 10.1074/jbc.M112.386854.

Zaniqueli D, de Oliveira Alvin R, Griep RH, Benseñor IM, Barreto SM, Lotufo PA, *et al*. (2020). Insulin resistance may be misdiagnosed by HOMA-IR in adults with greater fat-free mass: the ELSA-Brasil study. *Acta Diabetol* **58**, 73-80. doi: 10.1007/s00592-020-01594-6.

Zanotto TM, Quaresma PGF, Guadagnini D, Weissmann L, Santos AC, Vecina JF, *et al*. (2016). Blocking iNOS and endoplasmic reticulum stress synergistically improves insulin resistance in mice. *Mol Metab* **6**, 206-218. doi: 10.1016/j.molmet.2016.12.005.

Zeng M (2015). Phenotypic analysis of LUMAN/CREB3 deficient mice: a novel role of LUMAN in the regulation of emotion, locomotor activity, maternal response, and energy balance. PhD thesis, University of Guelph, Ontario, Canada.

Zhang D, Tong X, Arthurs B, Guha A, Rui L, Kamath A, *et al*. (2014). Liver clock protein BMAL1 promotes de novo lipogenesis through insulin-mTORC2-AKT signalling. *J Biol Chem* **289**, 25925-25935. doi: 10.1074/jbc.M114.567628.

Zhang L, Rajbhandari P, Priest C, Sandhu J, Wu X, Temel R, *et al*. (2017a). Inhibition of cholesterol biosynthesis through RNF145-dependent ubiquitination of SCAP. *Elife* **6**, e28766. doi: 10.7554/eLife.28766.

Zhang N, Ke Y & Zhang L (2017b). Interplay between Hepatitis C Virus and ARF4. *Virol Sin* **32**, 533-536. doi: 10.1007/s12250-017-4000-0.

Zhang W, Patil S, Chauhan B, Guo S, Powell DR, Le J, *et al*. (2006). FoxO1 regulates multiple metabolic pathways in the liver: effects on gluconeogenic, glycolytic, and lipogenic gene expression. *J Biol Chem* **281**, 10105-10117. doi: 10.1074/jbc.M600272200.

Zhang X, Cheng Q, Wang Y, Leung PS & Mak KK (2017c). Hedgehog signalling in bone regulates whole-body energy metabolism through a bone-adipose

endocrine relay mediated by PTHrP and adiponectin. *Cell Death Differ* **24**, 225-237. doi: 10.1038/cdd.2016.113.

Zhang X, Jiang L & Liu H (2021). Forkhead box protein O1: functional diversity and post-translational modification, a new therapeutic target? *Drug Des Devel Ther* **15**, 1851-1860. doi: 10.2147/DDDT.S305016.

Zhang X, Odom DT, Koo S-H, Conkright MD, Canettieri G, Best J, *et al*. (2005). Genome-wide analysis of cAMP-response element binding protein occupancy, phosphorylation, and target gene activation in human tissues. *Proc Natl Acad Sci U S A* **102**, 4459-4464. doi: 10.1073/pnas.0501076102.

Zhang Y, Higgins CB, Fortune HM, Chen P, Stothard AI, Mayer AL, *et al*. (2019). Hepatic arginase 2 (Arg2) is sufficient to convey the therapeutic metabolic effects of fasting. *Nat Commun* **10**, 1587. doi: 10.1038/s41467-019-09642-8.

Zhang Y, Ma R, Zou S, Tong G, Abula G, Hu M, *et al.* (2017d). Transcription of synaptic plasticity-related genes in patients with somnipathy combined with type 2 diabetes. *Biomed Res* **28**, 7035-7040.

Zhao F, Liu H, Wang N, Yu L, Wang A, Yi Y, *et al*. (2020). Exploring the role of Luman/CREB3 in regulating decidualisation of mice endometrial stromal cells by comparative transcriptomics. *BMC Genomics* **21**, 103. doi: 10.1186/s12864-020-6515-2.

Zhao F, Wang N, Yi Y, Lin P, Tang K, Wang A, *et al.* (2016). Knockdown of CREB3/Luman by shRNA in mouse granulosa cells results in decreased estradiol and progesterone synthesis and promotes cell proliferation. *PLoS One* **11**, e0168246. doi: 10.1371/journal.pone.0168246.

Zheng Z, Kim H, Qiu Y, Chen X, Mendez R, Dandekar A, *et al*. (2016). CREBH couples circadian clock with hepatic lipid metabolism. *Diabetes* **65**, 3369-3383. doi: 10.2337/db16-0298.

Zhong J-T, Yu J, Wang H-J, Shi Y, Zhao T-S, He B-X, *et al*. (2017). Effects of endoplasmic reticulum stress on the autophagy, apoptosis, and chemotherapy resistance of human breast cancer cells by regulating the PI3K/AKT/mTOR signalling pathway. *Tumour Biol* **39**, 1010428317697562. doi: 10.1177/1010428317697562.

Zhou R, Guo Q, Xiao Y, Guo Q, Huang Y, Li C, *et al*. (2021). Endocrine role of bone in the regulation of energy metabolism. *Bone Res* **9**, 25. doi: 10.1038/s41413-021-00142-4.

Zicker MC, Silveira ALM, Lacerda DR, Rodrigues DF, Oliveira CT, de Souza LM, *et al*. (2019). Virgin coconut oil is effective to treat metabolic and inflammatory dysfunction induced by high refined carbohydrate-containing diet in mice. *J Nutr Biochem* **63**, 117-128. doi: 10.1016/j.jnutbio.2018.08.013.

Zimmet P, Arblaster M & Thoma K (1978). The effect of Westernisation on native populations. Studies on a Micronesian community with a high diabetes prevalence. *Aust N Z J Med* **8**, 141-146. doi: 10.1111/j.1445-5994.1978.tb04500.x..

Zimmet P, Canteloube D, Genelle B, LeGonidec G, Couzigou P, Peghini M, *et al*. (1982). The prevalence of diabetes mellitus and impaired glucose tolerance in Melanesians and part-Polynesians in rural New Caledonia and Ouvea (Loyalty Islands). *Diabetologia* **23**, 393-398. doi: 10.1007/BF00260949.

Zimmet P, Faaiuso S, Ainuu J, Whitehouse S, Milne B & DeBoer W (1981). The prevalence of diabetes in the rural and urban Polynesian population of Western Samoa. *Diabetes* **30**, 45-51. doi: 10.2337/diab.30.1.45.

Zimmet P, Taft P, Guinea A, Guthrie W & Thoma K (1977). The high prevalence of diabetes mellitus on a Central Pacific Island. *Diabetologia* **13**, 111-115. doi: 10.1007/BF00745137.

Zimmet P, Whitehouse S & Kiss J (1979). Ethnic variability in the plasma insulin response to oral glucose in Polynesian and Micronesian subjects. *Diabetes* **28**, 624-628. doi: 10.2337/diab.28.7.624.

Zinker B, Mika A, Nguyen P, Wilcox D, Öhman L, von Geldern TW, *et al*. (2007). Liver-selective glucocorticoid receptor antagonism decreases glucose production and increases glucose disposal, ameliorating insulin resistance. *Metabolism* **56**, 380-387. doi: 10.1016/j.metabol.2006.10.021.

Zuloaga DG, Heck AL, De Guzman RM & Handa RJ (2020). Roles for androgens in mediating the differences of neuroendocrine and behavioural stress responses. *Biol Sex Differ* **11**, 44. doi: 10.1186/s13293-020-00319-2.

Zurlo F, Larson K, Bogardus C & Ravussin E (1990). Skeletal muscle metabolism is a major determinant of resting energy expenditure. *J Clin Invest* **86**, 1423-1427. doi: 10.1172/JCI114857.